Supporting Information

New α-Glucosidase Inhibitors from a Marine Sponge-derived Fungus *Aspergillus* sp. OUCMDZ-1583

Fandong Kong,[†] Chengying Zhao,[†] Jiejie Hao,[†] Cong Wang,[†] Wei Wang,[†] Xiaolong Huang,[‡] Weiming Zhu[*,†]

[†] *Key Laboratory of Marine Drugs, Ministry of Education of China, School of Medicine and Pharmacy, Ocean University of China, Qingdao 266003, China;* [‡] *College of Agriculture, Hainan University, Haikou 570228, China*

List of Supporting Information

Anti-influenza A Virus (H1N1) Assay

The antiviral activity against H1N1 was evaluated by the CPE inhibition assay.[6] Confluent MDCK cell monolayers were firstly incubated with influenza virus (A/Puerto Rico/8/34 (H1N1), PR/8) at 37 ºC for 1 h. After removing the virus dilution, cells were maintained in infecting media (RPMI 1640, 4 μg/mL of trypsin) containing different concentrations of test compounds at 37 ºC. After 48 h incubation at 37 ºC, the cells were fixed with 100 μL of 4% formaldehyde for 20 min at room temperature. After removal of the formaldehyde, the cells were stained with 0.1% crystal violet for 30 min. The plates were washed and dried, and the intensity of crystal violet staining for each well was measured in a microplate reader (Bio-Rad, USA) at 570 nm. The IC_{50} value was calculated as the compound concentration required inhibiting influenza virus yield at 48 h post-infection by 50%. Ribavirin was used as the positive control with an IC_{50} value of 137.3 ± 0.4 μM.

α-Glucosidase Inhibitory Effect Assay

The inhibitory effects were assayed as described preciously.[22] The sample was dissolved in sodium phosphate buffer (PBS, pH 6.8) at three concentrations. A volume of 10 μL of the sample solution, 20 μL of PBS and 20 μL of 2.5 *m*M *p*-nitrophenyl-α-D-glucopyranoside (PNPG) solution (in phosphate buffer) were mixed in a 96-well microplate and incubated at 37 °C for 5 min. A volume of 10 μL of α-glucosidase diluted to 0.2 U/mL by 0.01 M PBS was then added to each well. After incubating at 37 °C for 15 min, the absorbance at 405 nm was recorded by a Spectra max 190 micro plate reader (Molecular Devices Inc.). The blank was prepared by adding phosphate buffer instead of the α-glucosidase and acarbose was used as a positive control. Blank readings (no enzyme) were subtracted from each well and results were compared to the control. The inhibition (%) was calculated as $[1-(OD_{sample}/OD_{control})] \times 100$ %. The IC_{50} value was calculated as the compound concentration that is required for 50% inhibition and the IC_{50} value of the acarbose was 0.95 *m*M.

Antimicrobial Assays

The antimicrobial activities against *Escherichia coli*, *Enterobacter aerogenes*, *Pseudomonas aeruginosa*, *Bacillus subtilis*, *Staphylococcus aureus*, and *Candida albicans* were evaluated by an agar dilution method.[23] The tested strains were cultivated in LB agar plates for bacteria and in YPD agar plates for *C. albicans* at 37 °C. Compounds **1**–**23** and positive controls (ciprofloxacin lactate for bacteria and ketoconazole for *C. albicans*) were dissolved in MeOH at different concentrations from 100 to 0.05 μg/mL by the continuous 2-fold dilution methods. A 10 μL quantity of test solution was

absorbed by a paper disk (5 mm diameter) and placed on the assay plates. After 24 h incubation, zones of inhibition (mm in diameter) were recorded. The minimum inhibitory concentrations (MICs) were defined as the lowest concentration at which no microbial growth could be observed.

Cytotoxic Assays

Cytotoxicity was assayed by the MTT[24] and CCK-8 methods.[25] In the MTT assay, A549 and MCF-7 cell lines was grown in RPMI-1640 supplemented with 10% FBS under a humidified atmosphere of 5% CO_2 and 95% air at 37 °C, respectively. Cell suspension, 100 μL, at a density of 3 × 10^4 cell mL^{-1} was plated in 96-well microtiter plates, allowed to attach overnight, and then exposed to varying concentrations (10^{-5}-10^{-12} M) of compounds for 72 h. The MTT solution (20 μL, 5 mg/mL in IPMI-1640 medium) was then added to each well and incubated for 4 h. Old medium containing MTT was then gently replaced by DMSO and pipetted to dissolve any formazan crystals formed. Absorbance was then determined on a Spectra Max Plus plate reader at 540 nm. In the CCK-8 assay, K562 cell line was grown in RPMI-1640 supplemented with 10% FBS under a humidified atmosphere of 5% CO_2 and 95% air at 37 °C. Cell suspension, 100 μL, at a density of 5 × 10^5 cell mL^{-1} was plated in 96-well microtiter plates and then exposed to varying concentrations (10^{-5}-10^{-12} M) of compounds after cultivation for 24 h. Three days later, 10 μL of CCK-8 solution was added 4 h before detection. Then the absorbency (A450 value) was measured, and the growth rates of cells were computed.

ITS sequences of *Aspergillus* sp. OUCMDZ-1583

CGTAGGTGAACCTGCGGAAGGATCATTACTGAGTGCGGGCTGCCTCCGGGCGCCCAACCTCCCACCCG
TGAATACCTAACACTGTTGCTTCGGCGGGGAACCCCCTCGGGGGCGAGCCGCCGGGGACTACTGAACT
TCATGCCTGAGAGTGATGCAGTCTGAGTCTGAATATAAAATCAGTCAAAACTTTCAACAATGGATCTCT
TGGTTCCGGCATCGATGAAGAACGCAGCGAACTGCGATAAGTAATGTGAATTGCAGAATTCAGTGAAT
CATCGAGTCTTTGAACGCACATTGCGCCCCCTGGCATTCCGGGGGGCATGCCTGTCCGAGCGTCATTGC
TGCCCATCAAGCCCGGCTTGTGTGTTGGGTCGTCGTCCCCCCCCGGGGGACGGGCCCGAAAGGCAGC
GGCGGCACCGTGTCCGGTCCTCGAGCGTATGGGGCTTTGTCACCCGCTCGACTAGGGCCGGCCGGGCG
CCAGCCGACGTCTCCAACCATTTTTCTTCAGGTTGACCTCGGATCAGGTAGGGATACCCGCTGAACTTA
AGCATATCAATAAGCGGAG

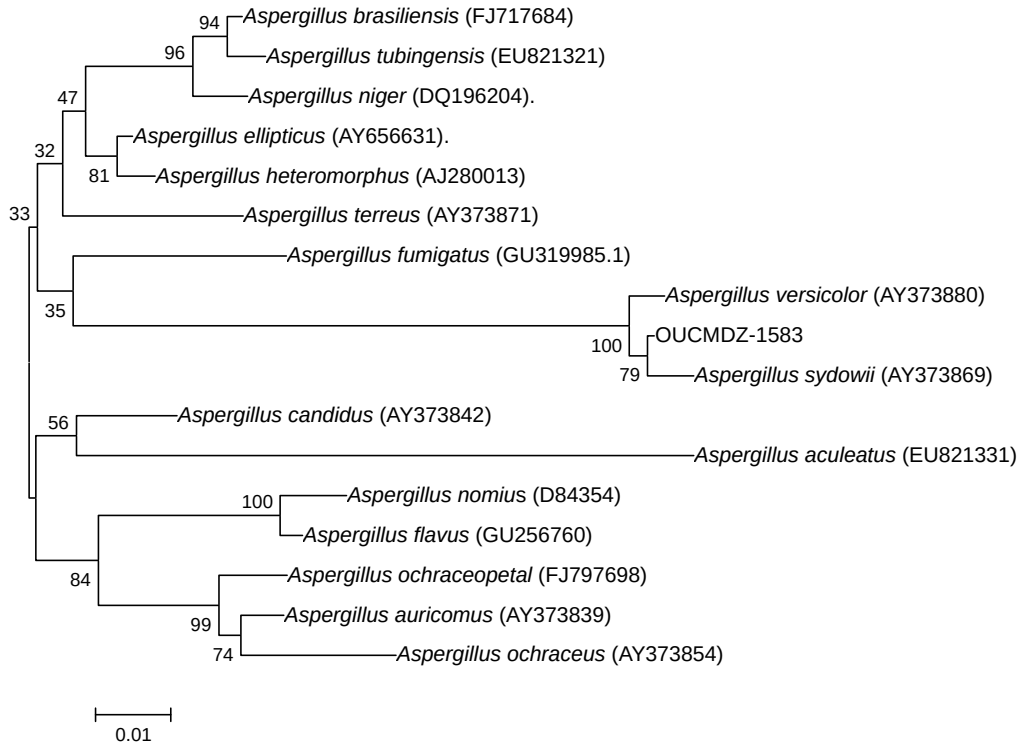

Neighbor-joining phylogenetic tree of strain OUCMDZ-1583 based on ITS gene sequences (ca. 565 bp). The values at each node represent the bootstrap values from 1000 replicates, and the scale bar represents 0.0005 substitutions per nucleotide. Phylogenetic analyses were conducted in MEGA4.

Theory and Calculation Details. The calculations were performed by using the density functional theory (DFT) as carried out in the Gaussian 03.[S1] The preliminary conformational distributions search was performed by HyperChem 7.5 software. All ground-state geometries were optimized at the B3LYP/6-31G(d) level. Solvent effects of methanol solution were evaluated at the same DFT level by using the SCRF/PCM method.[S2] TDDFT[S3] at B3LYP/6-31G(d) was employed to calculate the electronic excitation energies and rotational strengths in methanol.

(S1) Gaussian 03, Revision E.01, M. J. Frisch, G. W. Trucks, H. B. Schlegel, G. E. Scuseria, M. A. Robb, J. R. Cheeseman, J. A. Montgomery, Jr., T. Vreven, K. N. Kudin, J. C. Burant, J. M. Millam, S. S. Iyengar, J. Tomasi, V. Barone, B. Mennucci, M. Cossi, G. Scalmani, N. Rega, G. A. Petersson, H. Nakatsuji, M. Hada, M. Ehara, K. Toyota, R. Fukuda, J. Hasegawa, M. Ishida, T. Nakajima, Y. Honda, O. Kitao, H. Nakai, M. Klene, X. Li, J. E. Knox, H. P. Hratchian, J. B. Cross, V. Bakken, C. Adamo, J. Jaramillo, R. Gomperts, R. E. Stratmann, O. Yazyev, A. J. Austin, R. Cammi, C. Pomelli, J. W. Ochterski, P. Y. Ayala, K. Morokuma, G. A. Voth, P. Salvador, J. J. Dannenberg, V. G. Zakrzewski, S. Dapprich, A. D. Daniels, M. C. Strain, O. Farkas, D. K. Malick, A. D. Rabuck, K. Raghavachari, J. B. Foresman, J. V. Ortiz, Q. Cui, A. G. Baboul, S. Clifford, J. Cioslowski, B. B. Stefanov, G. Liu, A. Liashenko, P. Piskorz, I. Komaromi, R. L. Martin, D. J. Fox, T. Keith, M. A. Al-Laham, C. Y. Peng, A. Nanayakkara, M. Challacombe, P. M. W. Gill, B. Johnson, W. Chen, M. W. Wong, C. Gonzalez and J. A. Pople, Gaussian, Inc., Wallingford CT, 2004.

(S2) (a) S. Miertus and J. Tomasi, Chem. Phys., 1982, **65**, 239–245. (b) J. Tomasi and M. Persico, Chem. Rev., 1994, **94**, 2027–2094. (c) R. Cammi and J. Tomasi, J.Comp.Chem., 1995, **16**, 1449–1458.

(S3) (a) M. E. Casida, In Recent Advances in Density Functional Methods, part I; D. P. Chong, World Scientific: Singapore, 1995; pp 155–192. (b) E. K. U. Gross, J. F. Dobson and M. Petersilka, Top. Curr. Chem., 1996, **181**, 81–172. (c) E. K. U. Gross and W. Kohn, Adv. Quantum Chem., 1990, **21**, 255–291. (d) E. Runge and E. K. U. Gross, Phys. Rev. Lett., 1984, **52**, 997–1000.

Table S1. ^{1}H (500 MHz) and ^{13}C (125 MHz) NMR Data of Compounds **19**–**23**

position	**19**[a]		**20**[b]		**21**[b]		**22**[a]		**23**[a]	
	δ_C	δ_H (J in Hz)	δ_C	δ_H (J in Hz)	δ_C	δ_H (J in Hz)	δ_C	δ_H (J in Hz)	δ_C	δ_H (J in Hz)
1	128.1, C		168.0, C		167.8, C		170.2, C		169.6, C	
2	148.9, C									
3	195.1, C		81.7, CH	5.05, br d	81.2, CH	5.03, m	77.5, CH	4.73, m	79.8, CH	4.67, m
4	52.5, CH	3.47, d (4.0)	74.5, CH	4.52, br d	74.4, CH	4.52, d (3.0)	42.8, CH_2	2.90, dd (16.0, 4.0); 2.83, dd (16.0, 12.0)	65.7, CH	4.46, br d (2.5)
4a			127.0, C		131.2, C		131.7, C		136.1, C	
5	55.8, CH	3.74, d (1.6, 4.0)	104.2, CH	6.59, s	104.4, CH	6.57, s	103.0, CH	6.51, s	103.9, CH	6.72, s
6	61.9, CH	4.86, d (1.6)	152.3, C		158.6, C		154.0, C		158.8, C	
7	128.1, CH	6.60, d (16.2)	134.3, C		137.2, C		132.8, C		139.0, C	
8	136.2, CH	6.47, dq (16.2, 6.8)	149.5, C		156.2, C		150.6, C		155.2, C	
8a			101.8, C		102.0, C		102.6, C		102.3, C	
9	19.7, CH	1.87, d (6.8)	19.2, CH_2	2.57, m; 2.13, m	19.2, CH_2	2.57, m; 2.13, m	33.0, CH_2	1.81, ddd (14.7, 10.4, 2.8); 1.56, ddd (14.7, 10.8, 3.6)	38.6, CH_2	1.94, m; 1.58,m
10	53.3, CH_2	4.07, d (11.3); 4.27, d (11.3)	78.7, CH	4.09, m	78.7, CH	4.10, m	65.7, CH	3.70, m	66.1, CH	3.70, m
11			39.1, CH_2	1.67, m; 1.54, m	39.8, CH_2	1.67, m; 1.52, m	40.4, CH_2	1.38, m; 1.35, m	40.5, CH_2	1.40, m; 1.38, m
12			38.1, CH_2	1.39, m; 1.34, m	38.0, CH_2	1.40, m; 1.31, m	18.9, CH_2	1.33, m; 1.30, m	18.9, CH_2	1.32, m; 1.37m
13			14.1, CH_3	0.88, t (7.5)	19.2, CH_3	0.89, t (7.4)	14.4, CH_3	0.86, t (7.2)	14.6, CH_3	0.89, t (7.1)
6-OCH_3			56.4, CH_3	3.93, s	56.2, CH_3	3.87, s	56.5, CH_3	3.83, s	56.7, CH	3.88, s
7-OCH_3					60.7, CH_3	3.93, s			60.5, CH_3	3.70, s
8-OH				11.11, s		11.3, br s		10.87, br s		11.03, br s

[a] recorded in DMSO-d_6. [b] recorded in $CDCl_3$.

Figure S1. The ^{1}H-NMR spectrum of compound **1** in $CDCl_3$

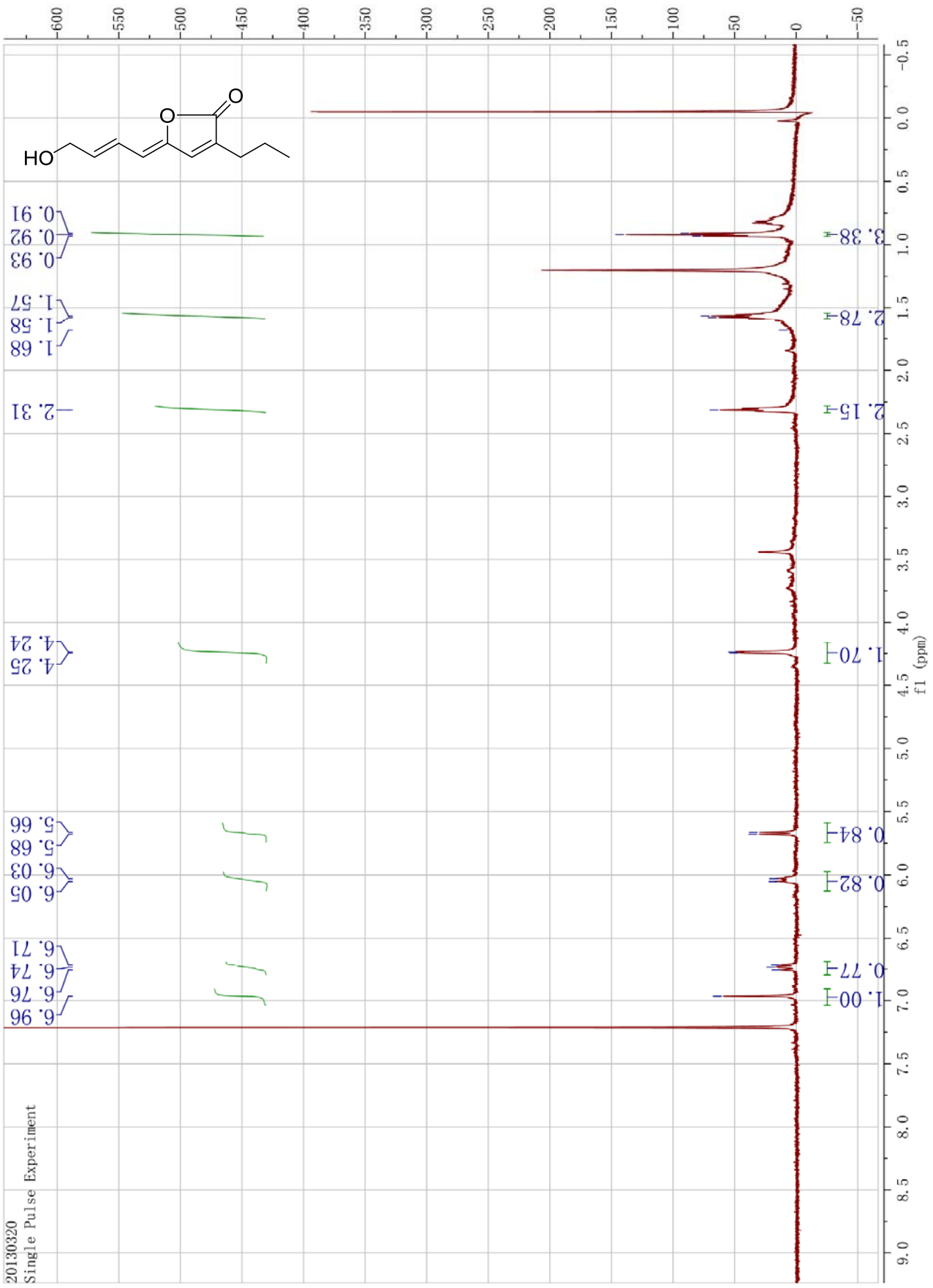

Figure S2. The DEPTQ spectrum of compound **1** in $CDCl_3$

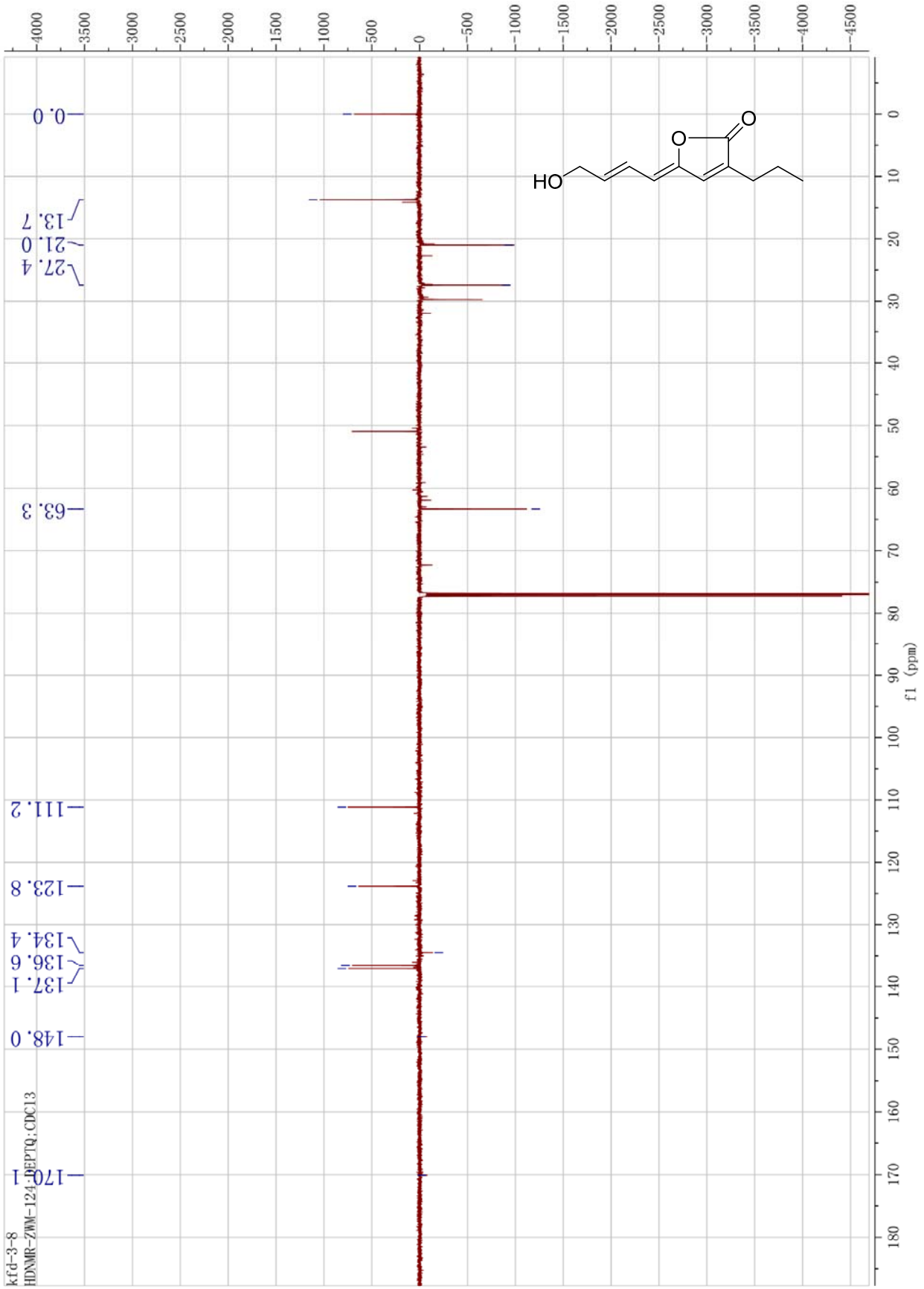

Figure S3. The HSQC spectrum of compound **1** in $CDCl_3$

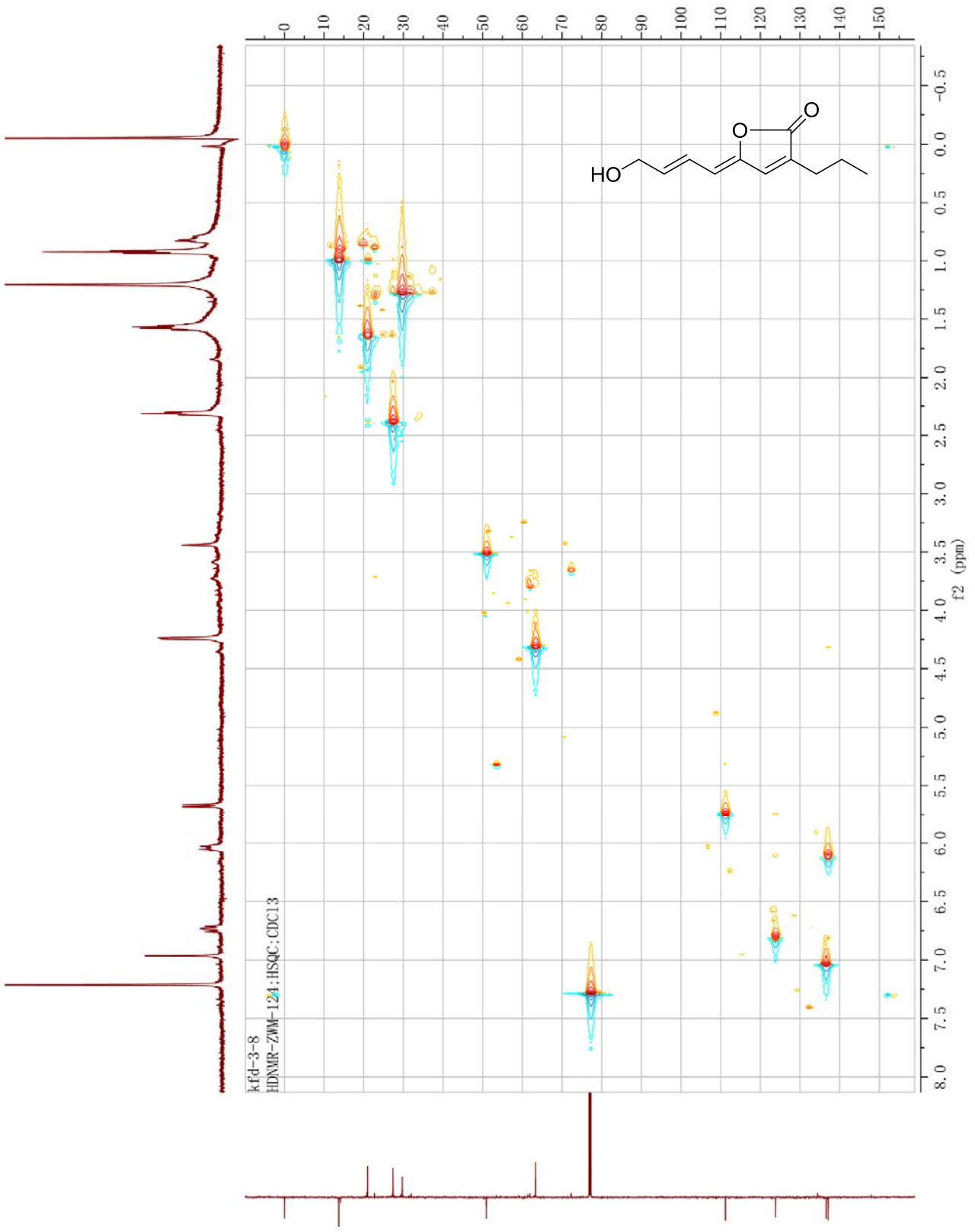

Figure S4. The HMBC spectrum of compound **1** in $CDCl_3$

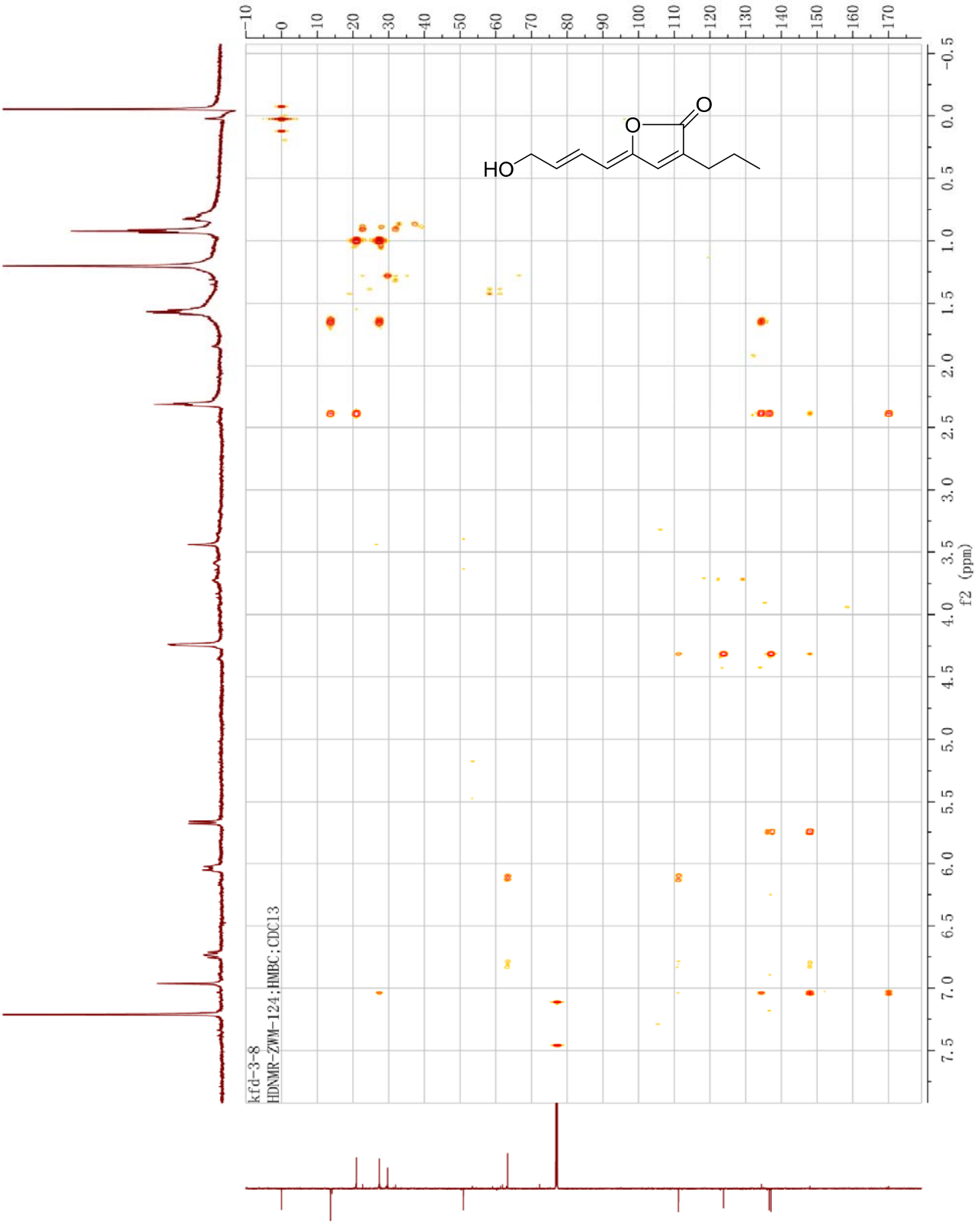

Figure S5. The ^{1}H-^{1}H COSY spectrum of compound **1** in $CDCl_3$

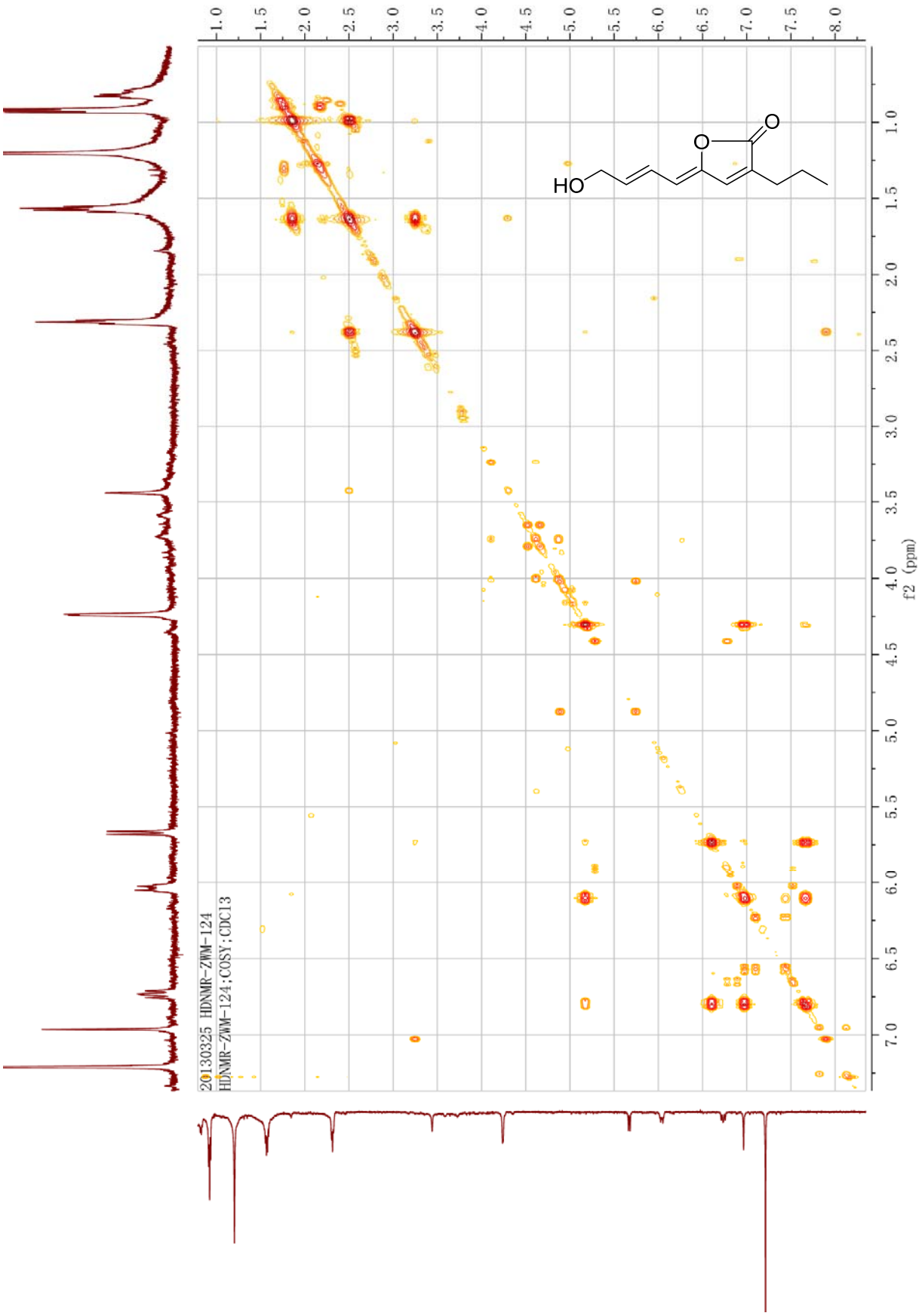

Figure S6. The NOE difference spectrum of compound **1** in $CDCl_3$

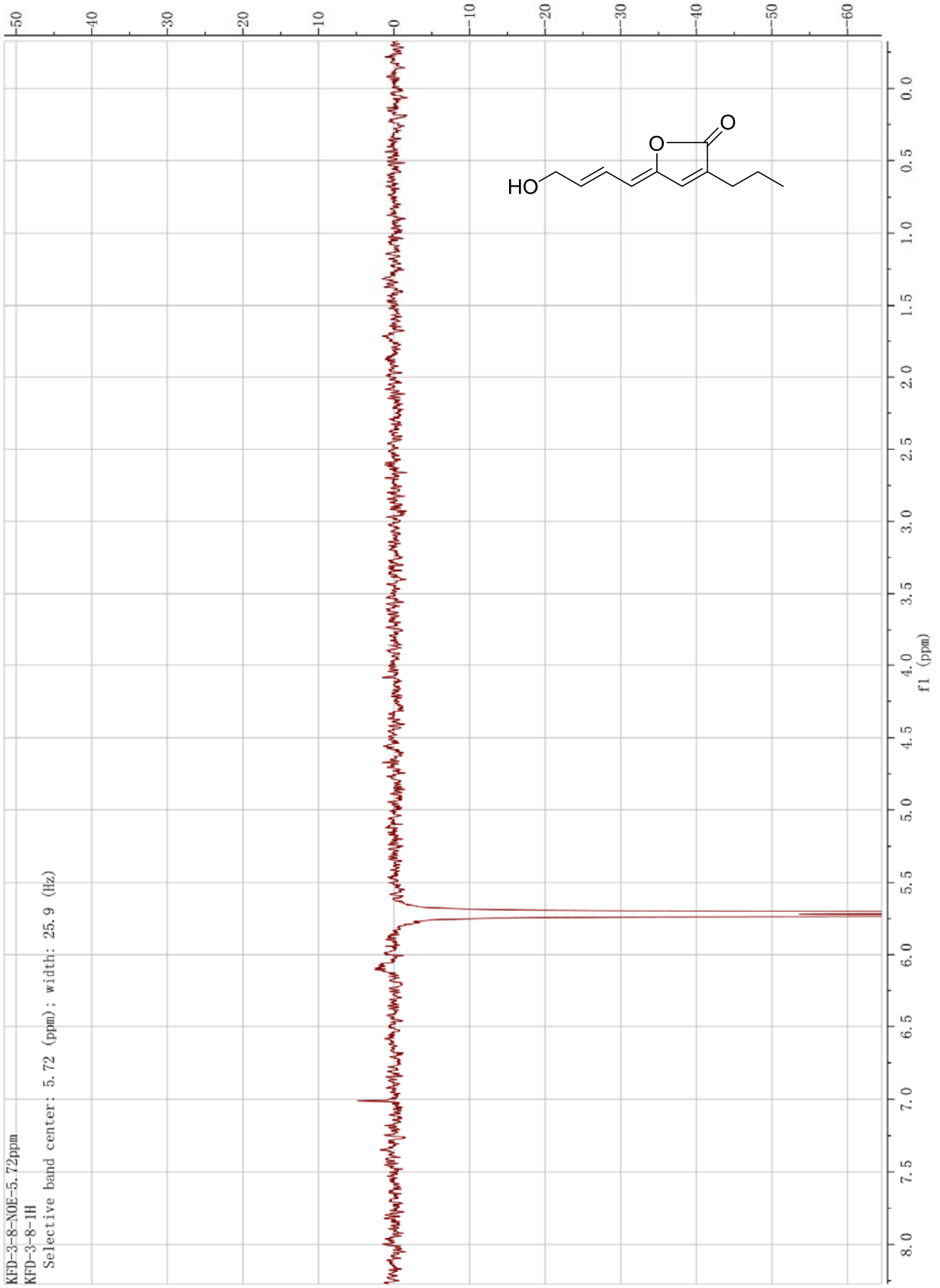

Figure S7. The ^{1}H-NMR spectrum of compound **2** in $CDCl_3$

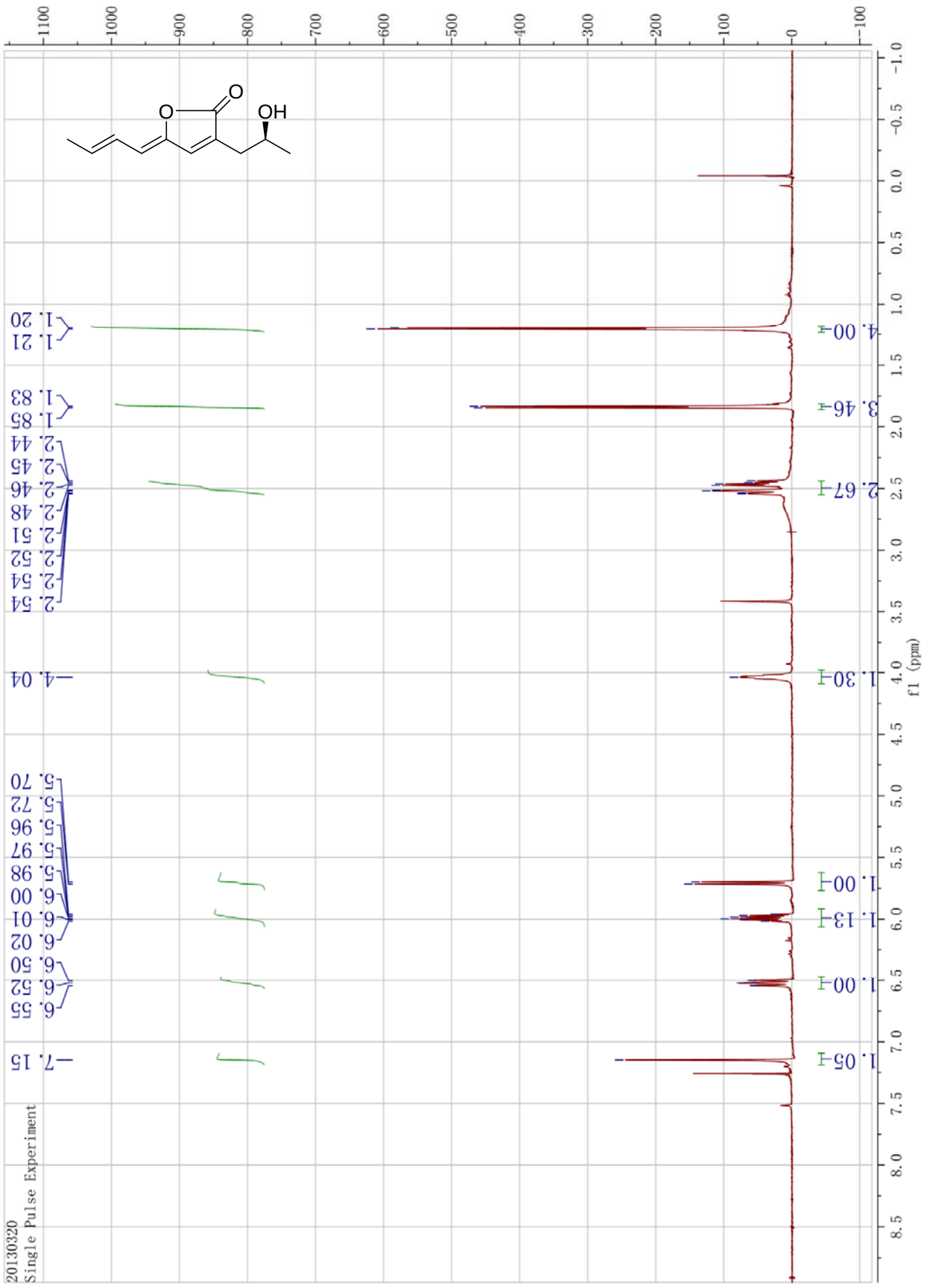

Figure S8. The ^{13}C-NMR spectrum of compound **2** in $CDCl_3$

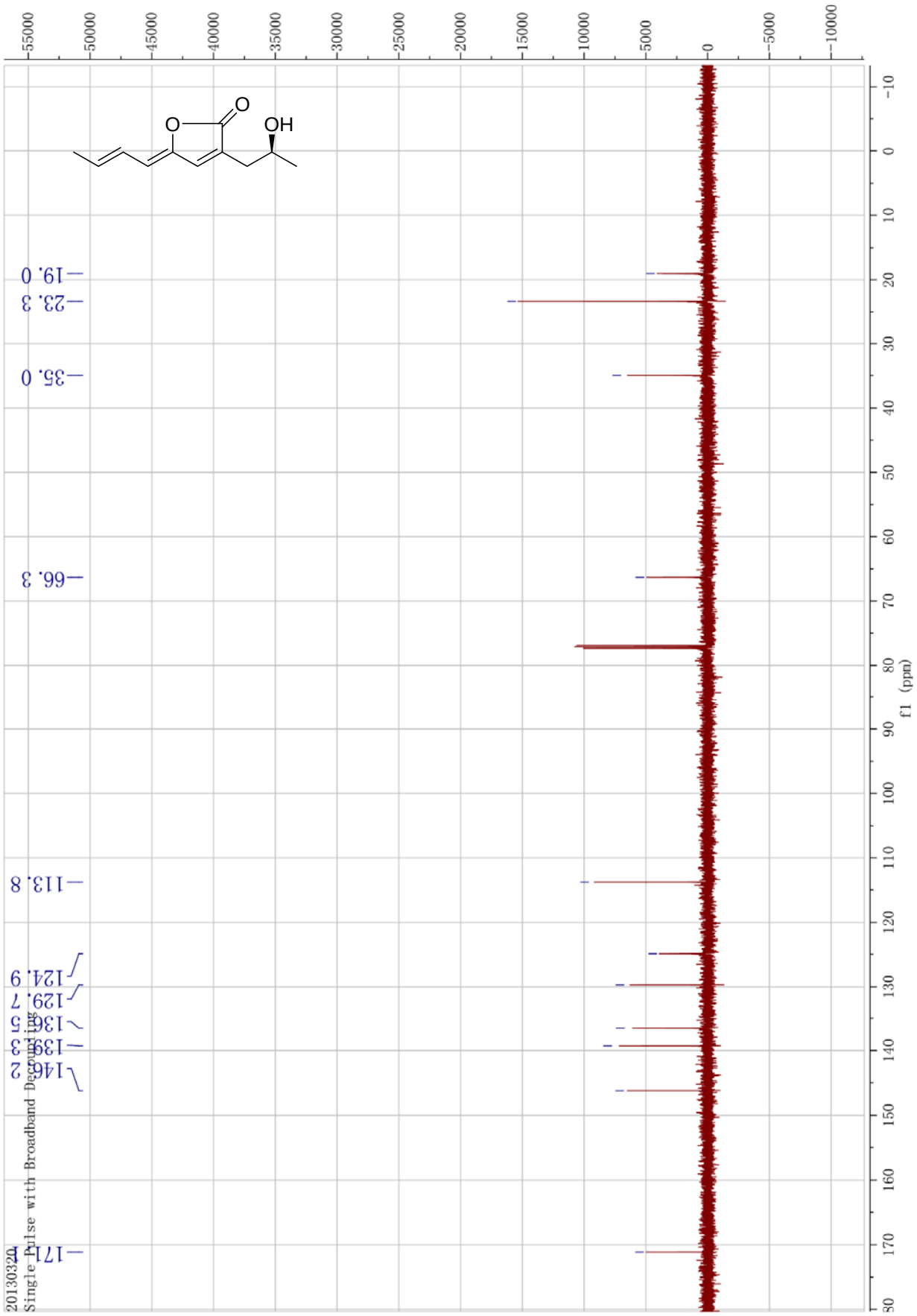

Figure S9. The DEPT spectrum of compound **2** in $CDCl_3$

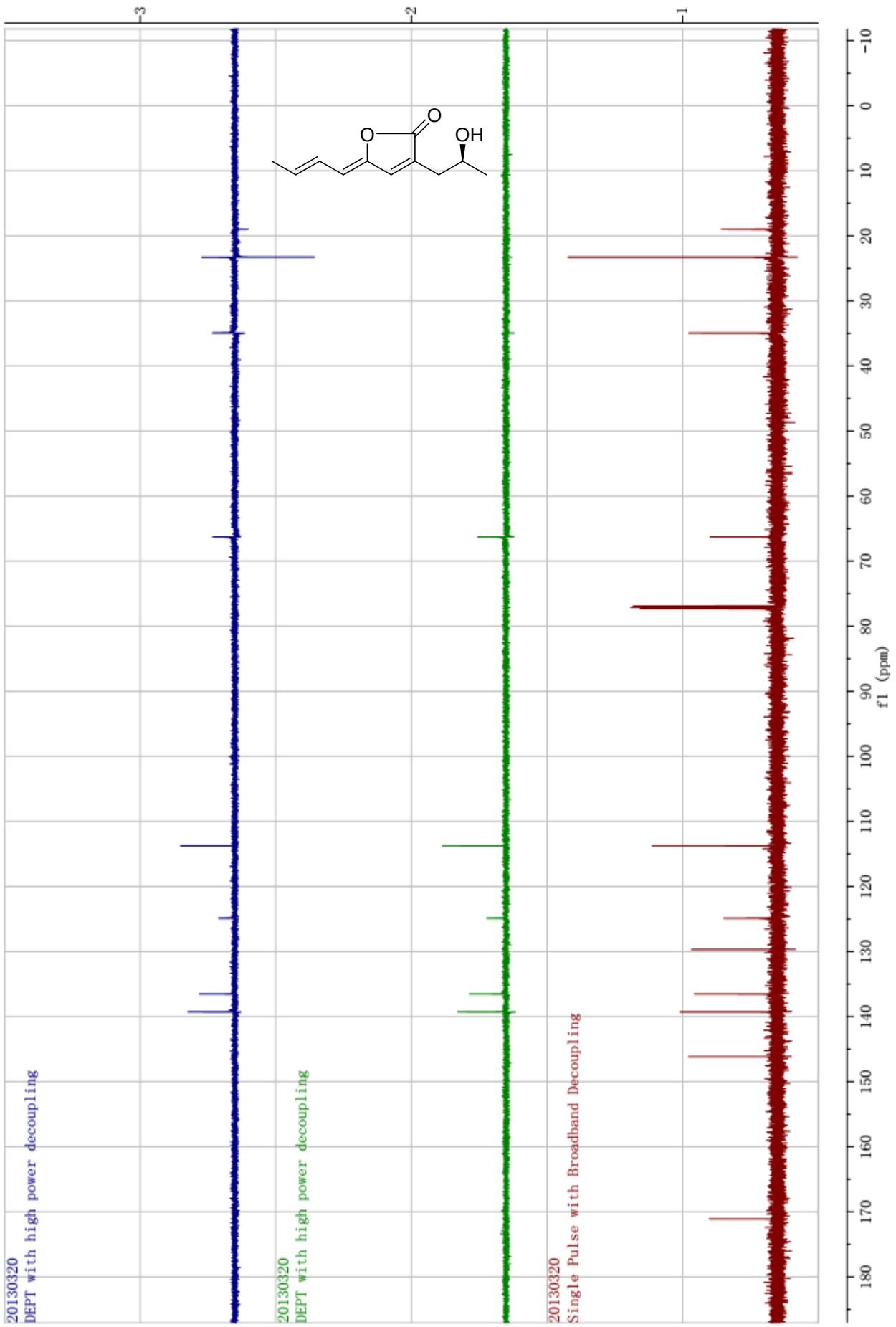

Figure S10. The HMQC spectrum of compound **2** in $CDCl_3$

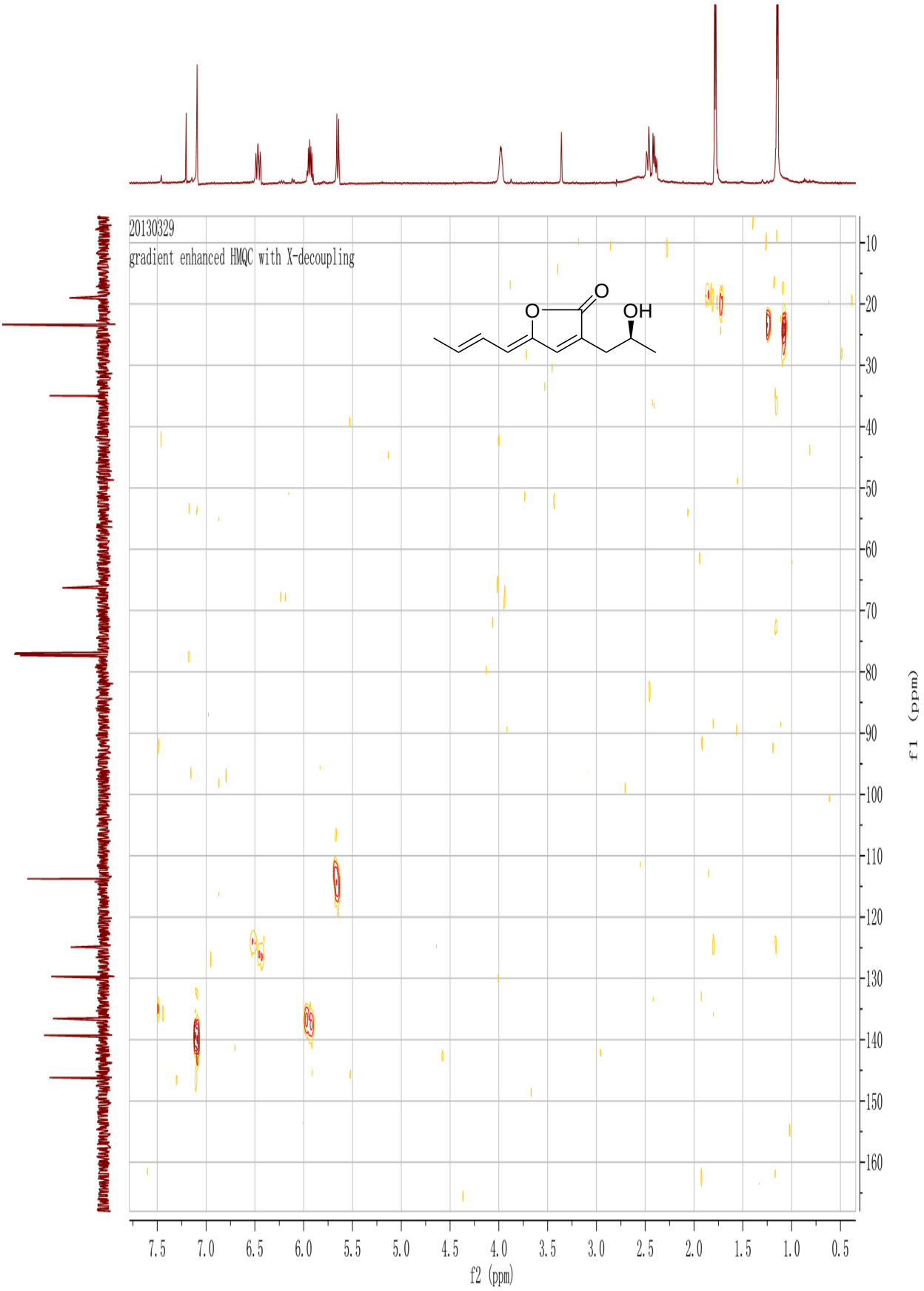

Figure S11. The ^{1}H-^{1}H COSY spectrum of compound **2** in $CDCl_3$

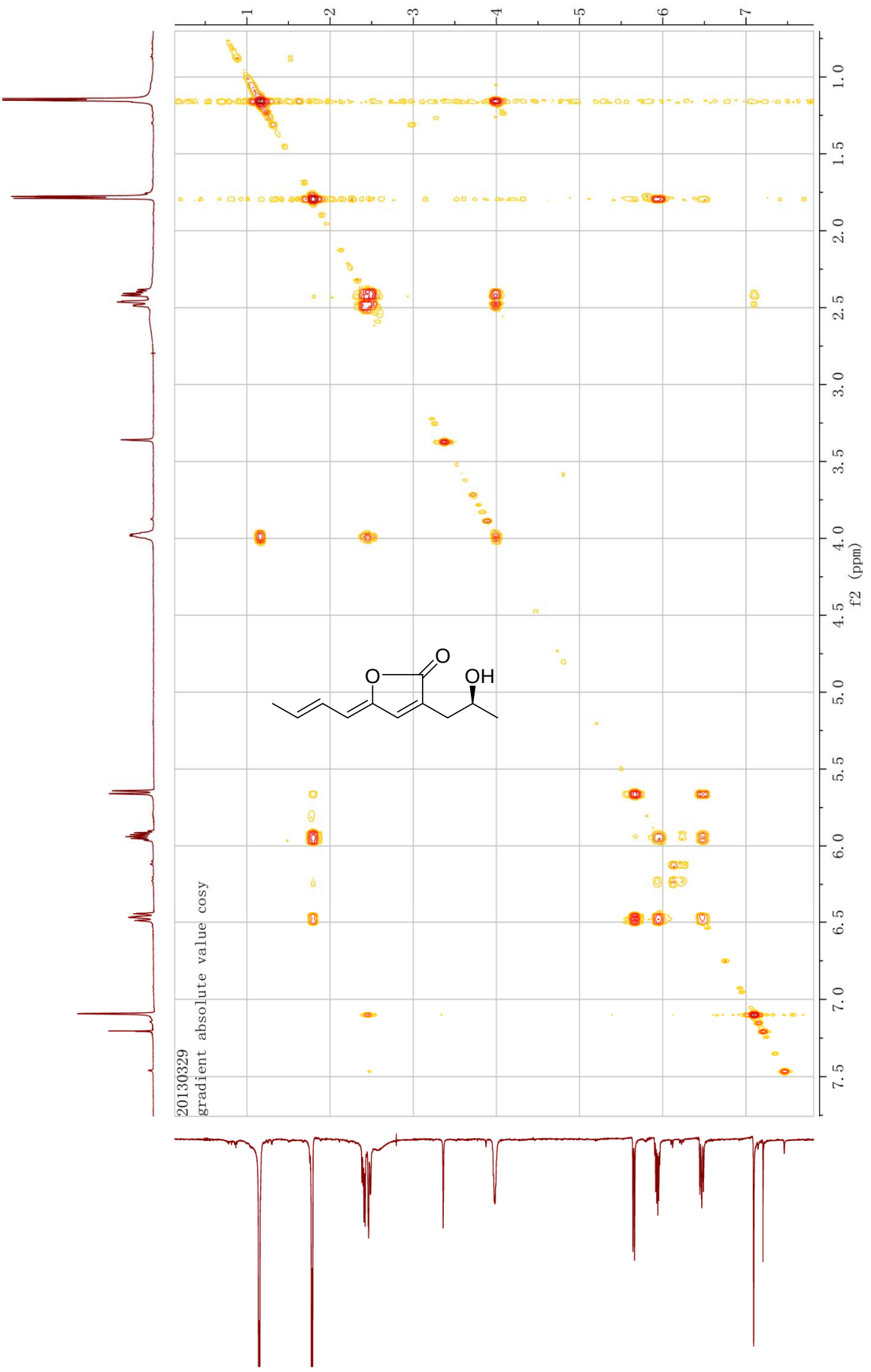

Figure S12. The HMBC spectrum of compound **2** in $CDCl_3$

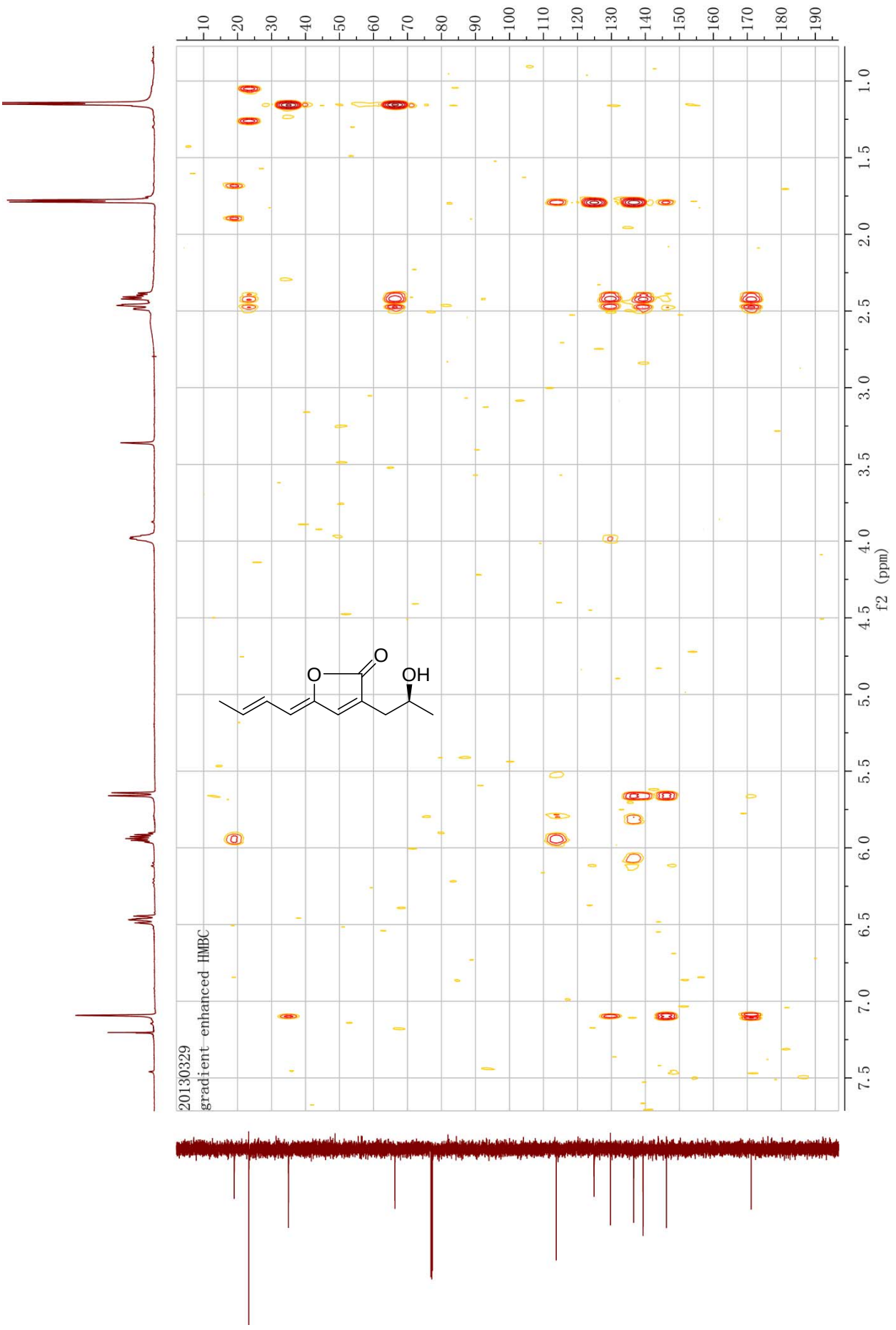

Figure S13. The NOE difference spectrum of compound **2** in $CDCl_3$

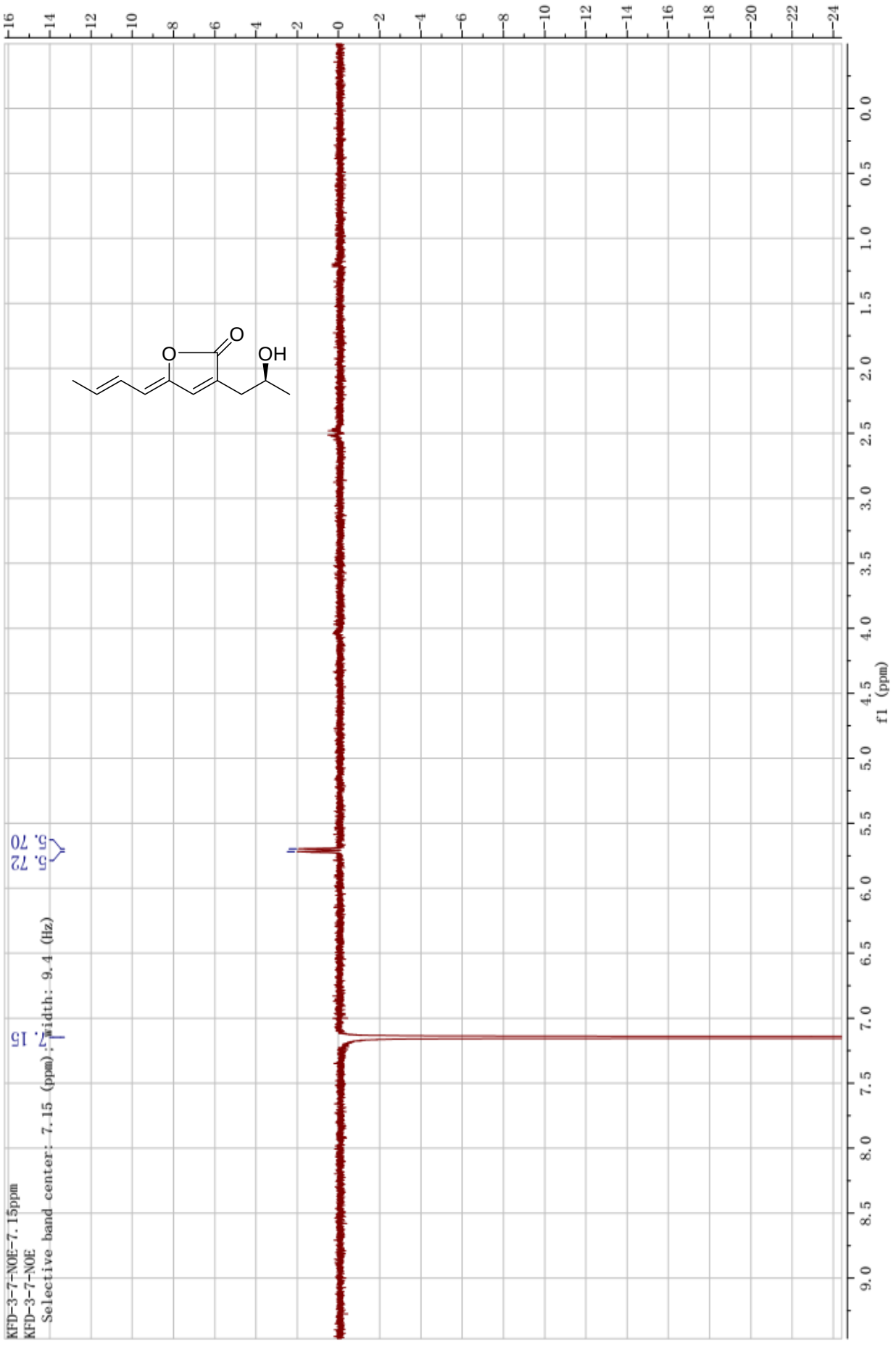

Figure S14. The ^{1}H-NMR spectrum of compounds **3** and **4** in $CDCl_3$

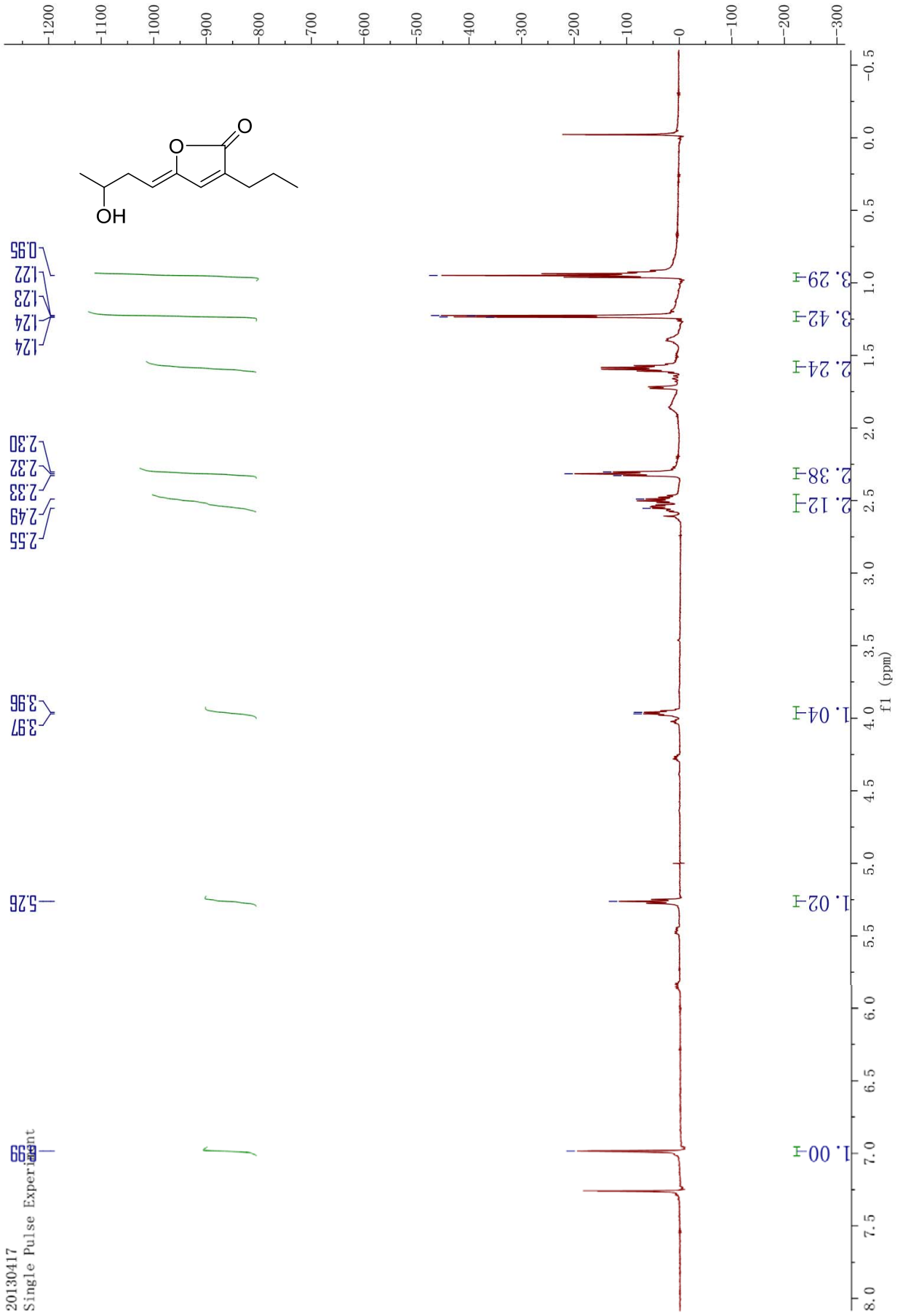

Figure S15. The ^{13}C-NMR spectrum of compounds **3** and **4** in $CDCl_3$

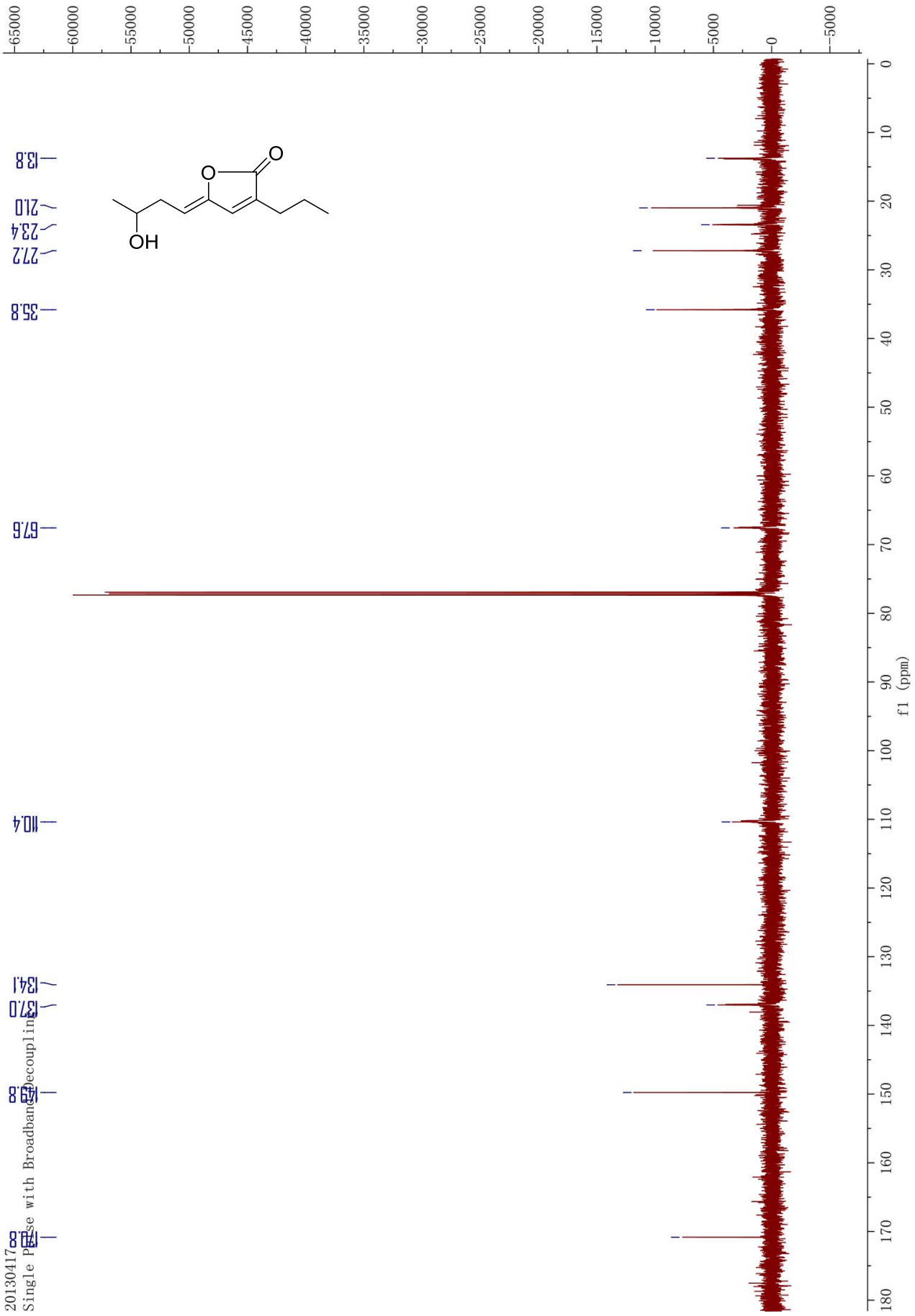

Figure S16. The DEPT spectrum of compounds **3** and **4** in $CDCl_3$

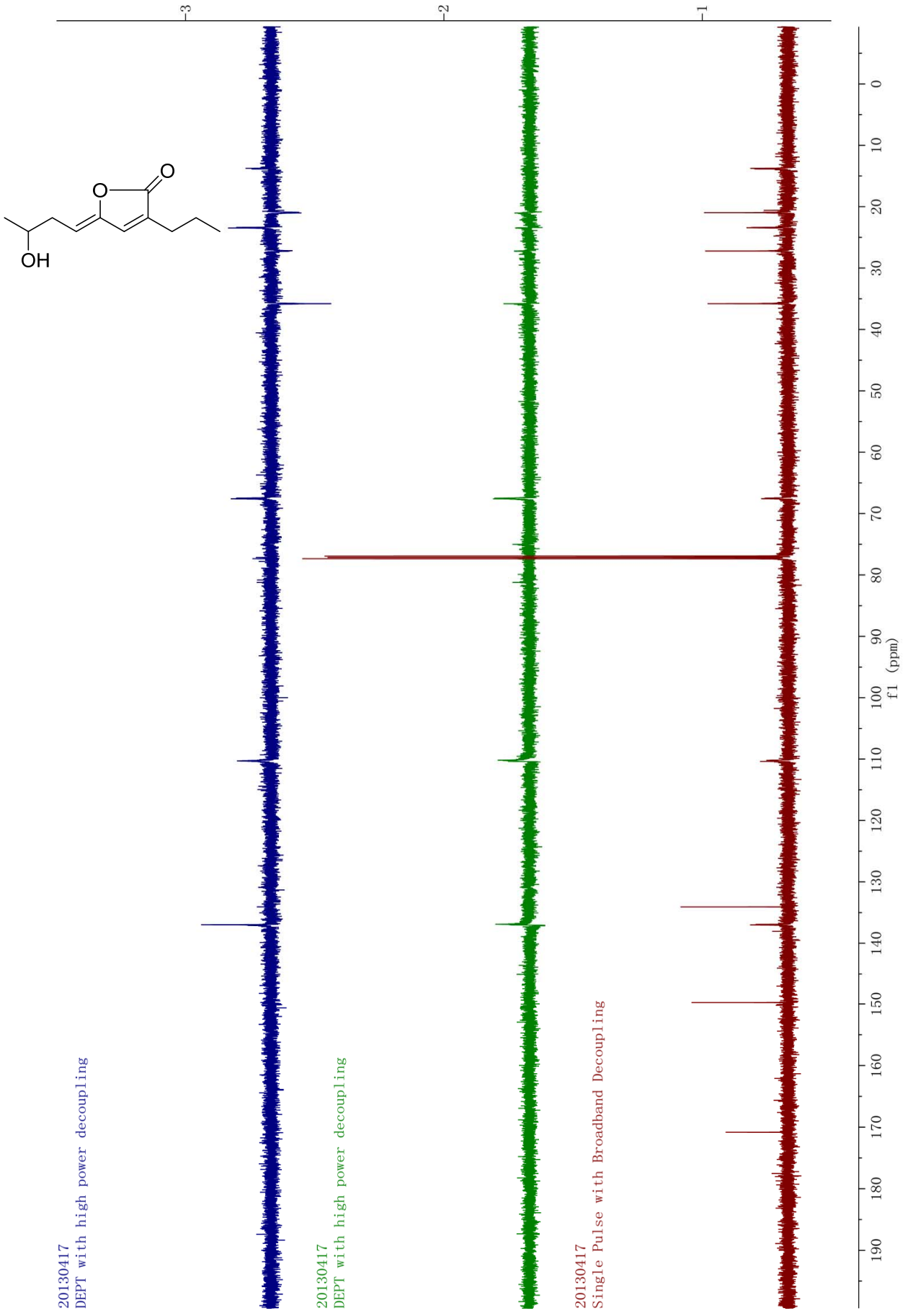

Figure S17. The HMQC spectrum of compounds **3** and **4** in $CDCl_3$

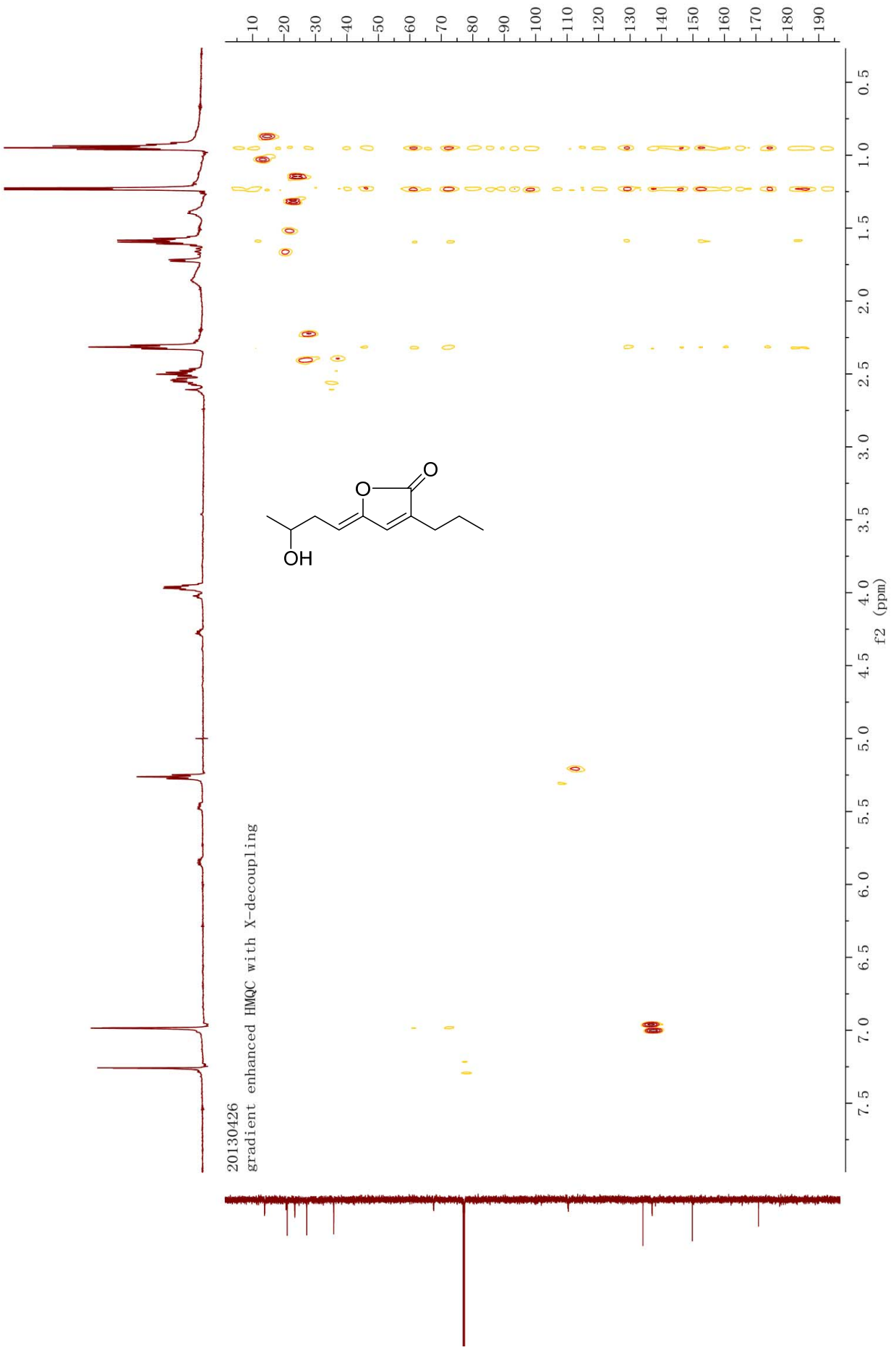

Figure S18. The ^{1}H-^{1}H COSY spectrum of compounds **3** and **4** in $CDCl_3$

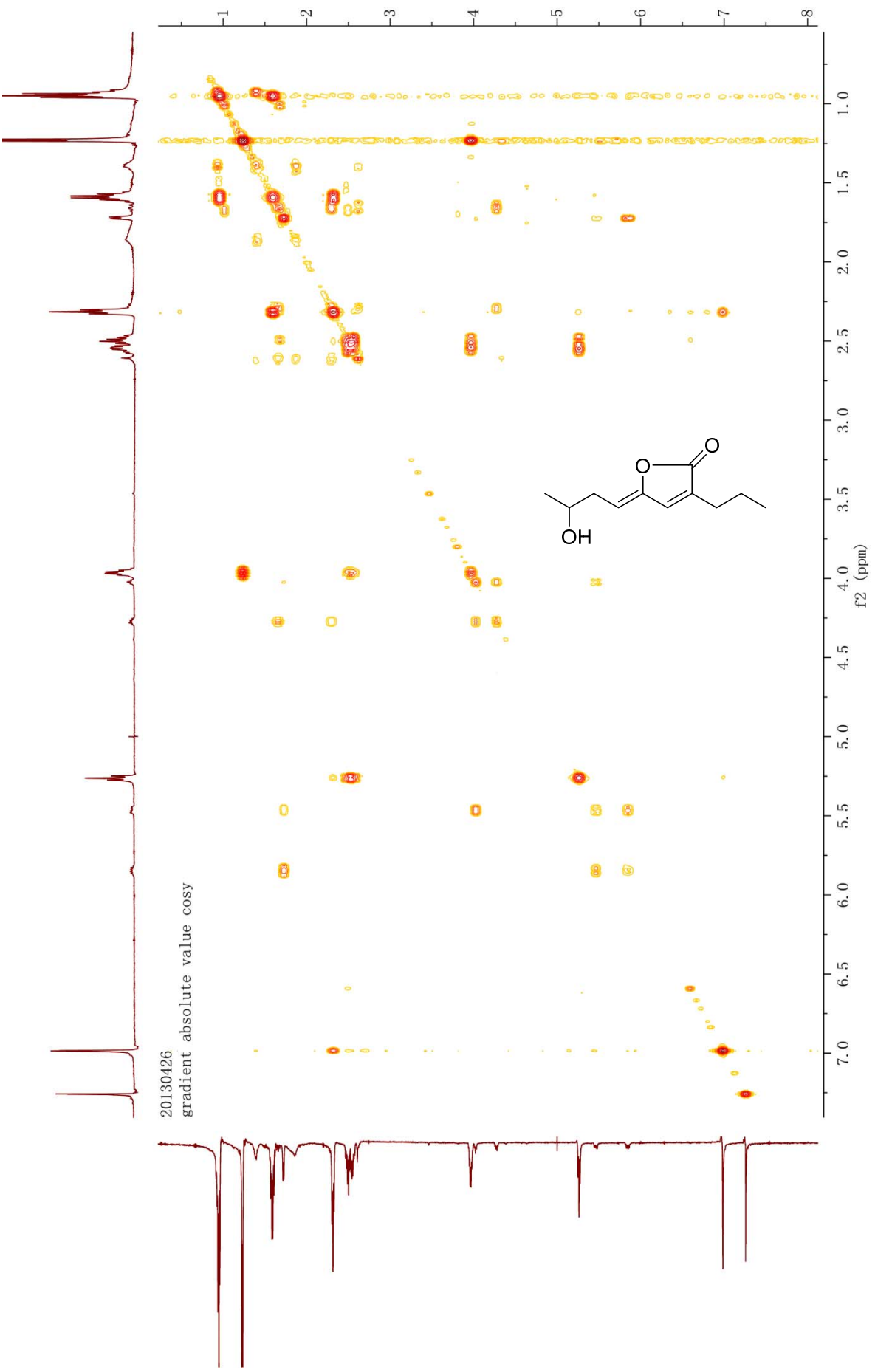

Figure S19. The HMBC spectrum of compounds **3** and **4** in $CDCl_3$

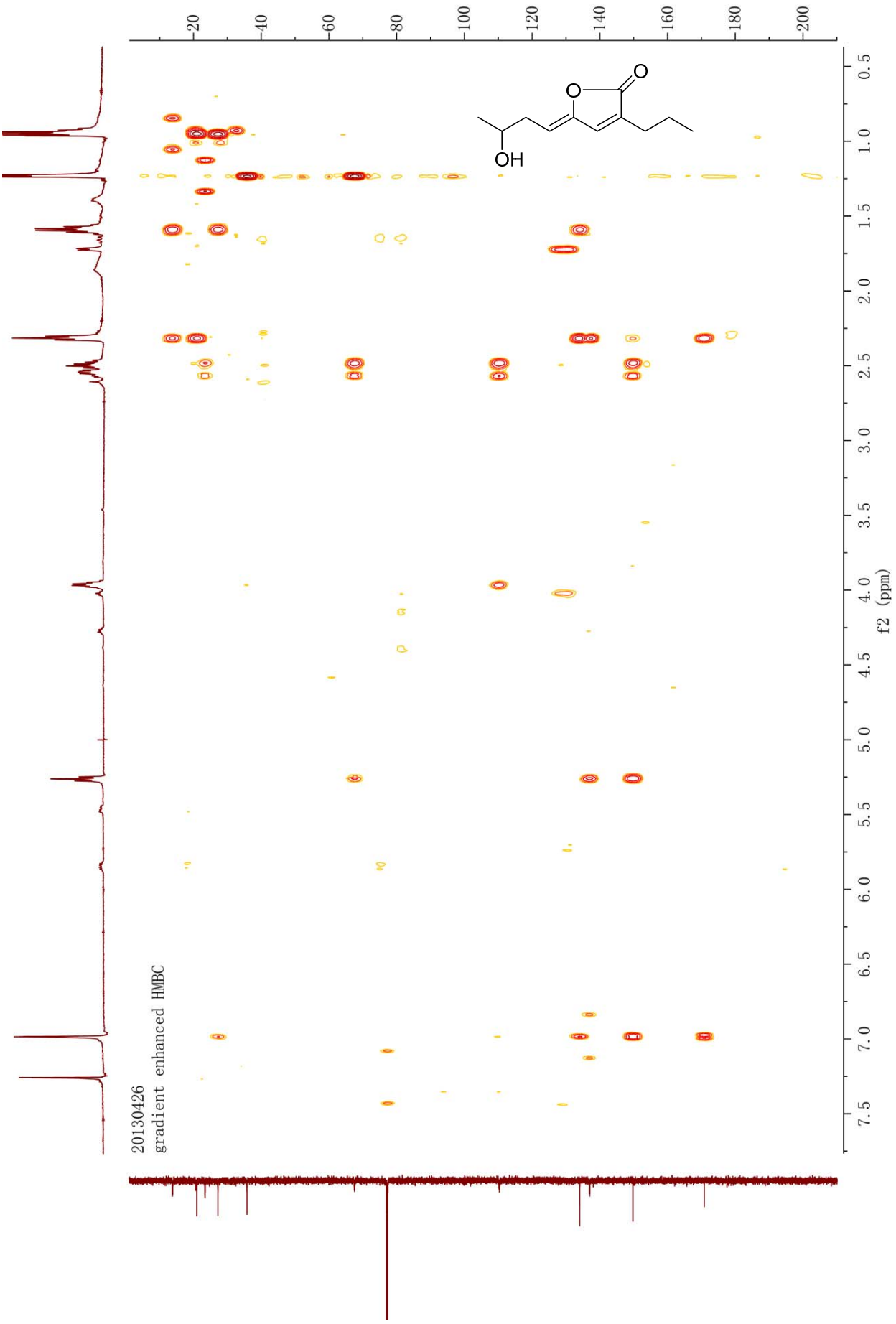

Figure S20. The NOE difference spectrum of compounds **3** and **4** in $CDCl_3$

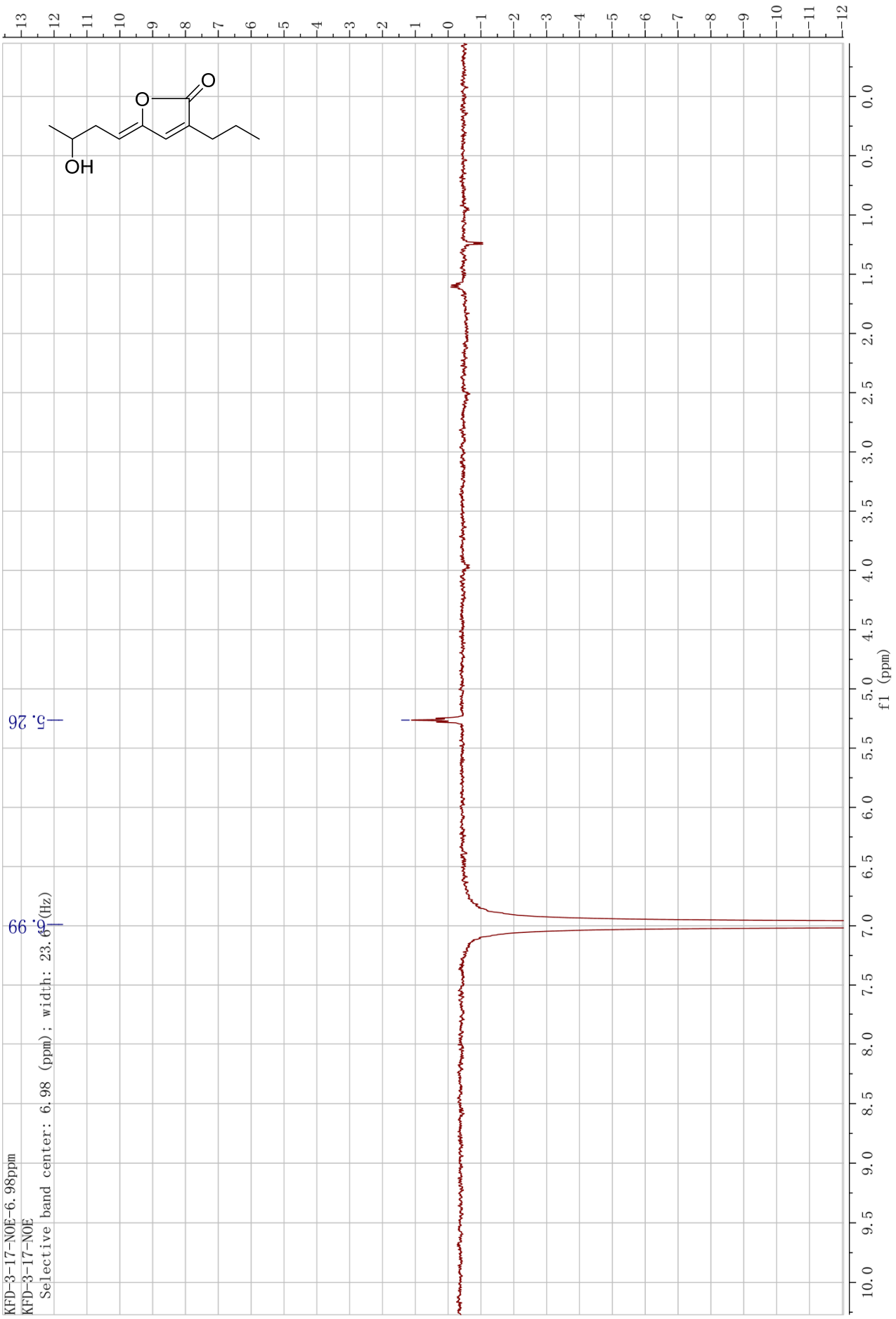

Figure S21. The ^{1}H-NMR spectrum of compound **5** in $CDCl_3$

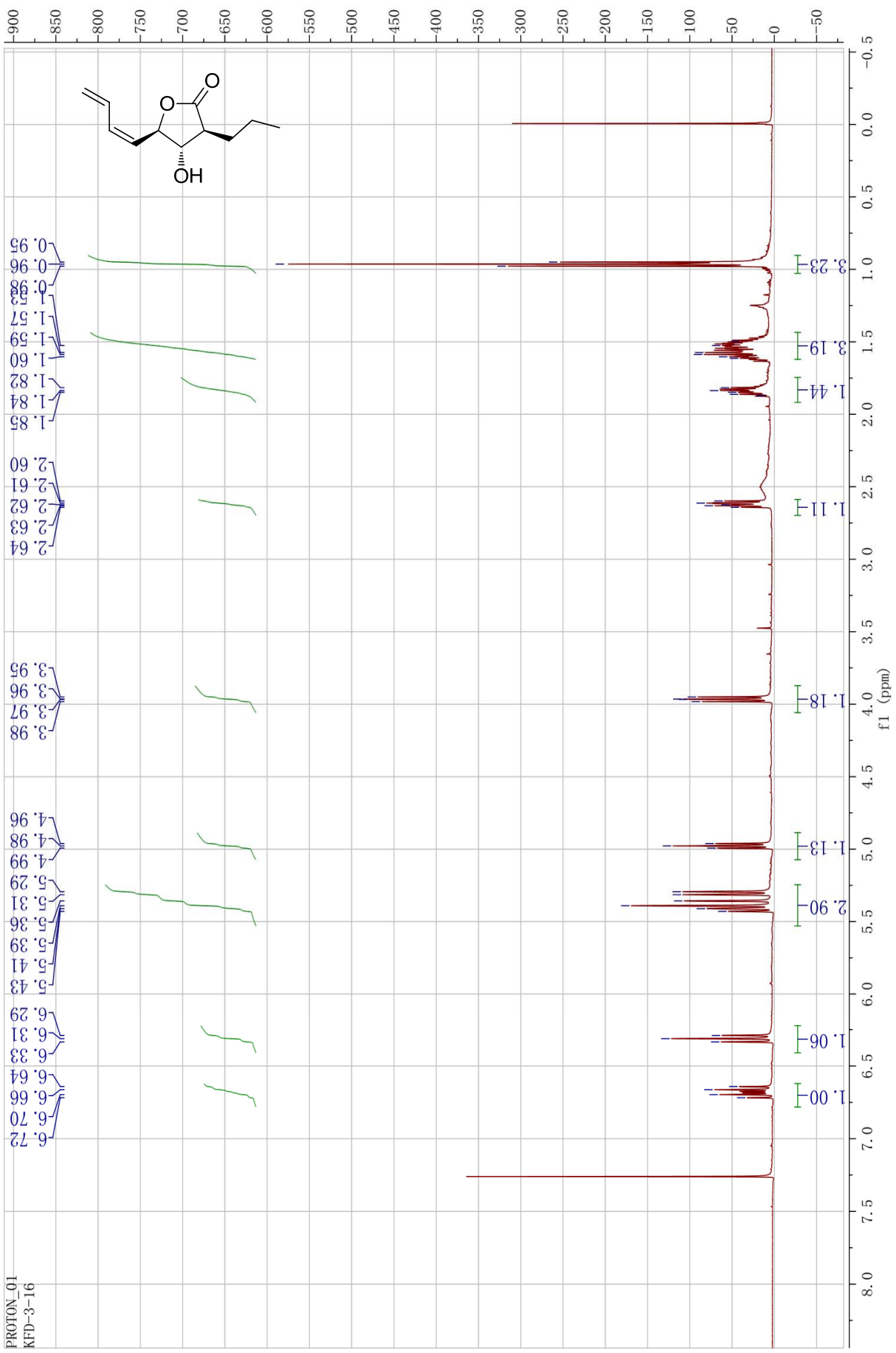

Figure S22. The ^{13}C-NMR spectrum of compound **5** in $CDCl_3$

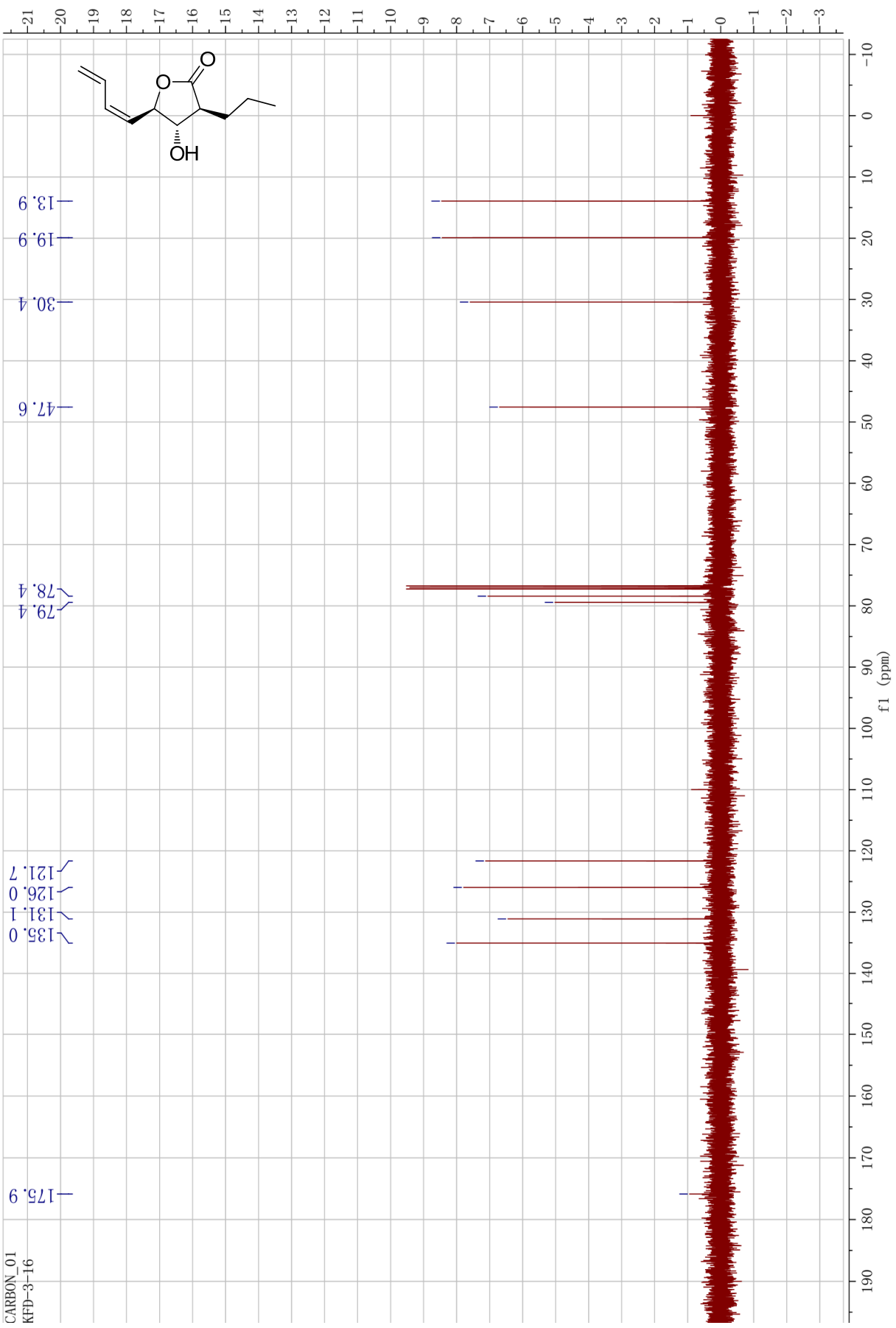

Figure S23. The DEPT spectrum of compound **5** in $CDCl_3$

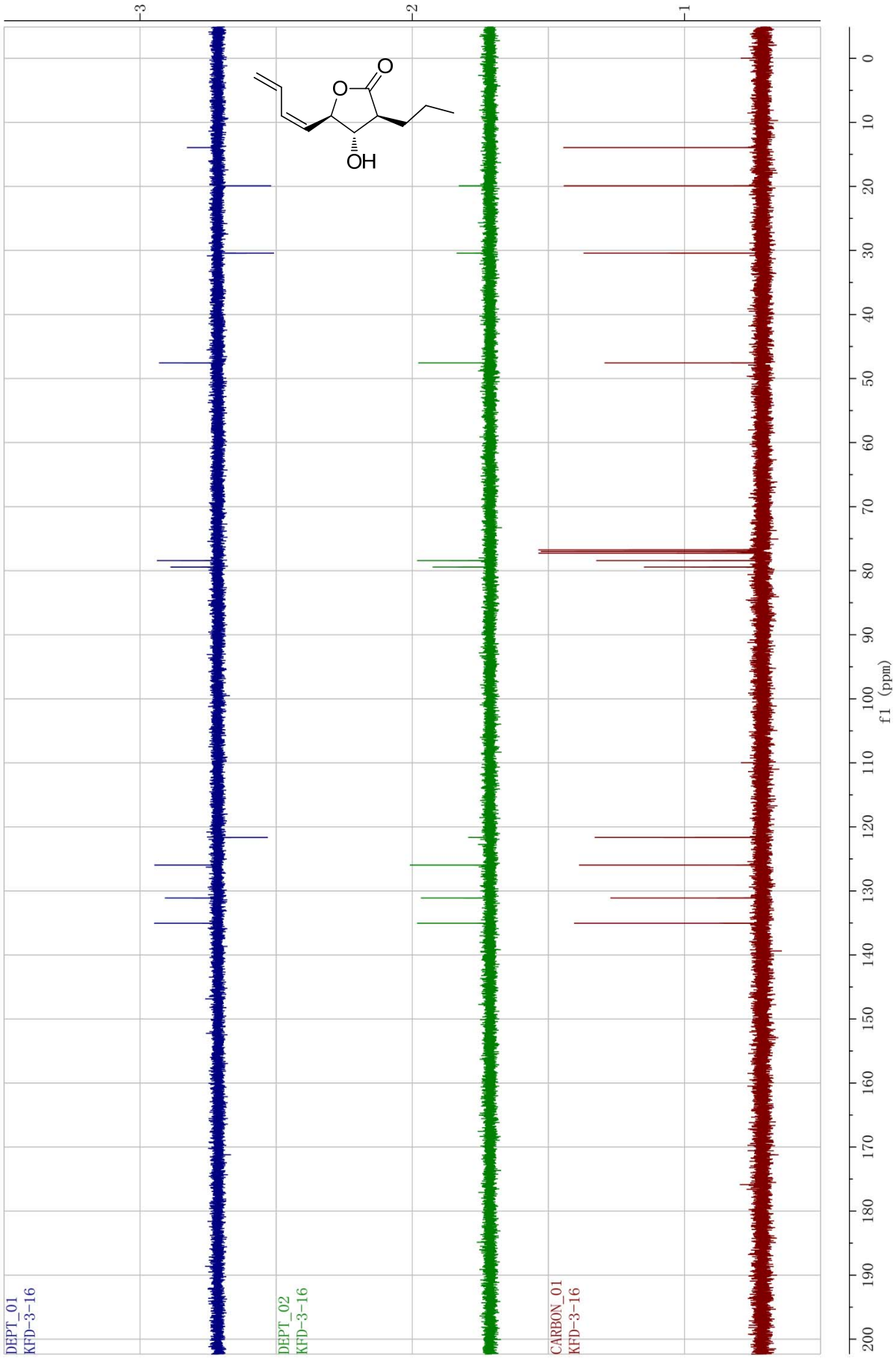

Figure S24. The HMQC spectrum of compound **5** in $CDCl_3$

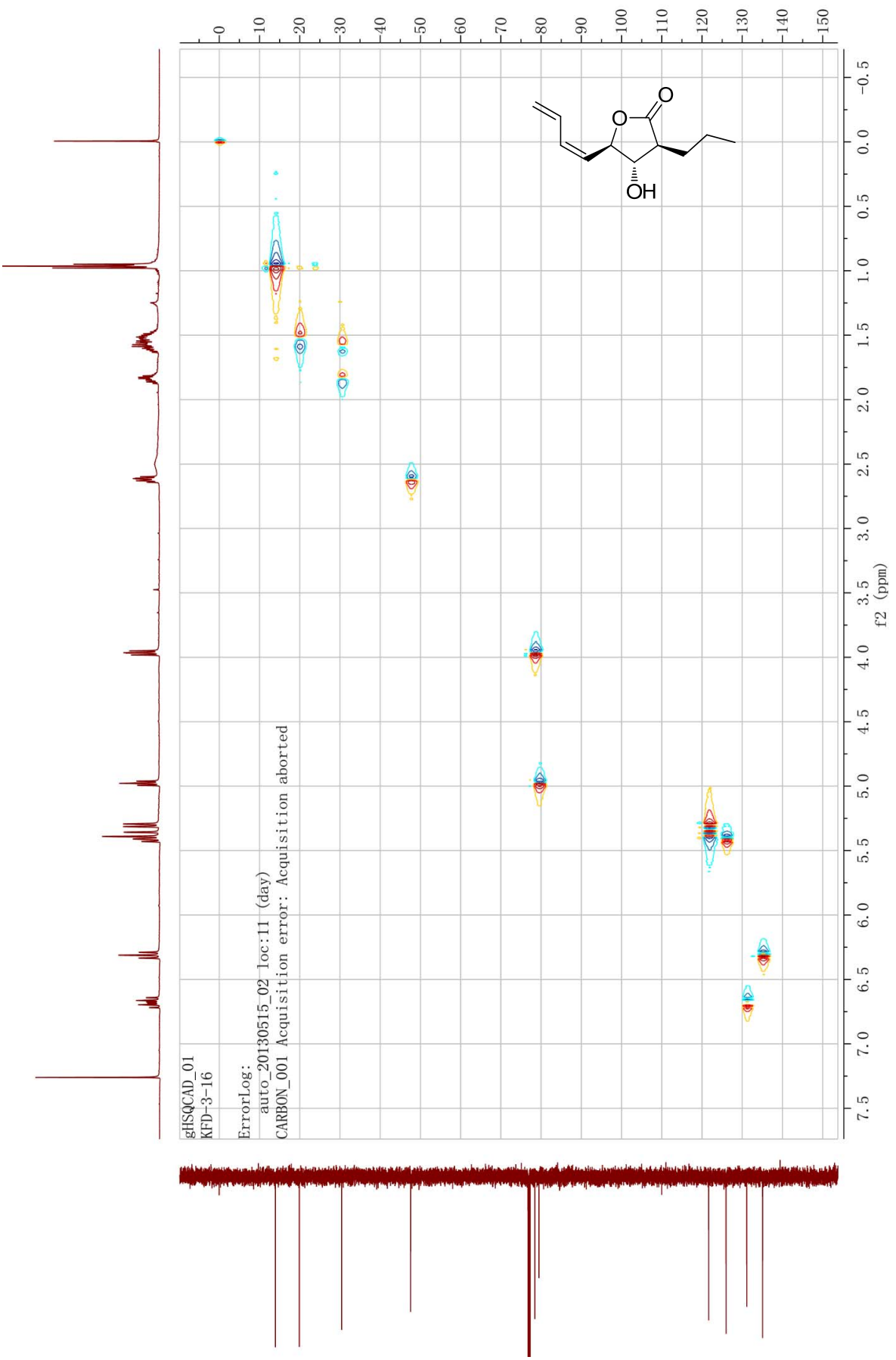

Figure S25. The ^{1}H-^{1}H COSY spectrum of compound **5** in $CDCl_3$

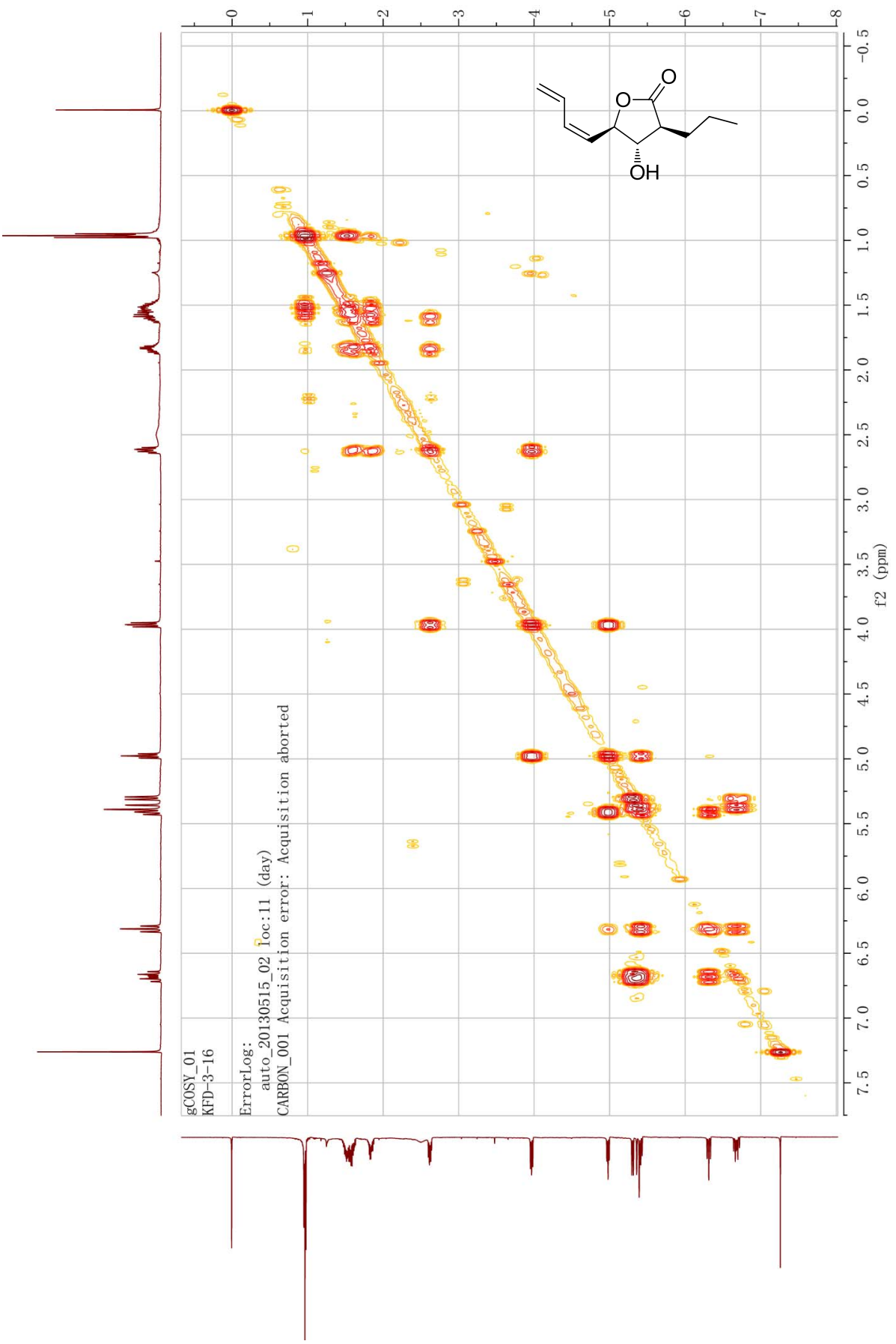

Figure S26. The HMBC spectrum of compound **5** in $CDCl_3$

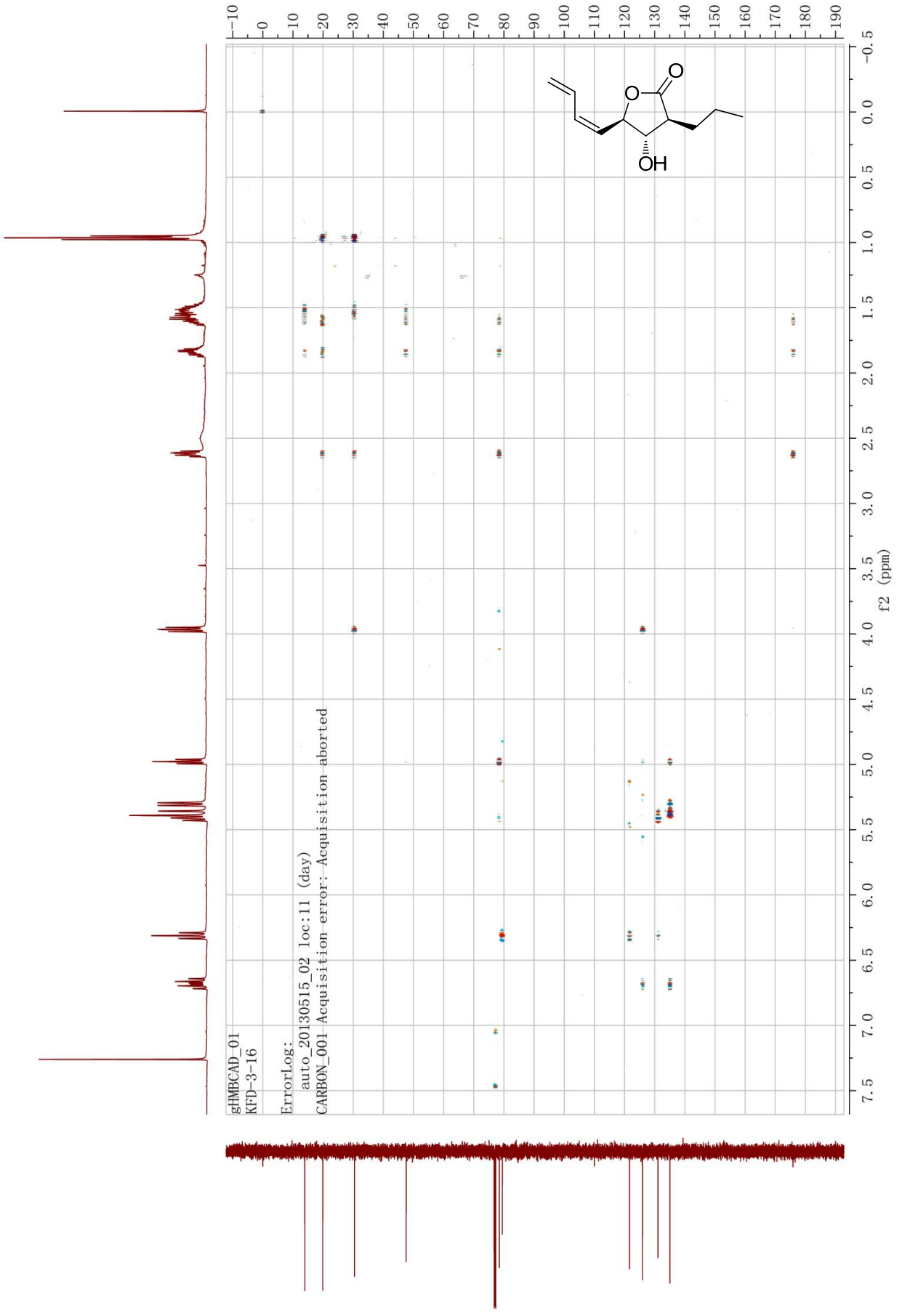

Figure S27. The NOE difference spectrum of compound **5** in $CDCl_3$ (I)

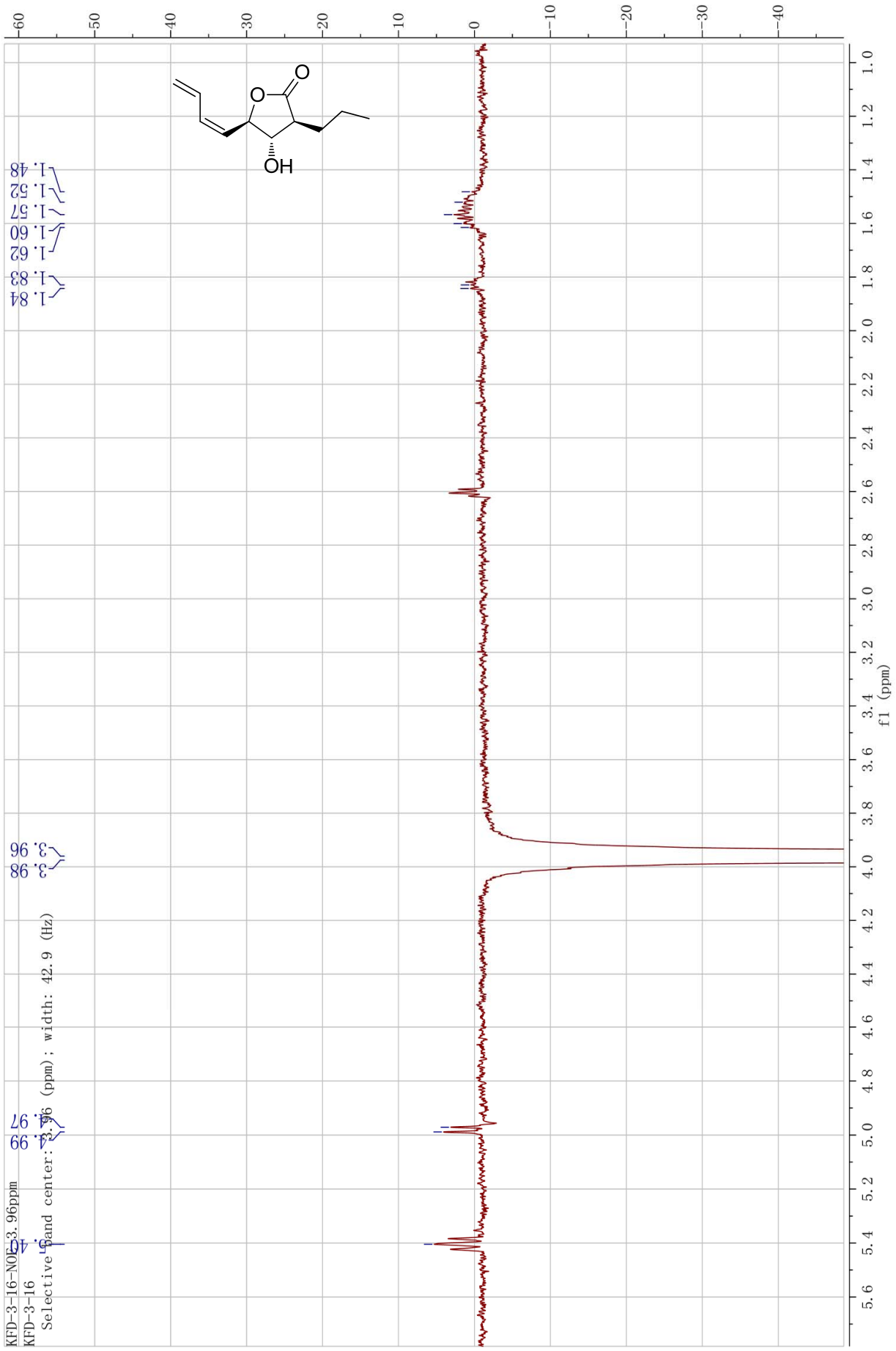

Figure S28. The NOE difference spectrum of compound **5** in $CDCl_3$ (II)

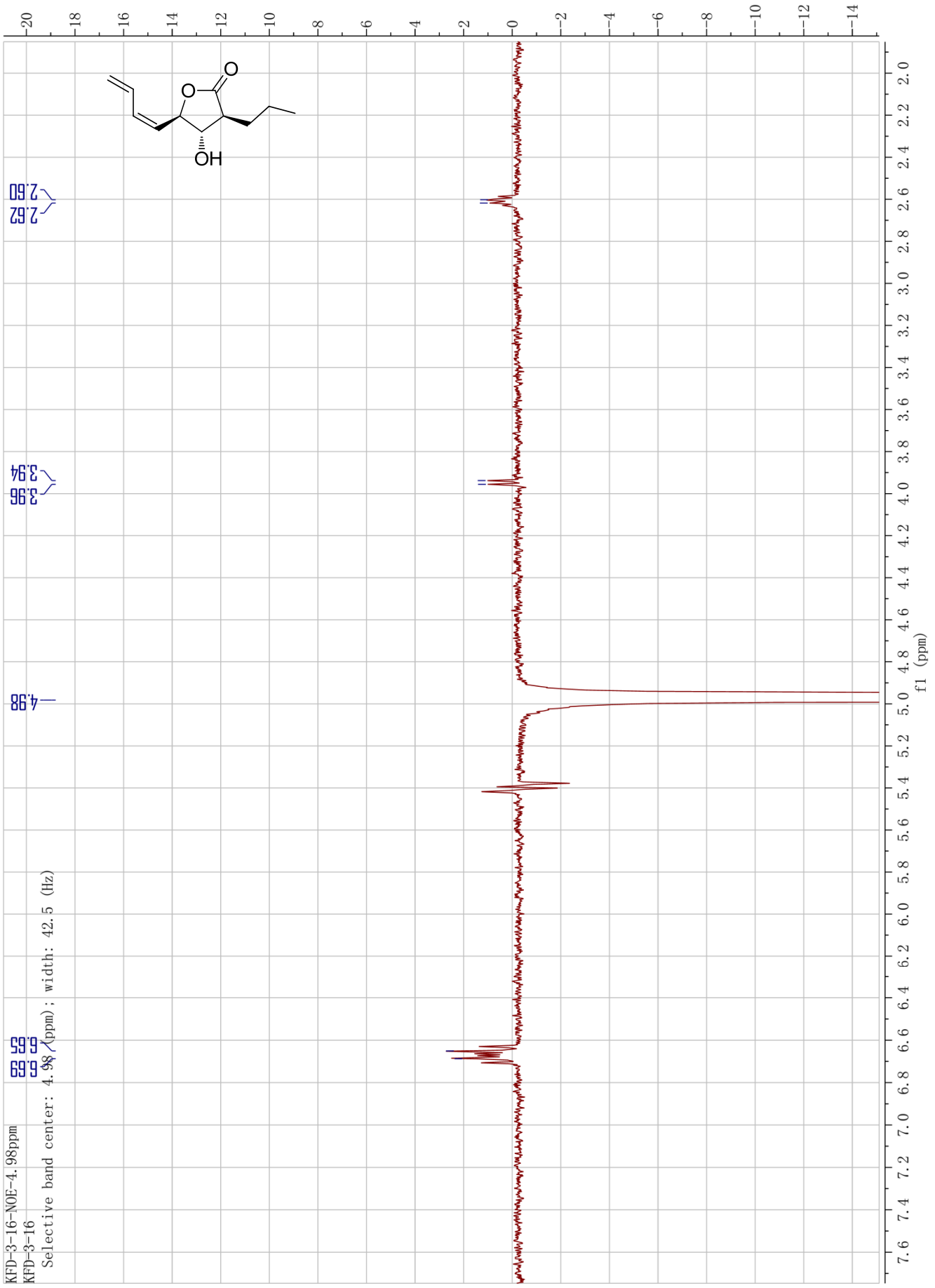

Figure S29. The ^{1}H-NMR spectrum of compound **6** in DMSO-d_6

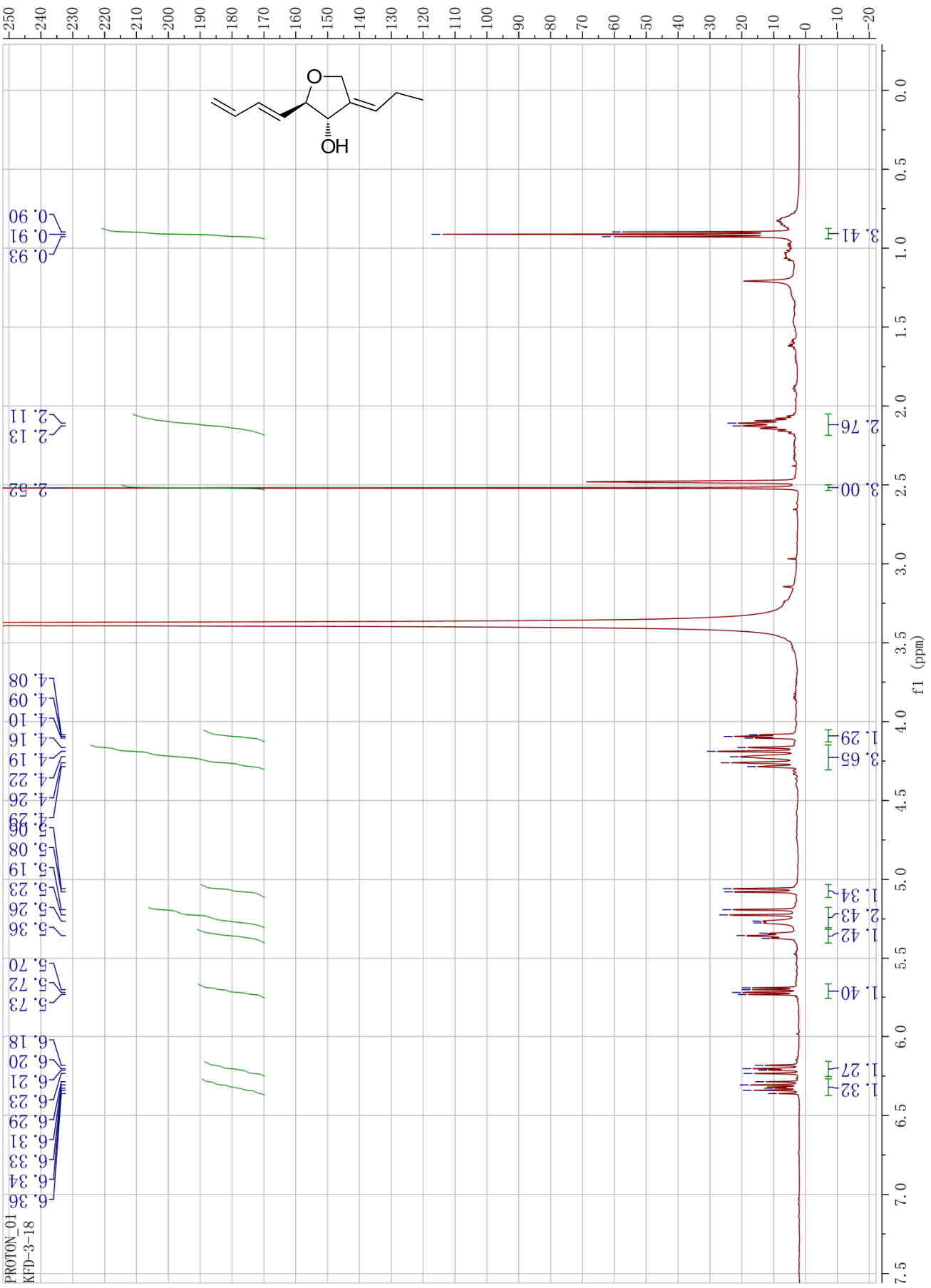

Figure S30. The ^{13}C-NMR spectrum of compound **6** in DMSO-d_6

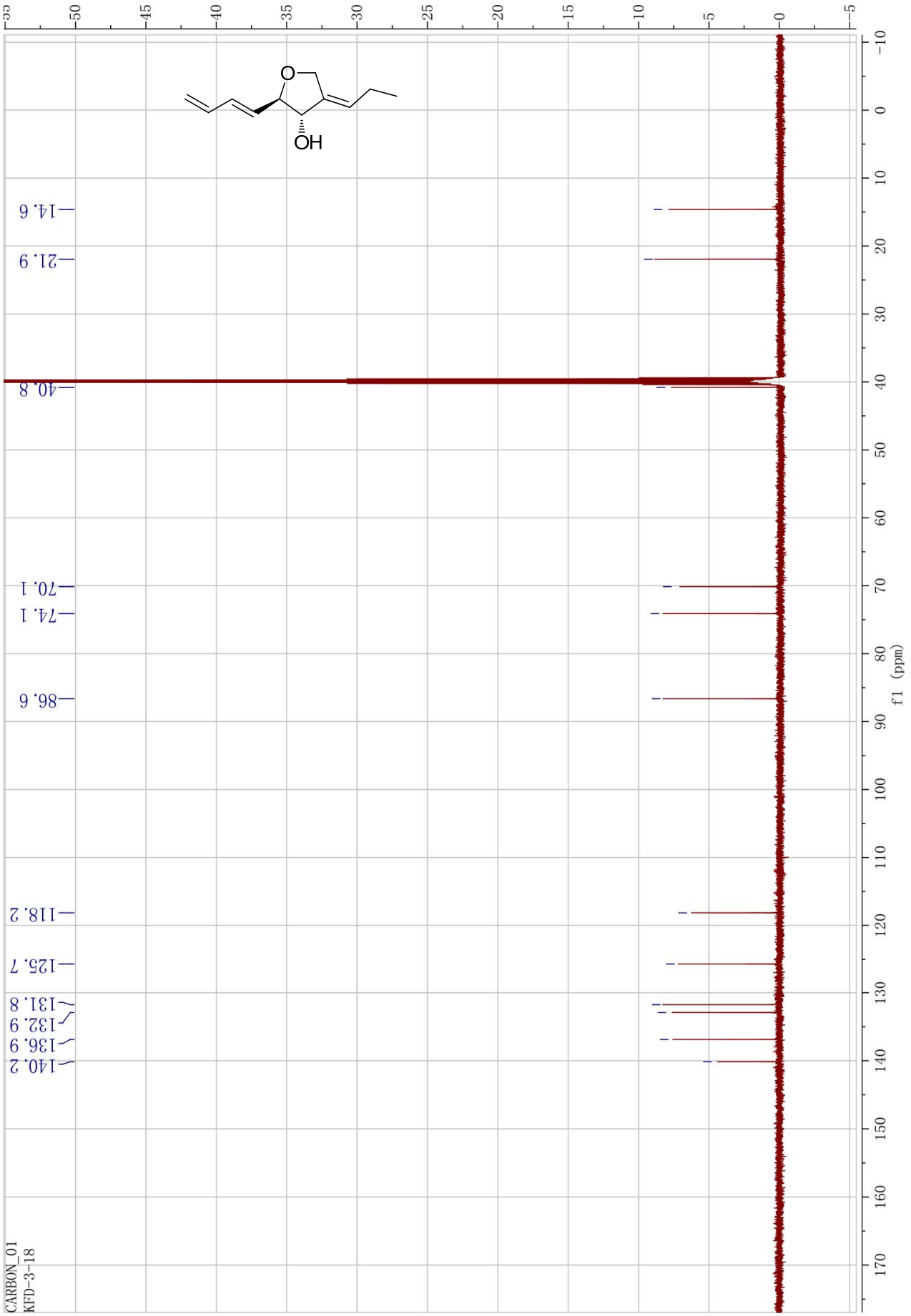

Figure S31. The DEPT spectrum of compound **6** in DMSO-d_6

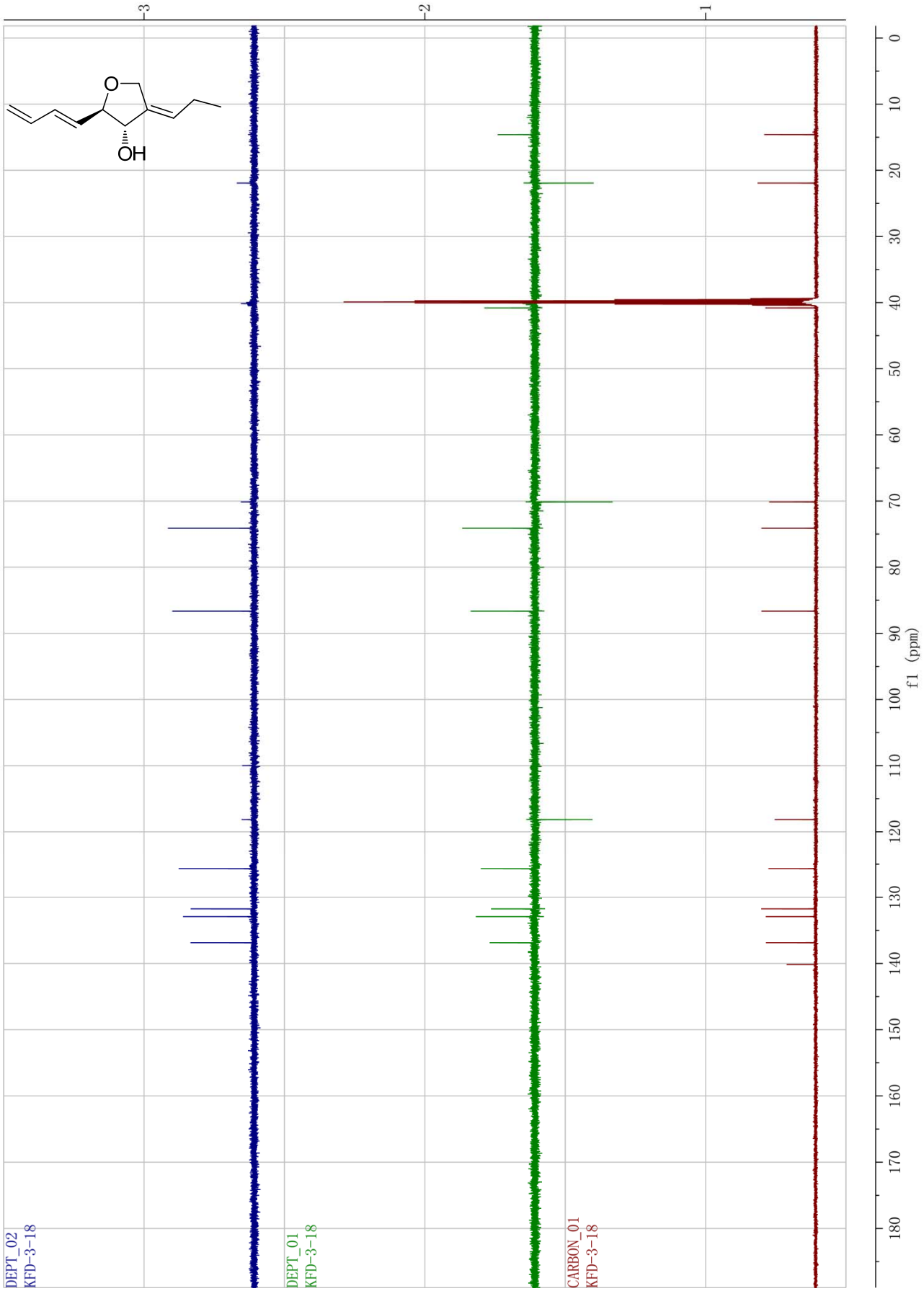

Figure S32. The HMQC spectrum of compound **6** in DMSO-d_6

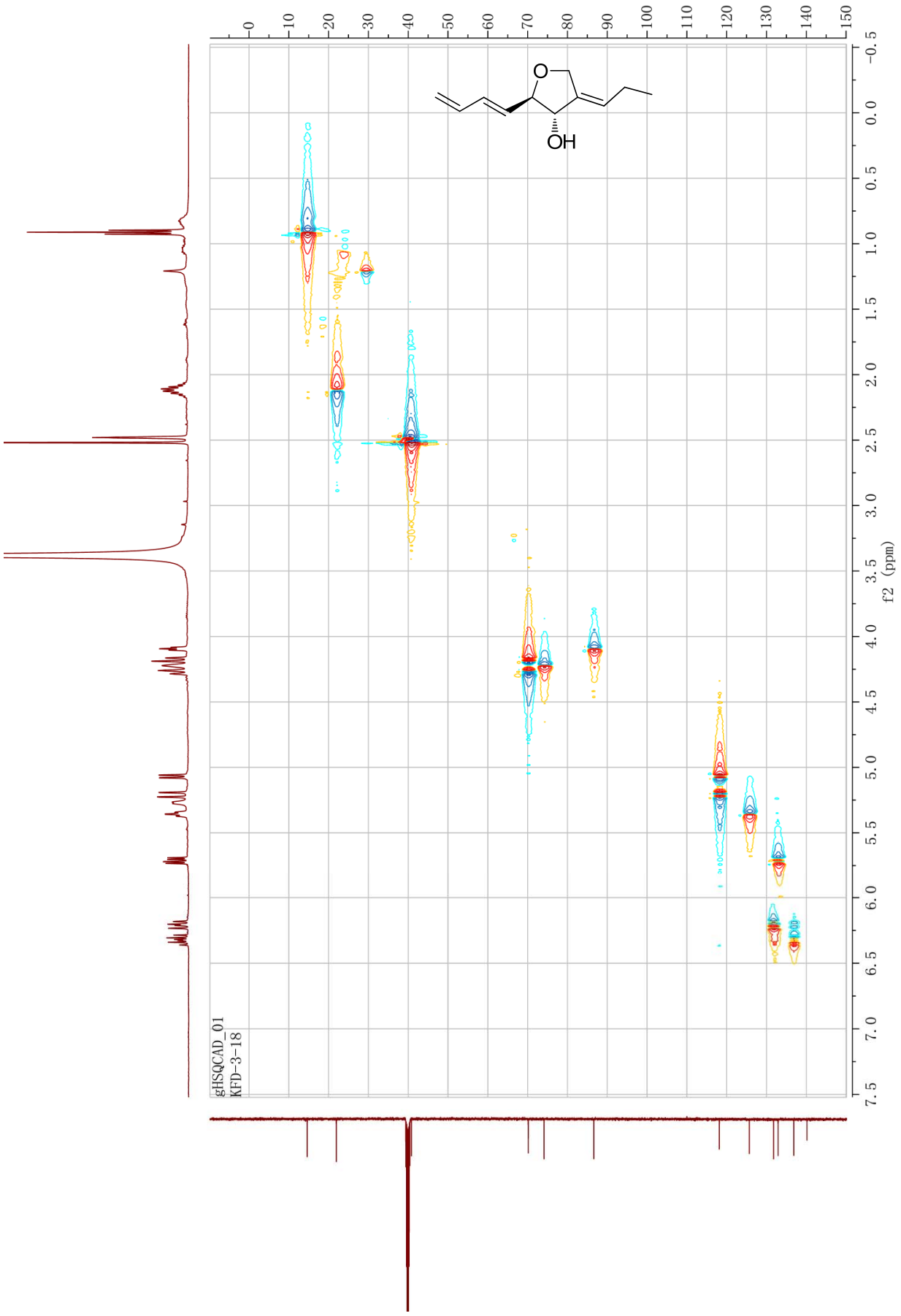

Figure S33. The ^{1}H-^{1}H COSY spectrum of compound **6** in DMSO-d_6

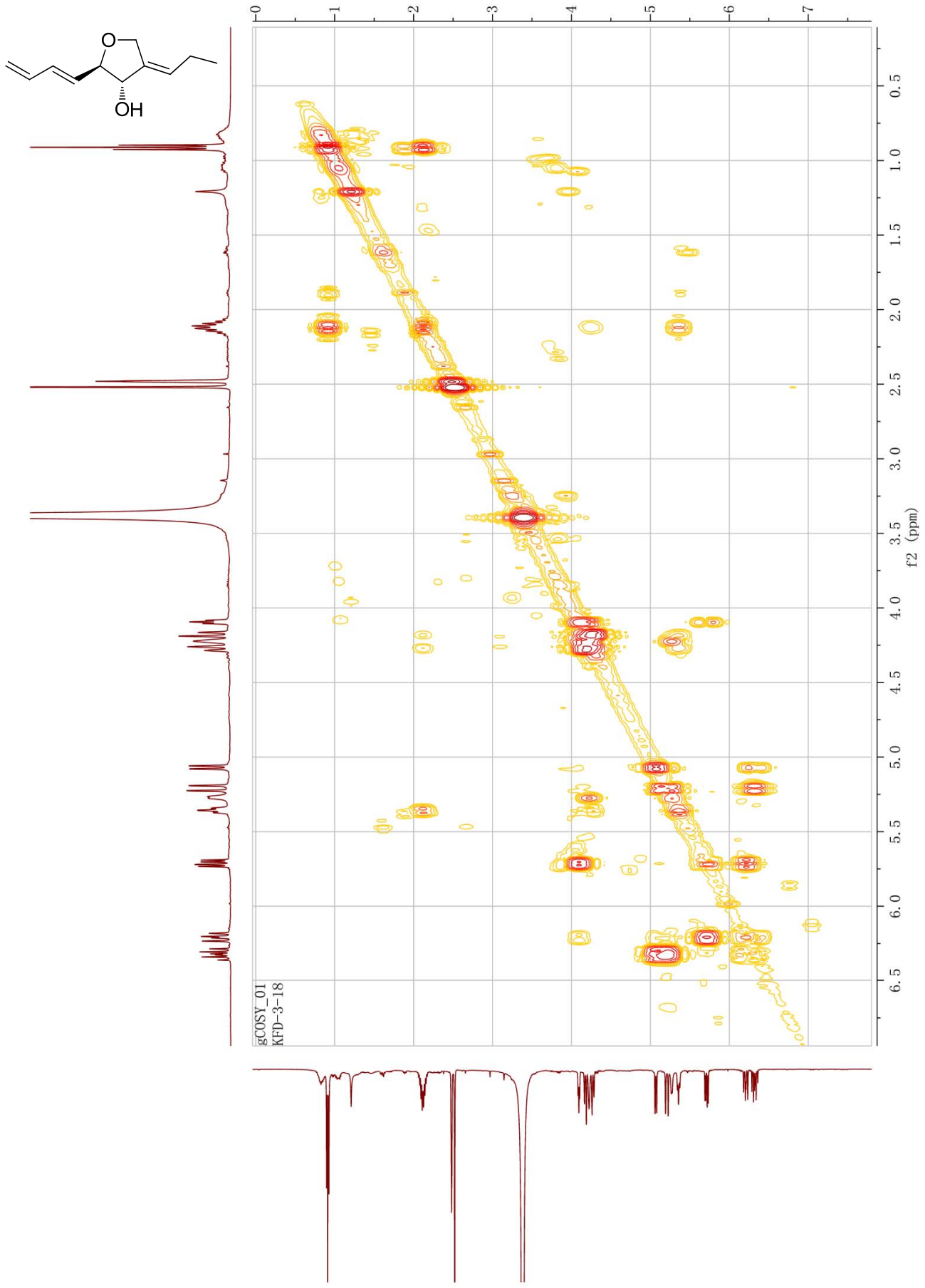

Figure S34. The HMBC spectrum of compound **6** in DMSO-d_6

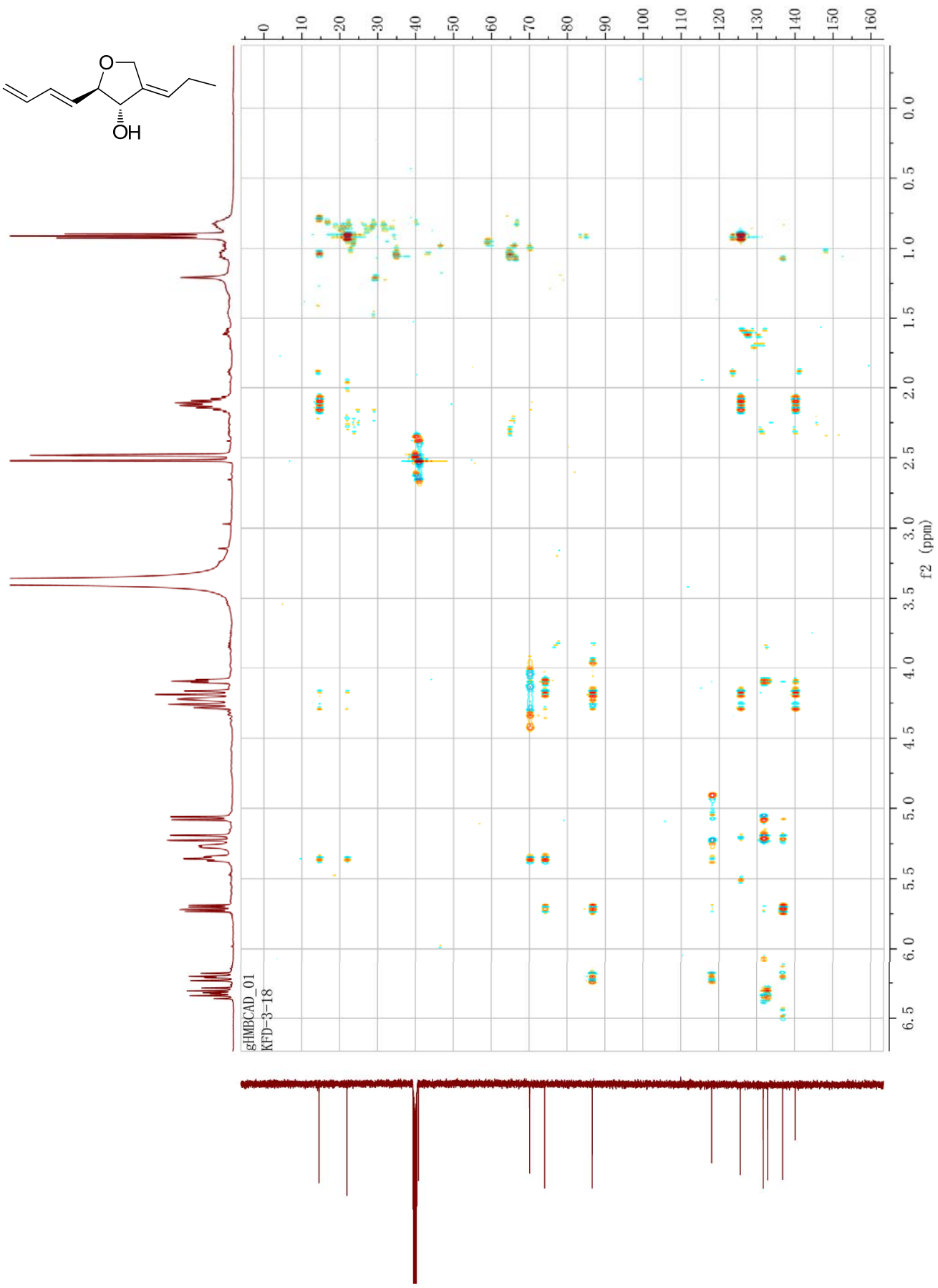

Figure S35. The NOE difference spectrum of compound **6** in DMSO-d_6 (I)

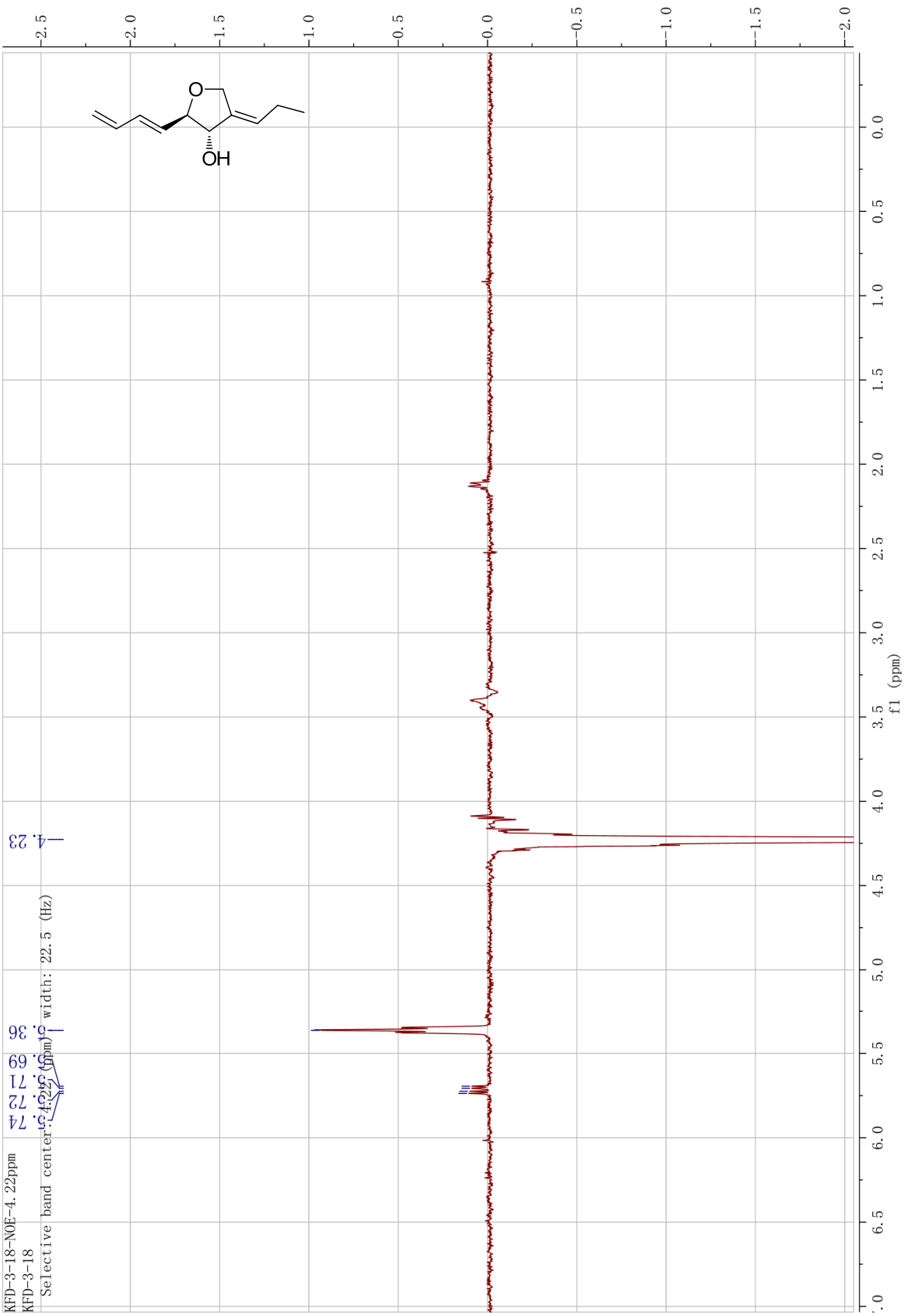

Figure S36. The NOESY difference spectrum of compound **6** in DMSO-d_6 (II)

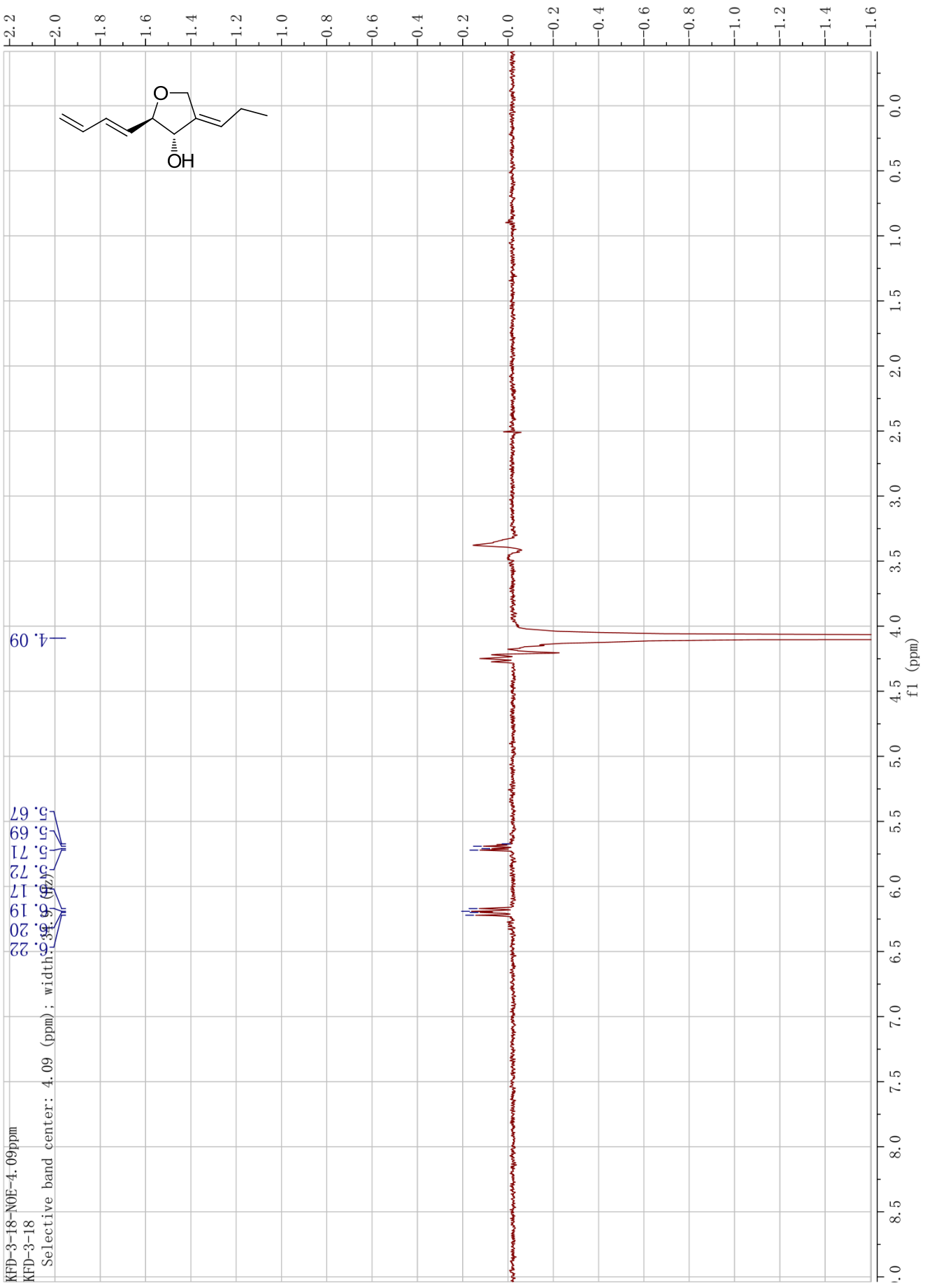

Figure S37. The ^{1}H-NMR spectrum of compounds **7** and **8** in $CDCl_3$

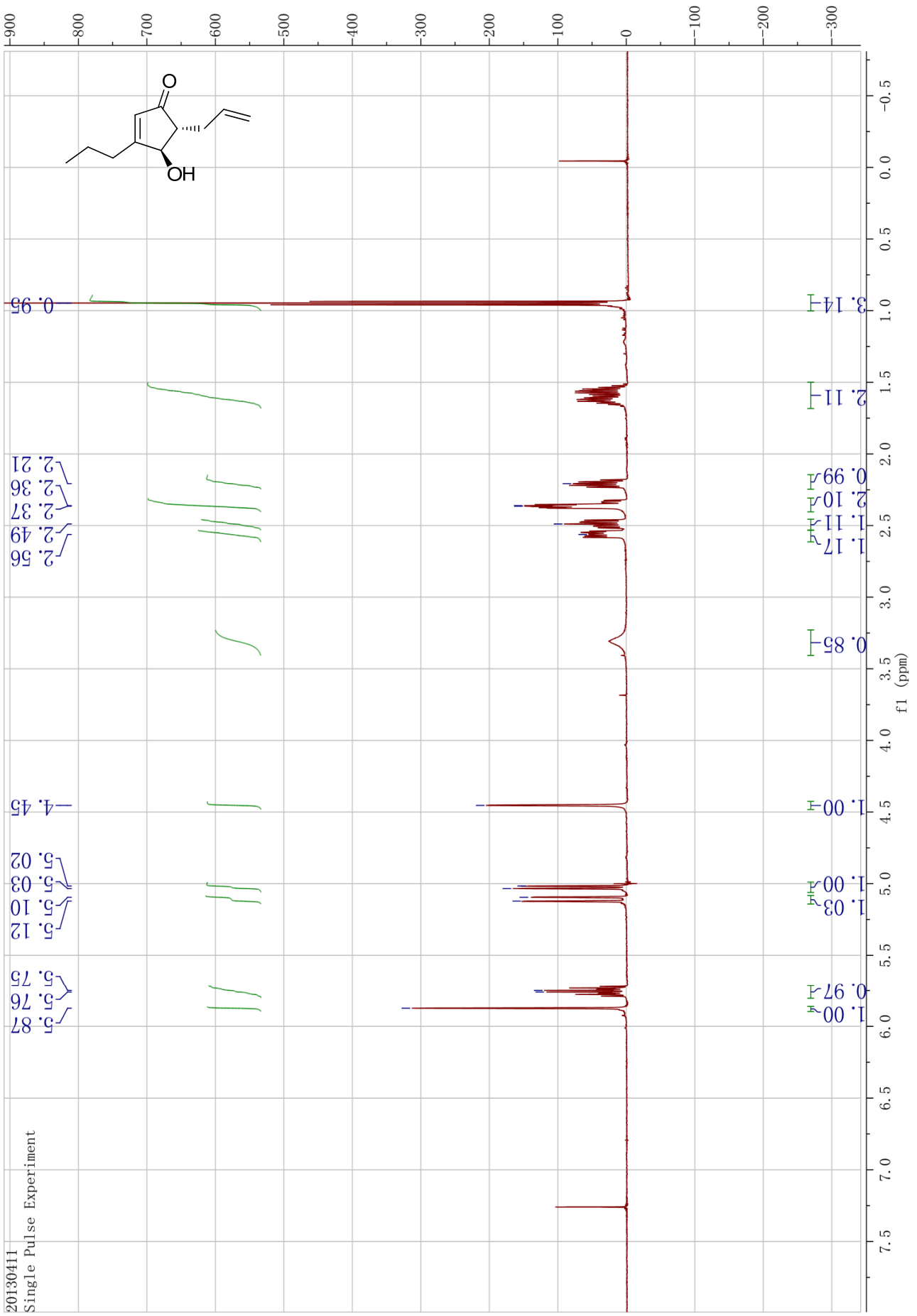

Figure S38. The ^{13}C-NMR spectrum of compounds **7** and **8** in $CDCl_3$

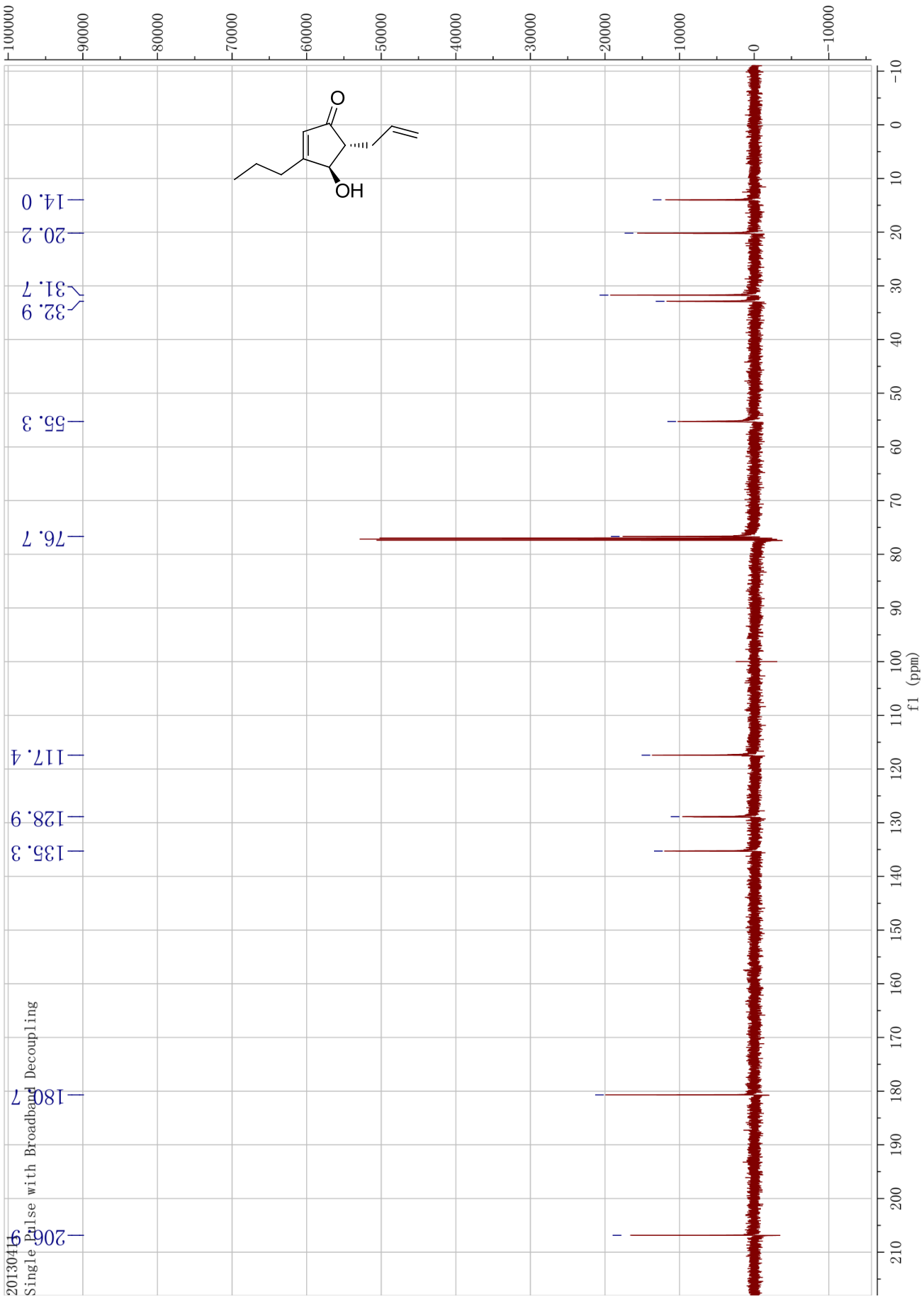

Figure S39. The DEPT spectrum of compounds **7** and **8** in $CDCl_3$

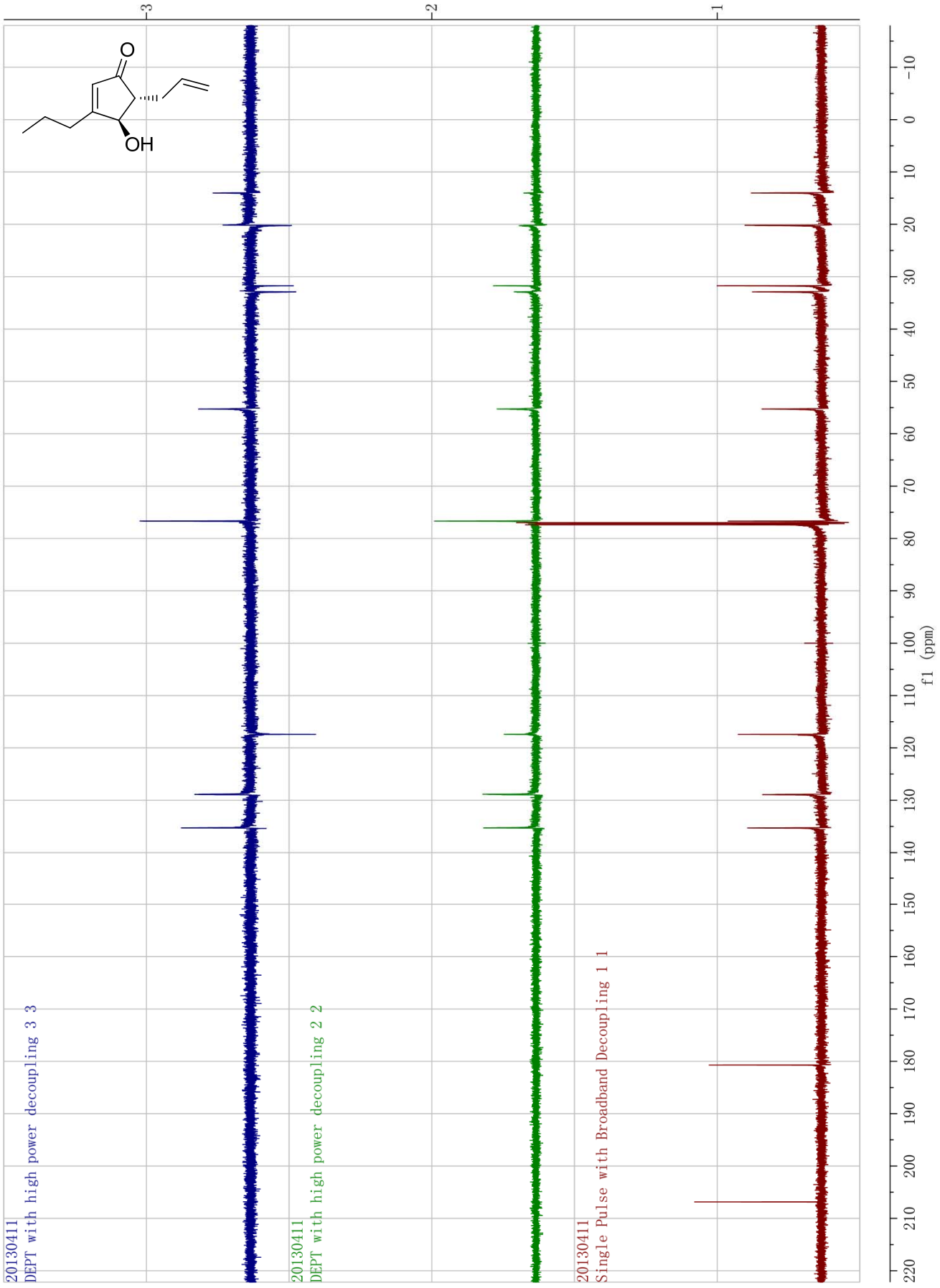

Figure S40. The HMQC spectrum of compounds **7** and **8** in $CDCl_3$

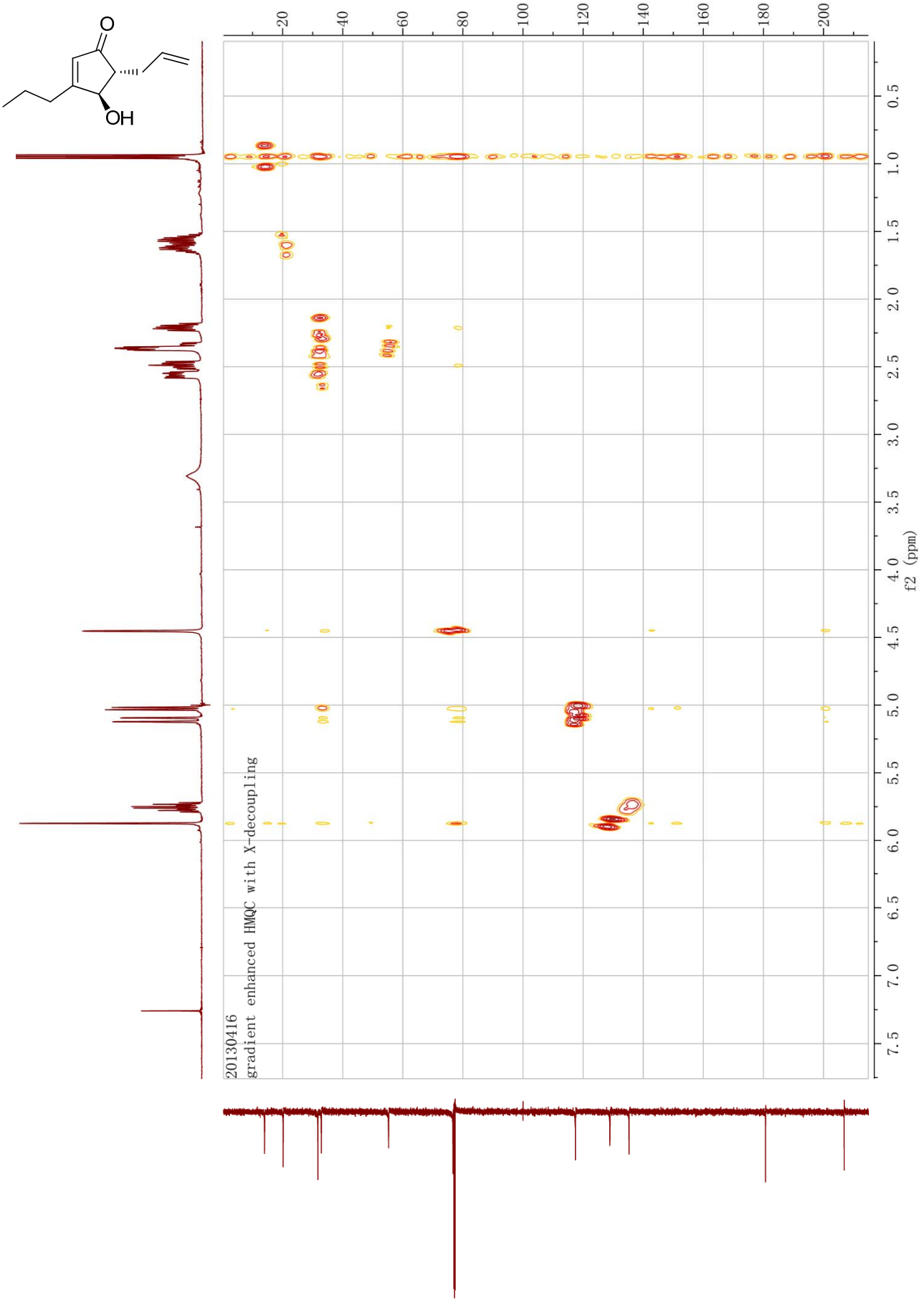

Figure S41. The ^{1}H-^{1}H COSY spectrum of compounds **7** and **8** in $CDCl_3$

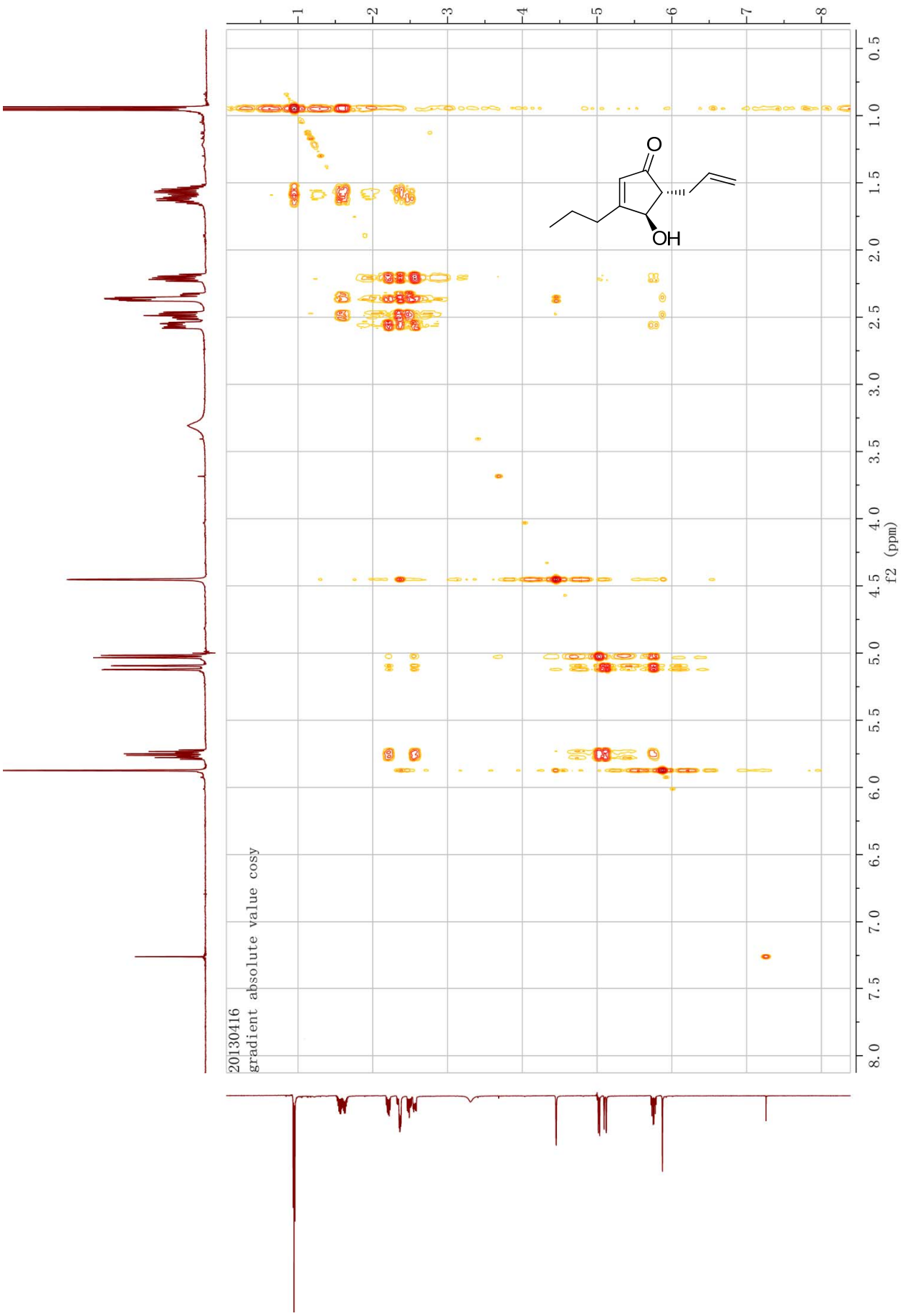

Figure S42. The HMBC spectrum of compounds **7** and **8** in $CDCl_3$

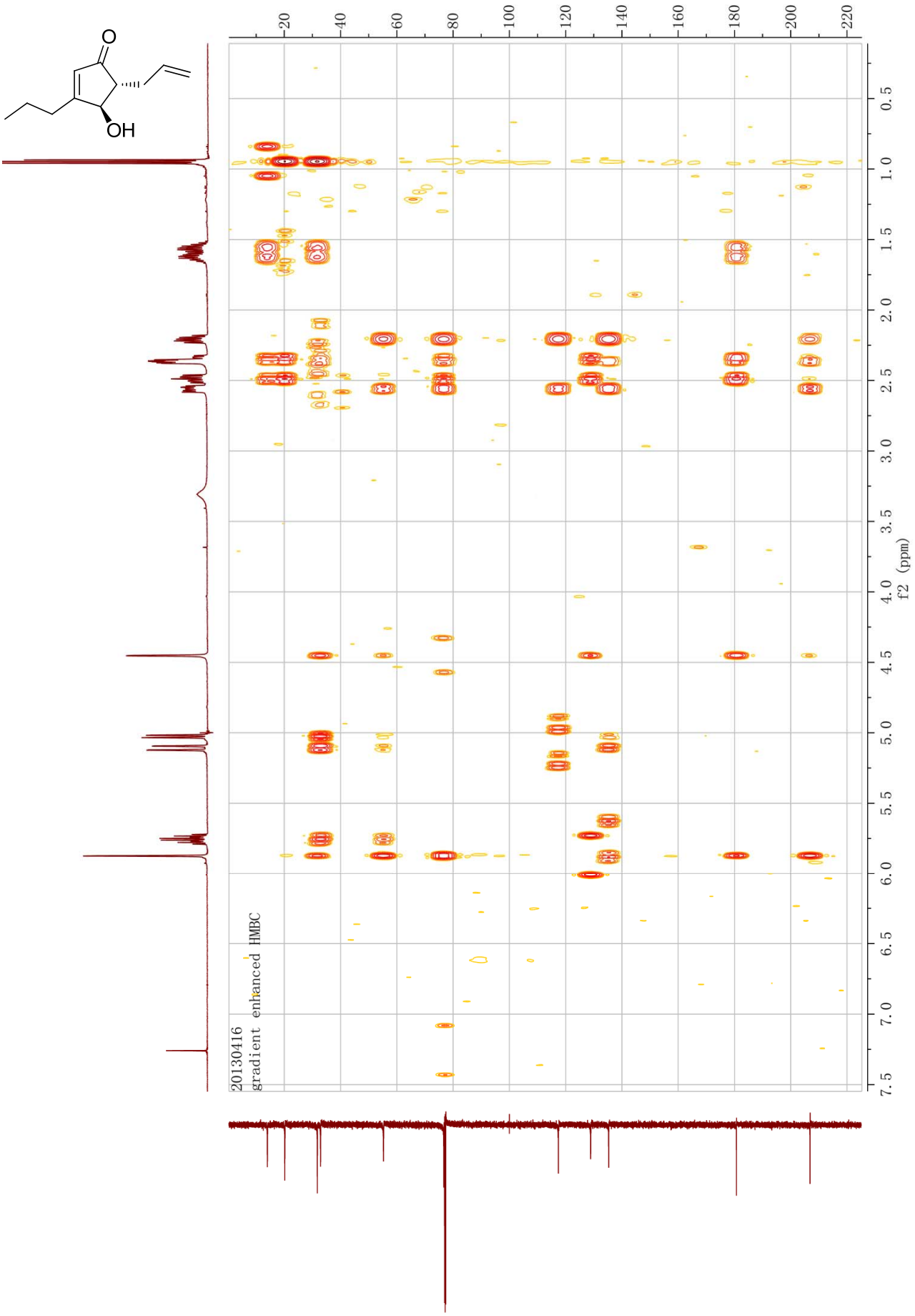

Figure S43. The NOE difference spectrum of compounds **7** and **8** in $CDCl_3$

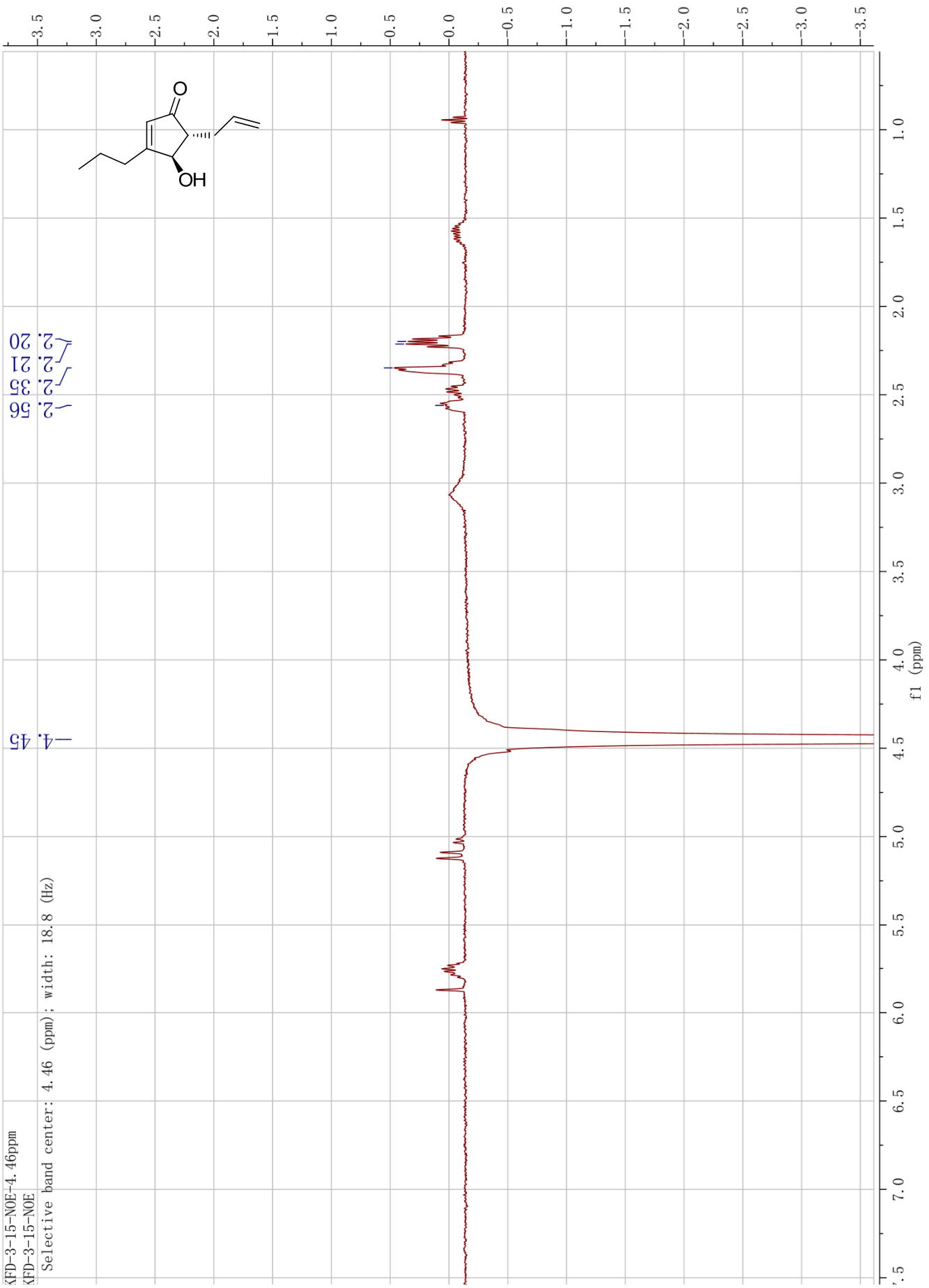

Figure S44. The ^{1}H-NMR spectrum of compound **9** in $CDCl_3$

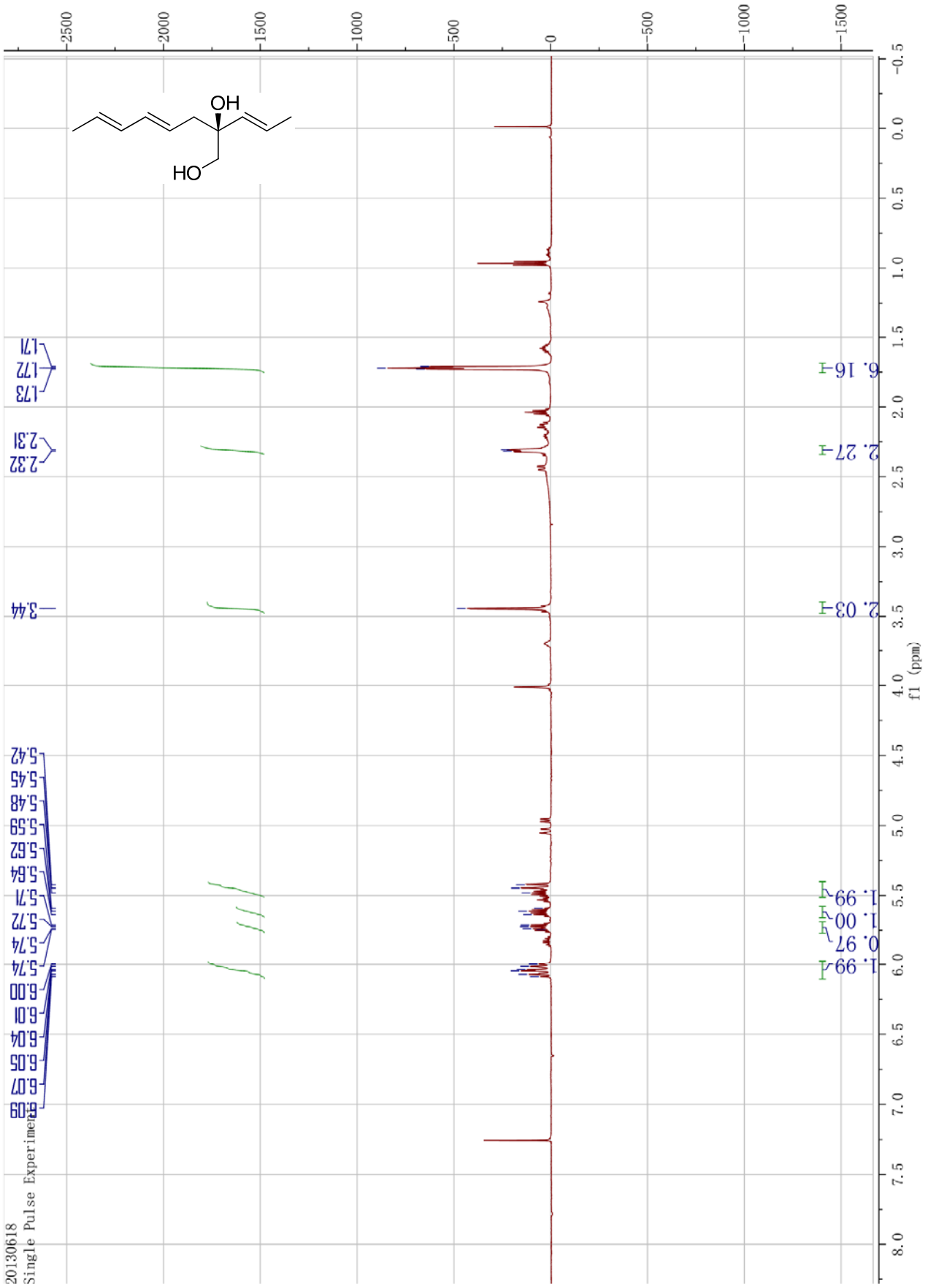

Figure S45. The ^{13}C-NMR spectrum of compound **9** in $CDCl_3$

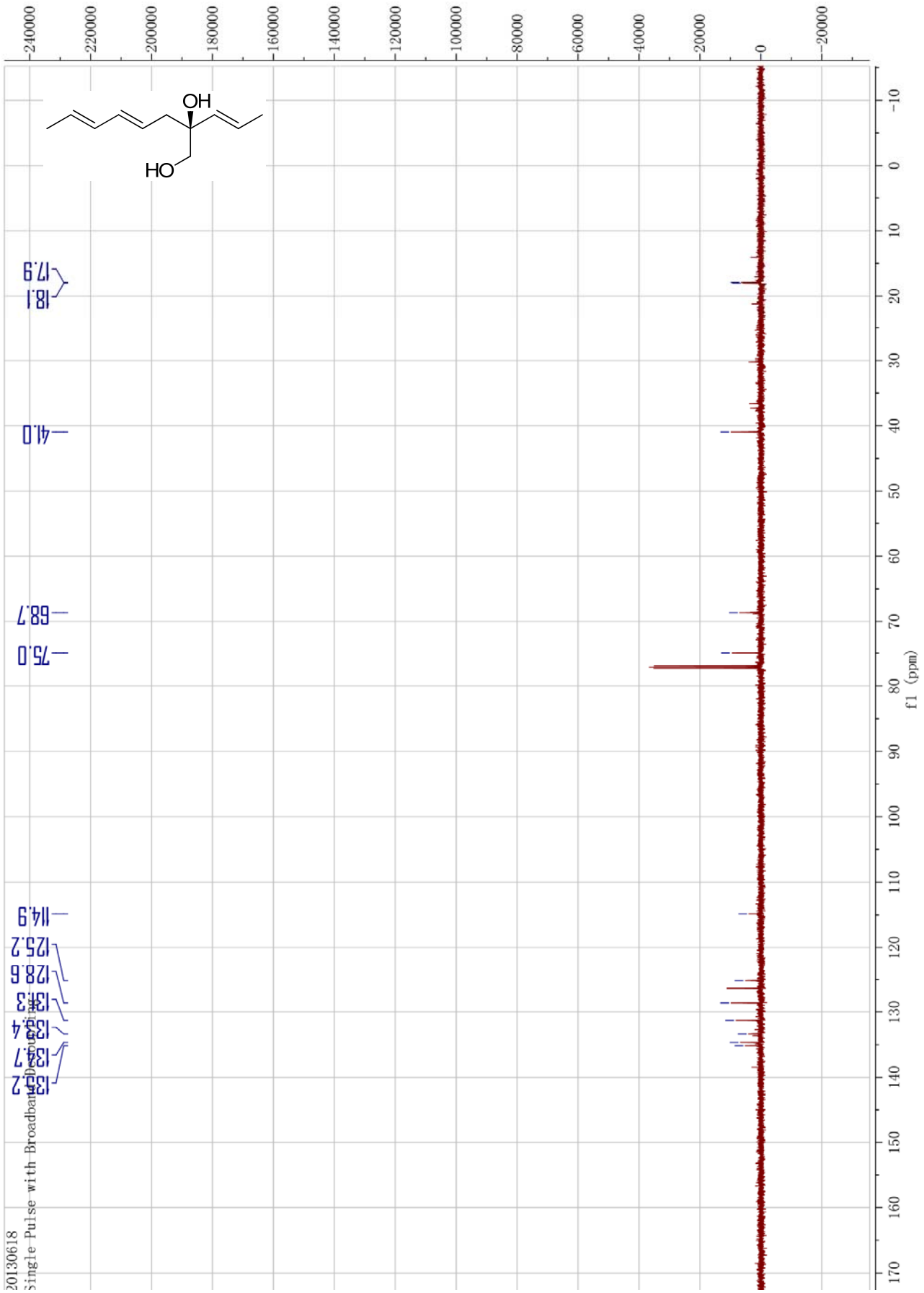

Figure S46. The DEPT spectrum of compound **9** in $CDCl_3$

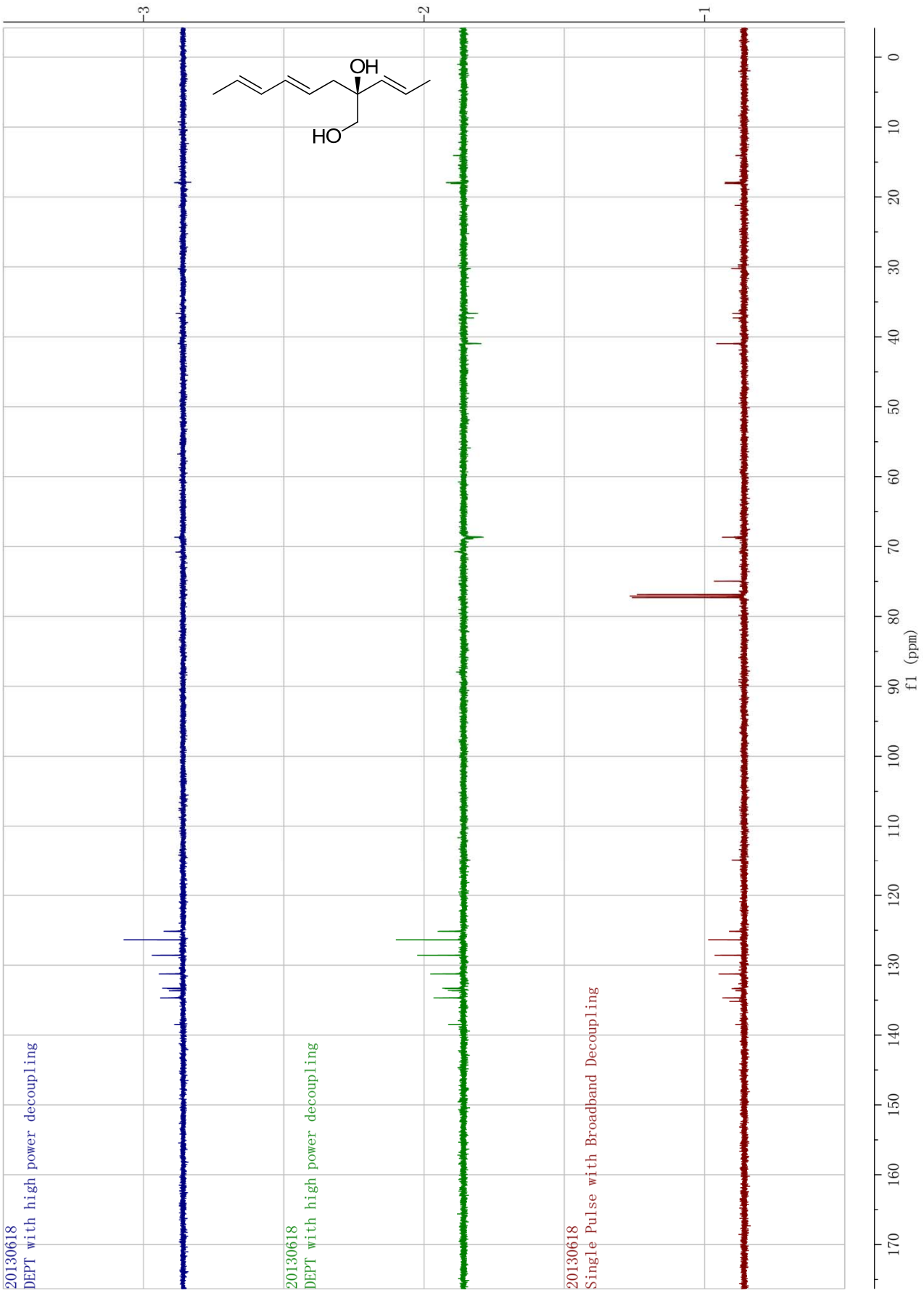

Figure S47. The HMQC spectrum of compound **9** in $CDCl_3$

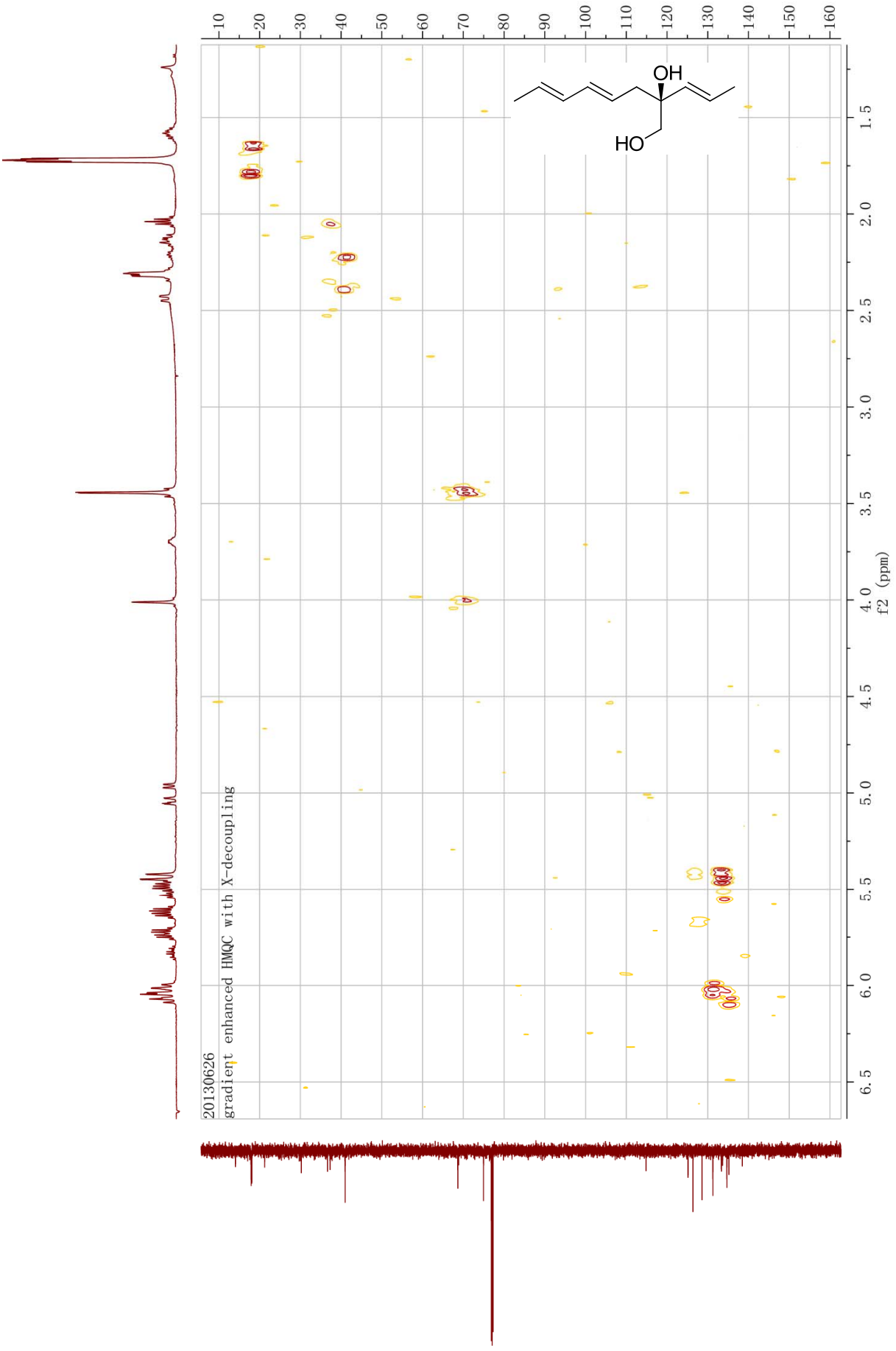

Figure S48. The ^{1}H-^{1}H COSY spectrum of compound **9** in $CDCl_3$

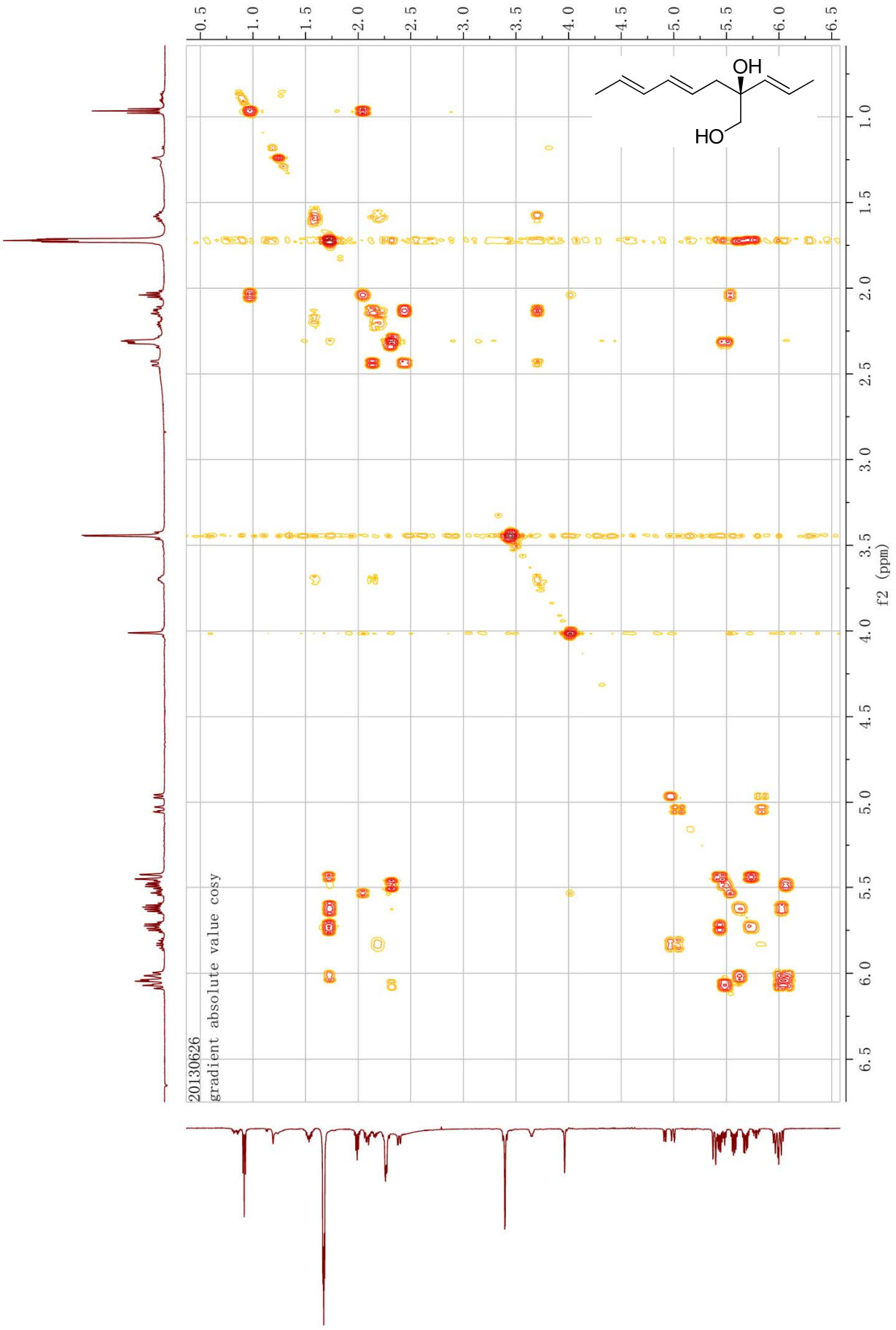

Figure S49. The HMBC spectrum of compound **9** in $CDCl_3$

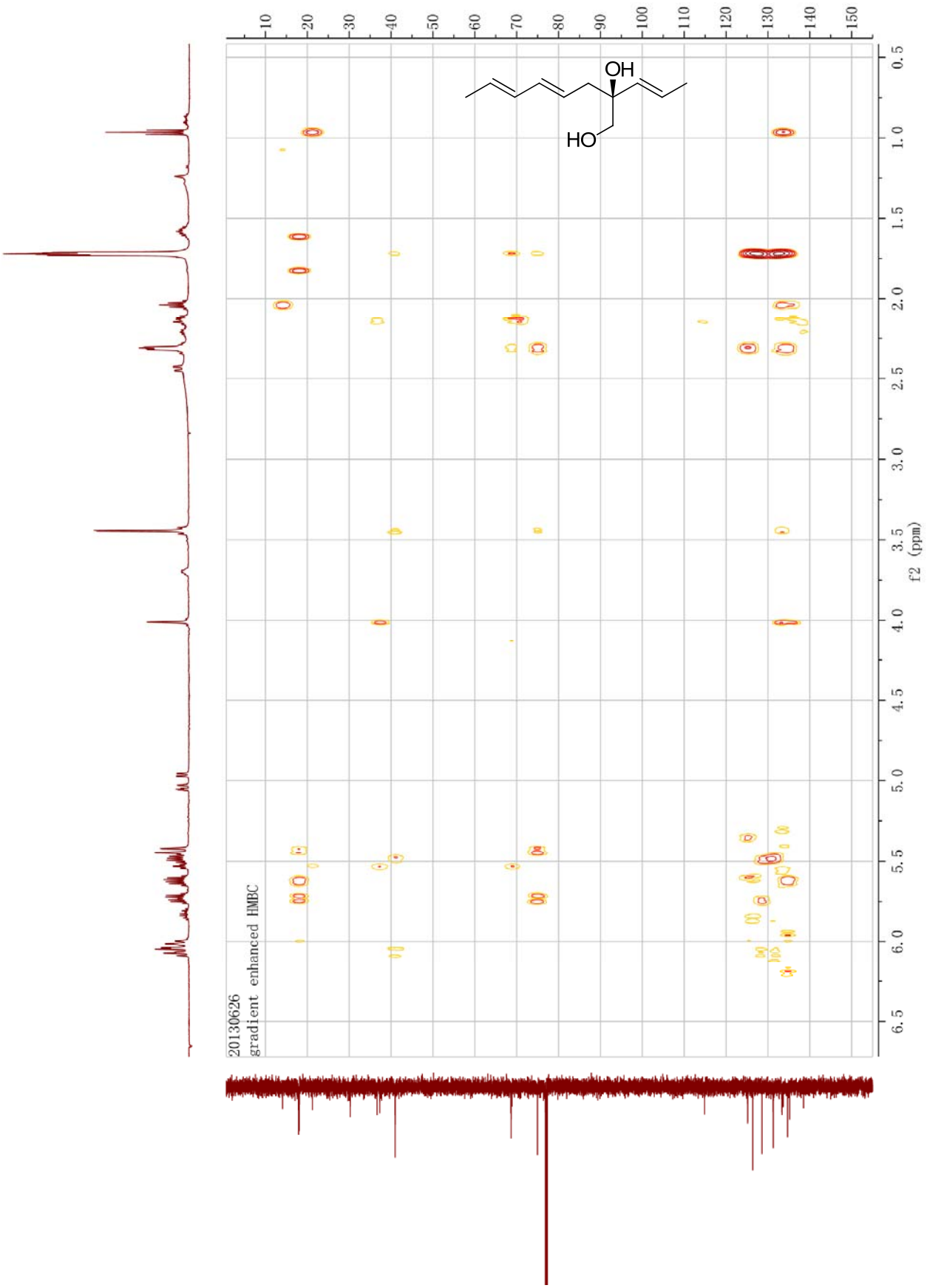

Figure S50. The ^{1}H-NMR spectrum of compound **10** in DMSO-d_6

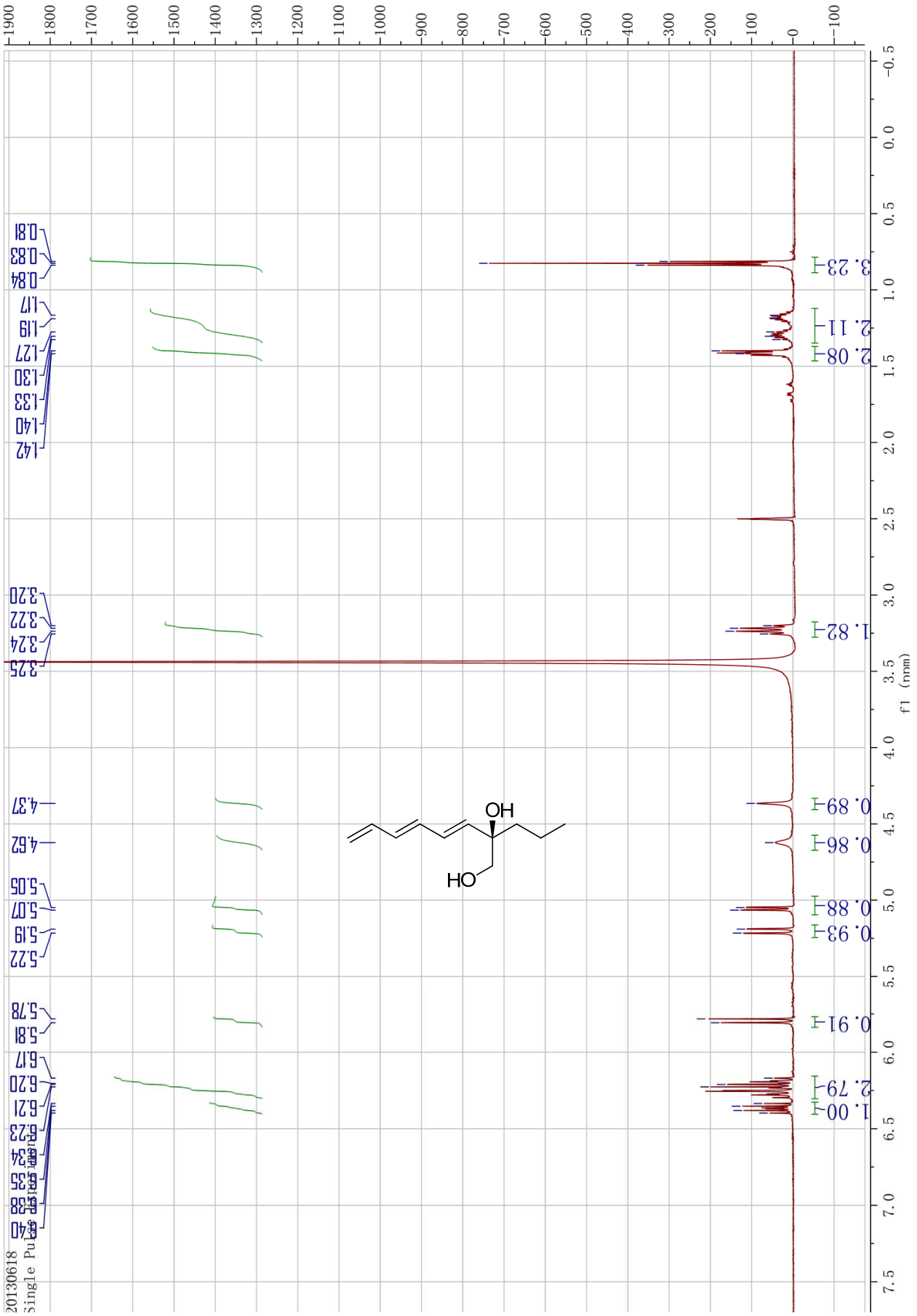

Figure S51. The ^{13}C-NMR spectrum of compound **10** in DMSO-d_6

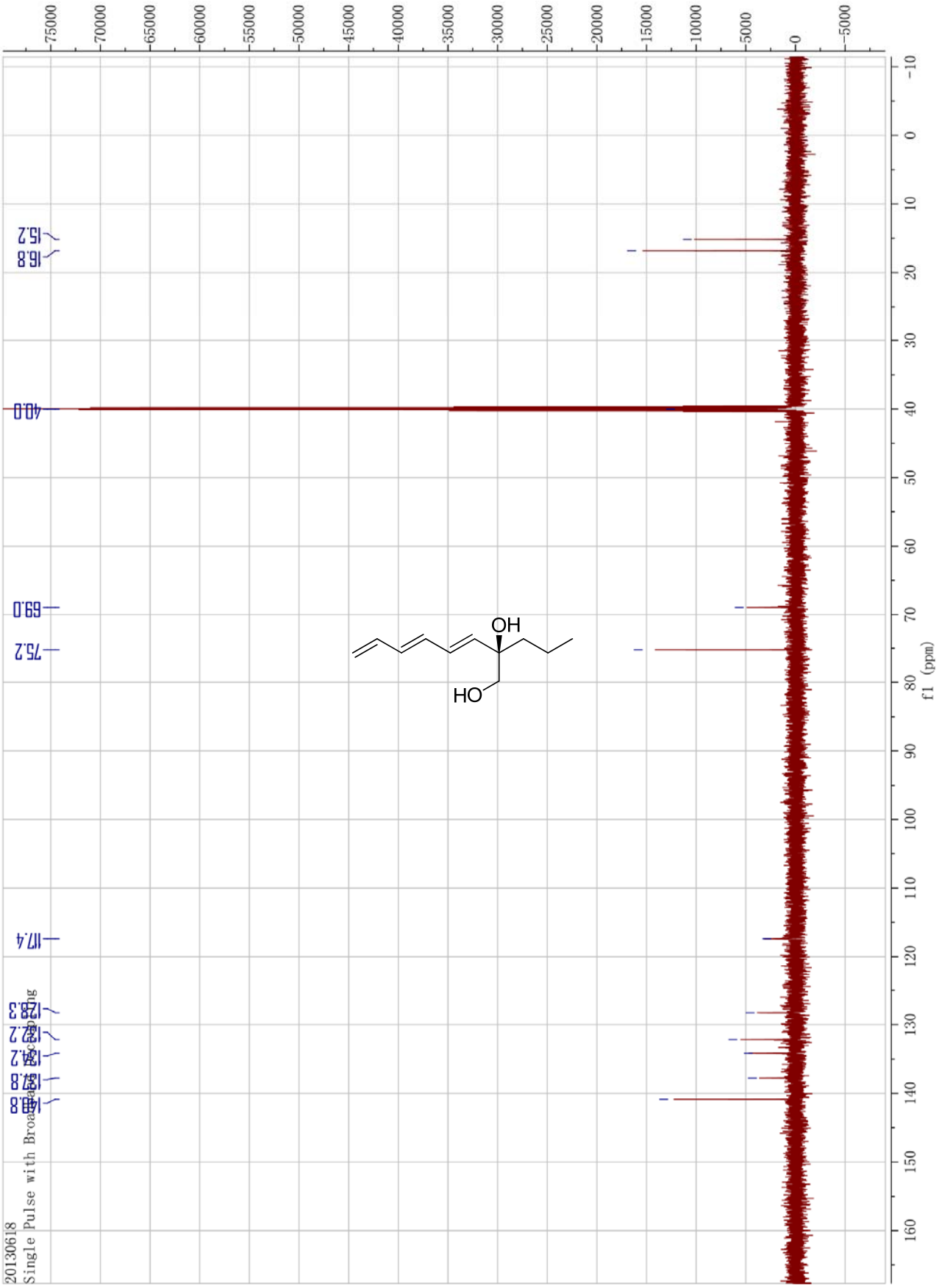

Figure S52. The DEPT spectrum of compound **10** in DMSO-d_6

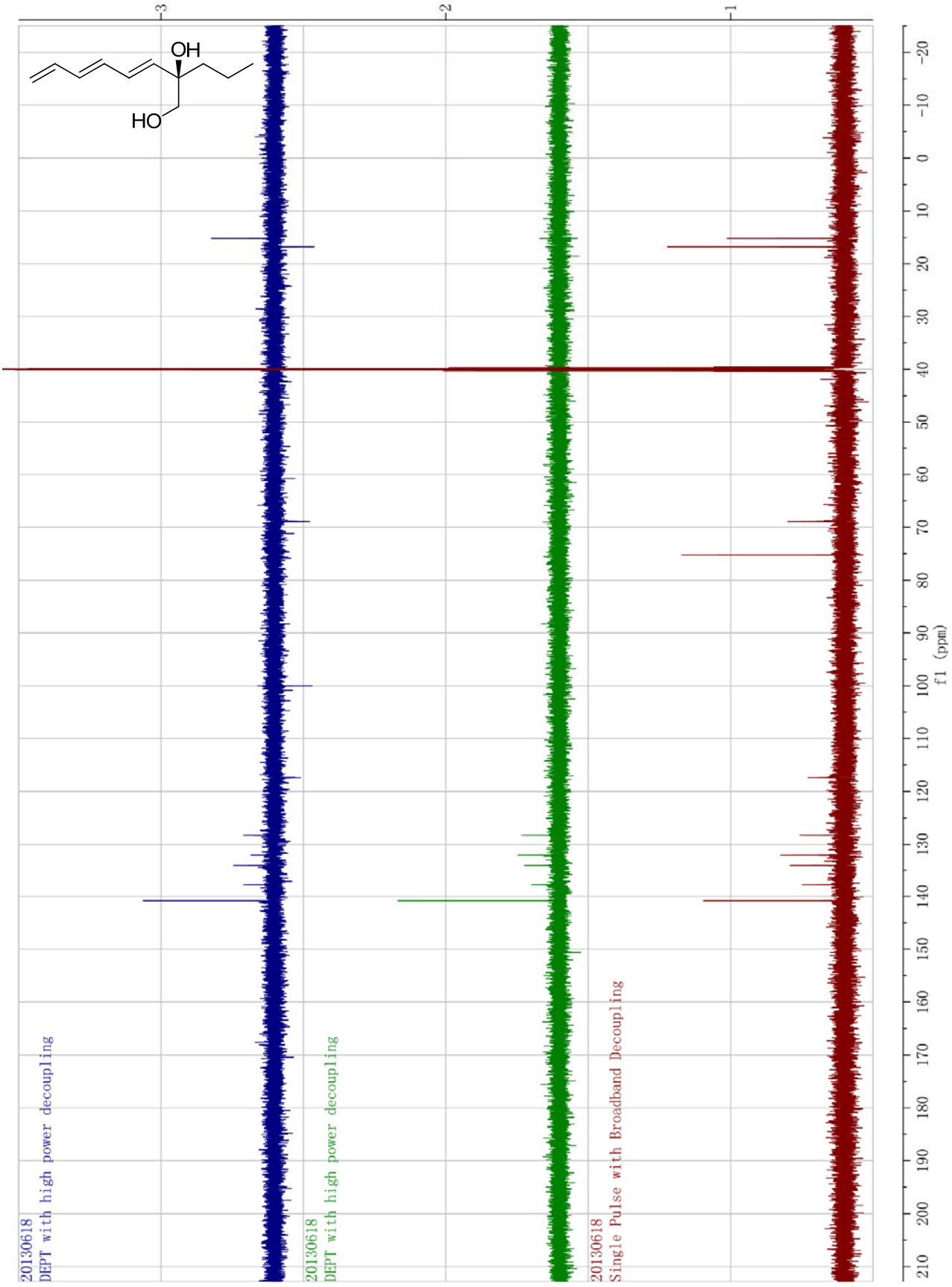

Figure S53. The HMQC spectrum of compound **10** in DMSO-d_6

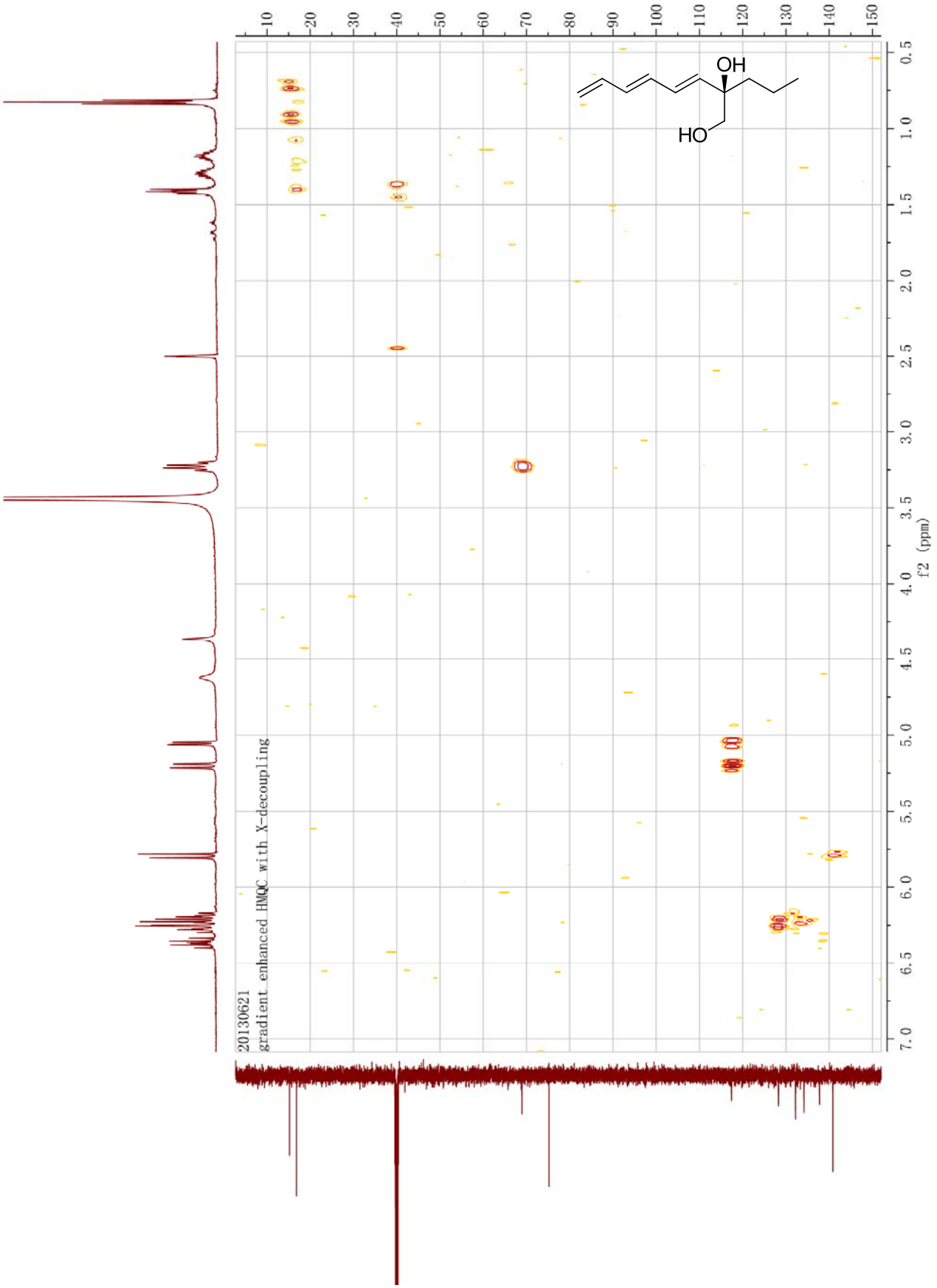

Figure S54. The ^{1}H-^{1}H COSY spectrum of compound **10** in DMSO-d_6

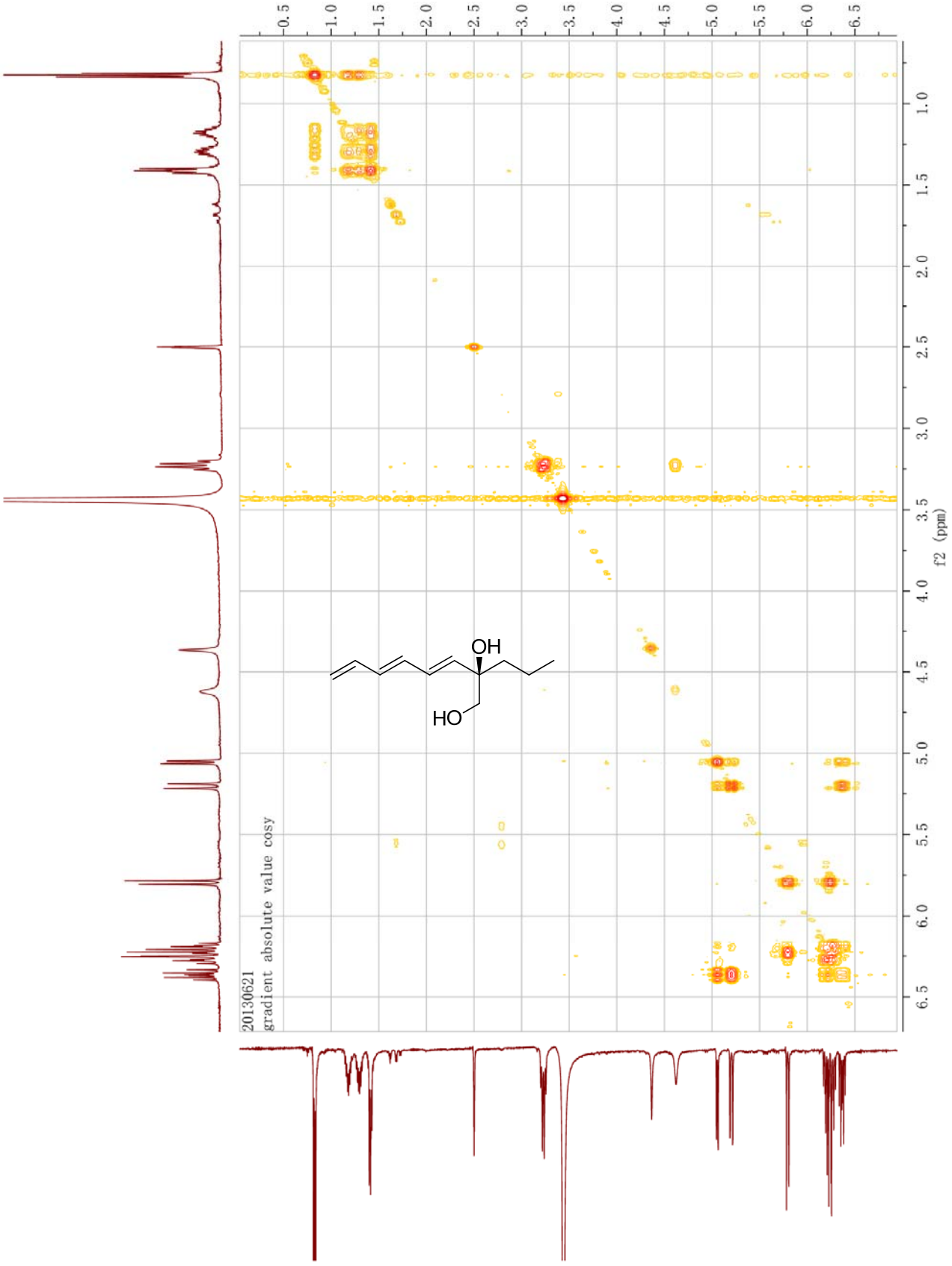

Figure S55. The HMBC spectrum of compound **10** in DMSO-d_6

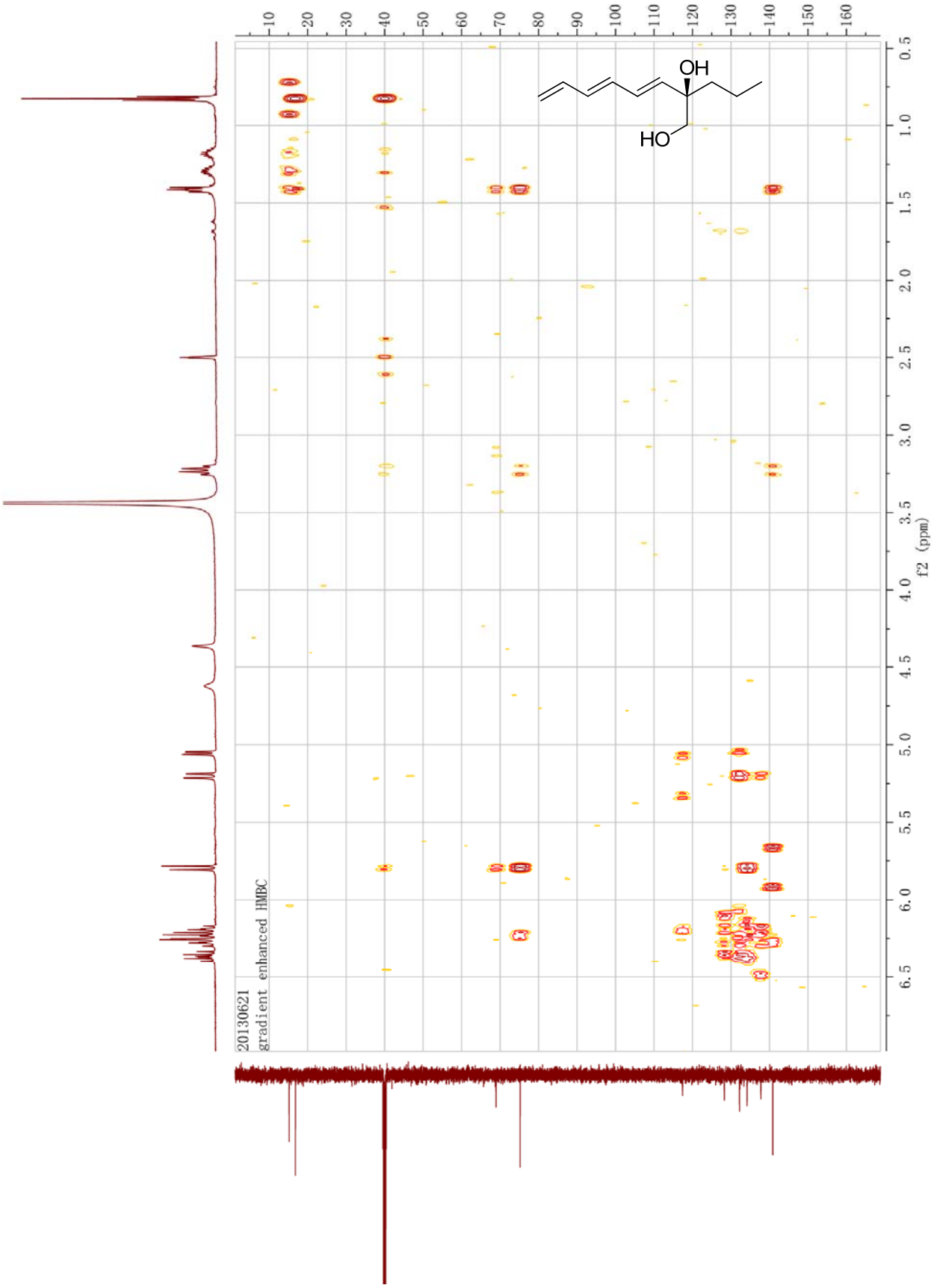

Figure S56. The [1]H-NMR spectrum of compound **11** in DMSO-d_6

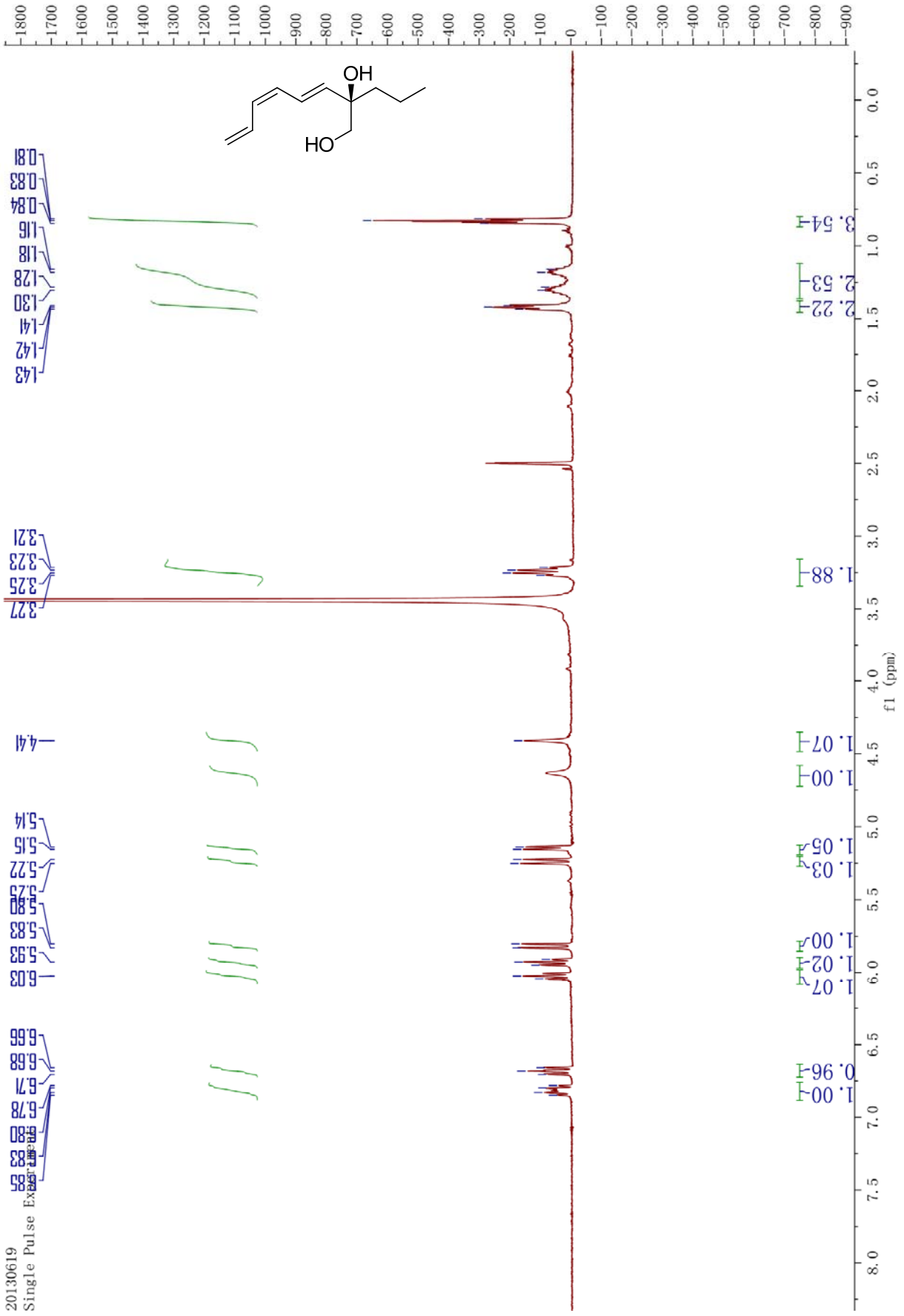

Figure S57. The ^{13}C-NMR spectrum of compound **11** in DMSO-d_6

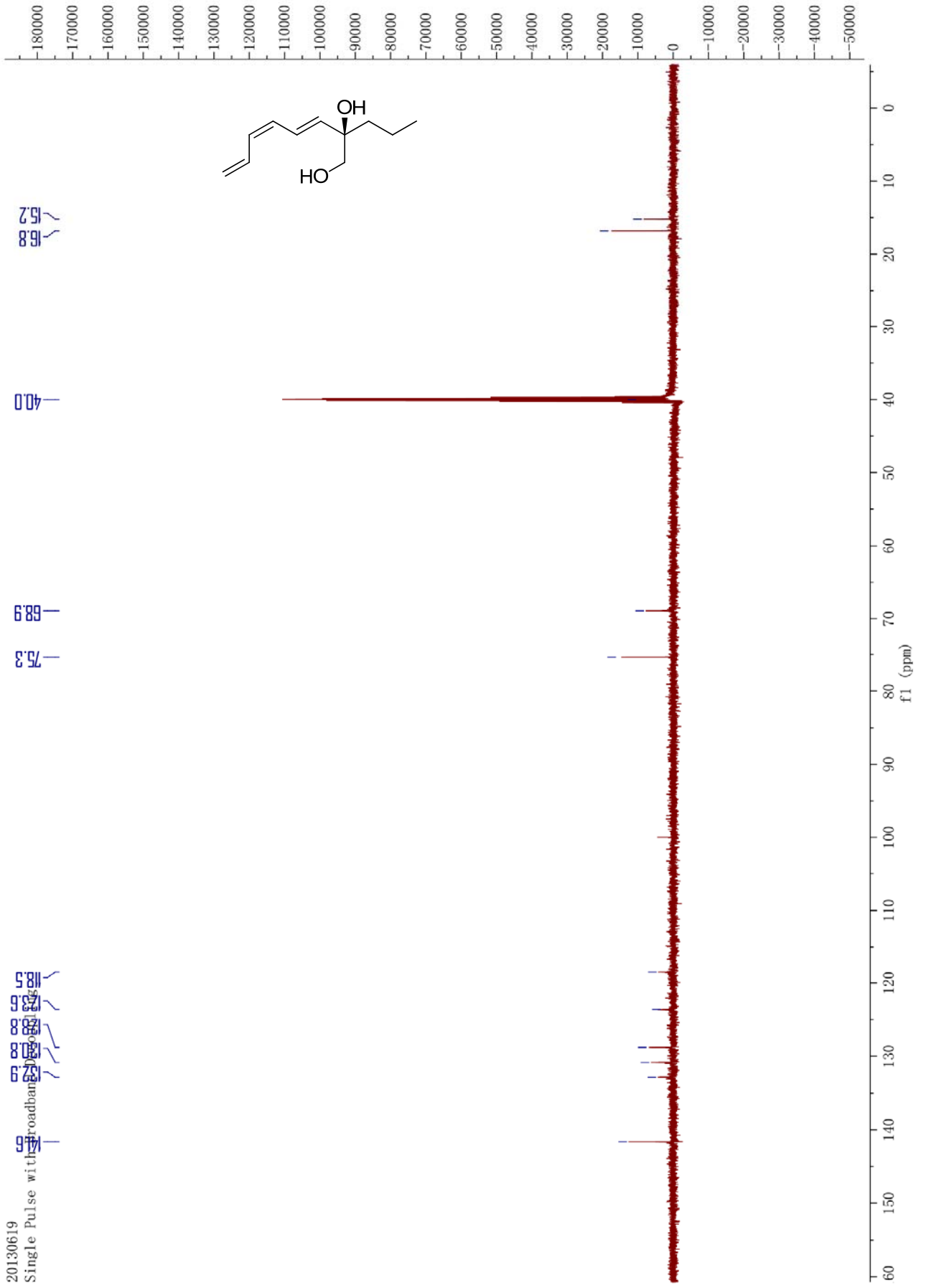

Figure S58. The DEPT spectrum of compound **11** in DMSO-d_6

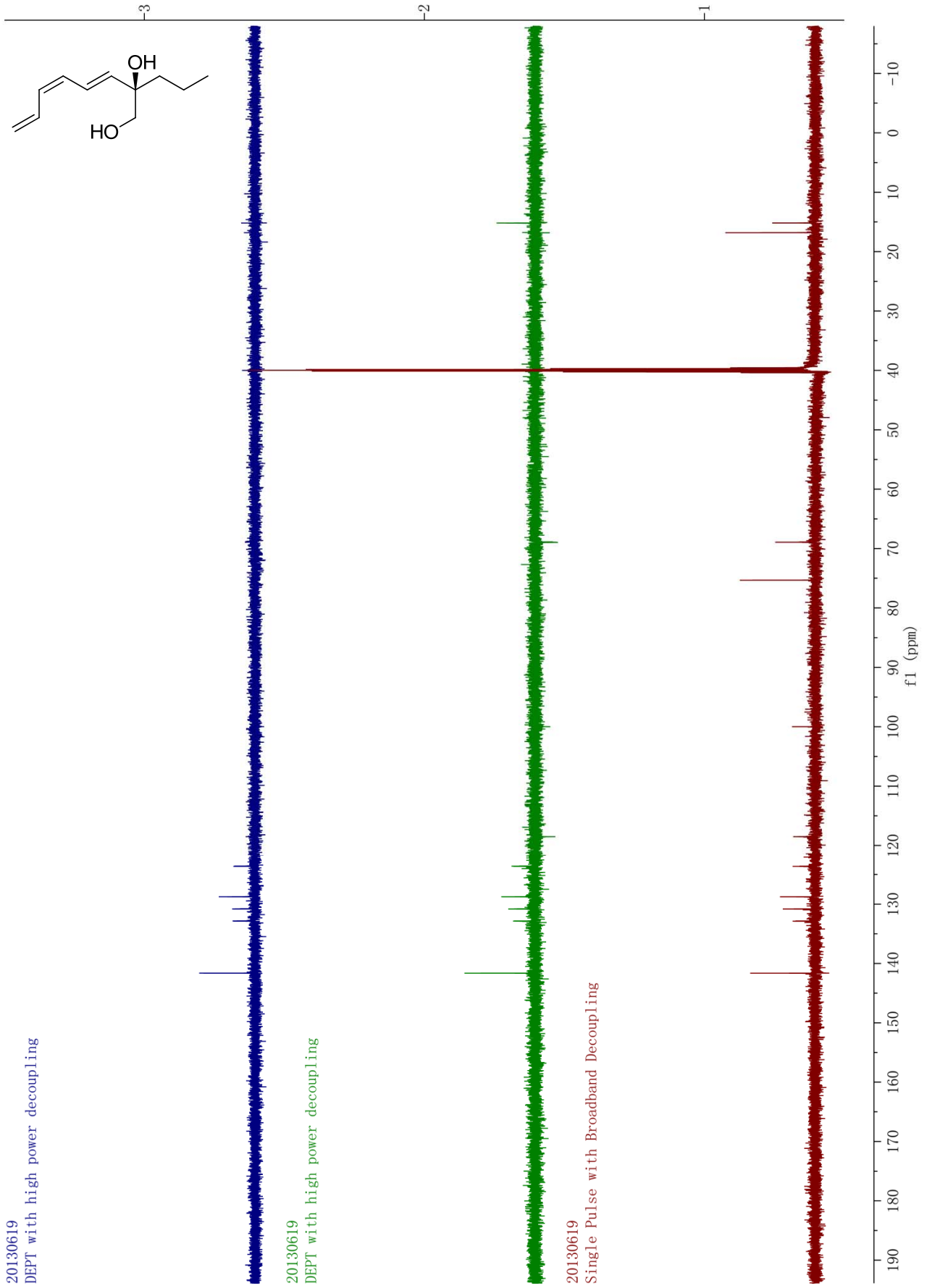

Figure S59. The HMQC spectrum of compound **11** in DMSO-d_6

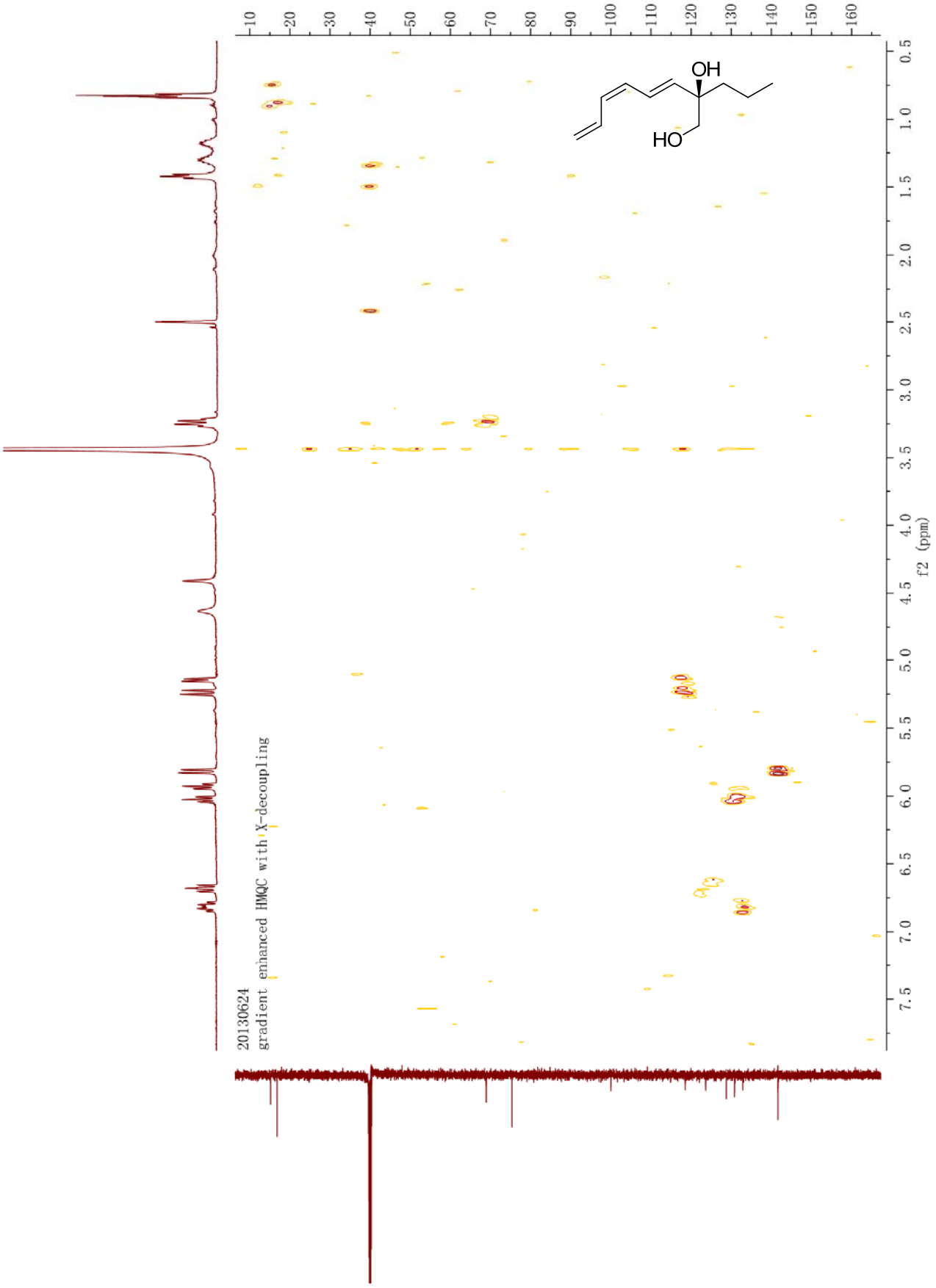

Figure S60. The ^{1}H-^{1}H COSY spectrum of compound **11** in DMSO-d_6

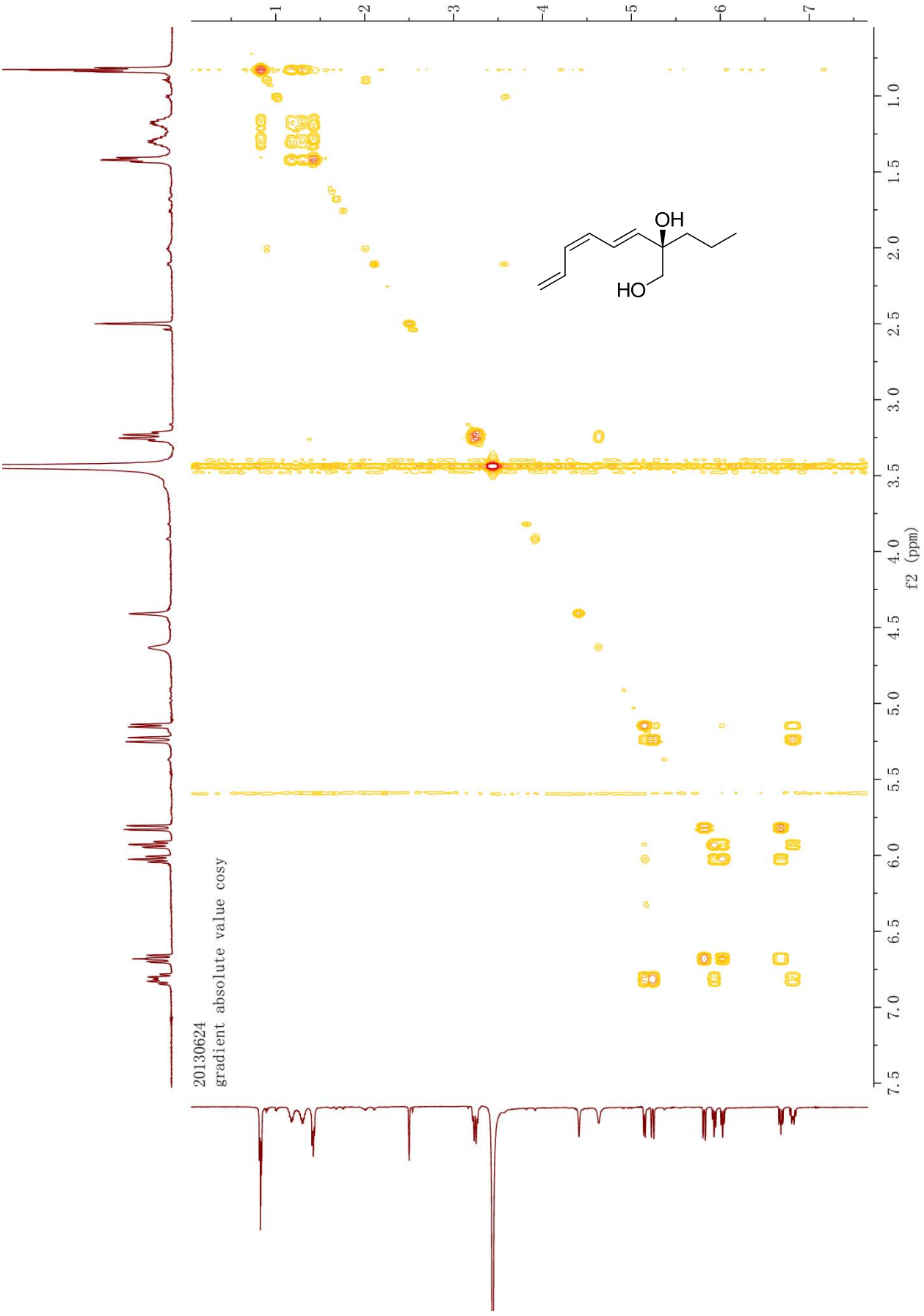

Figure S61. The HMBC spectrum of compound **11** in DMSO-d_6

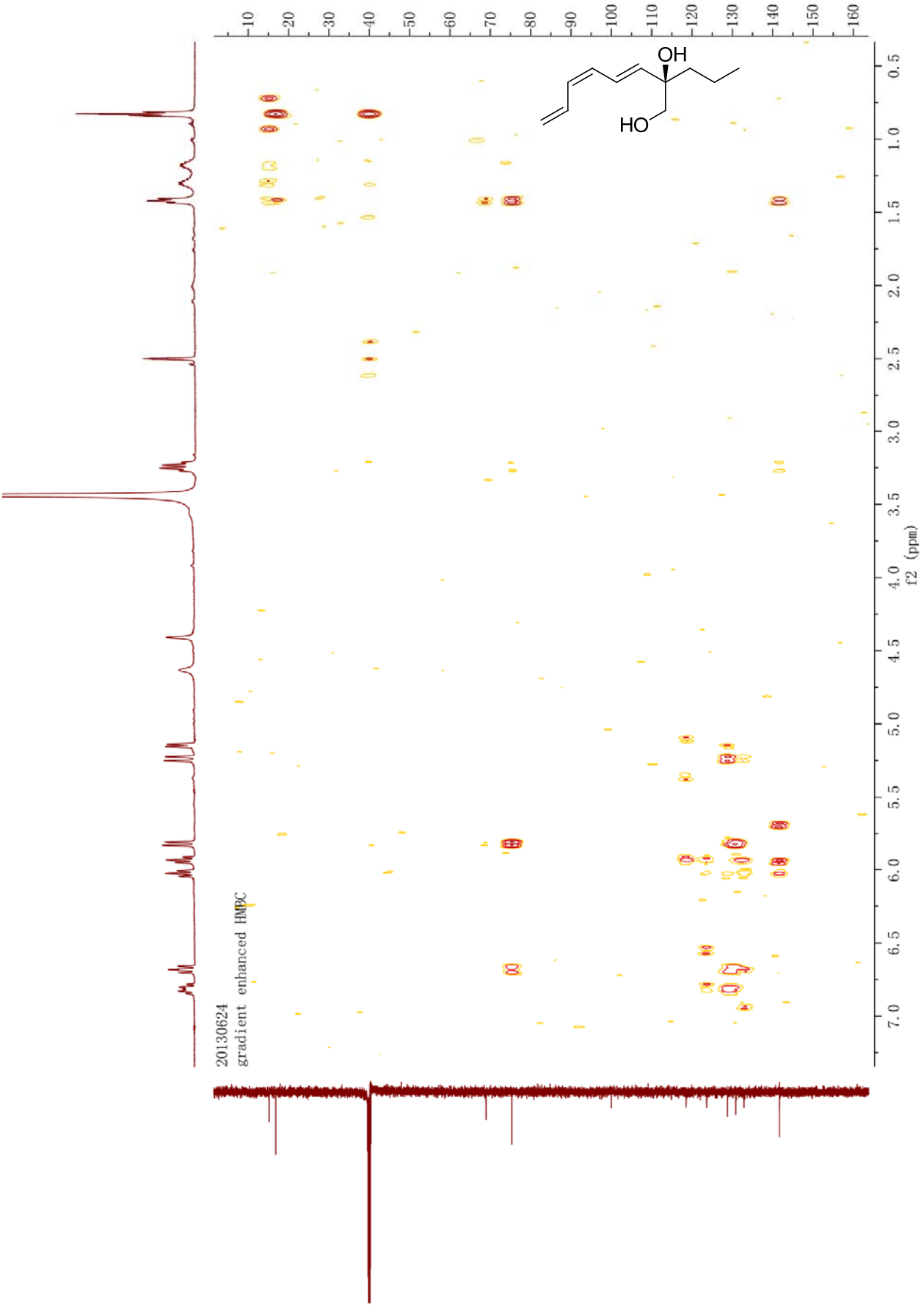

Figure S62. The ^{1}H-NMR spectrum of compound **12** in DMSO-d_6

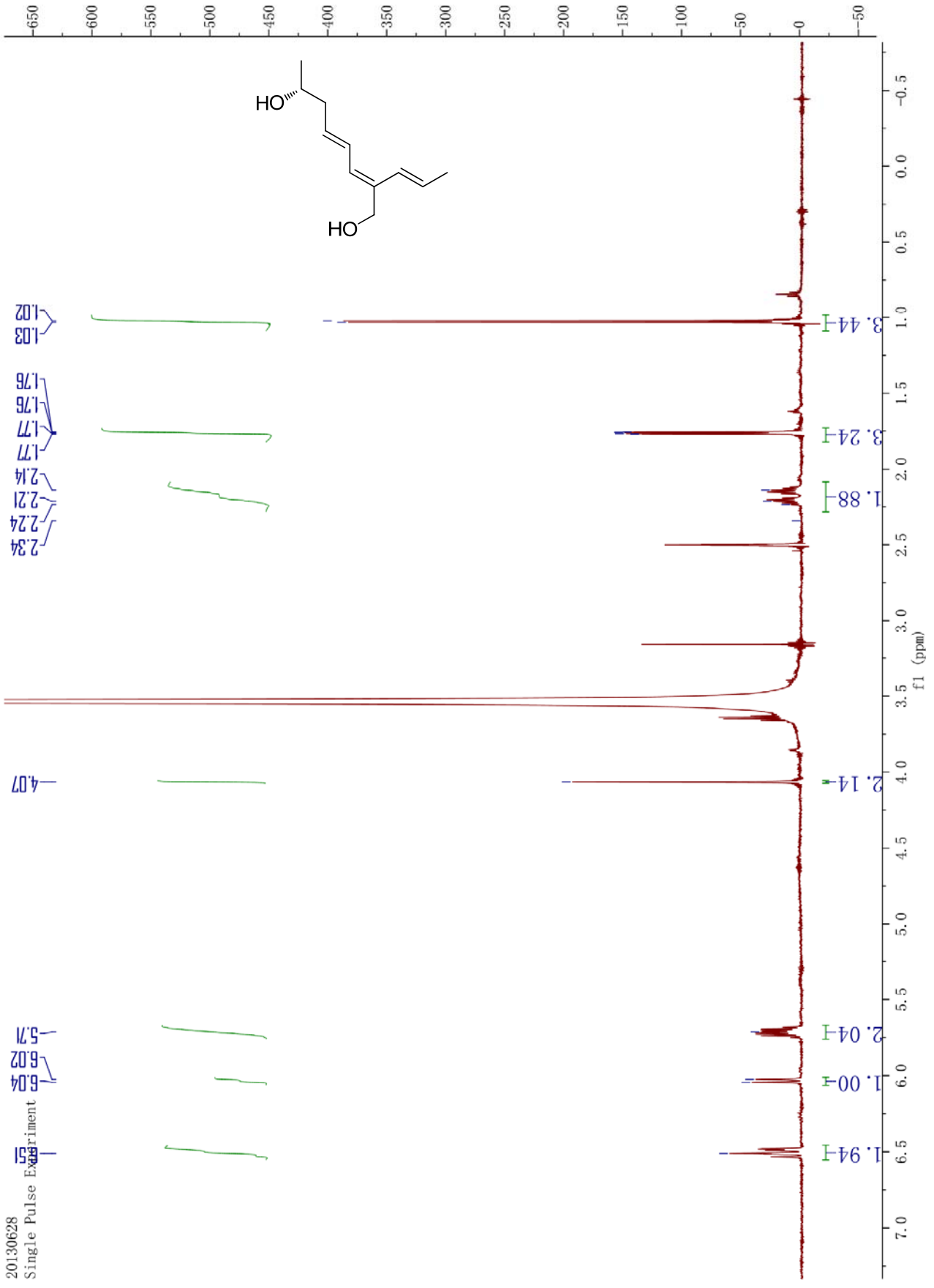

Figure S63. The ^{13}C-NMR spectrum of compound **12** in DMSO-d_6

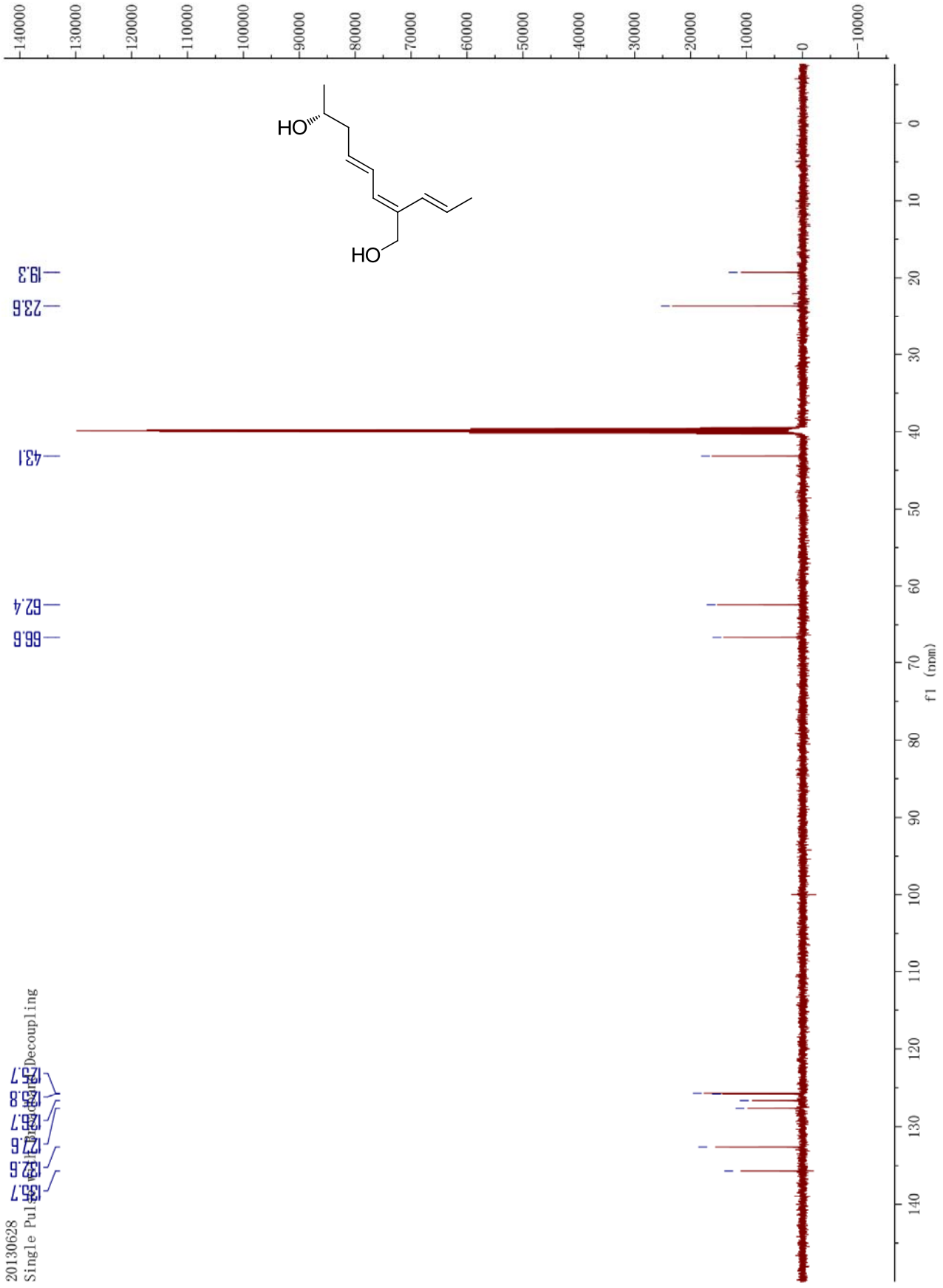

Figure S64. The DEPT spectrum of compound **12** in DMSO-d_6

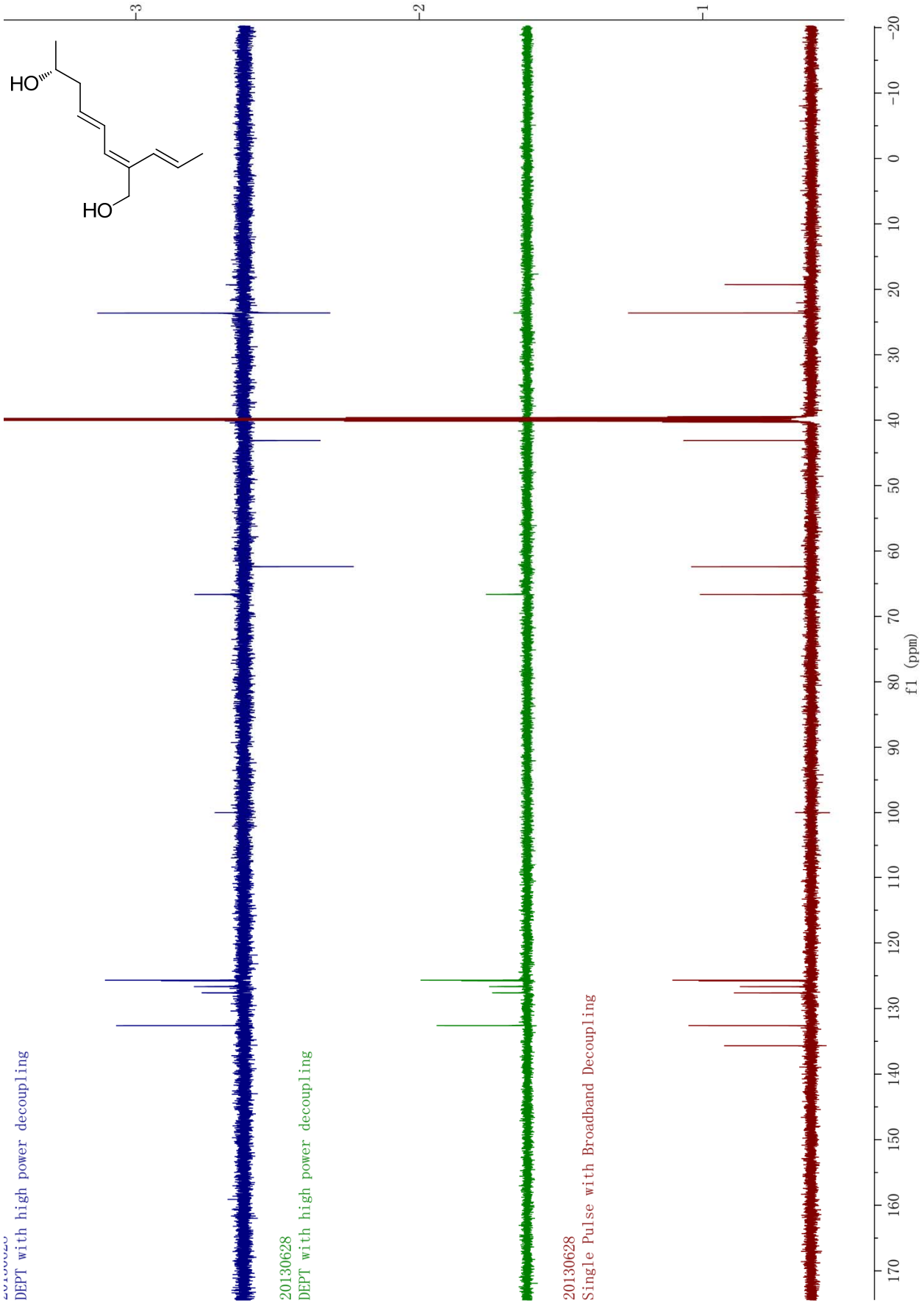

Figure S65. The HMQC spectrum of compound **12** in DMSO-d_6

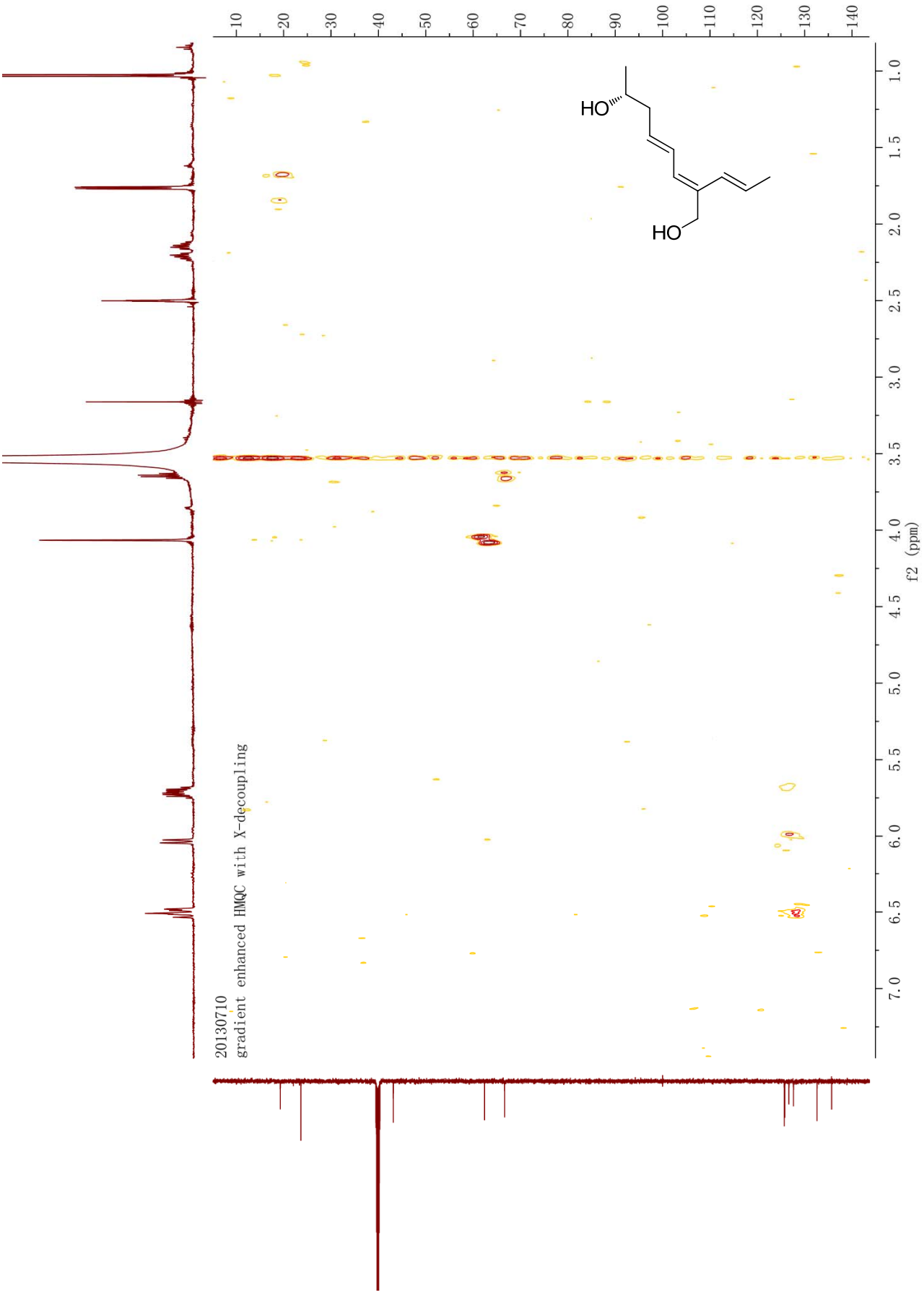

Figure S66. The ^{1}H-^{1}H COSY spectrum of compound **12** in DMSO-d_6

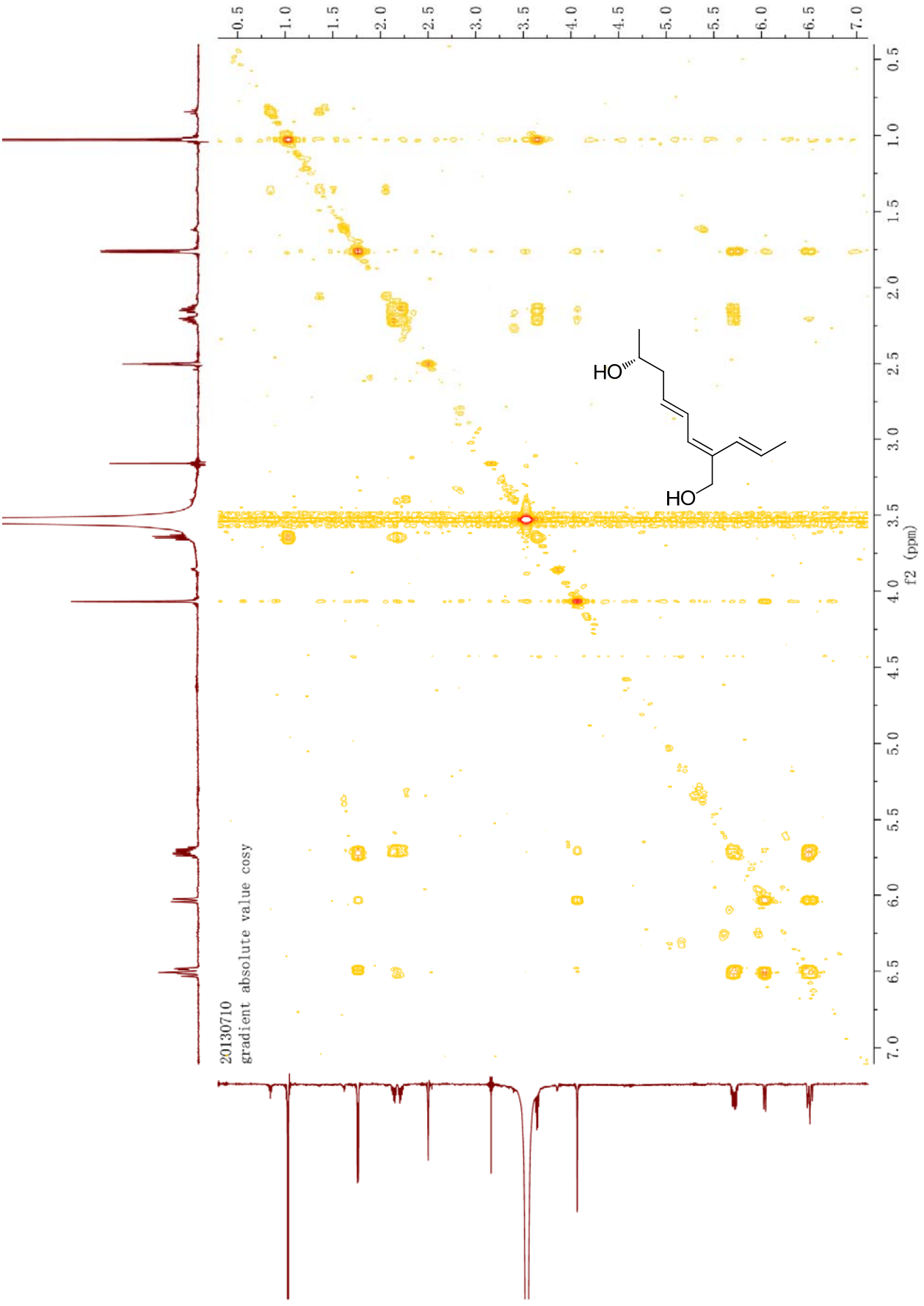

Figure S67. The HMBC spectrum of compound **12** in DMSO-d_6

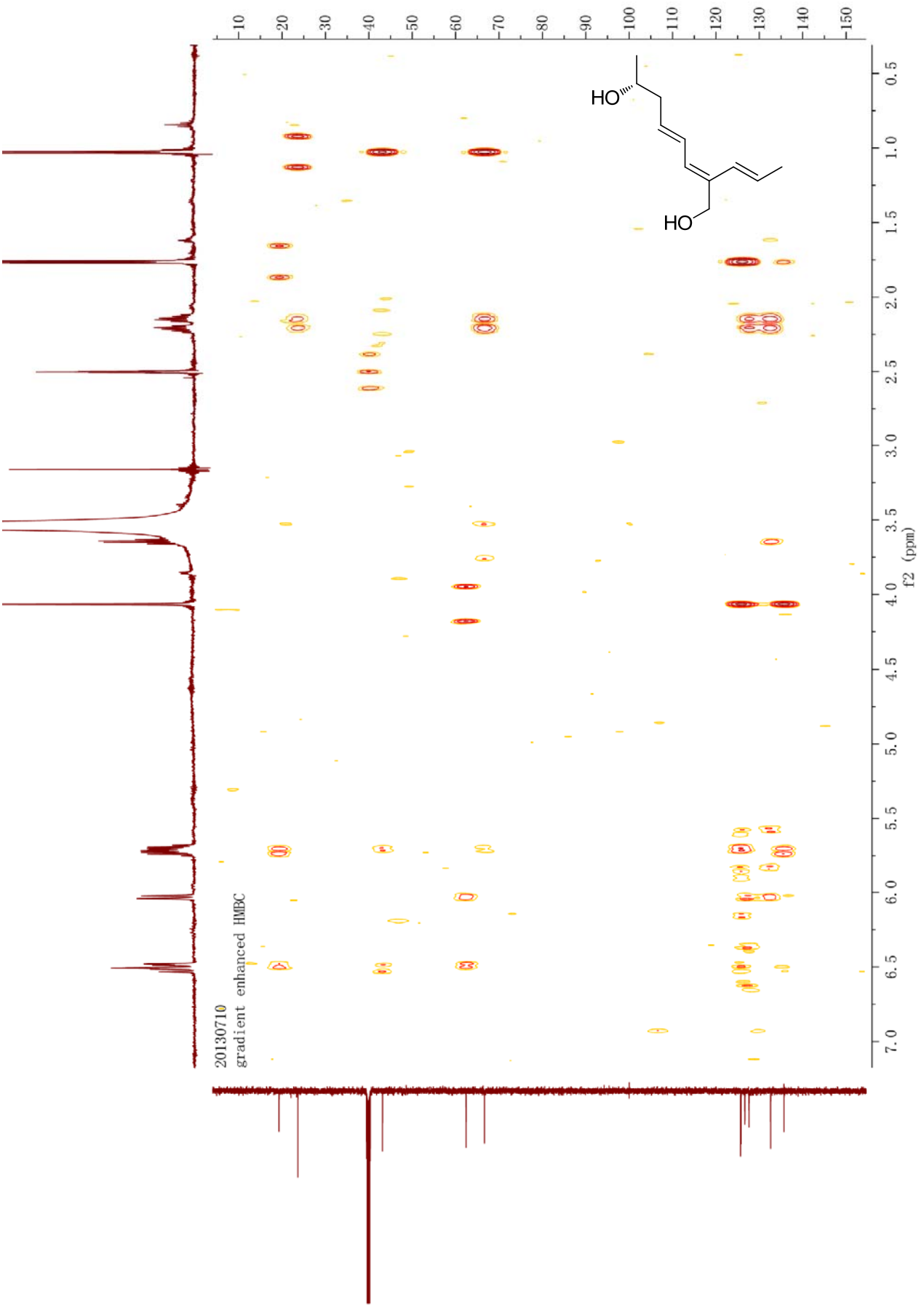

Figure S68. The NOESY spectrum of compound **12** in DMSO-d_6

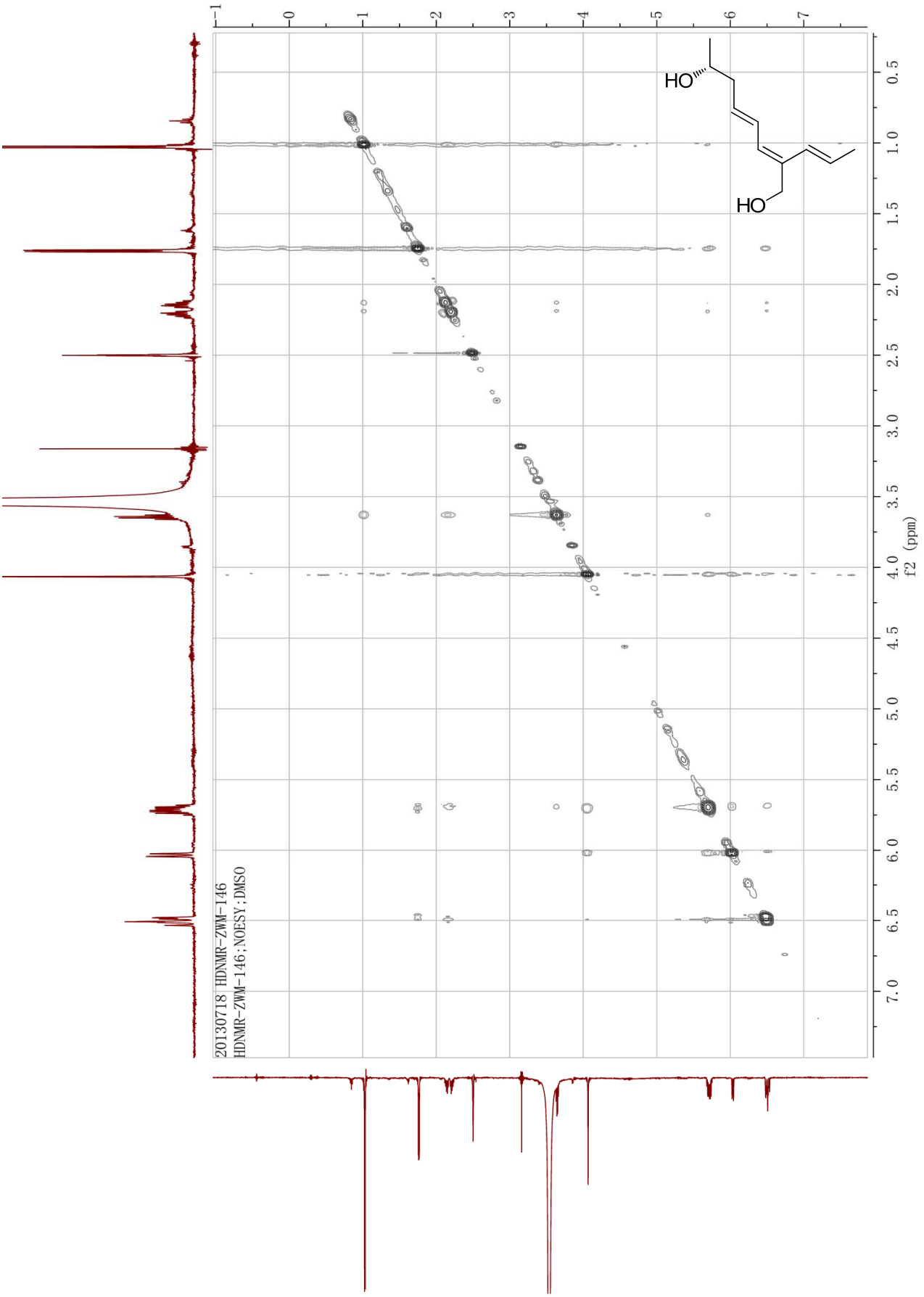

Figure S69. The ^{1}H-NMR spectrum of compound **13** in DMSO-d_6

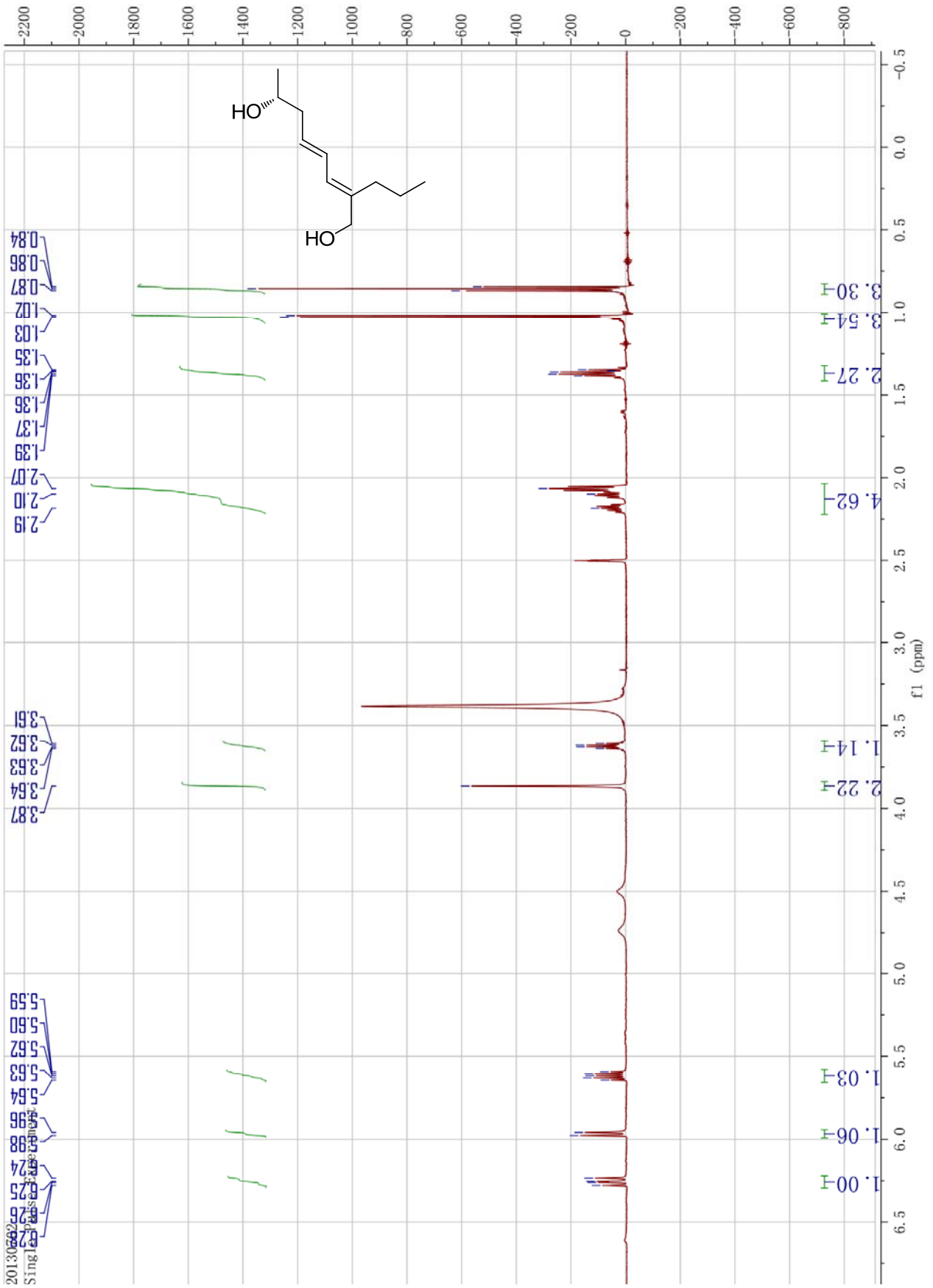

Figure S70. The ^{13}C-NMR spectrum of compound **13** in DMSO-d_6

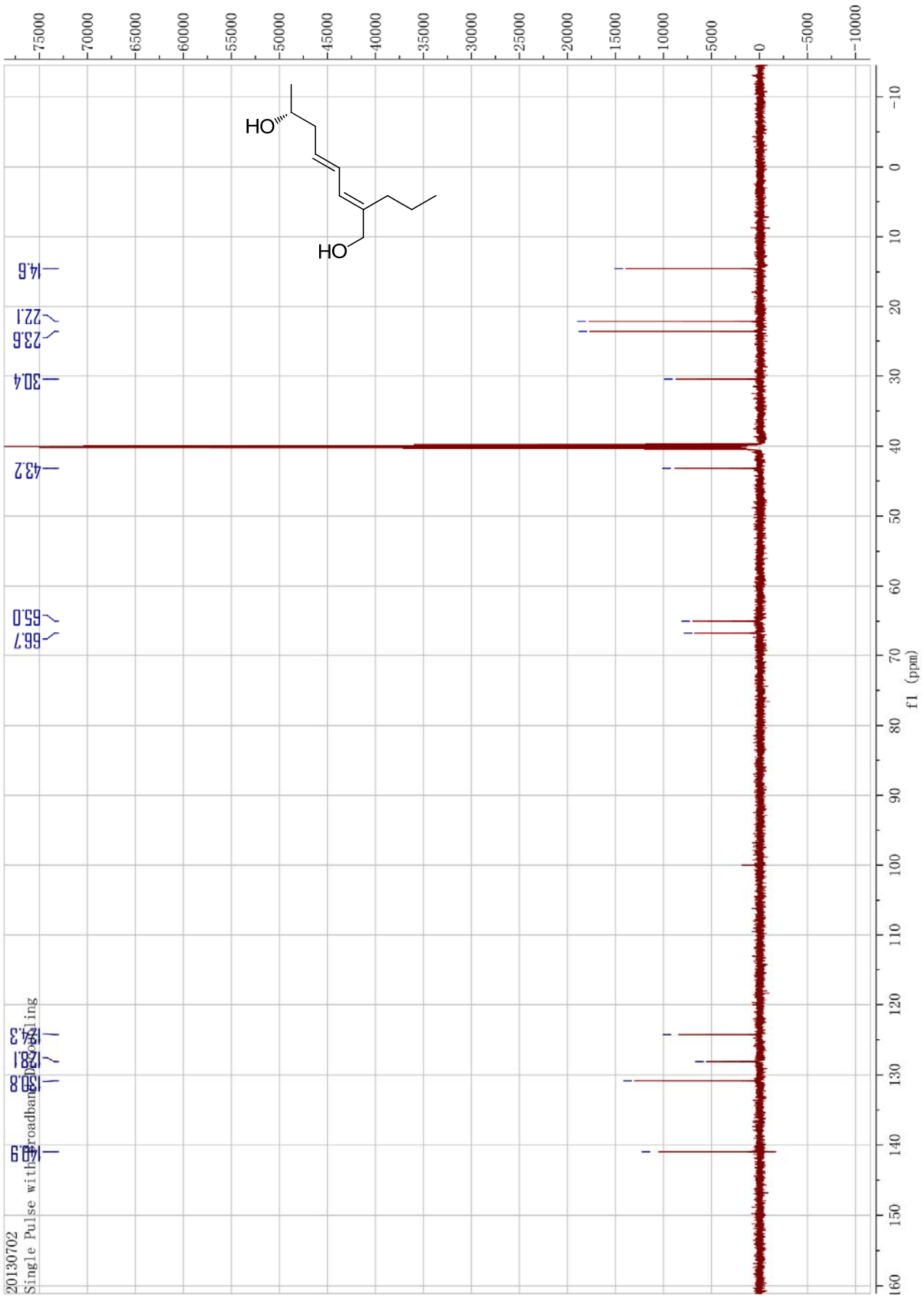

Figure S71. The DEPT spectrum of compound **13** in DMSO-d_6

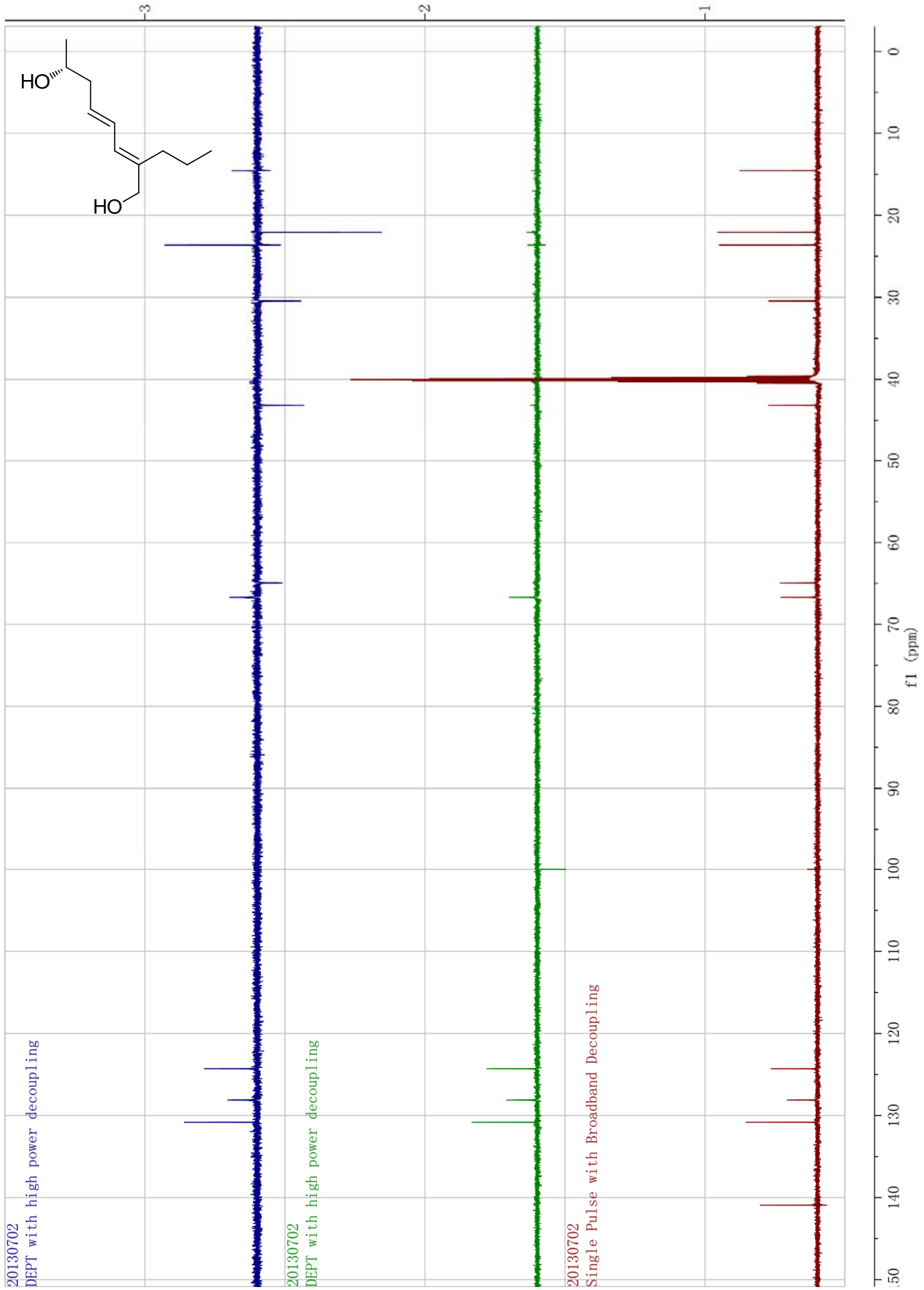

Figure S72. The HMQC spectrum of compound **13** in DMSO-d_6

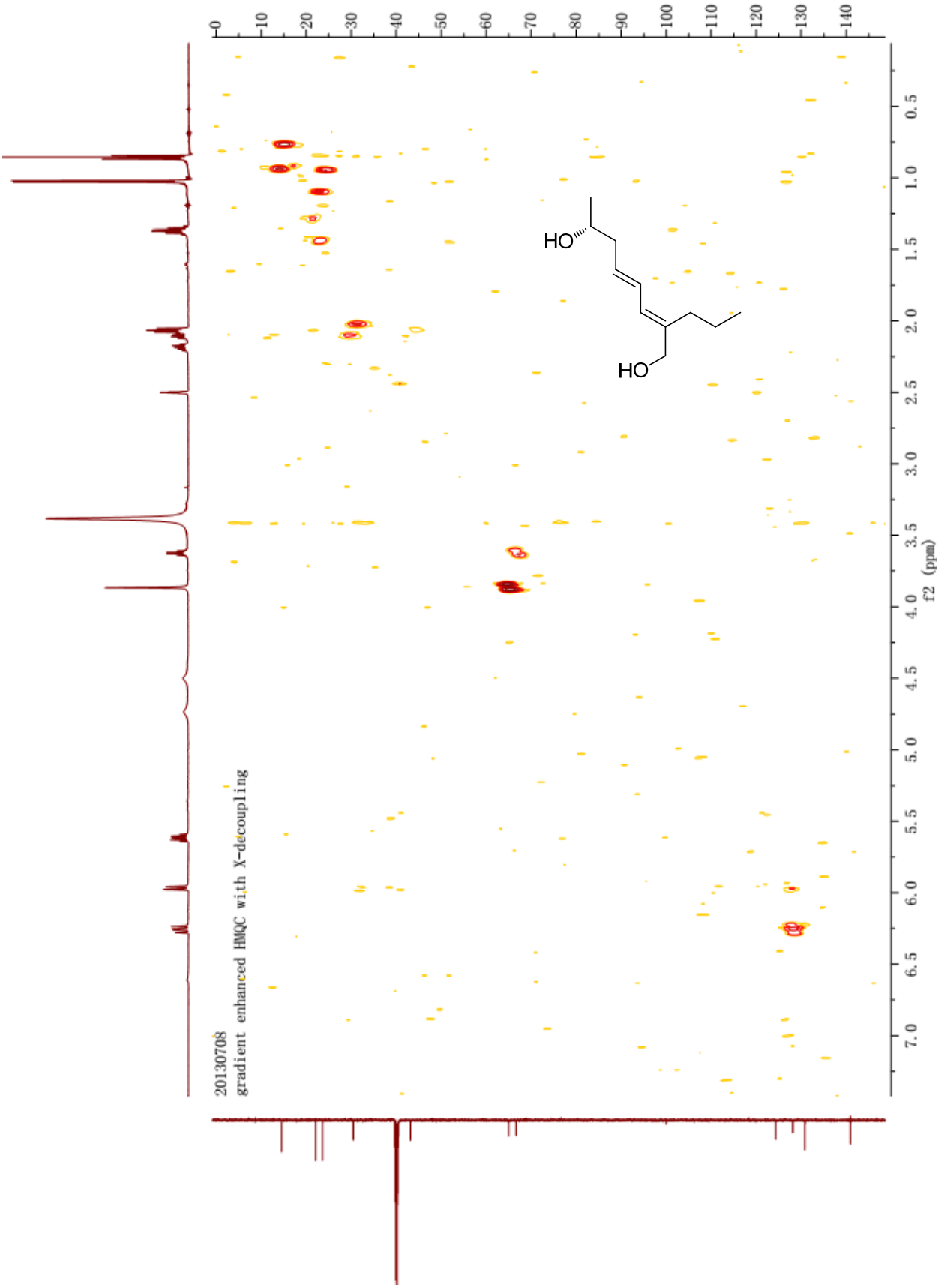

Figure S73. The ^{1}H-^{1}H COSY spectrum of compound **13** in DMSO-d_6

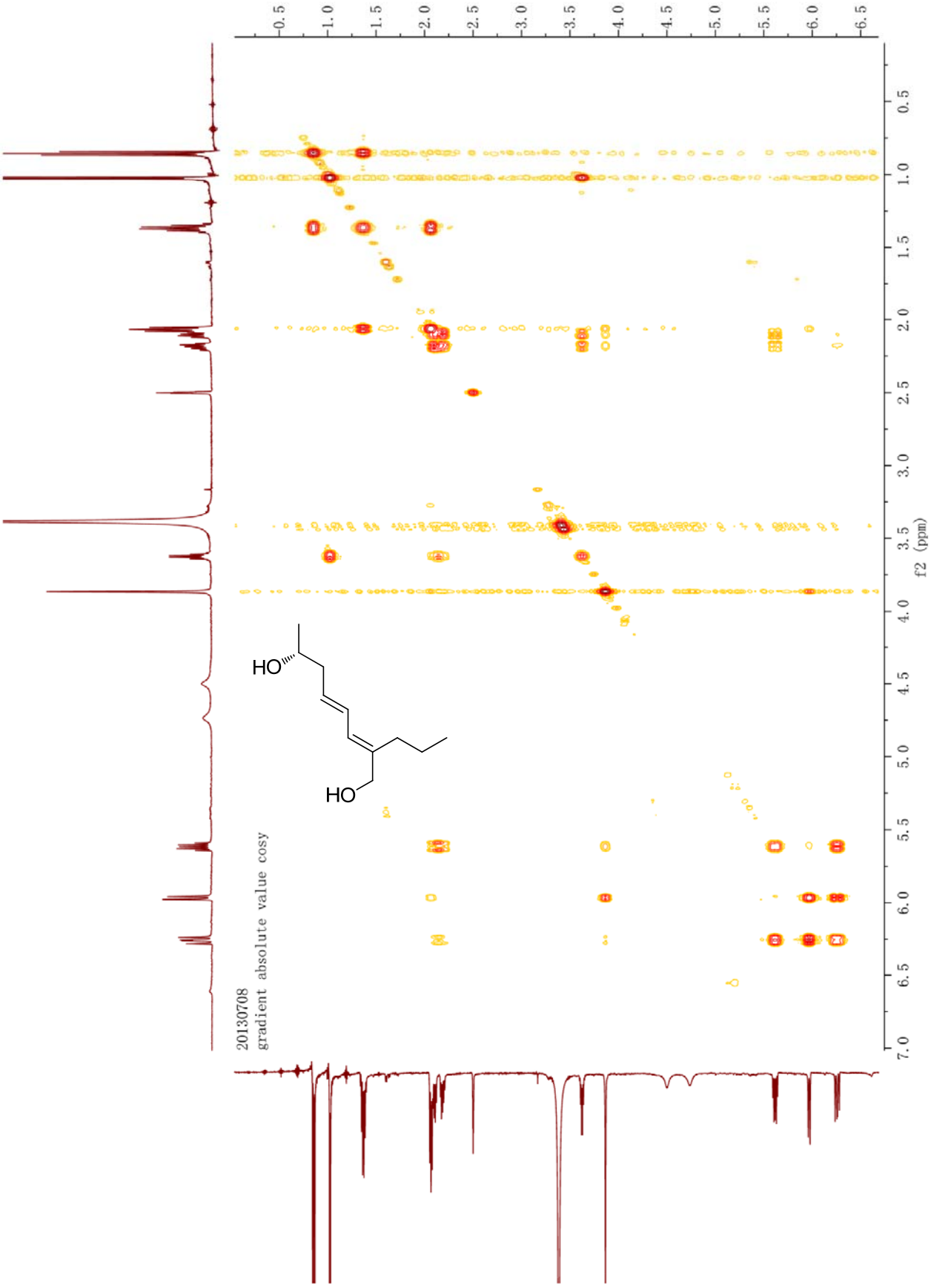

Figure S74. The HMBC spectrum of compound **13** in DMSO-d_6

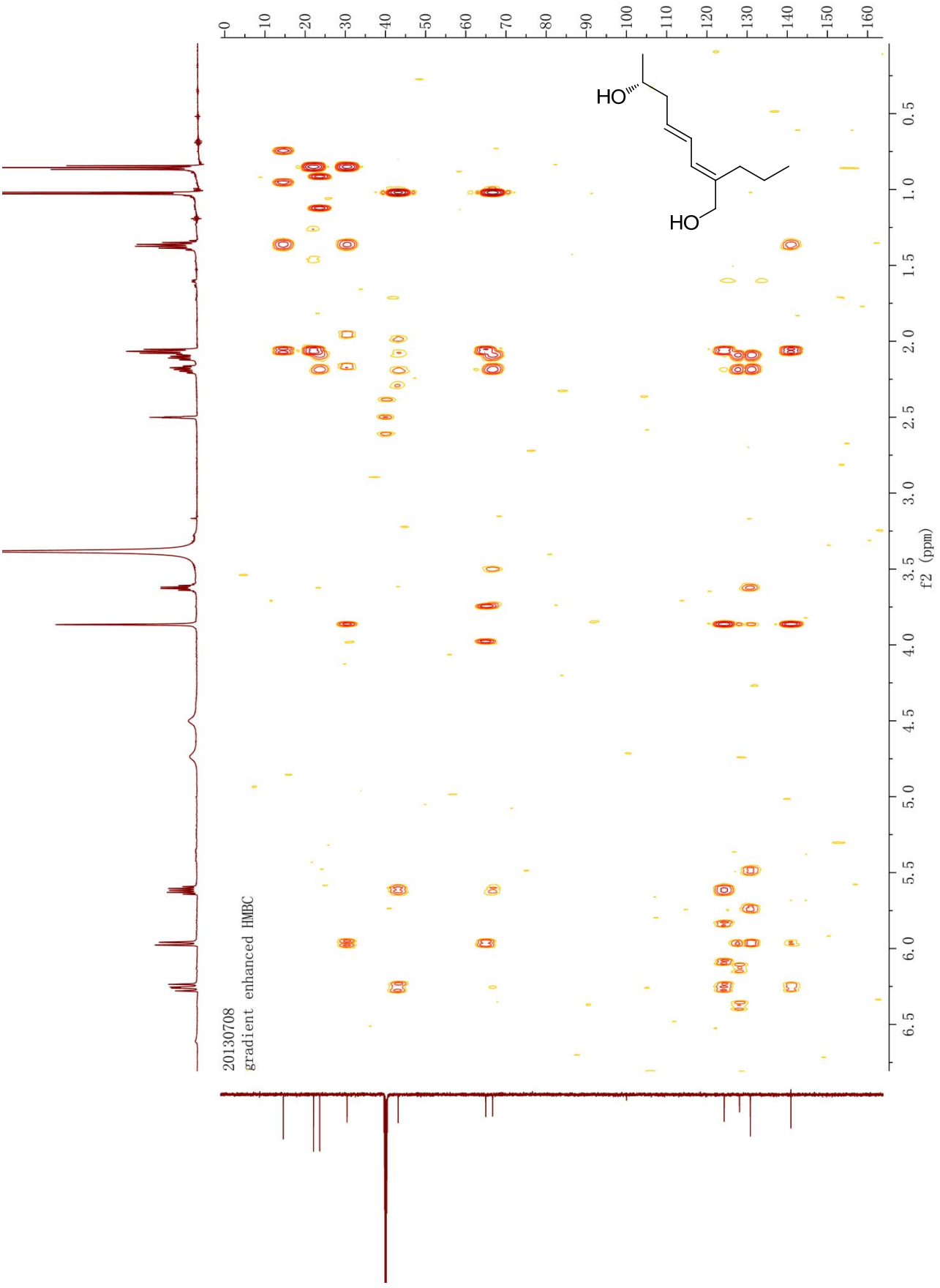

Figure S75. The NOESY spectrum of compound **13** in DMSO-d_6

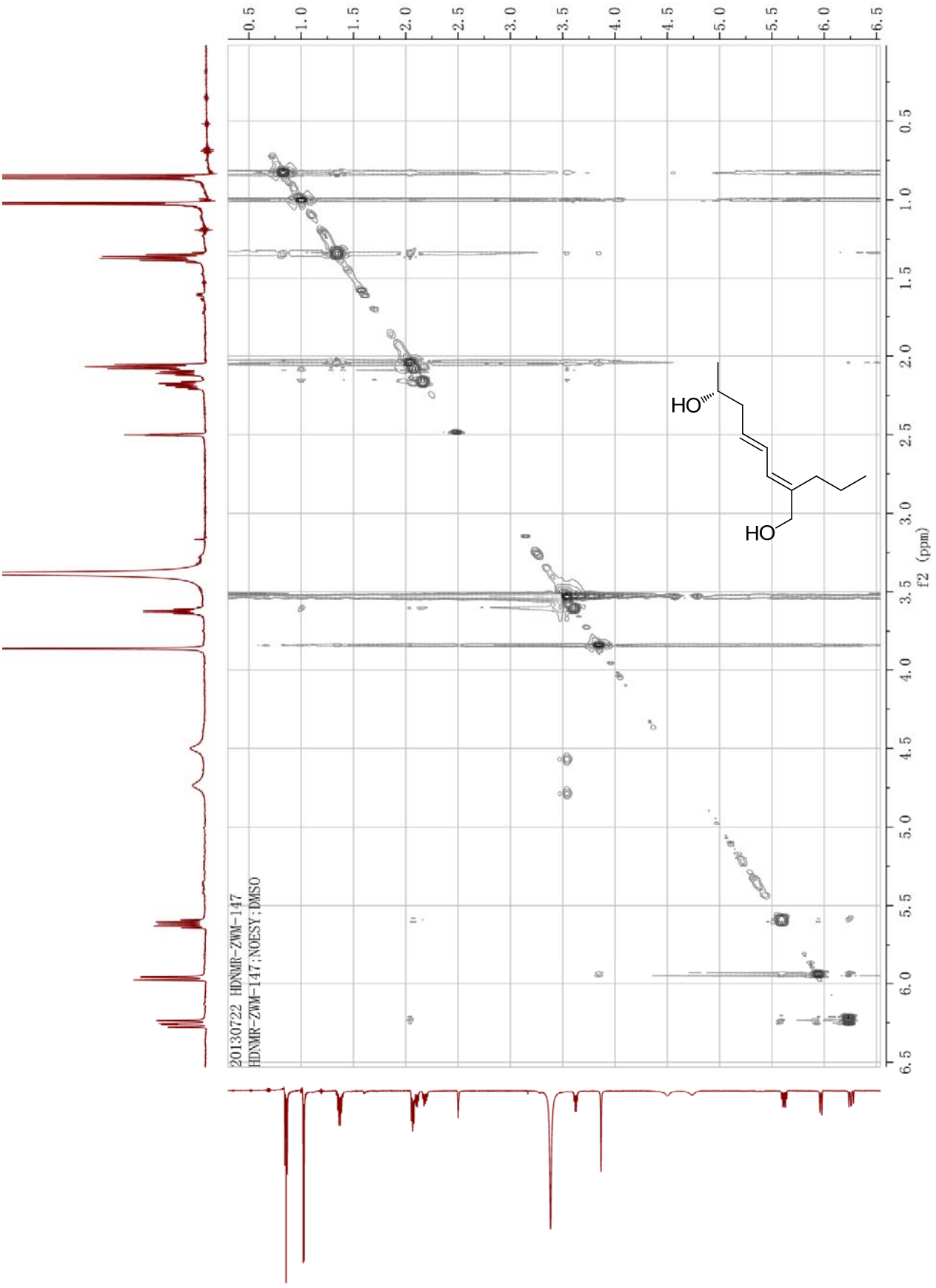

Figure S76. The ^{1}H-NMR spectrum of compound **14** in DMSO-d_6

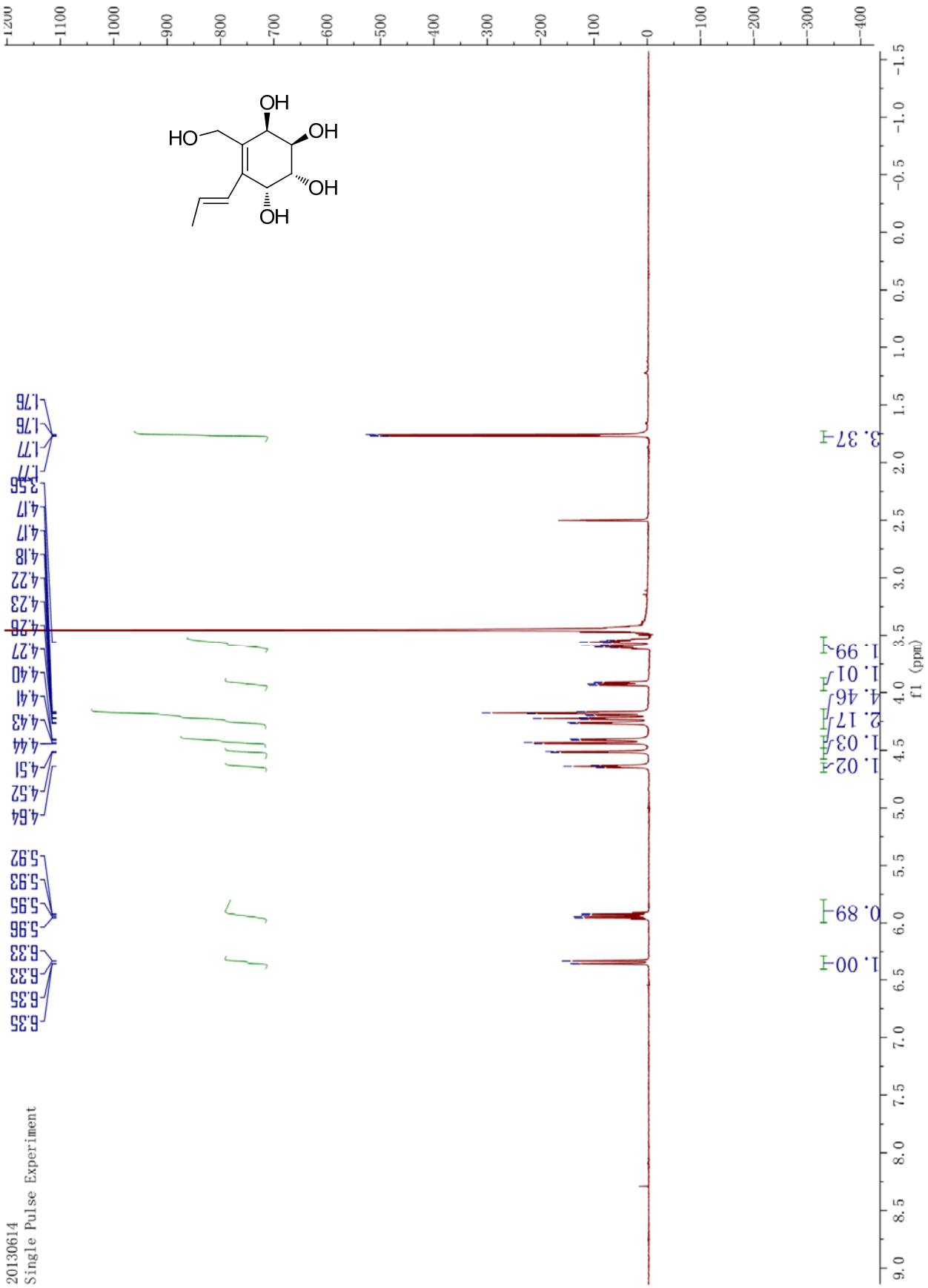

Figure S77. The ^{13}C-NMR spectrum of compound **14** in DMSO-d_6

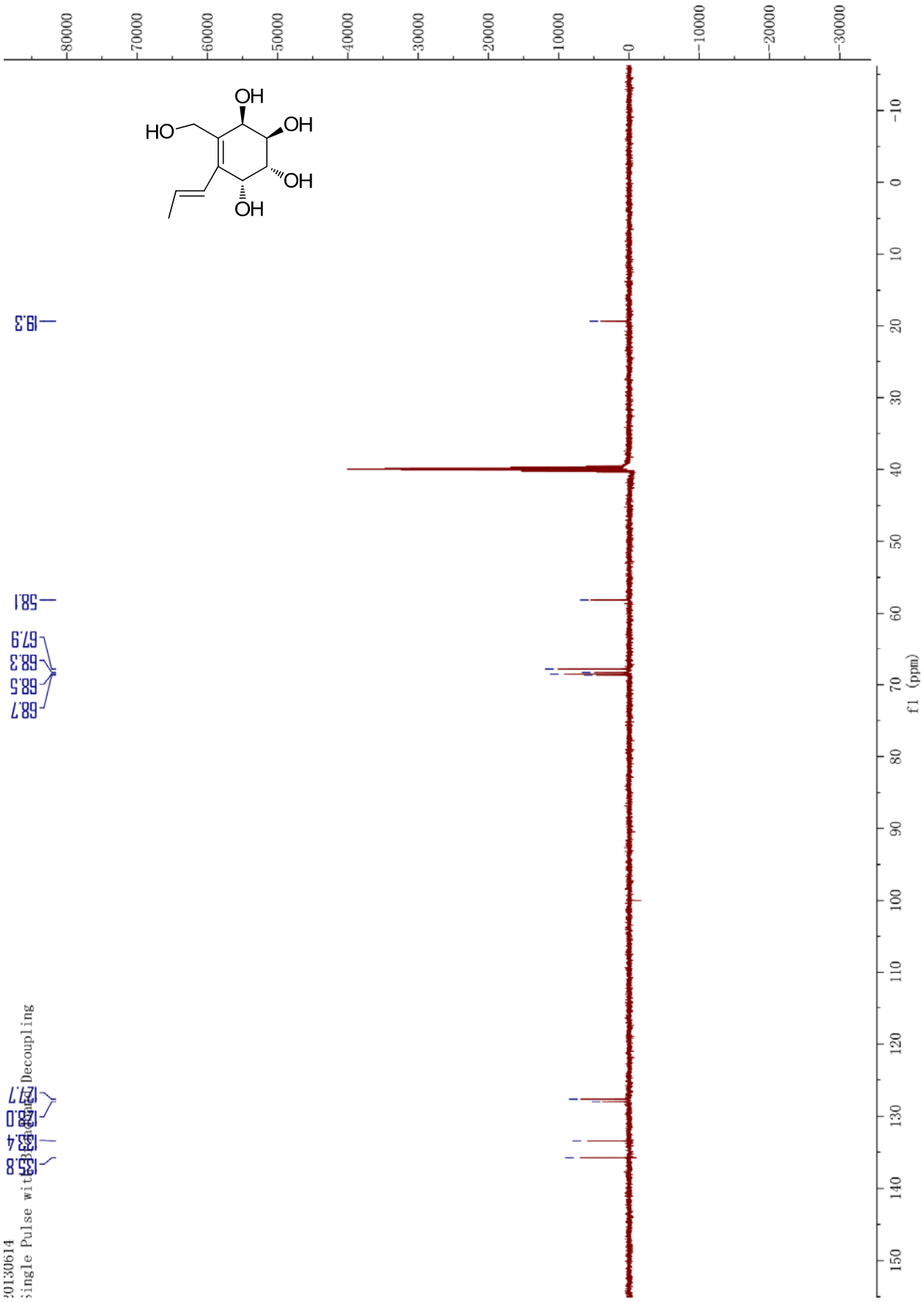

Figure S78. The DEPT spectrum of compound **14** in DMSO-d_6

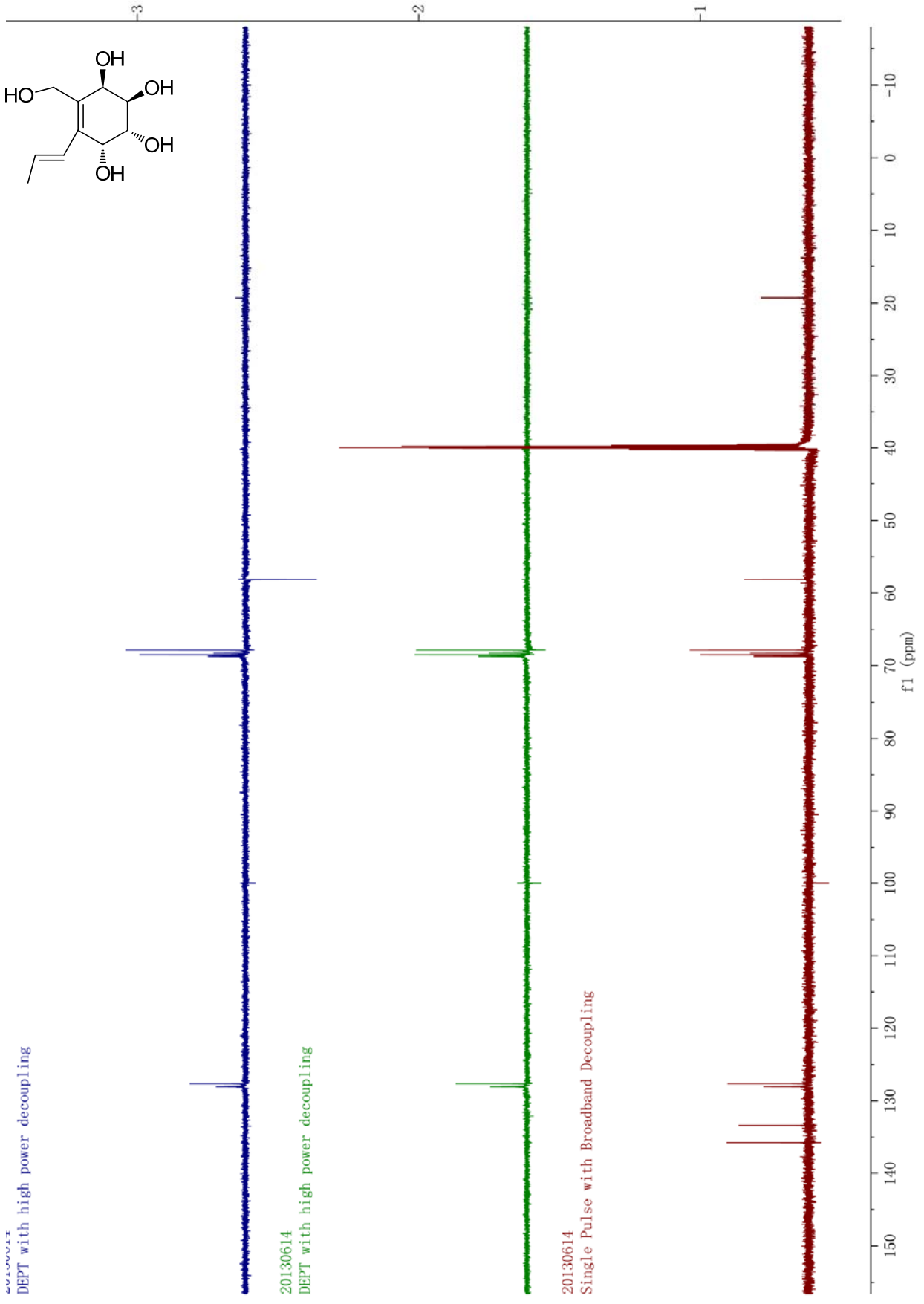

Figure S79. The HMQC spectrum of compound **14** in DMSO-d_6

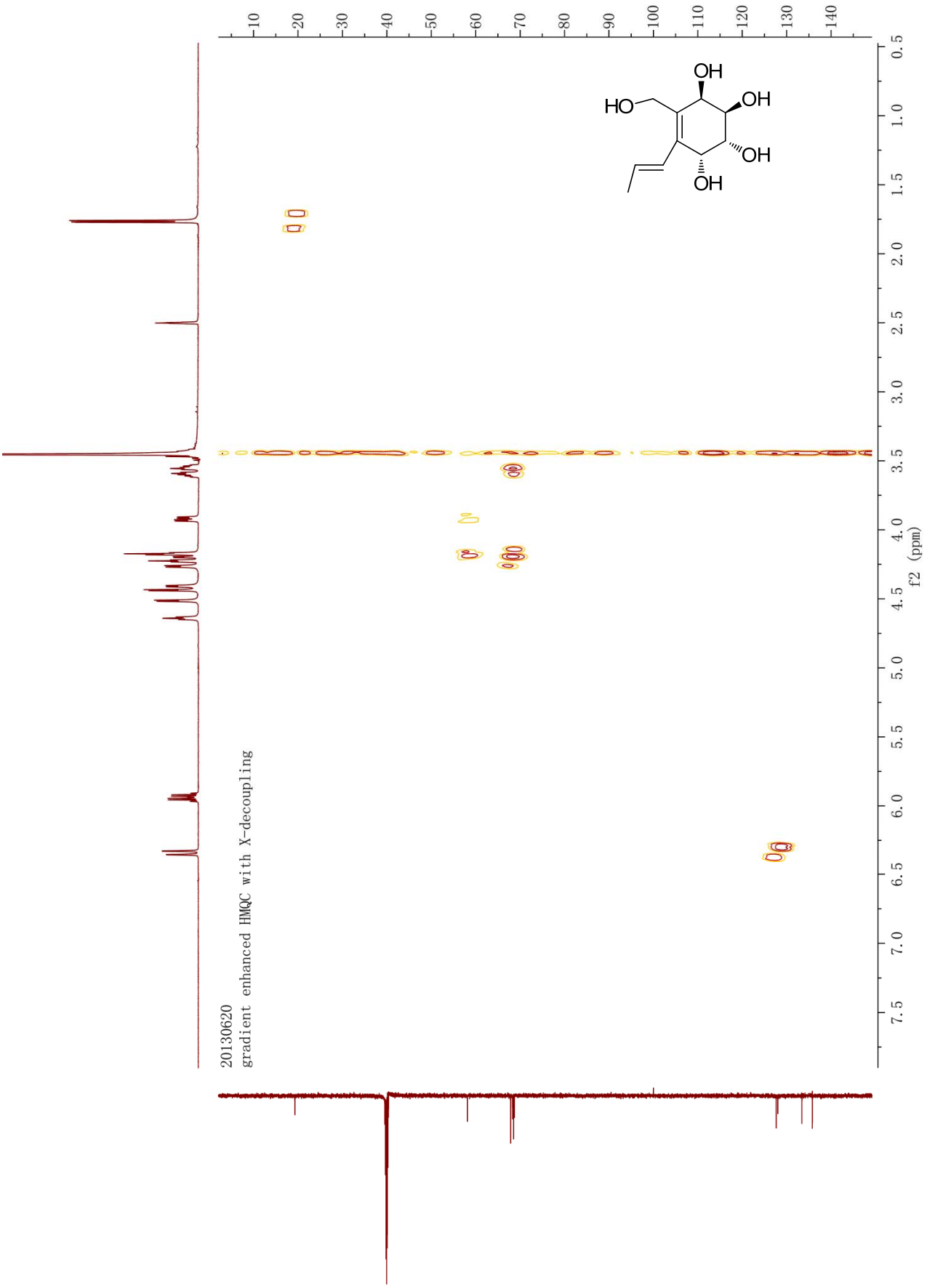

Figure S80. The ^{1}H-^{1}H COSY spectrum of compound **14** in DMSO-d_6

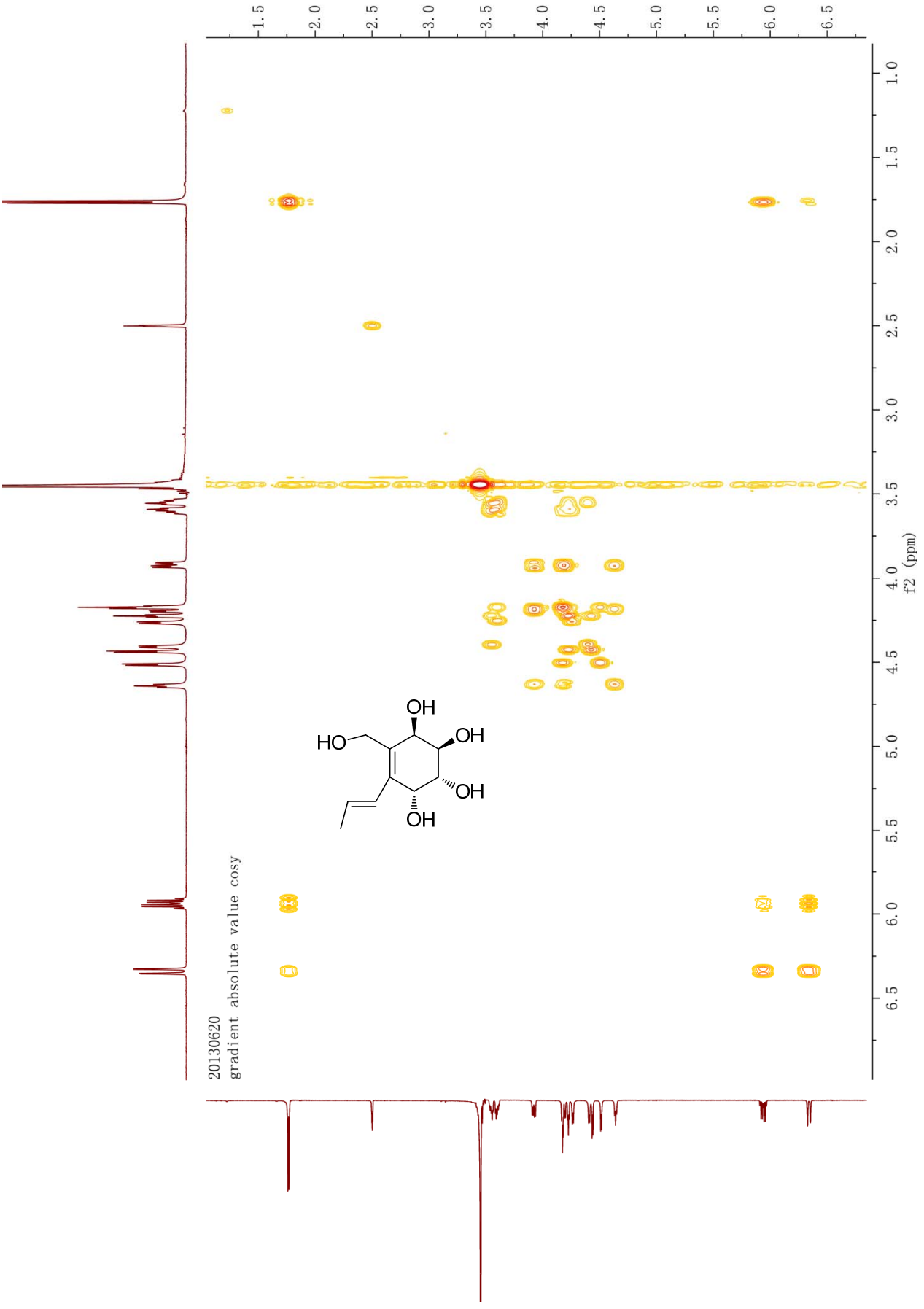

Figure S81. The HMBC spectrum of compound **14** in DMSO-d_6

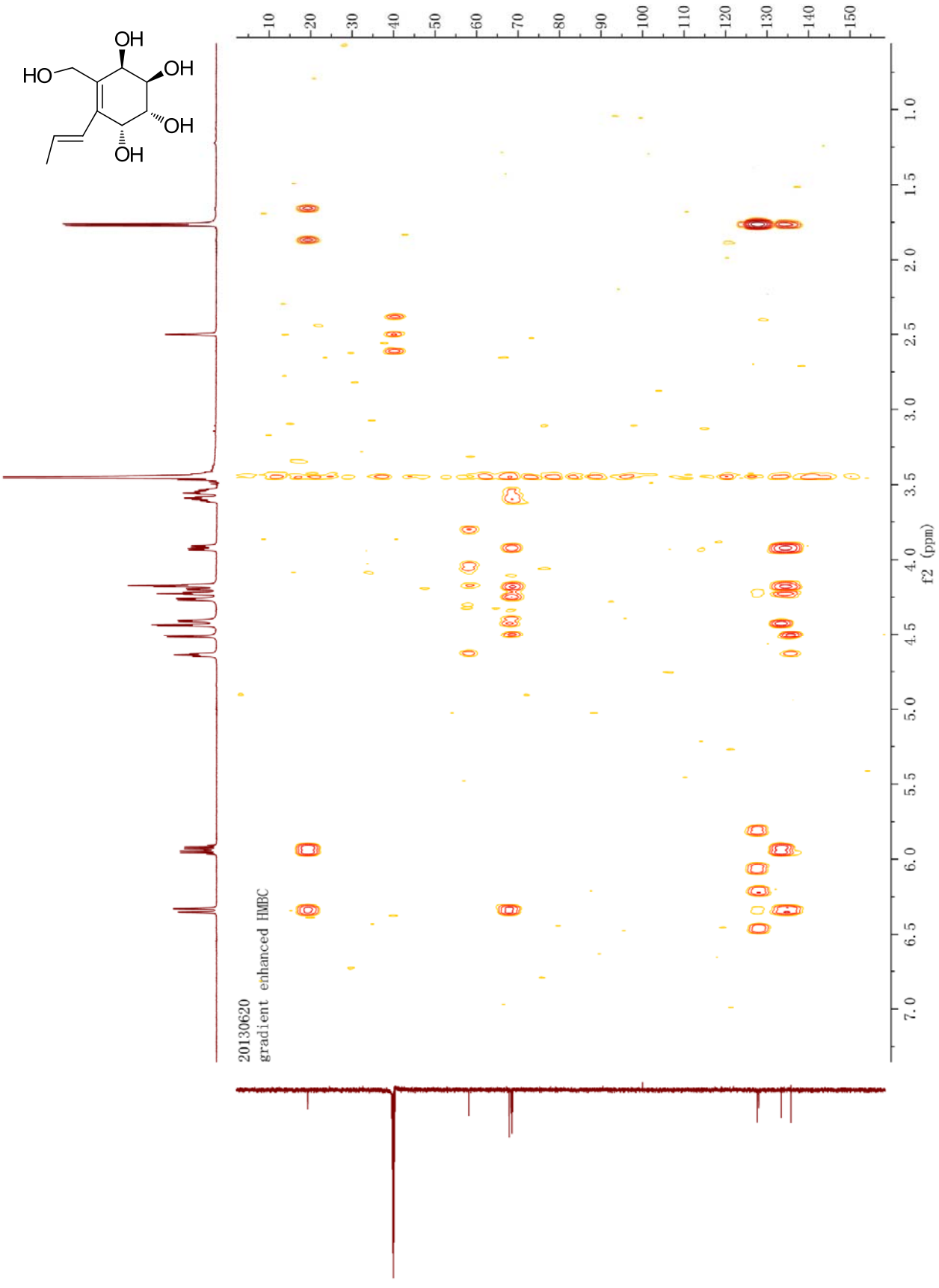

Figure S82. The ^{1}H-NMR spectrum of compound **15** in DMSO-d_6

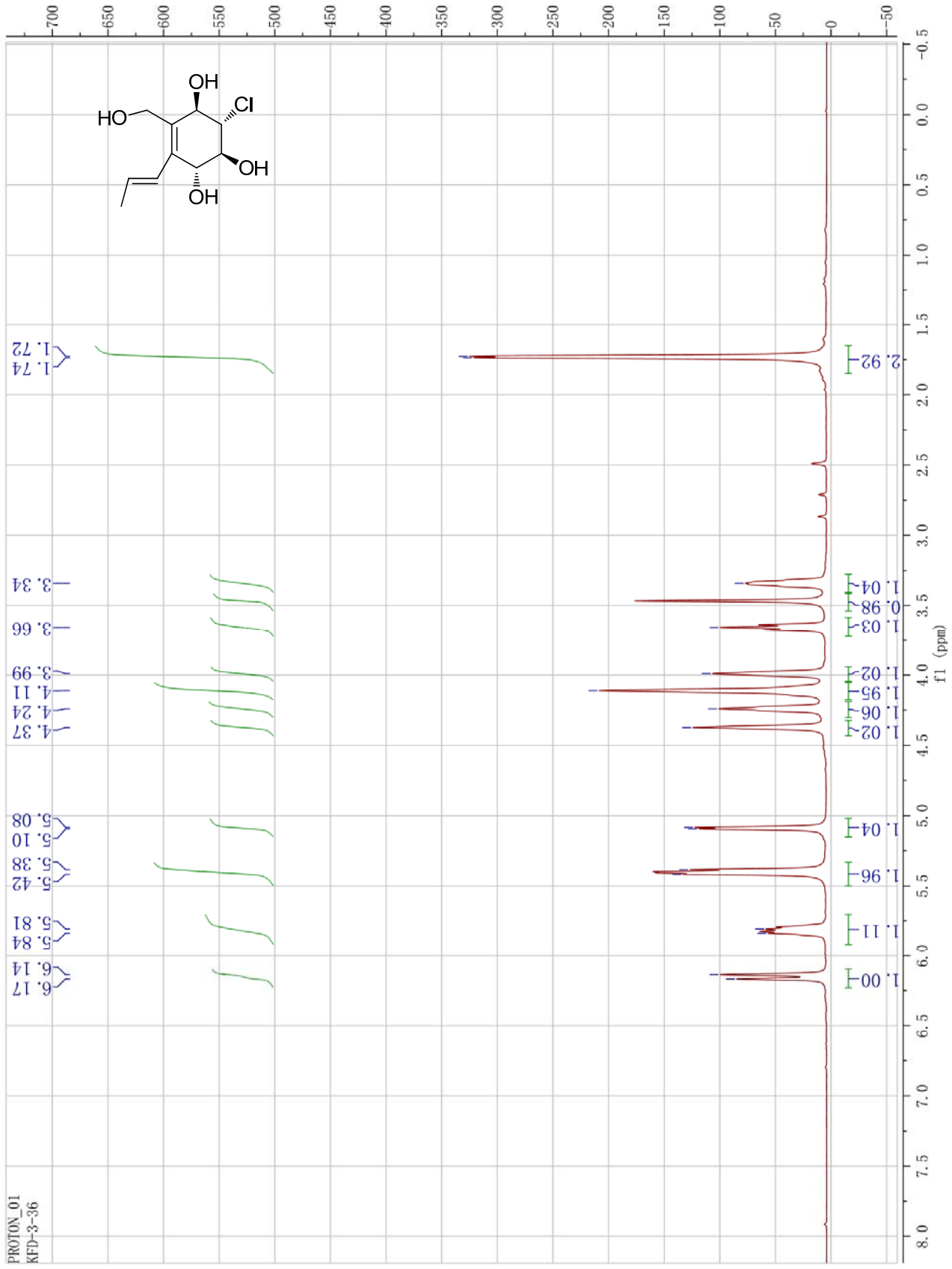

Figure S83. The ^{13}C-NMR spectrum of compound **15** in DMSO-d_6

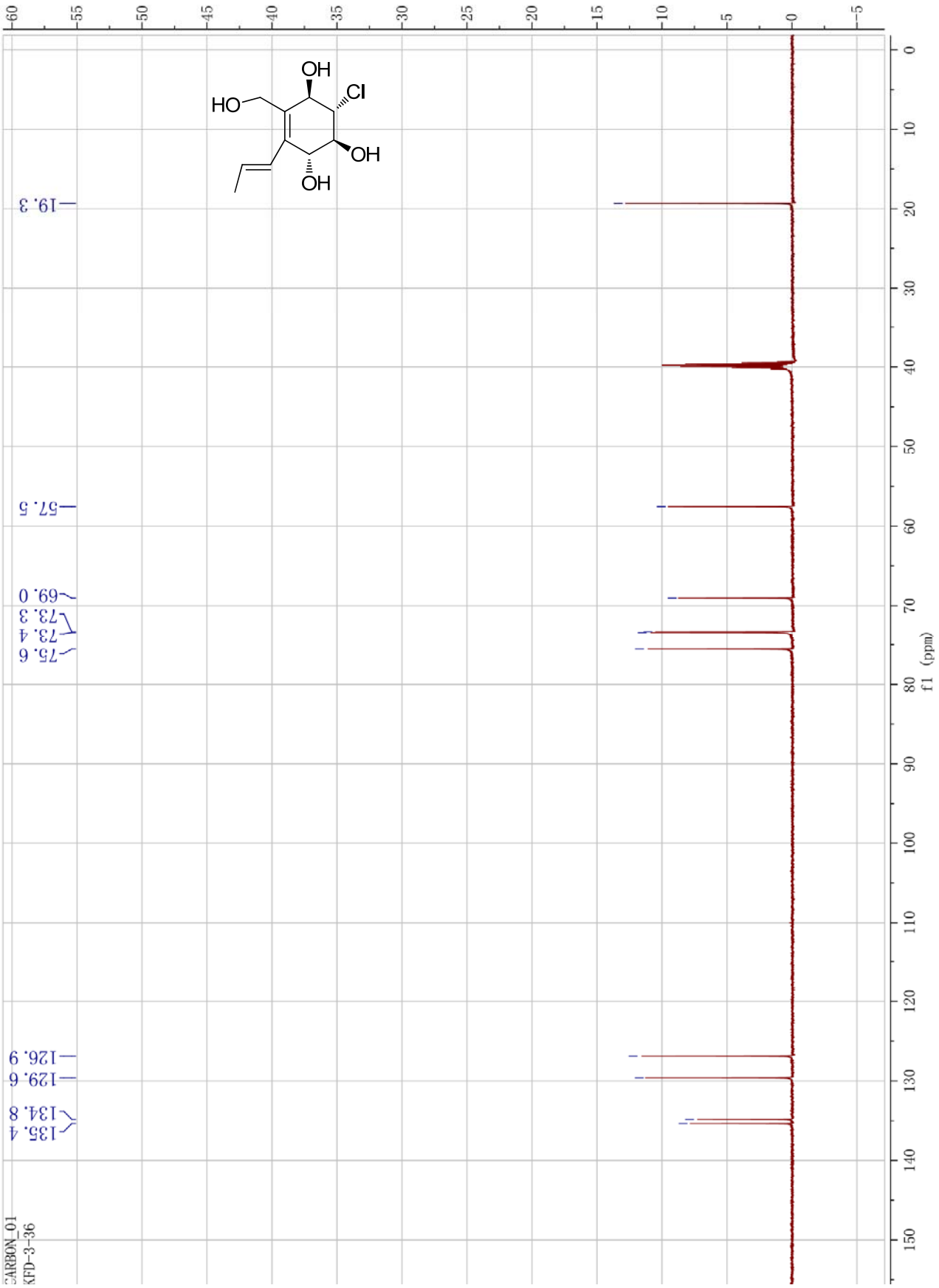

Figure S84. The DEPT spectrum of compound **15** in DMSO-d_6

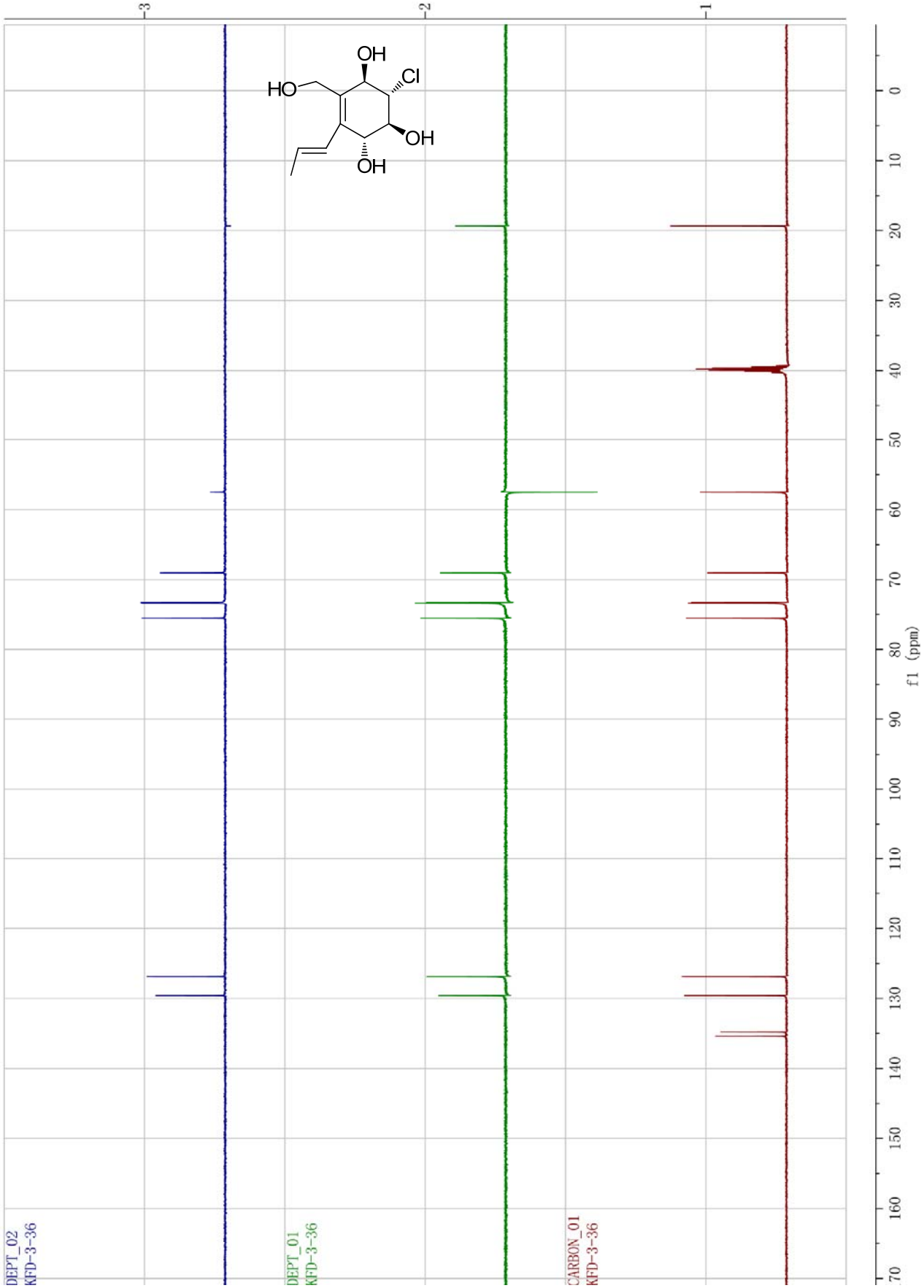

Figure S85. The HMQC spectrum of compound **15** in DMSO-d_6

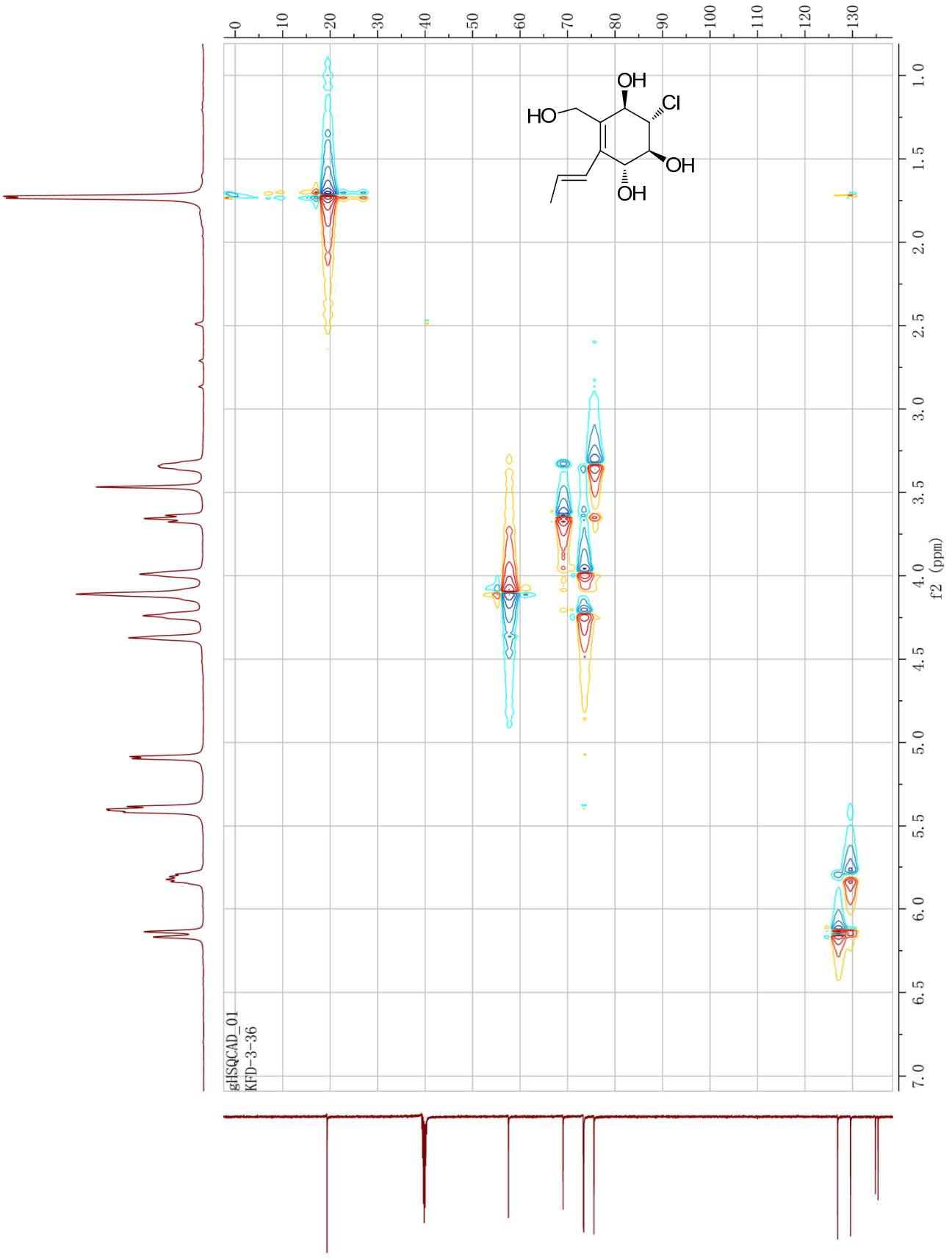

Figure S86. The ^{1}H-^{1}H COSY spectrum of compound **15** in DMSO-d_6

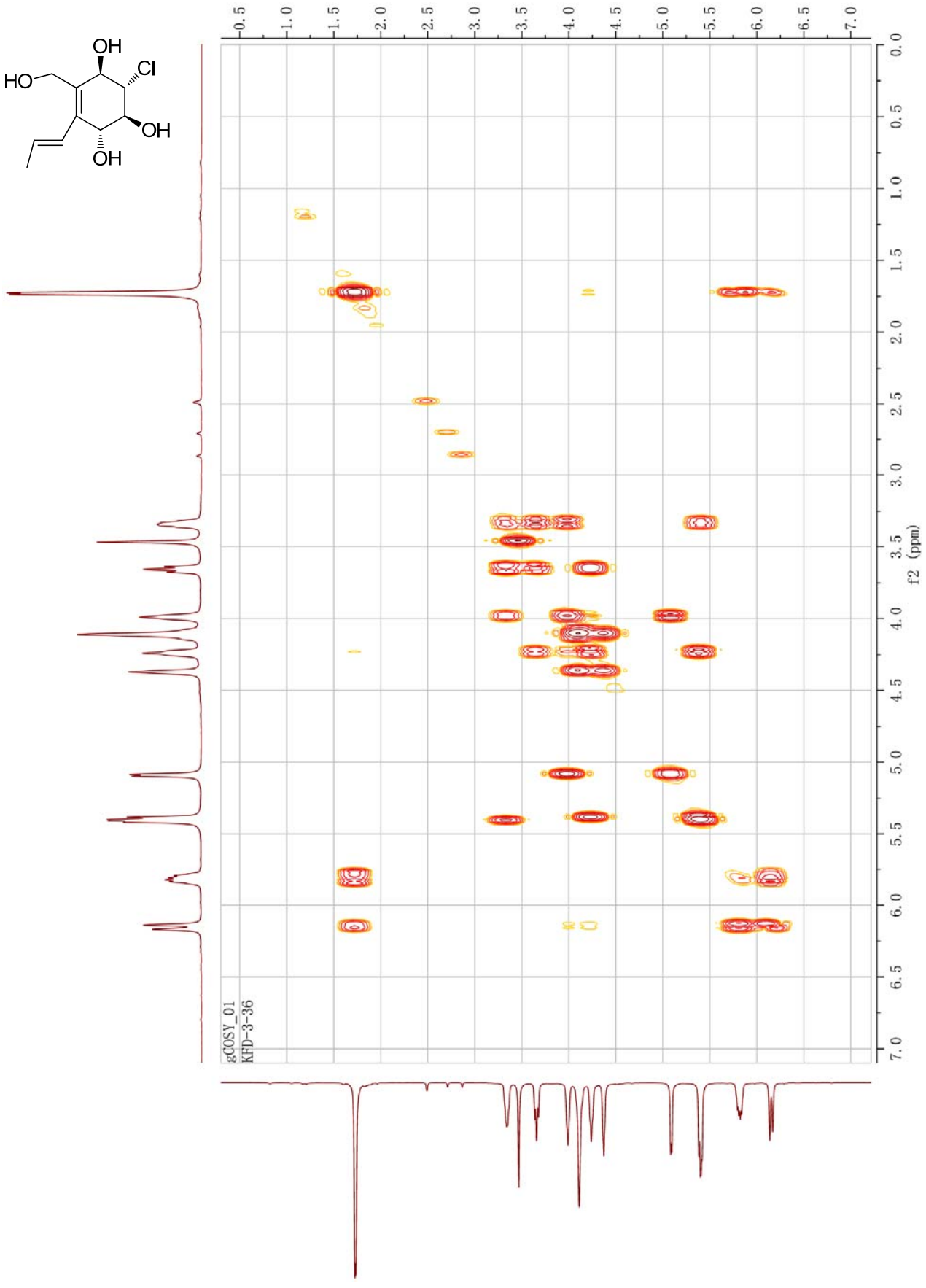

Figure S87. The HMBC spectrum of compound **15** in DMSO-d_6

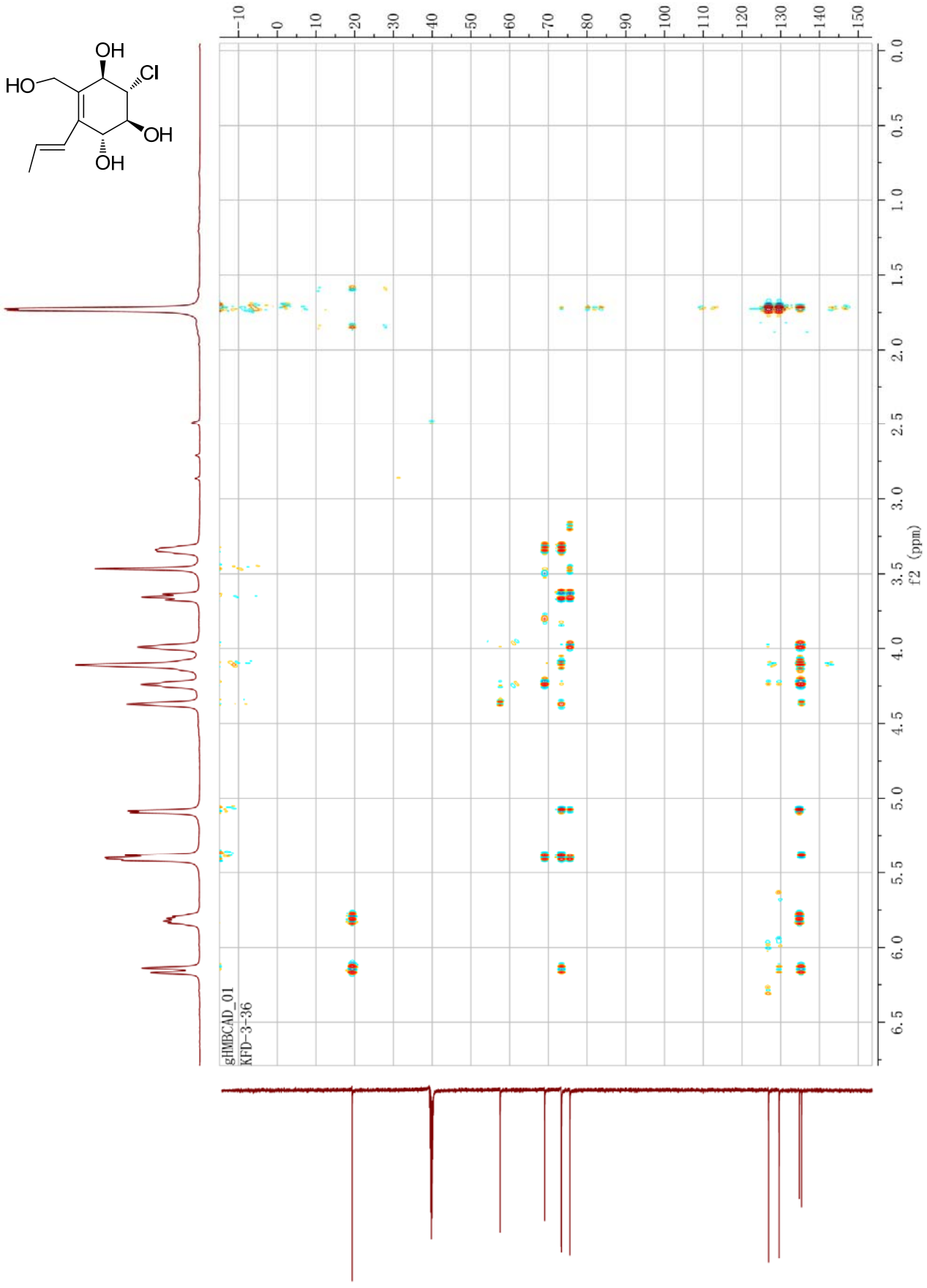

Figure S88. The ^{1}H-NMR spectrum of compound **16** in DMSO-d_6

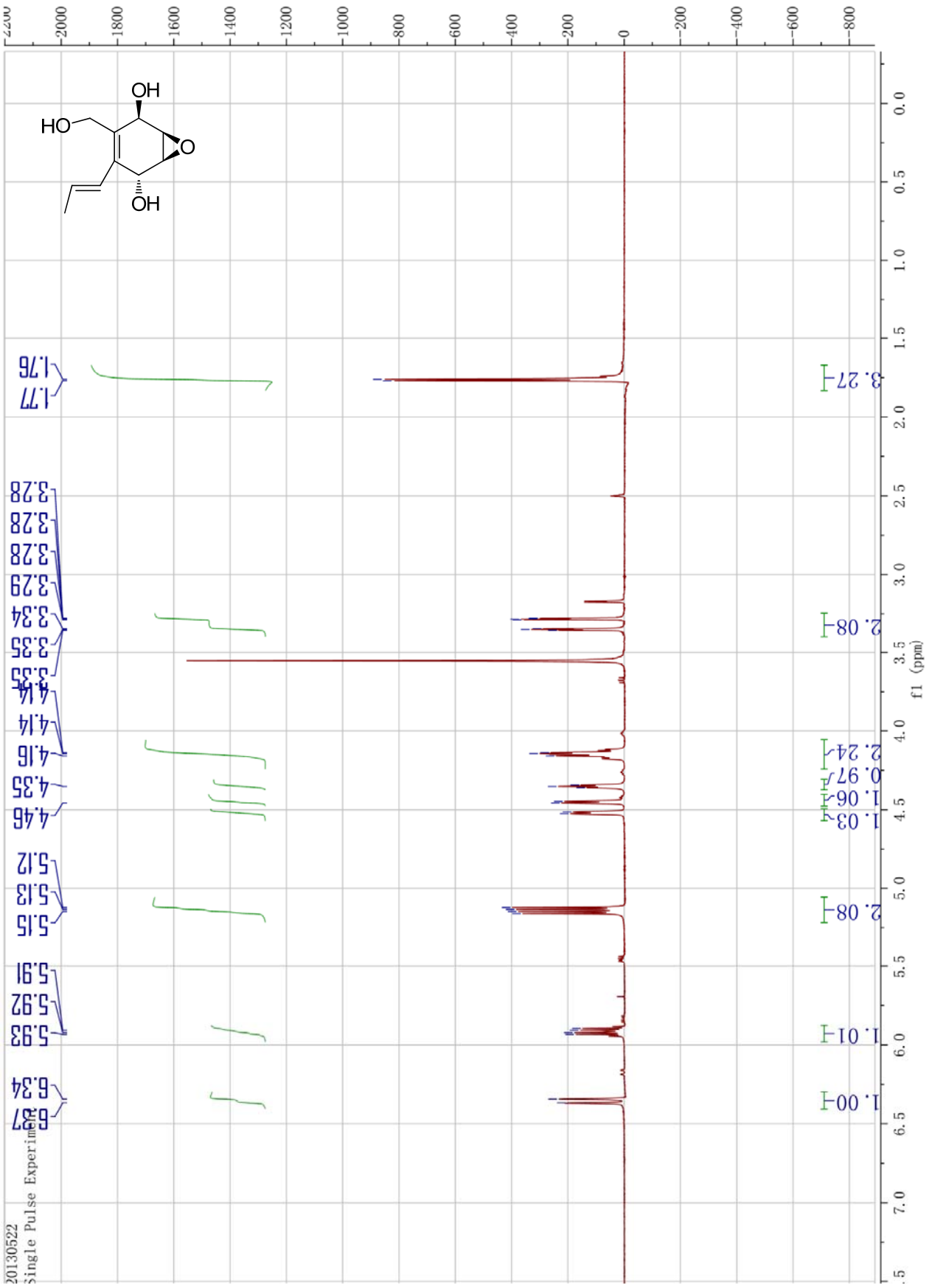

Figure S89. The ^{13}C-NMR spectrum of compound **16** in DMSO-d_6

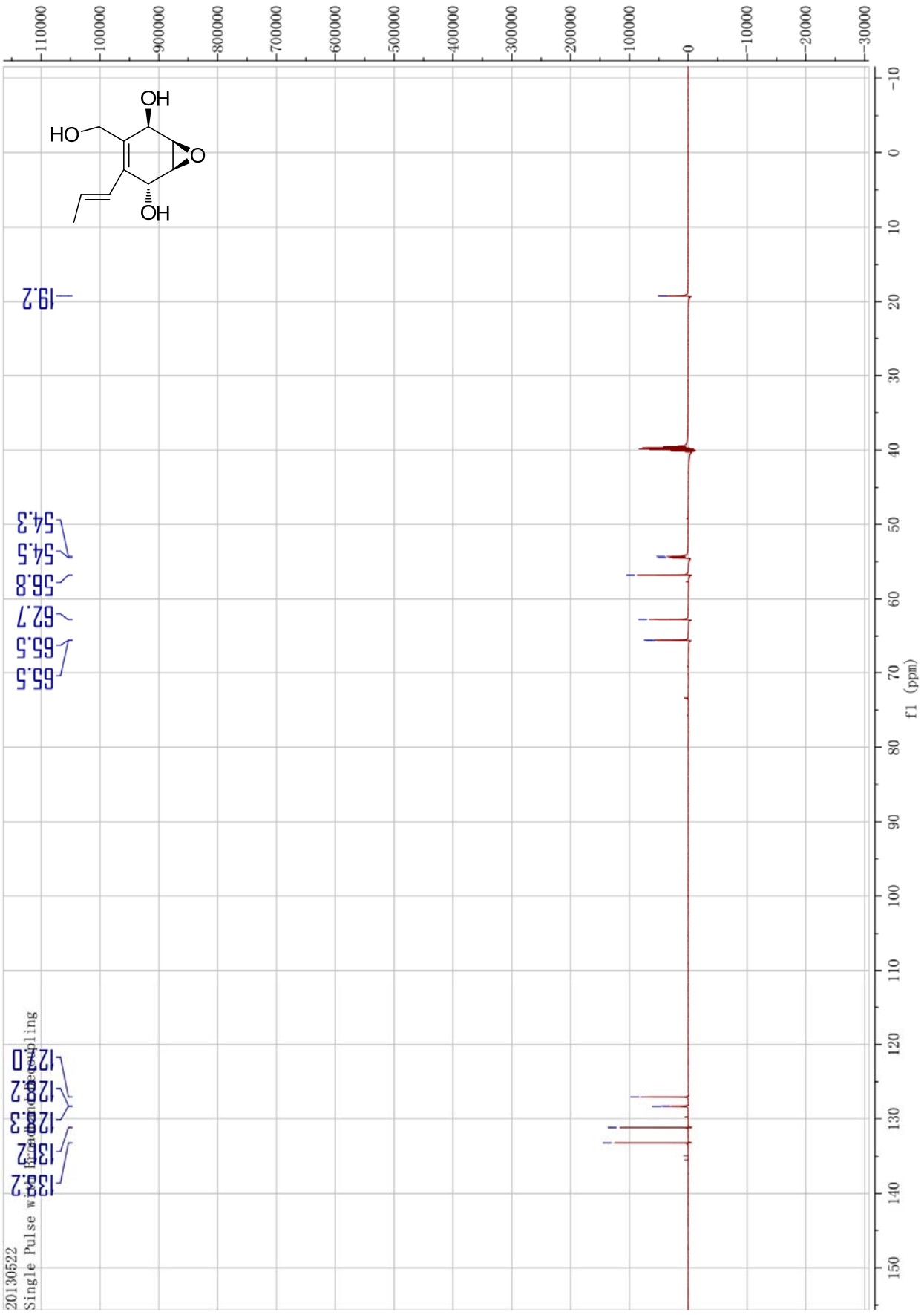

Figure S90. The DEPT spectrum of compound **16** in DMSO-d_6

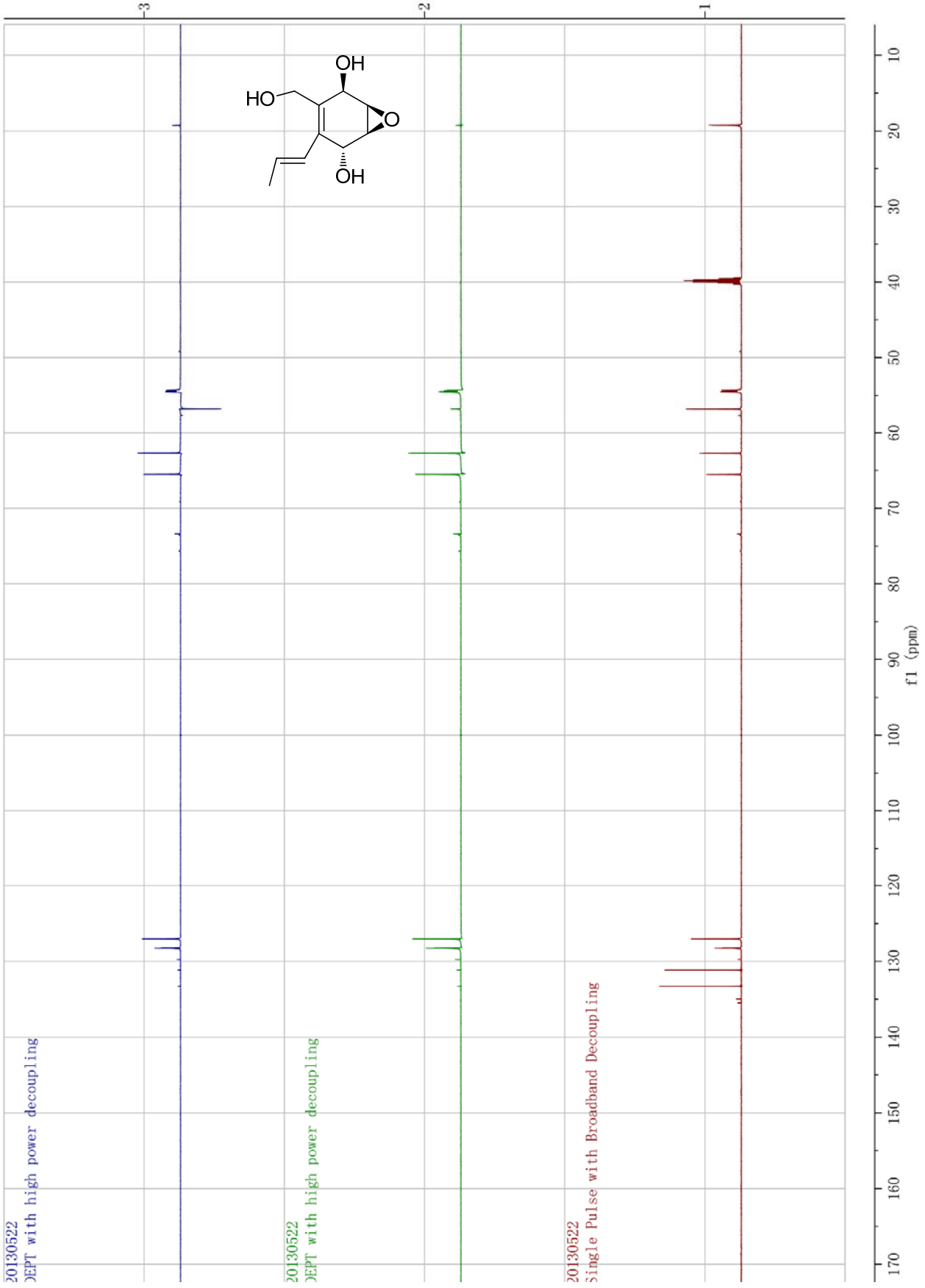

Figure S91. The HMQC spectrum of compound **16** in DMSO-d_6

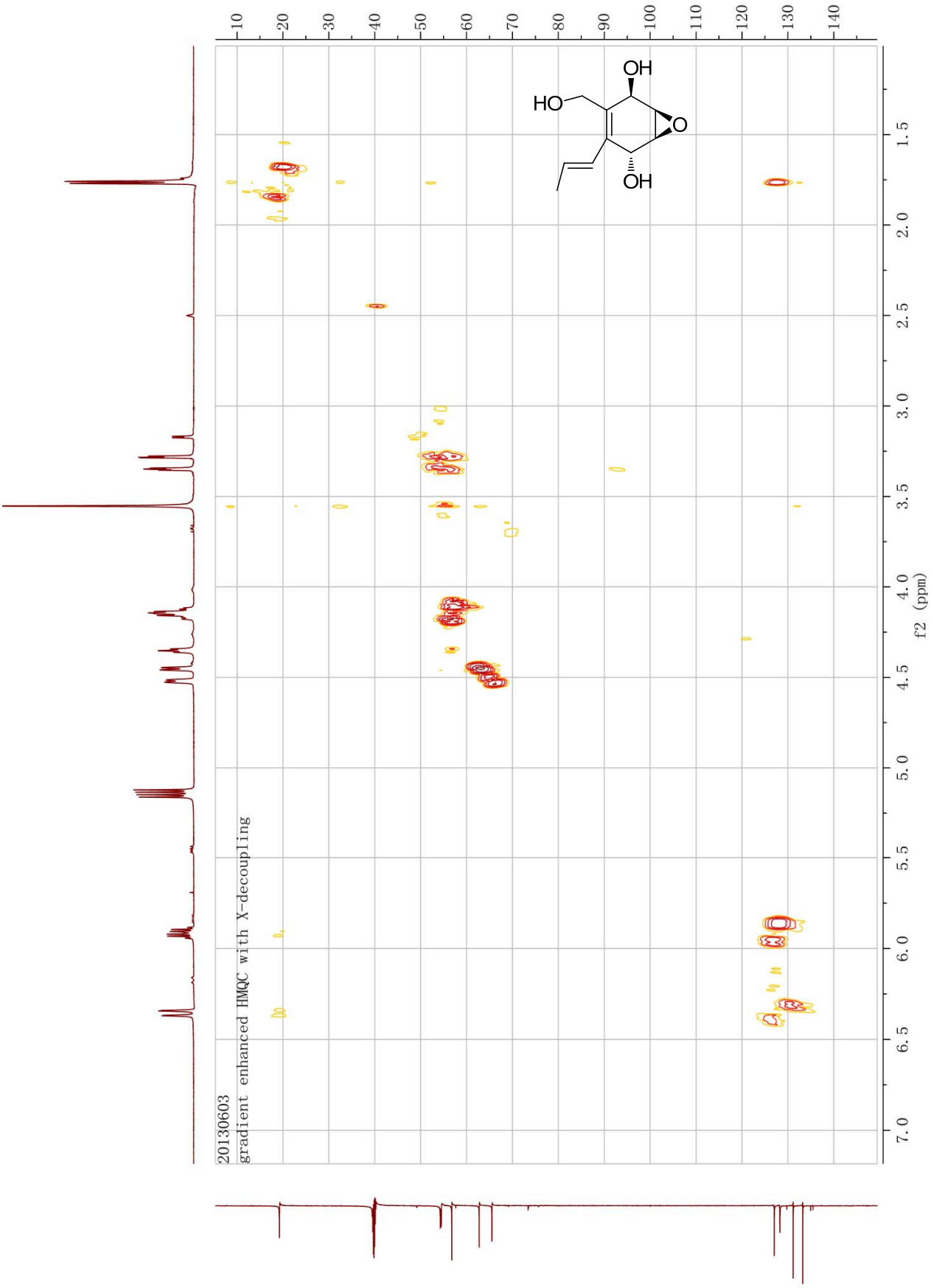

Figure S92. The ^{1}H-^{1}H COSY spectrum of compound **16** in DMSO-d_6

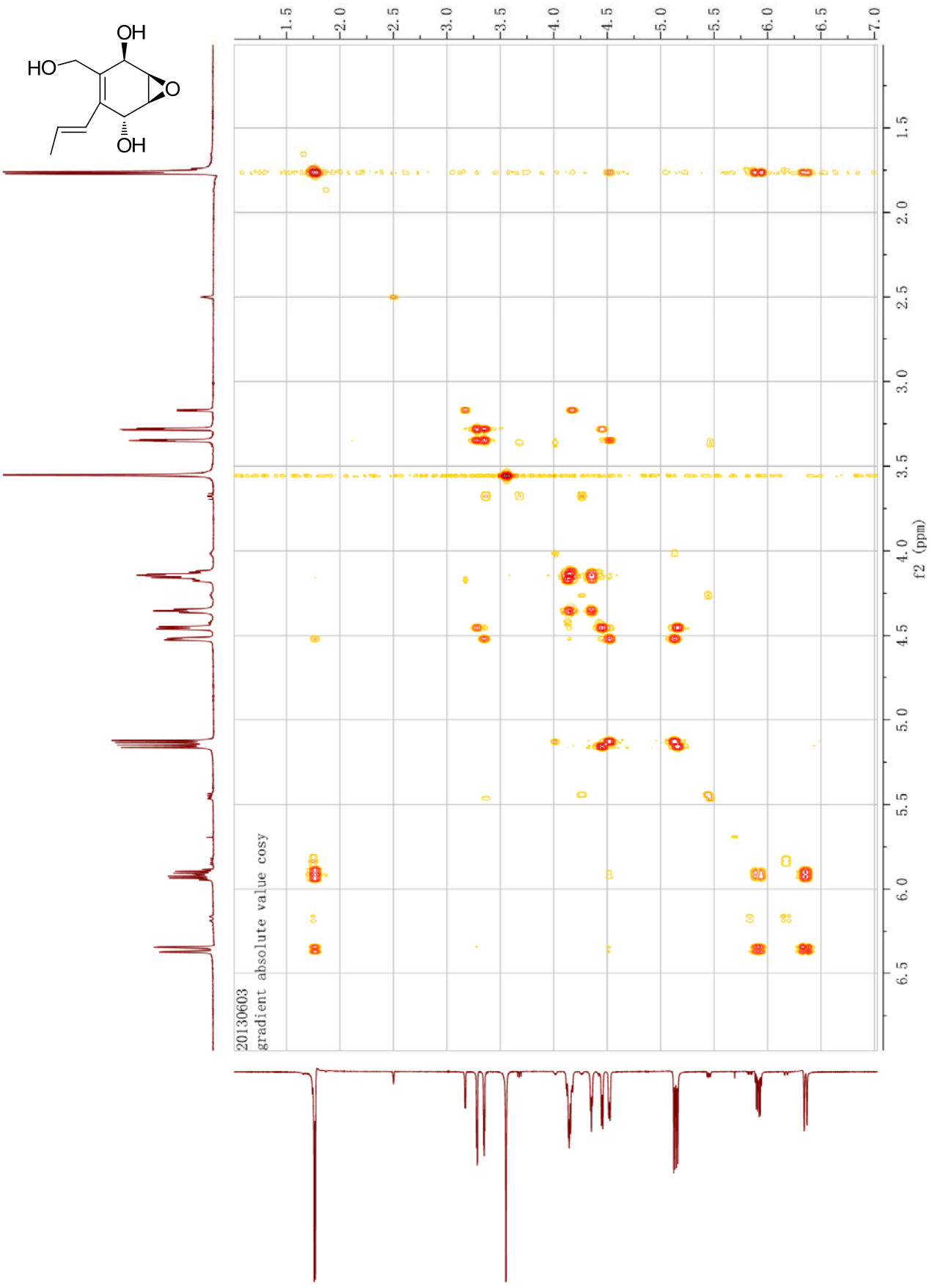

Figure S93. The HMBC spectrum of compound **16** in DMSO-d_6

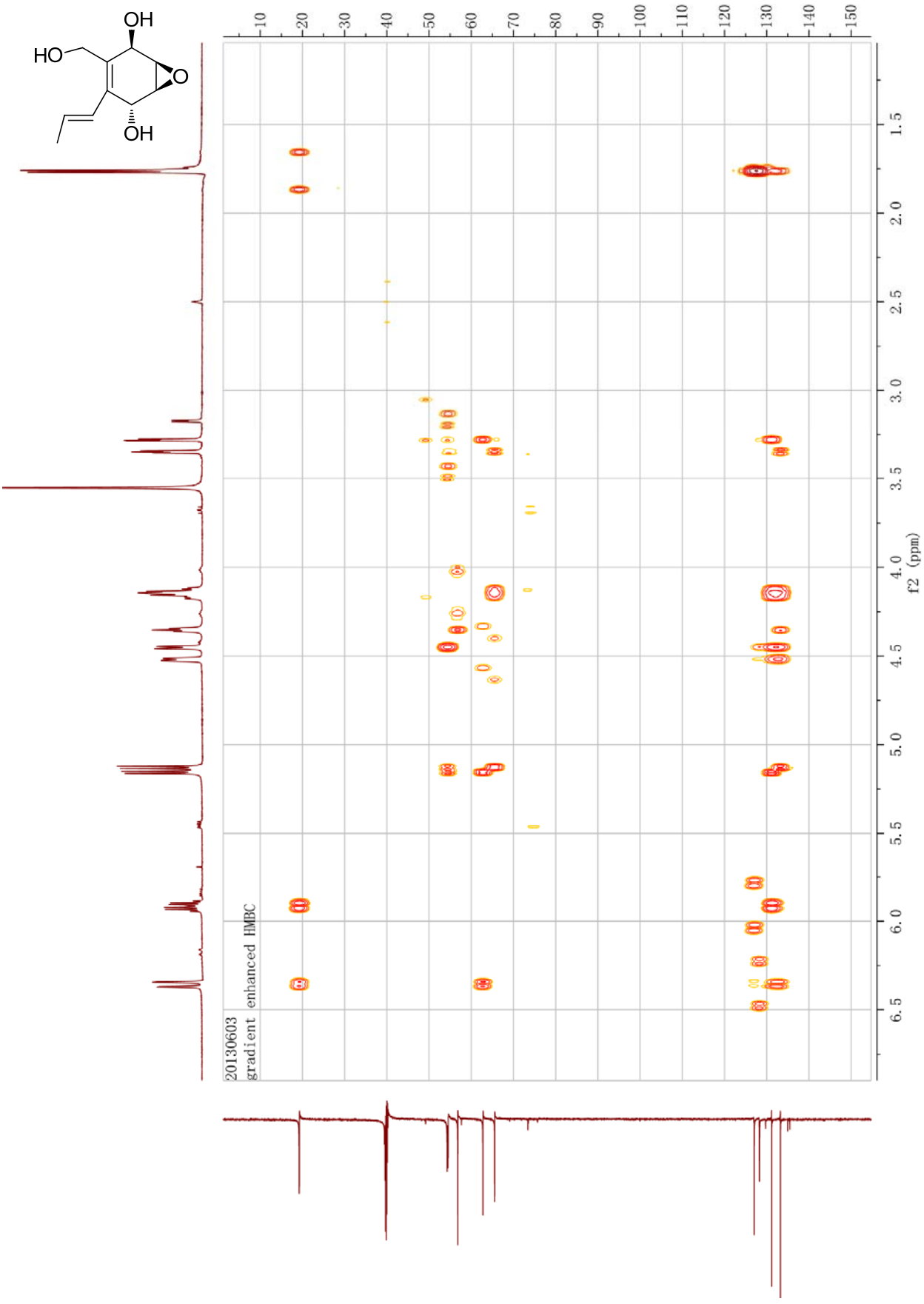

Figure S94. The ^{1}H-NMR spectrum of compound **17** in DMSO-d_6

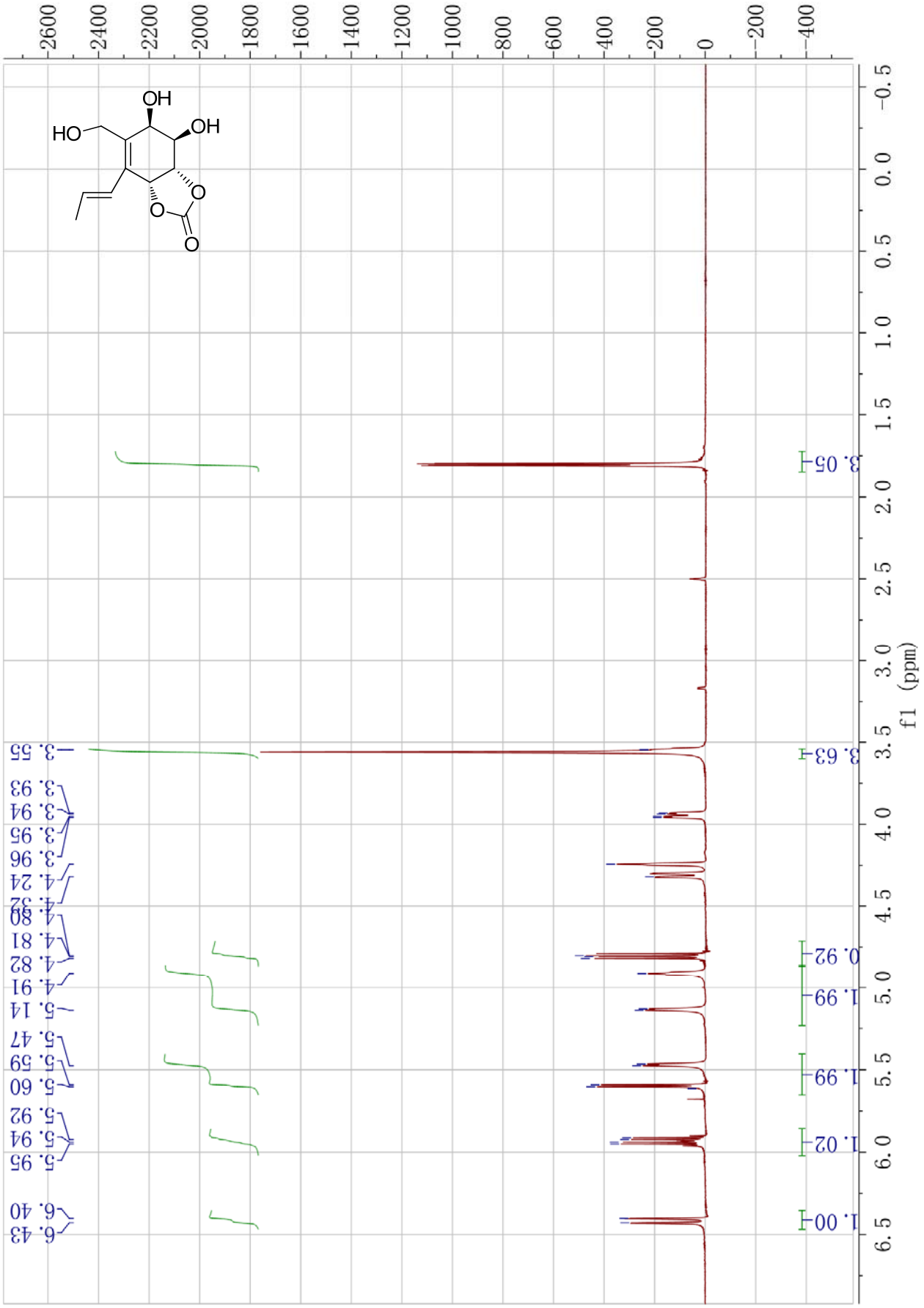

Figure S95. The ^{13}C-NMR spectrum of compound **17** in DMSO-d_6

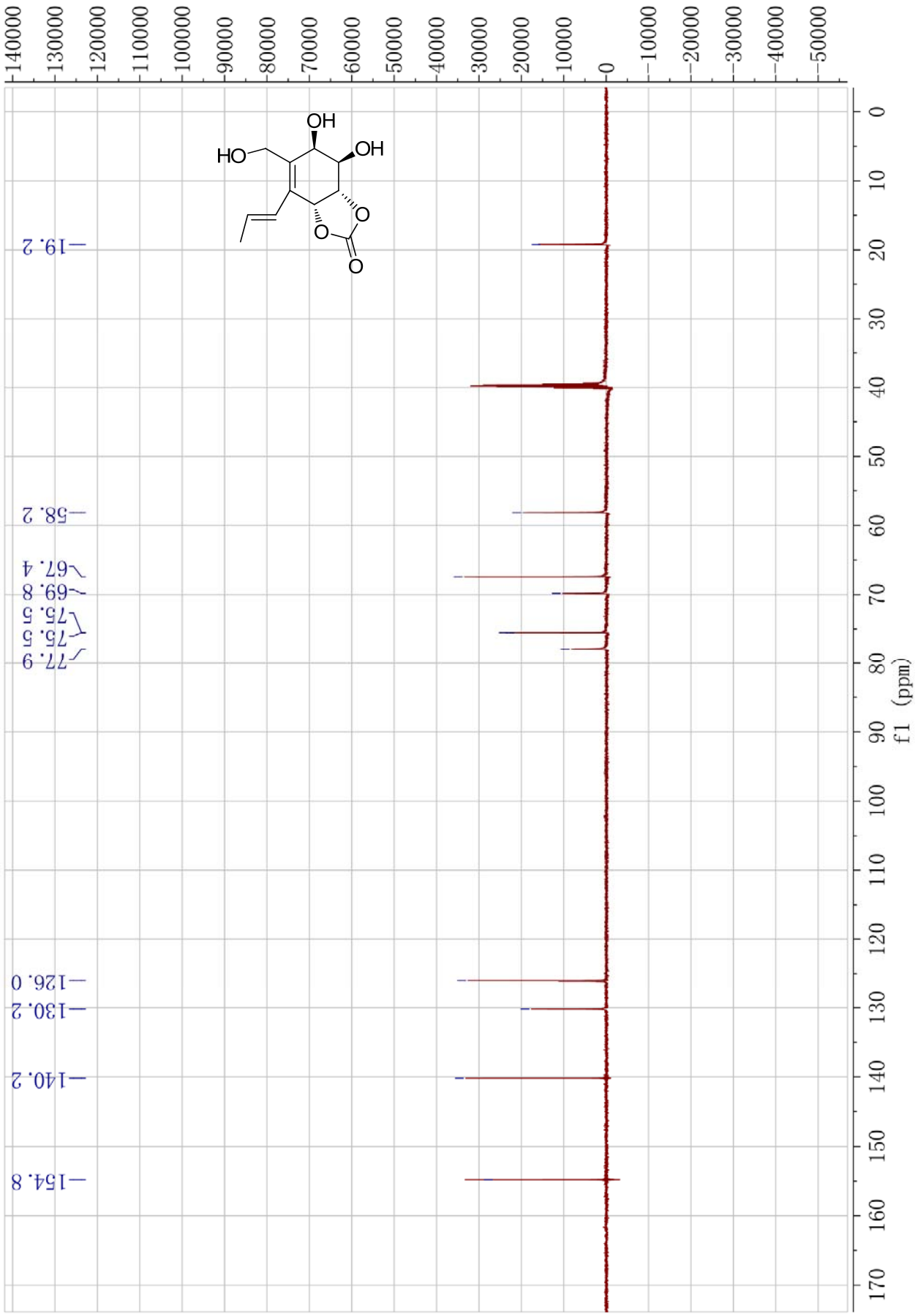

Figure S96. The DEPT spectrum of compound **17** in DMSO-d_6

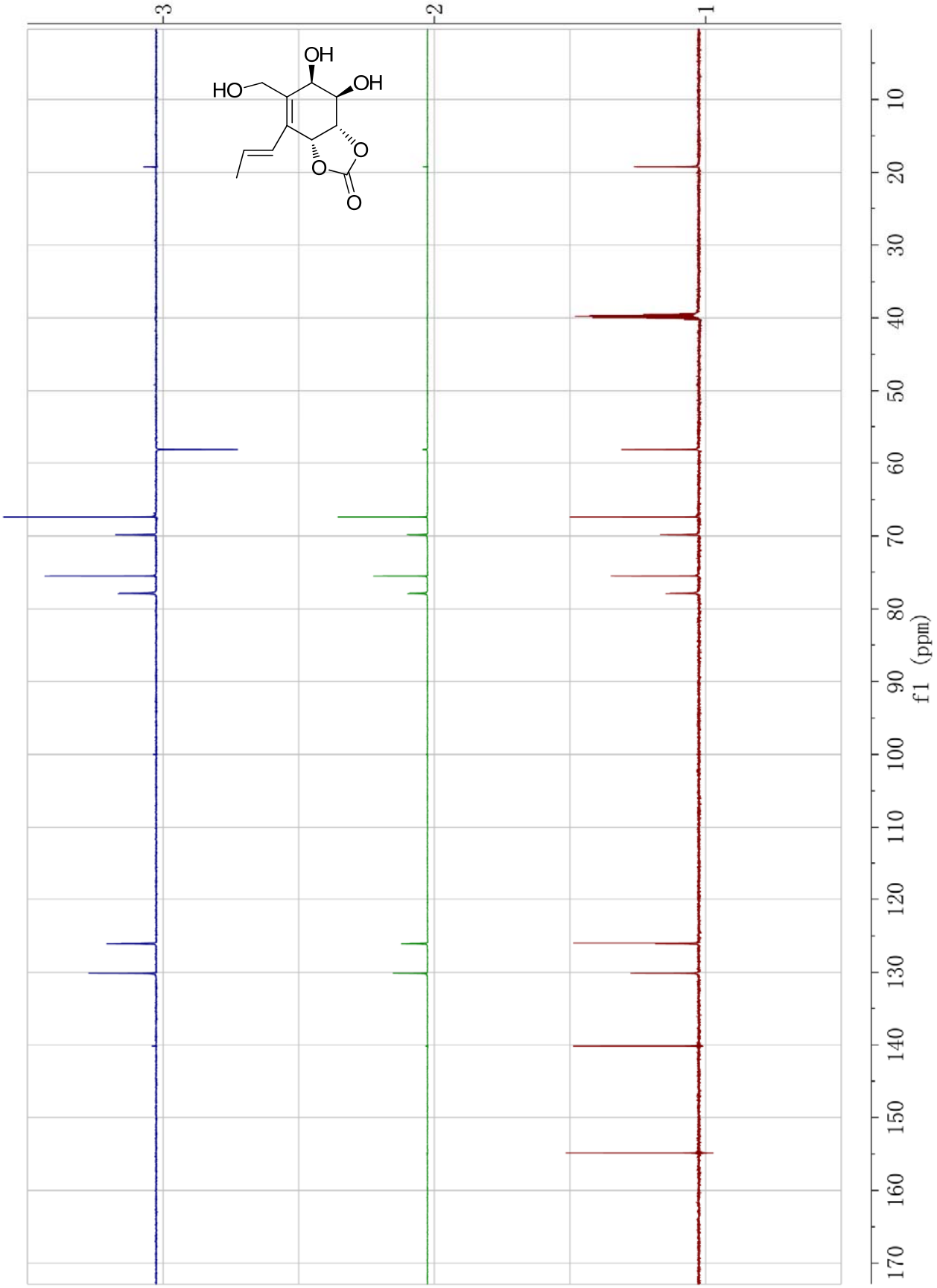

Figure S97. The HMQC spectrum of compound **17** in DMSO-d_6

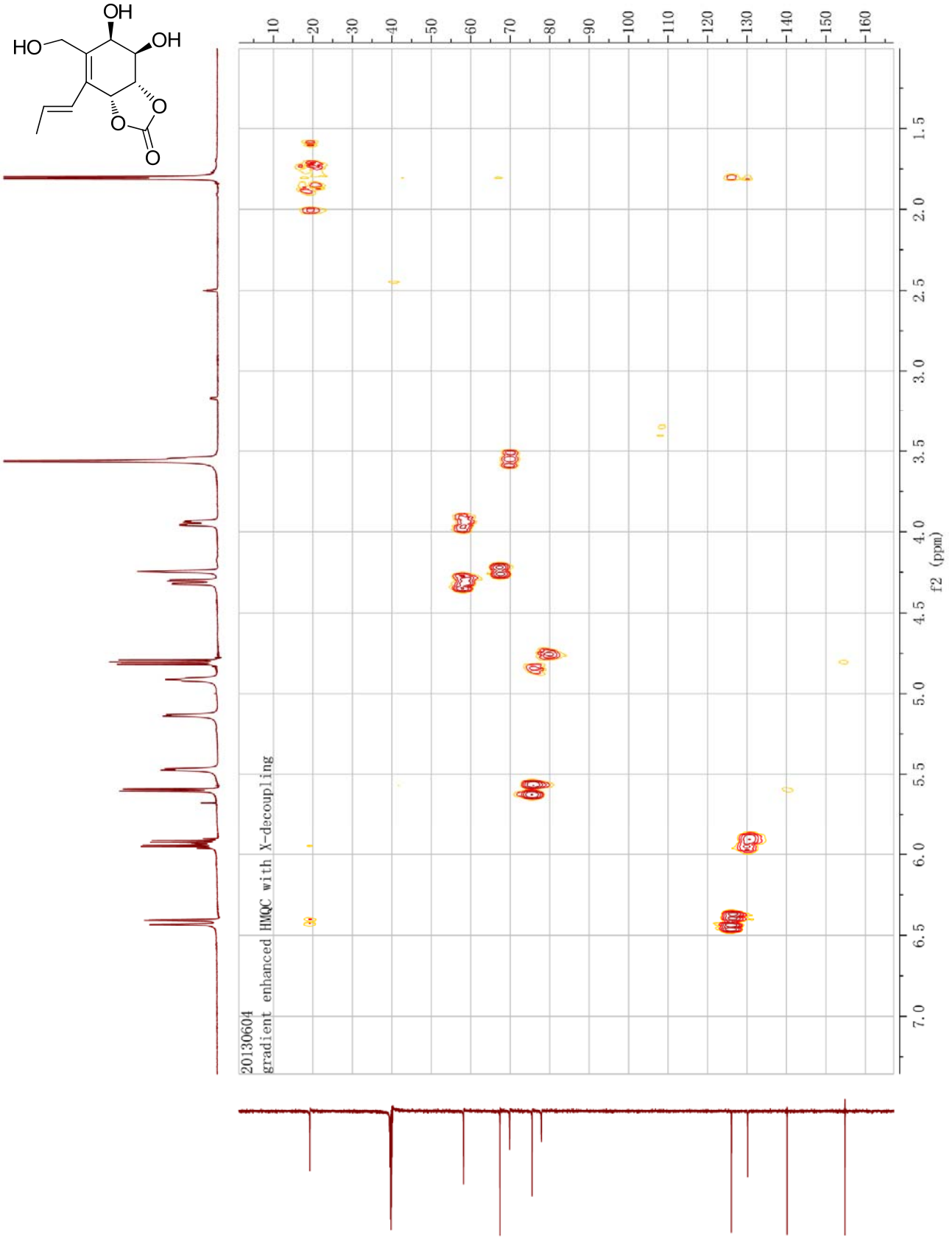

Figure S98. The ^{1}H-^{1}H COSY spectrum of compound **17** in DMSO-d_6

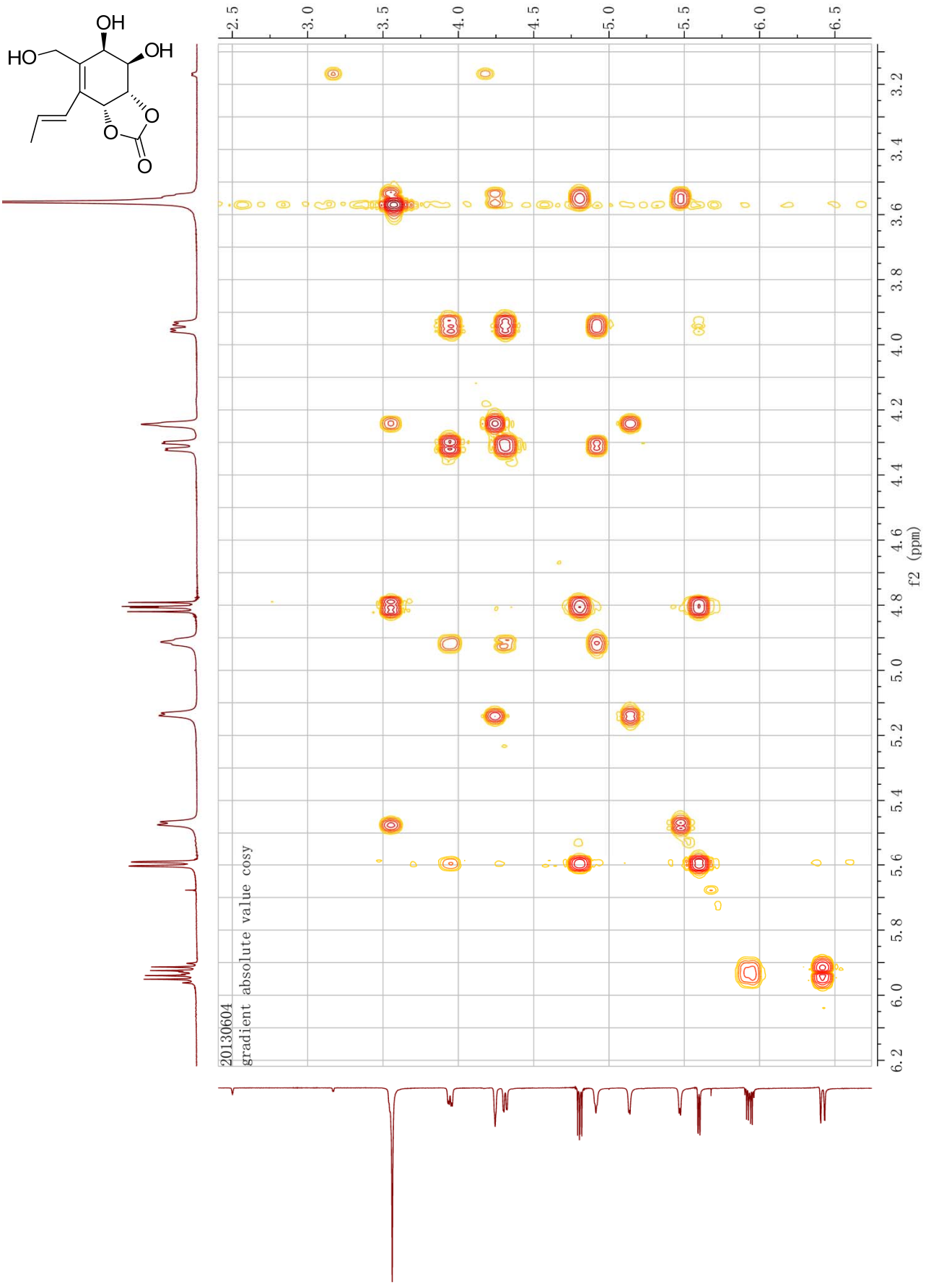

Figure S99. The HMBC spectrum of compound **17** in DMSO-d_6

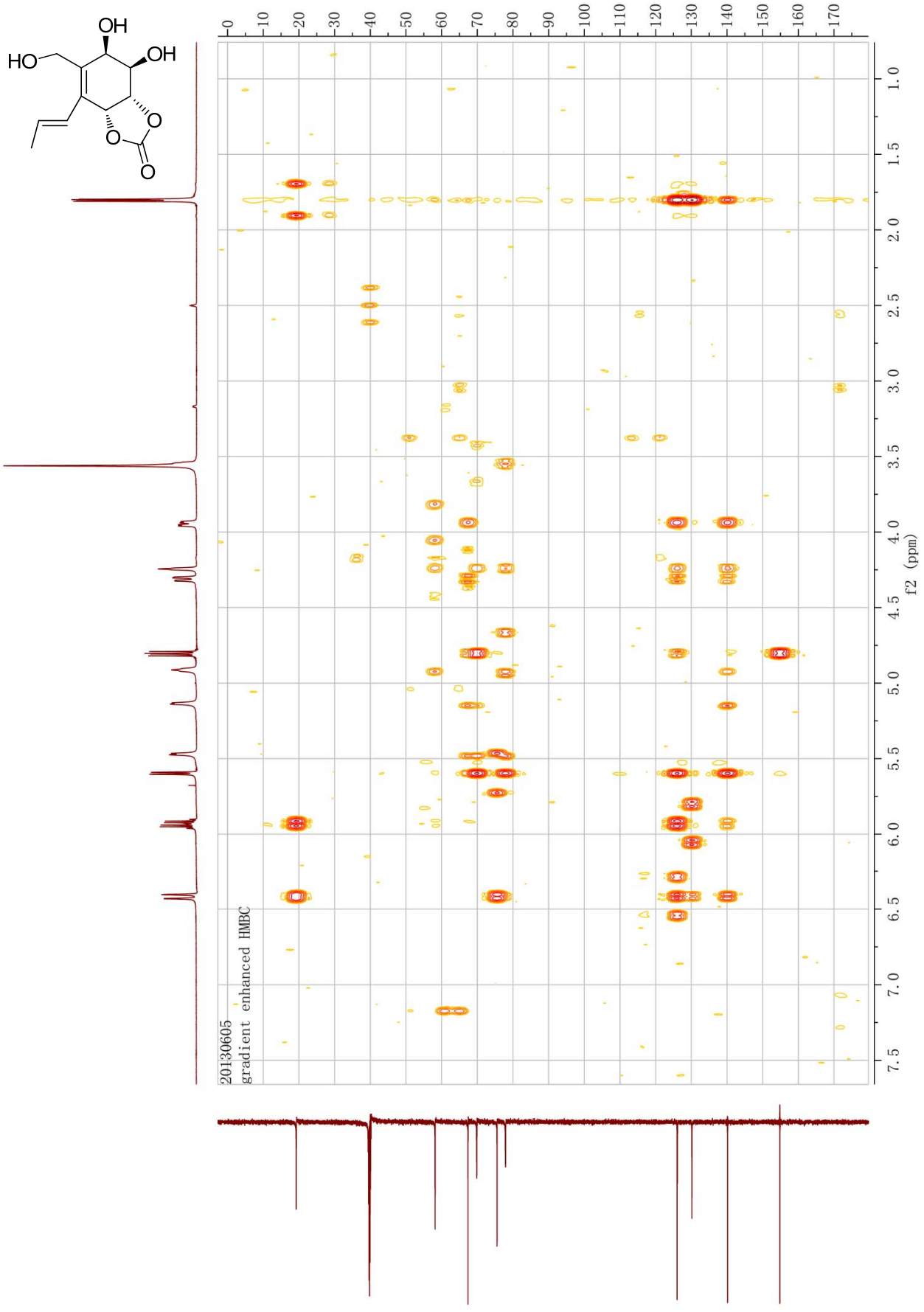

Figure S100. The ^{1}H-NMR spectrum of compound **18** in $CDCl_3$

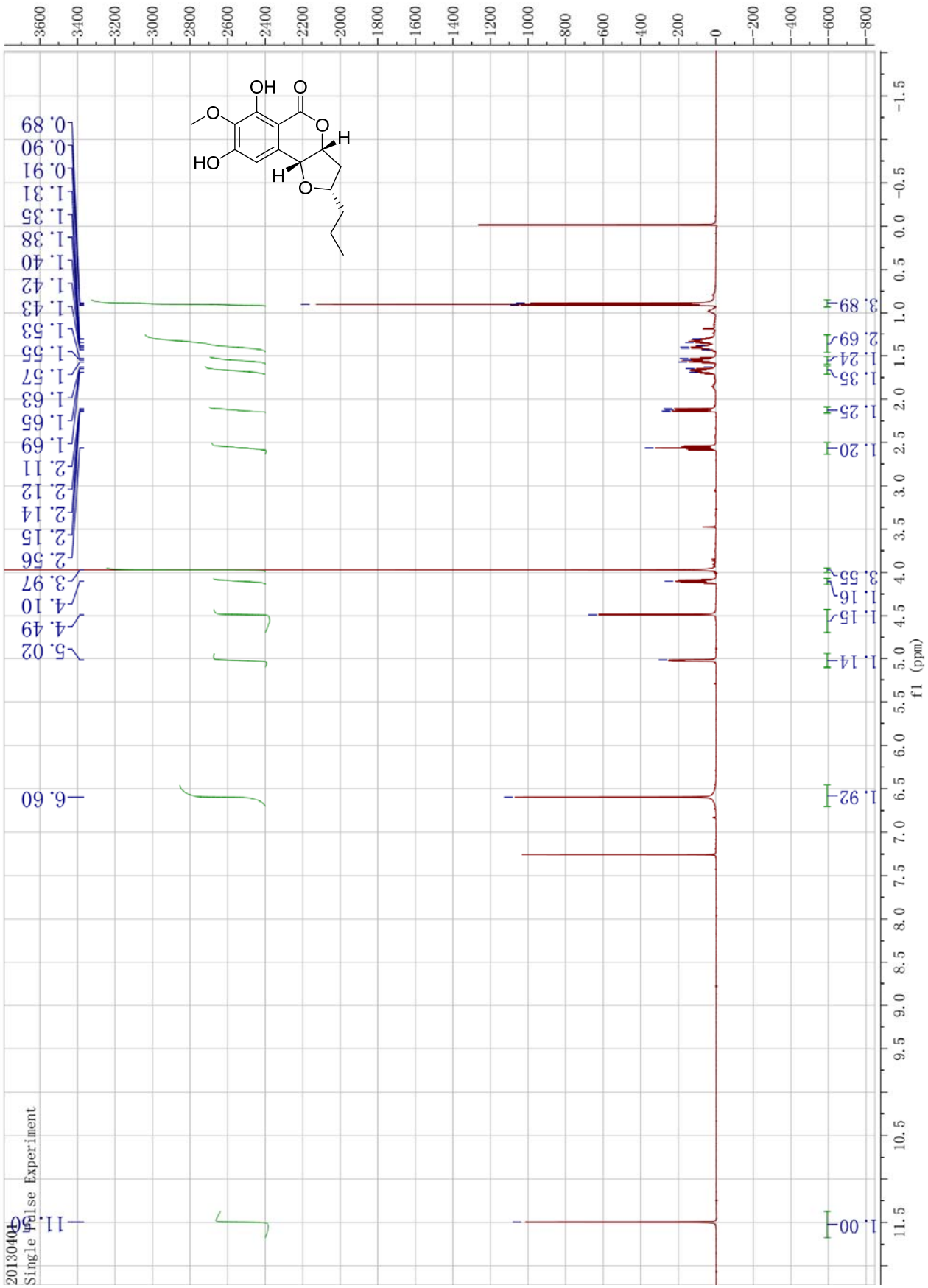

Figure S101. The ^{13}C-NMR spectrum of compound **18** in $CDCl_3$

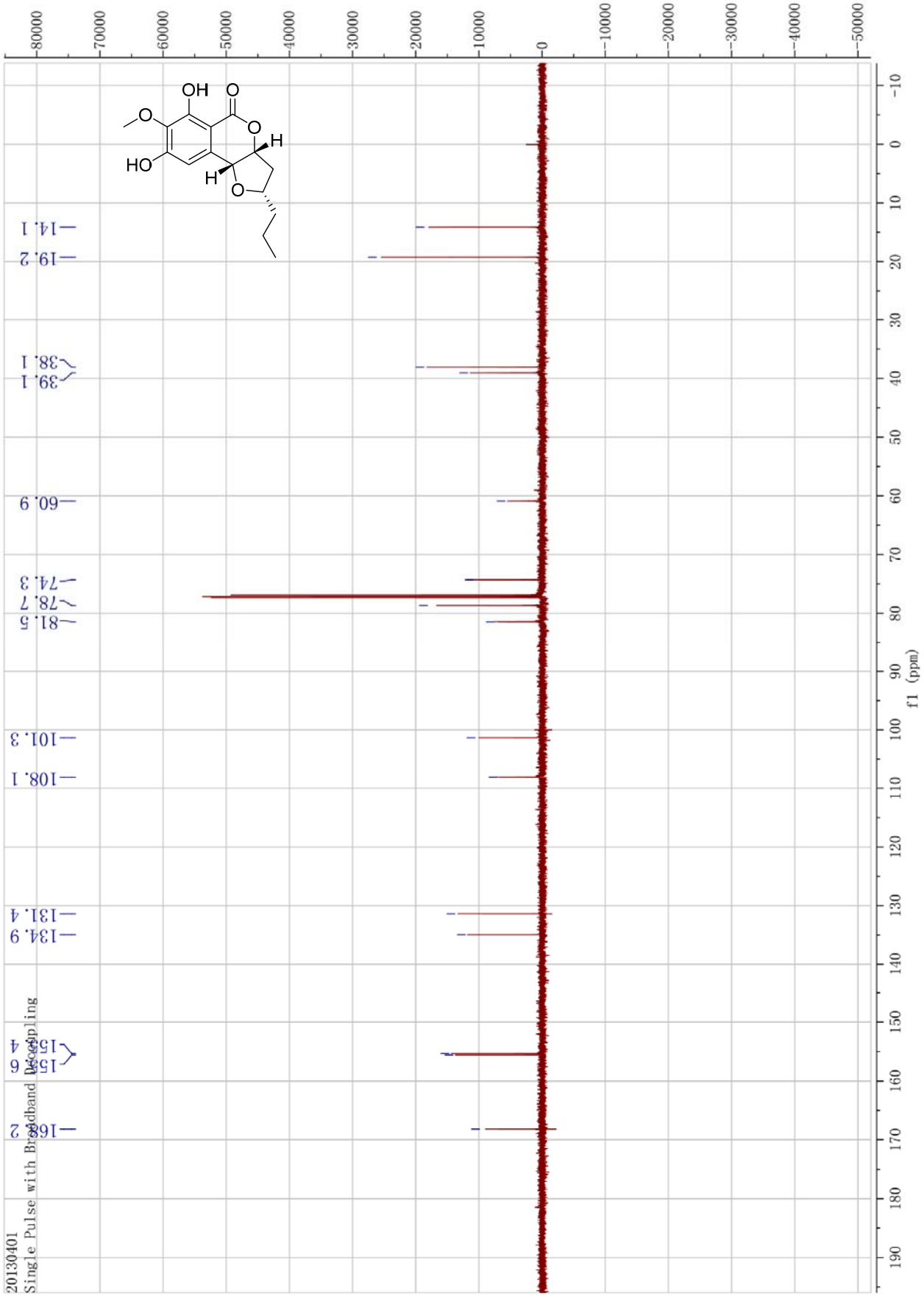

Figure S102. The DEPT spectrum of compound **18** in $CDCl_3$

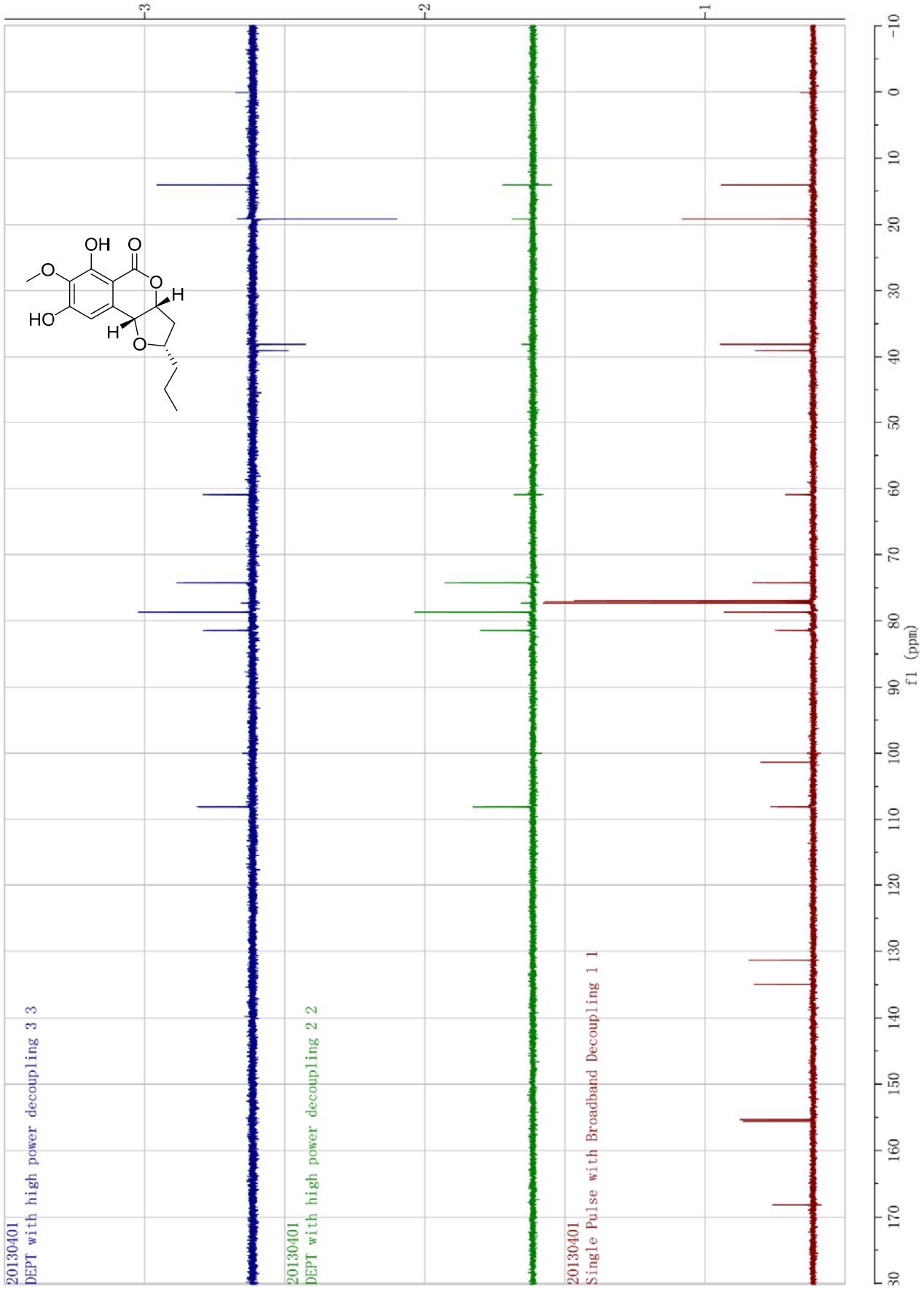

Figure S103. The HMQC spectrum of compound **18** in $CDCl_3$

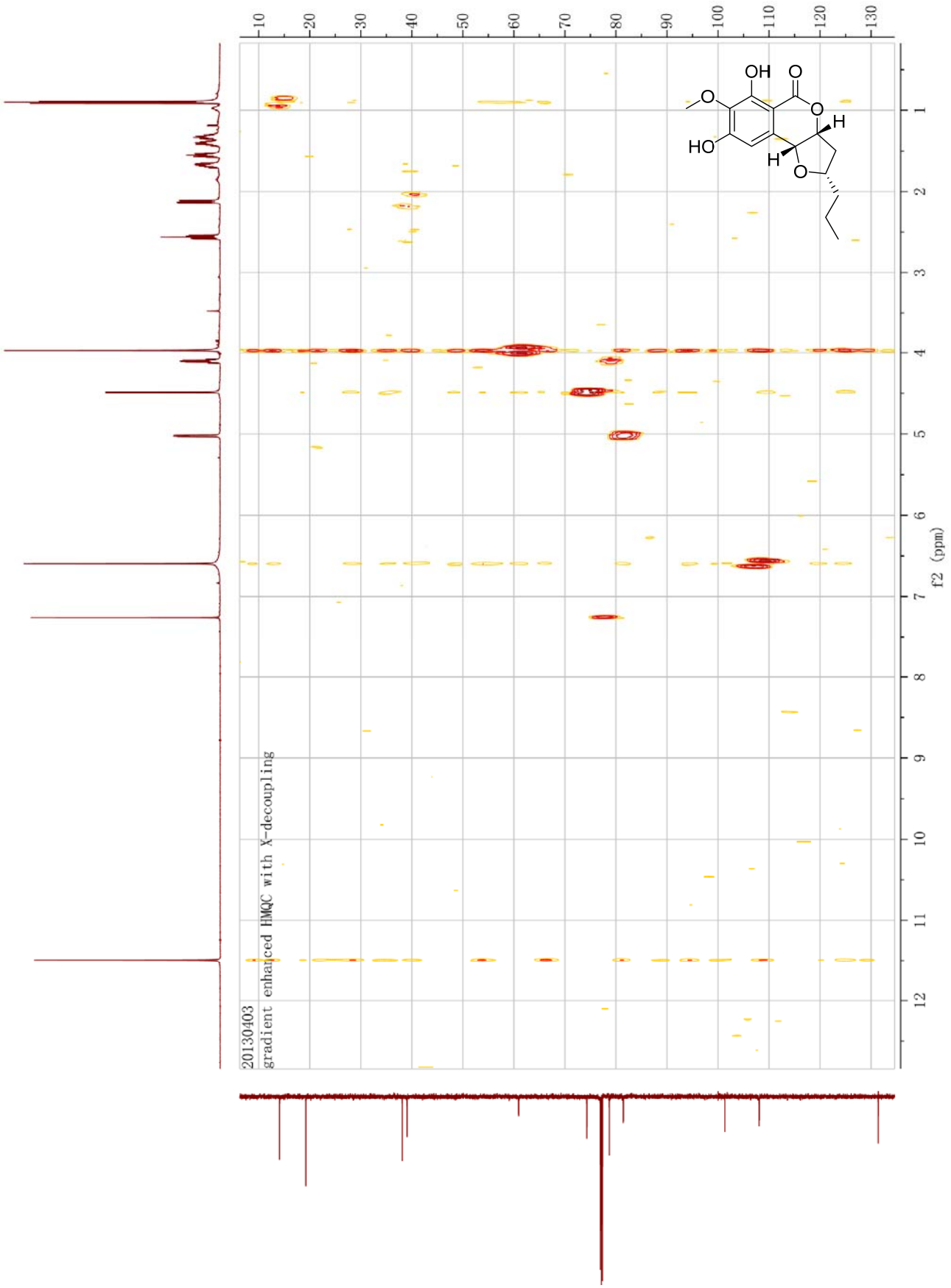

Figure S104. The ^{1}H-^{1}H COSY spectrum of compound **18** in $CDCl_3$

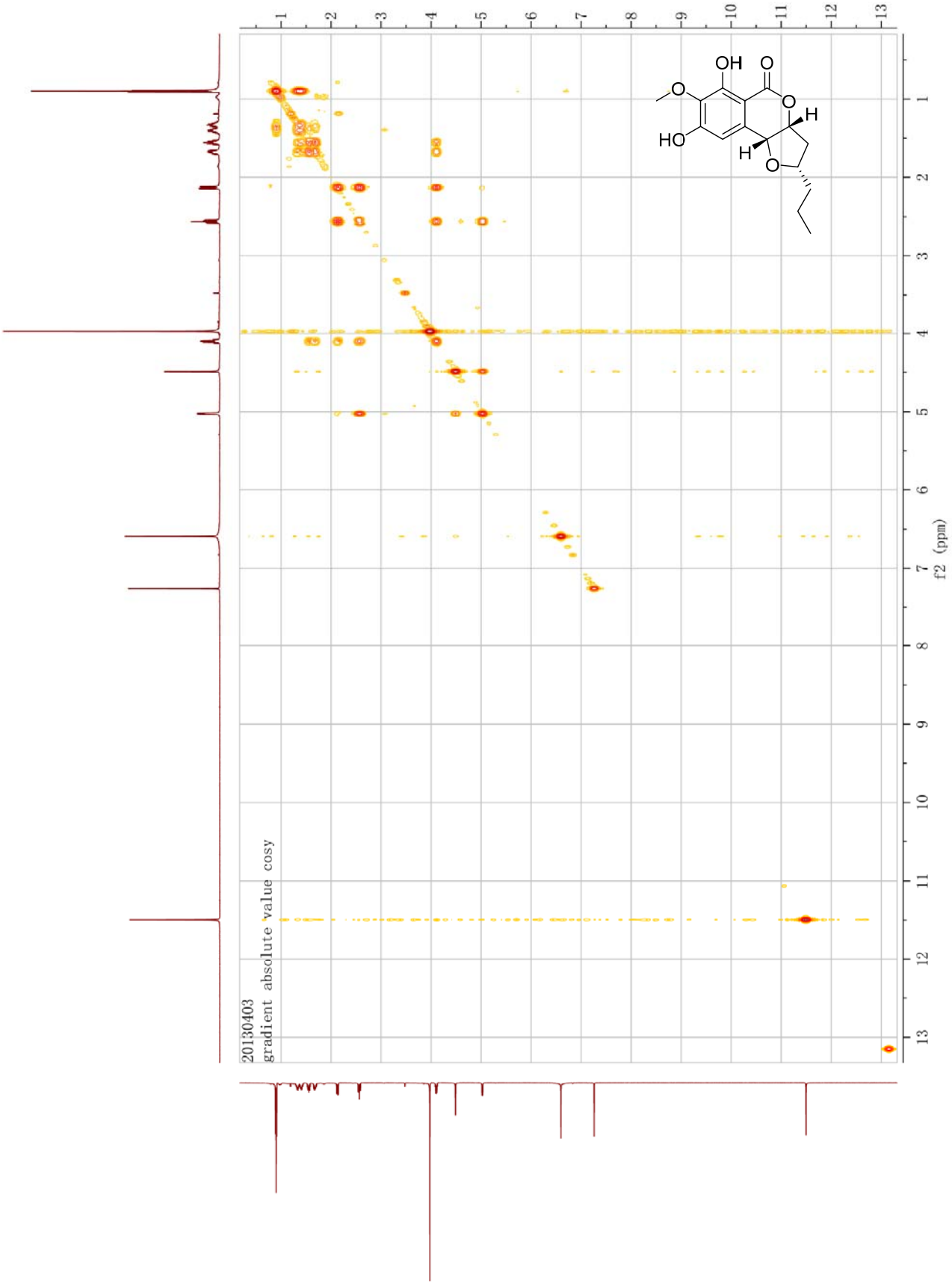

Figure S105. The HMBC spectrum of compound **18** in $CDCl_3$

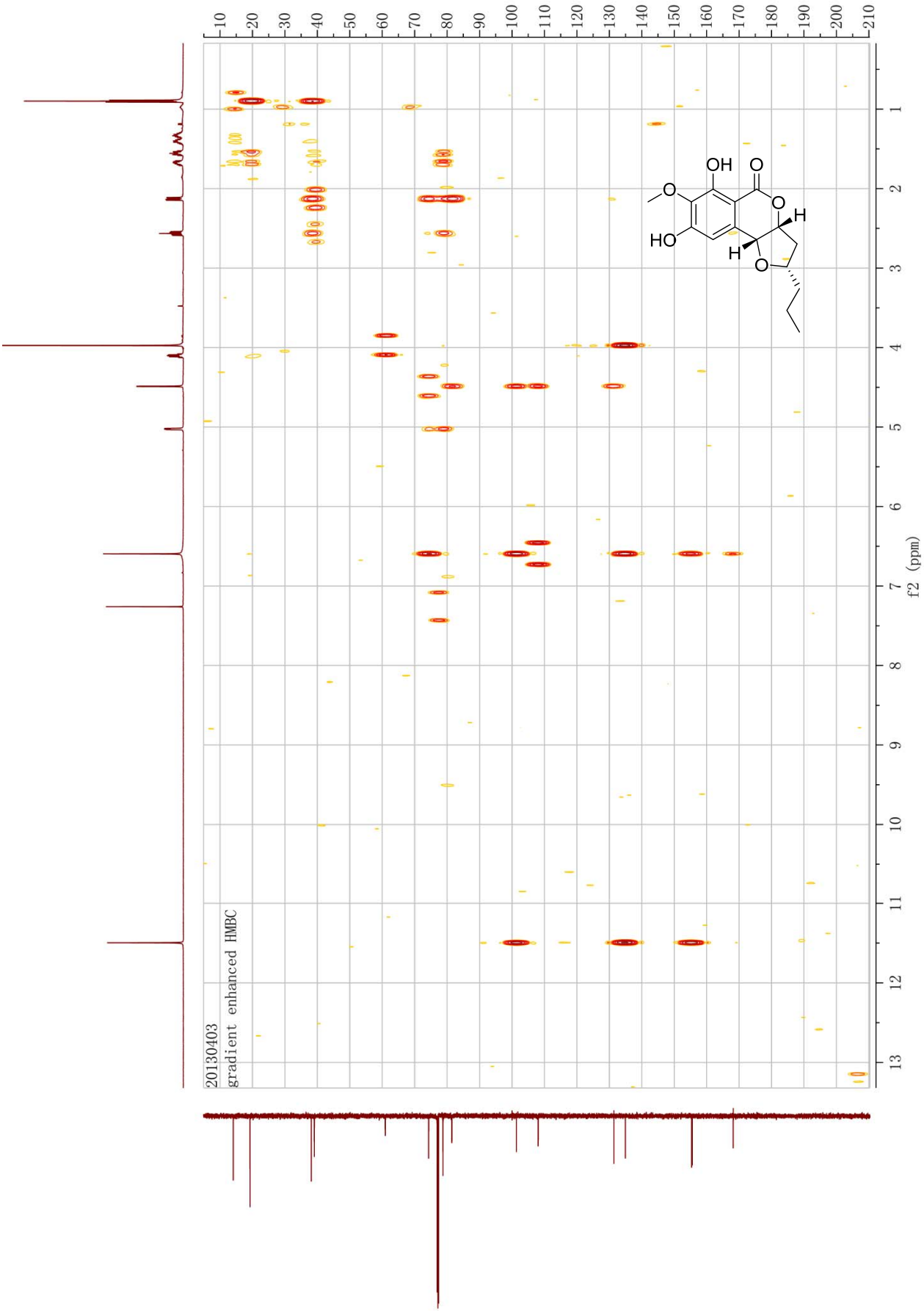

Figure S106. The NOESY spectrum of compound **18** in $CDCl_3$

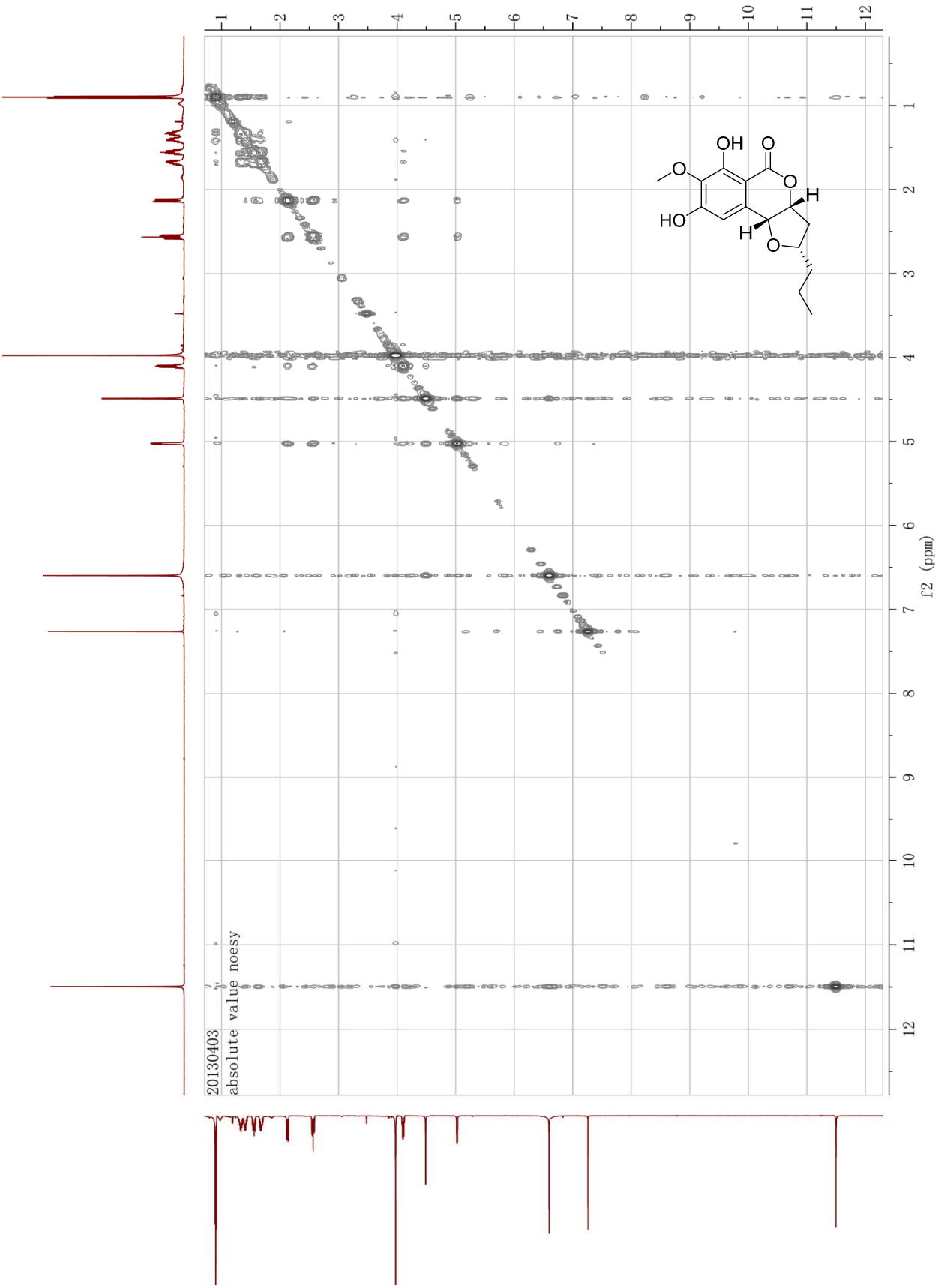

Figure S107. X-ray data and structure of compound **20**

7-*O*-Demethylmonocerin (**20**): Colorless Monoclinic crystals from MeOH-H_2O (1:1, v/v) with molecular formula of $C_{15}H_{18}O_6$; space group *P*2(1) with a = 7.7687(7) Å, b = 7.4049(5) Å, c = 12.6454(9) Å, V = 703.08(9) Å^3, Z = 2, D_{calcd} = 1.390 Mg/m^3, μ= 0.906 mm^{-1}, and F(000) = 312; crystal size: 0.32 × 0.27 × 0.07 mm^3. T = 293(2) K. Absolute structure parameter: 0.0(3). These data were obtained on a Bruker APEX DUO area detector diffractometer with graphite monochromatic Cu-Kα radiation (λ = 1.54178 Å) and have been deposited in the Cambridge Crystallographic Data Centre with supplementary publication No 995362. The structure was solved by direct methods (SHELXS-97) and expanded using Fourier techniques (SHELXL-97). The final cycle of full-matrix least-squares refinement was based on 1549 unique reflections (2θ < 50°) and 193 variable parameters and converged with unweighted and weighted agreement factors of R1 = 0.0409, wR2 = 0.1015, and R = 0.0499 for I > 2σ(I) data. These data can be obtained free of charge from The Cambridge Crystallographic Data Centre via www.ccdc.cam.ac.uk/data_request/cif.

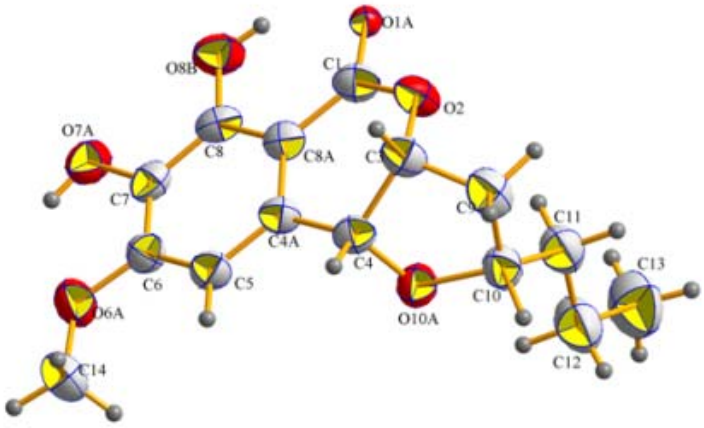

ORTEP drawing of **20**

Figure S108. The ^{1}H-NMR spectrum of compound **12a** in $CDCl_3$

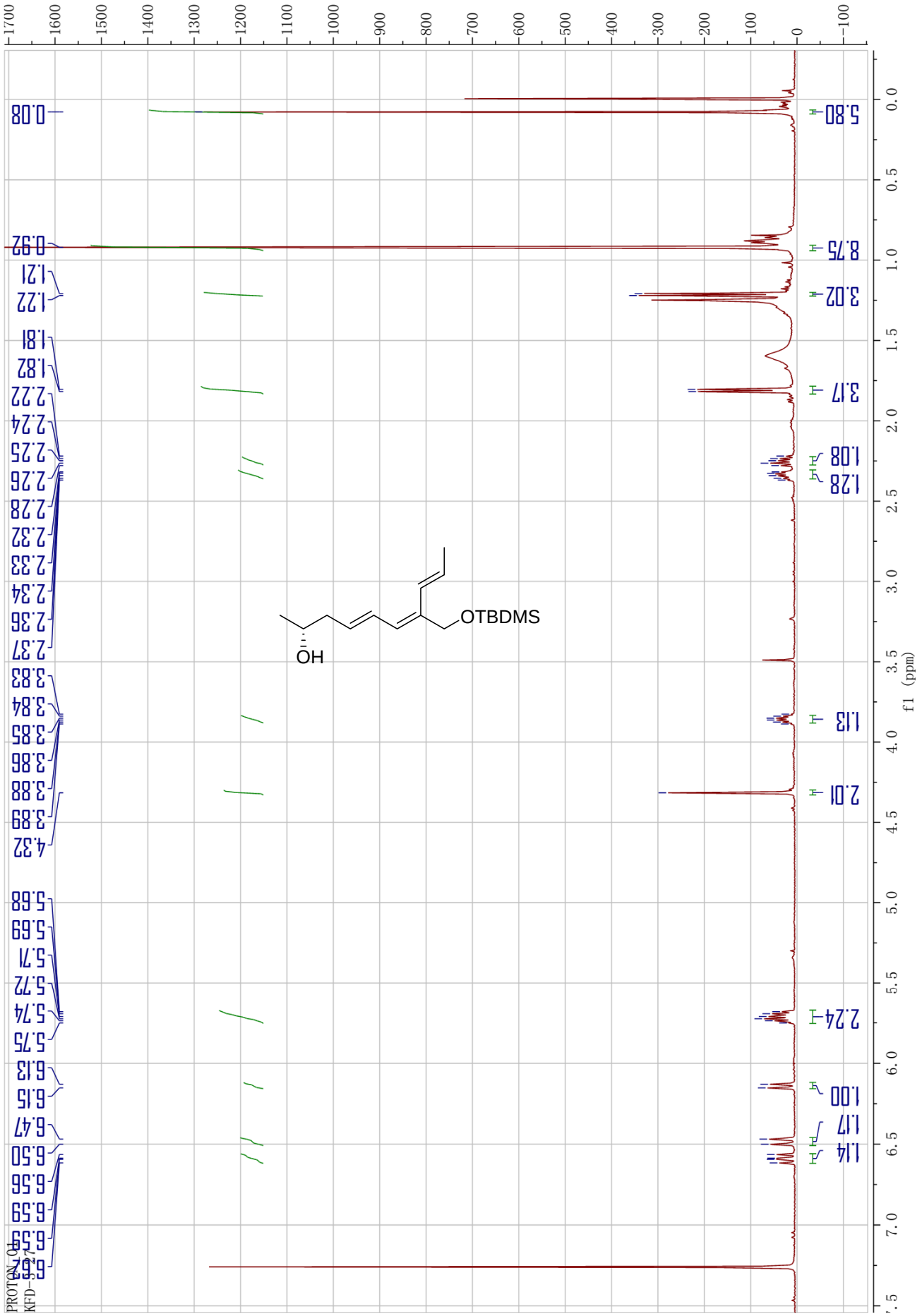

Figure S109. The DEPTQ spectrum of compound **12a** in $CDCl_3$

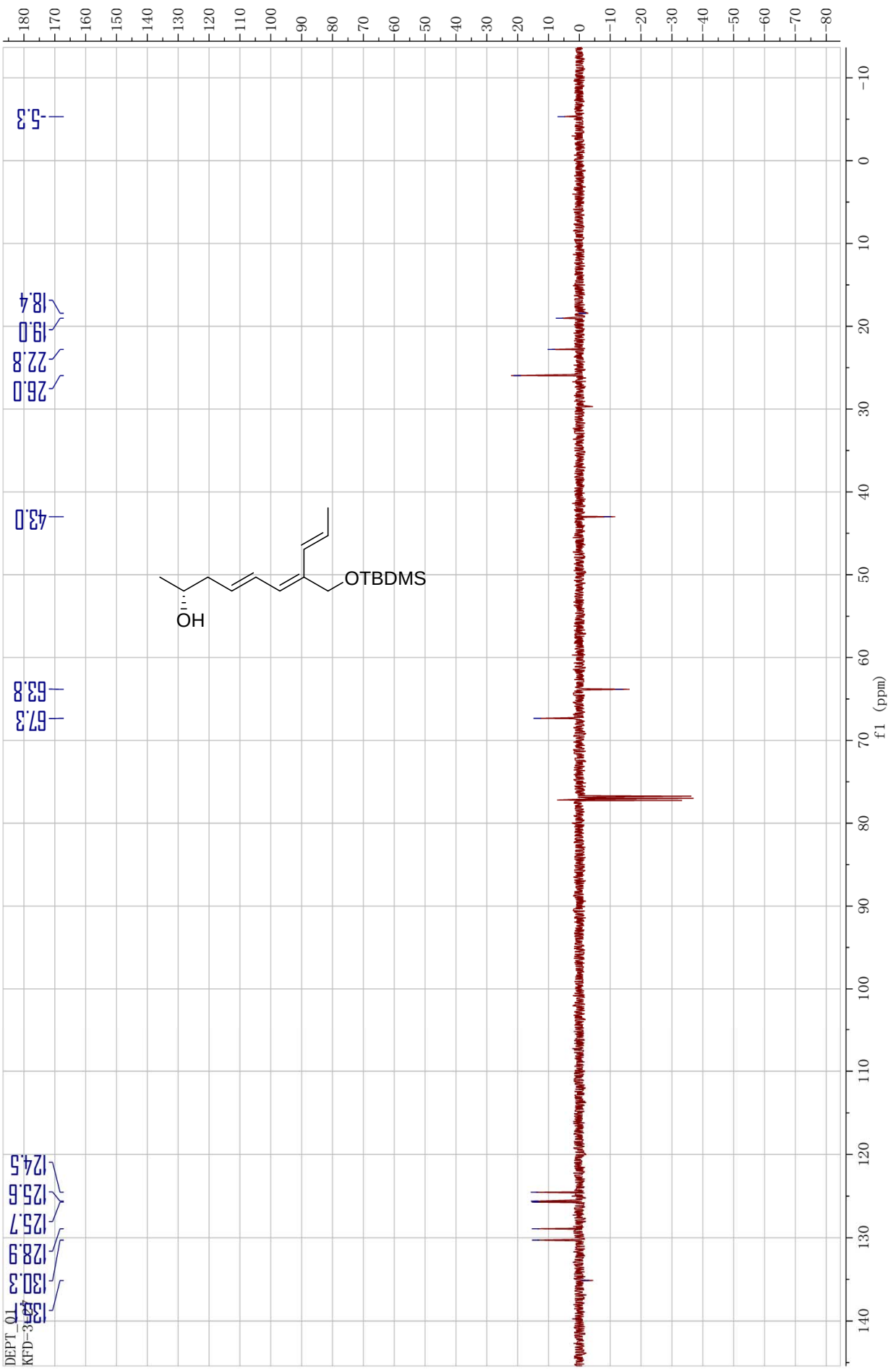

Figure S110. The HMQC spectrum of compound **12a** in $CDCl_3$

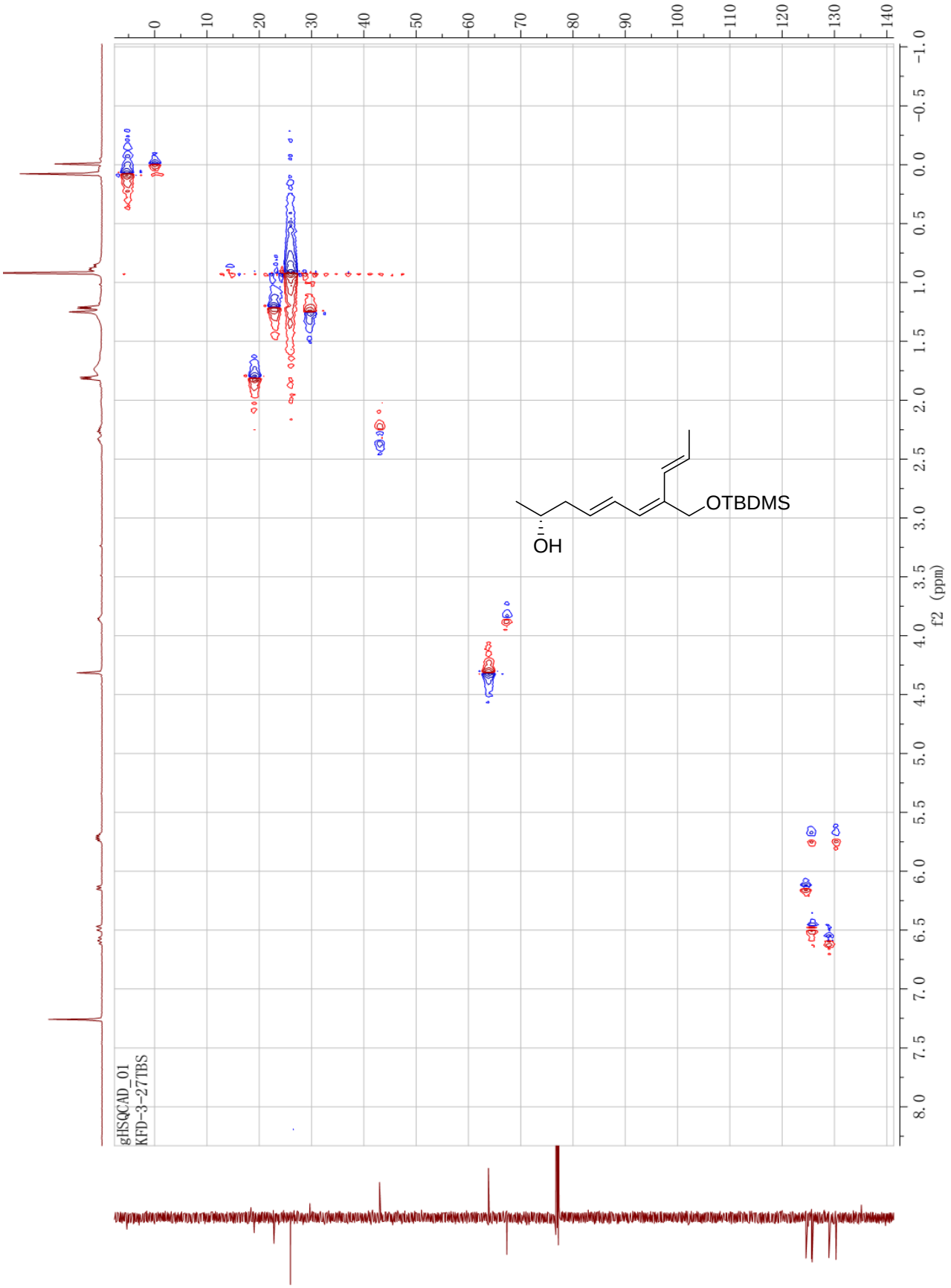

Figure S111. The ^{1}H-^{1}H COSY spectrum of compound **12a** in $CDCl_3$

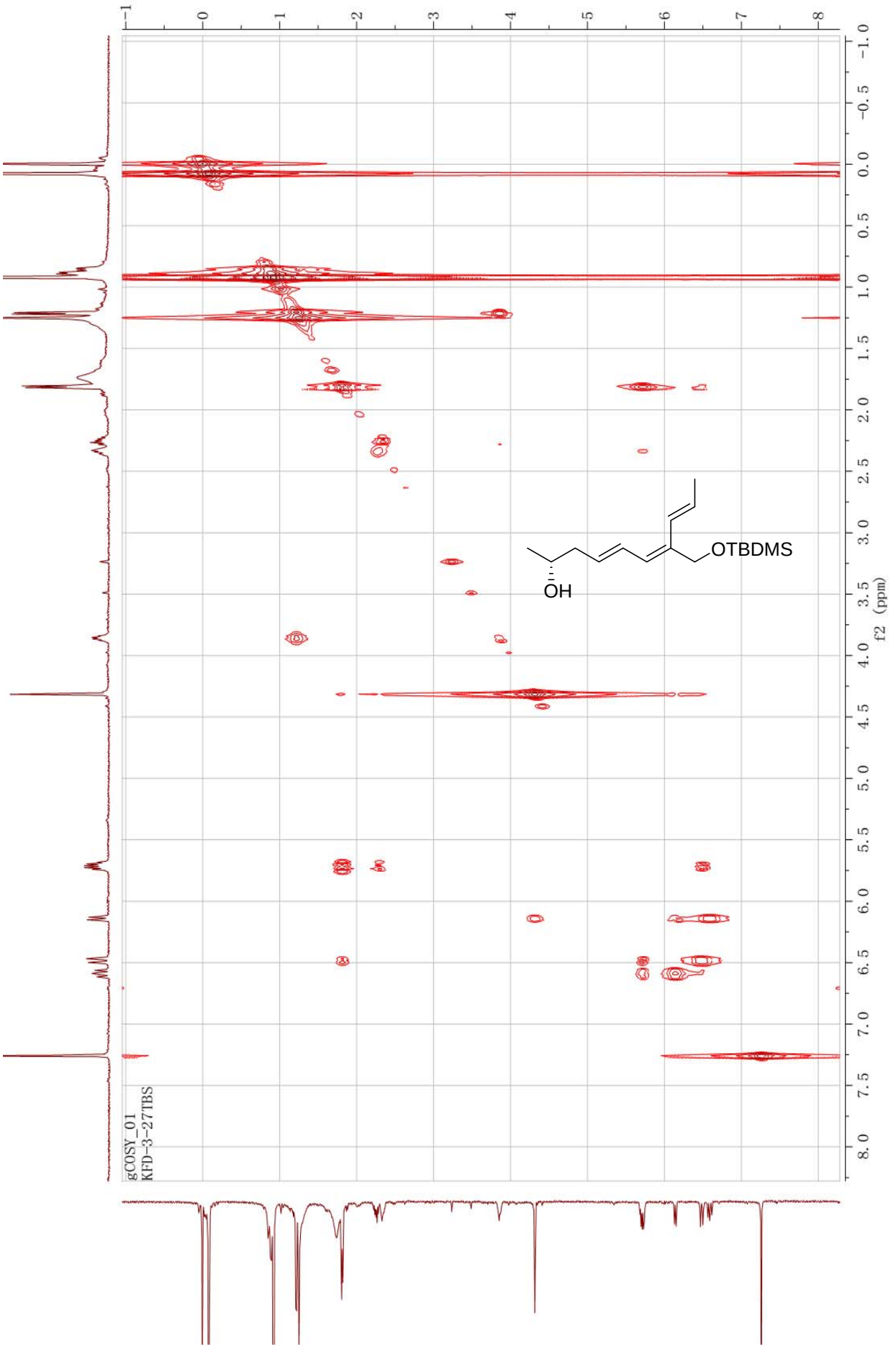

Figure S112. The HMBC spectrum of compound **12a** in $CDCl_3$

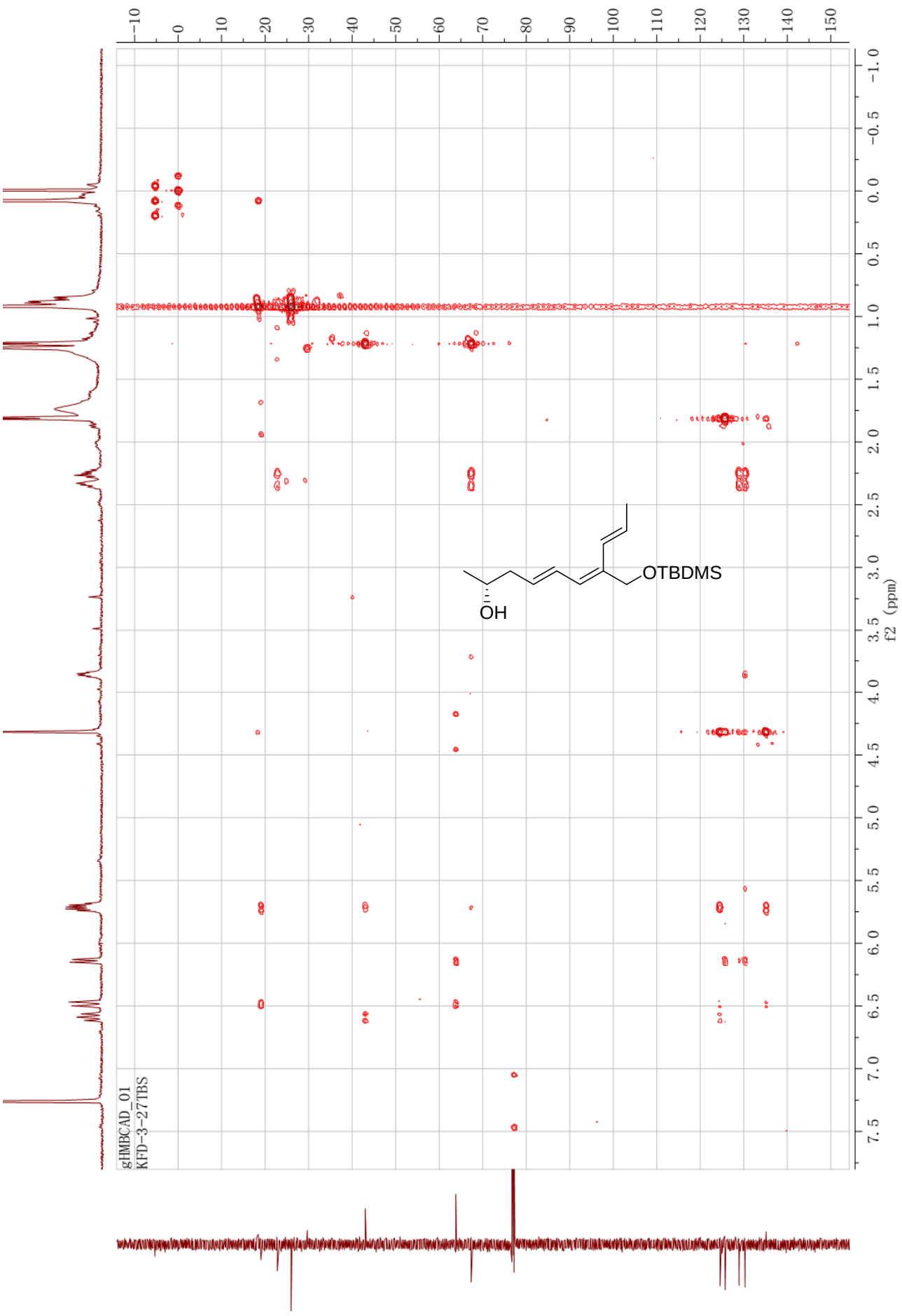

Figure S113. The ^{1}H-NMR spectrum of compounds **2a** and **2b** in $CDCl_3$

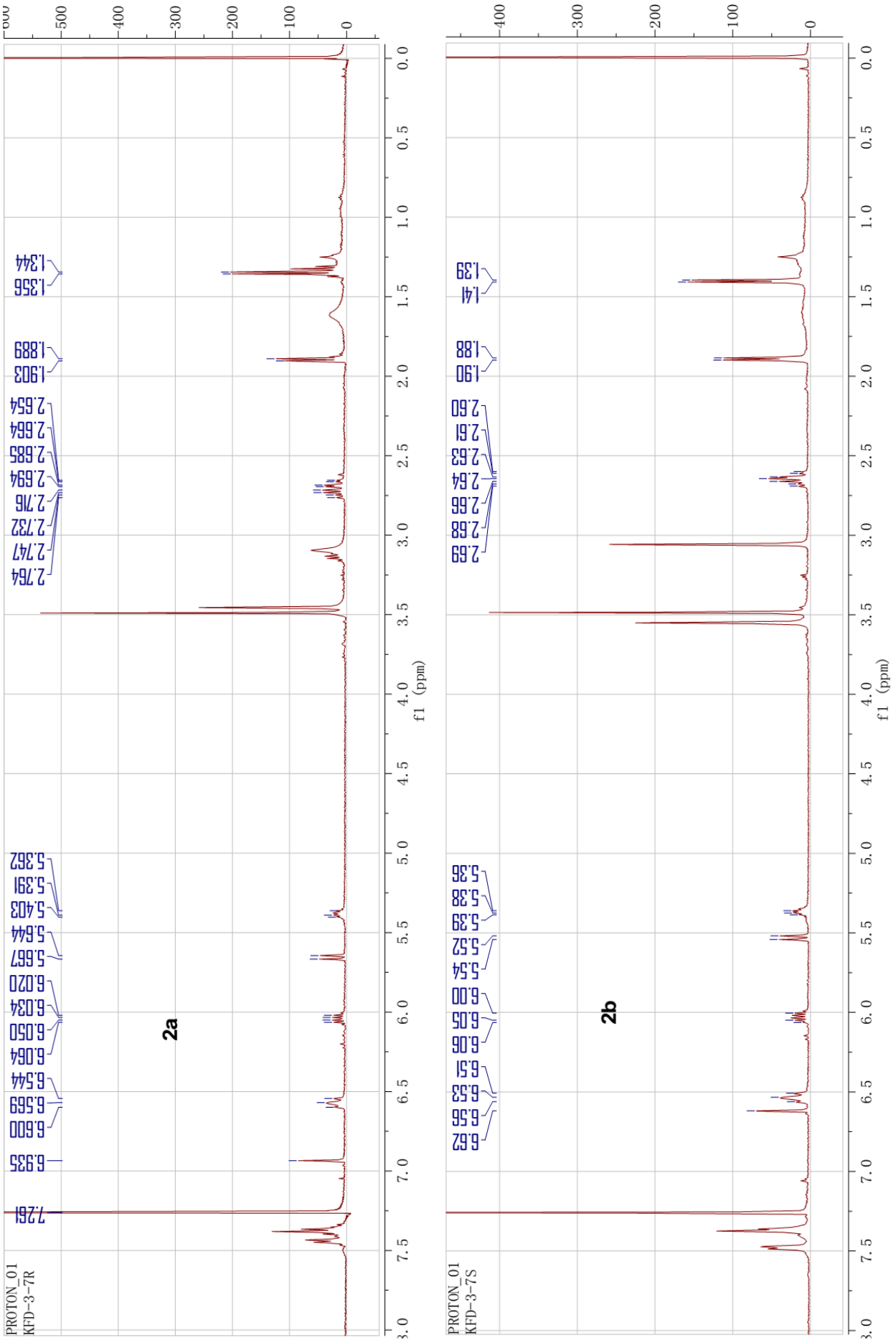

Figure S114. The ^{1}H-NMR spectrums of compounds **3a** and **3b** in $CDCl_3$

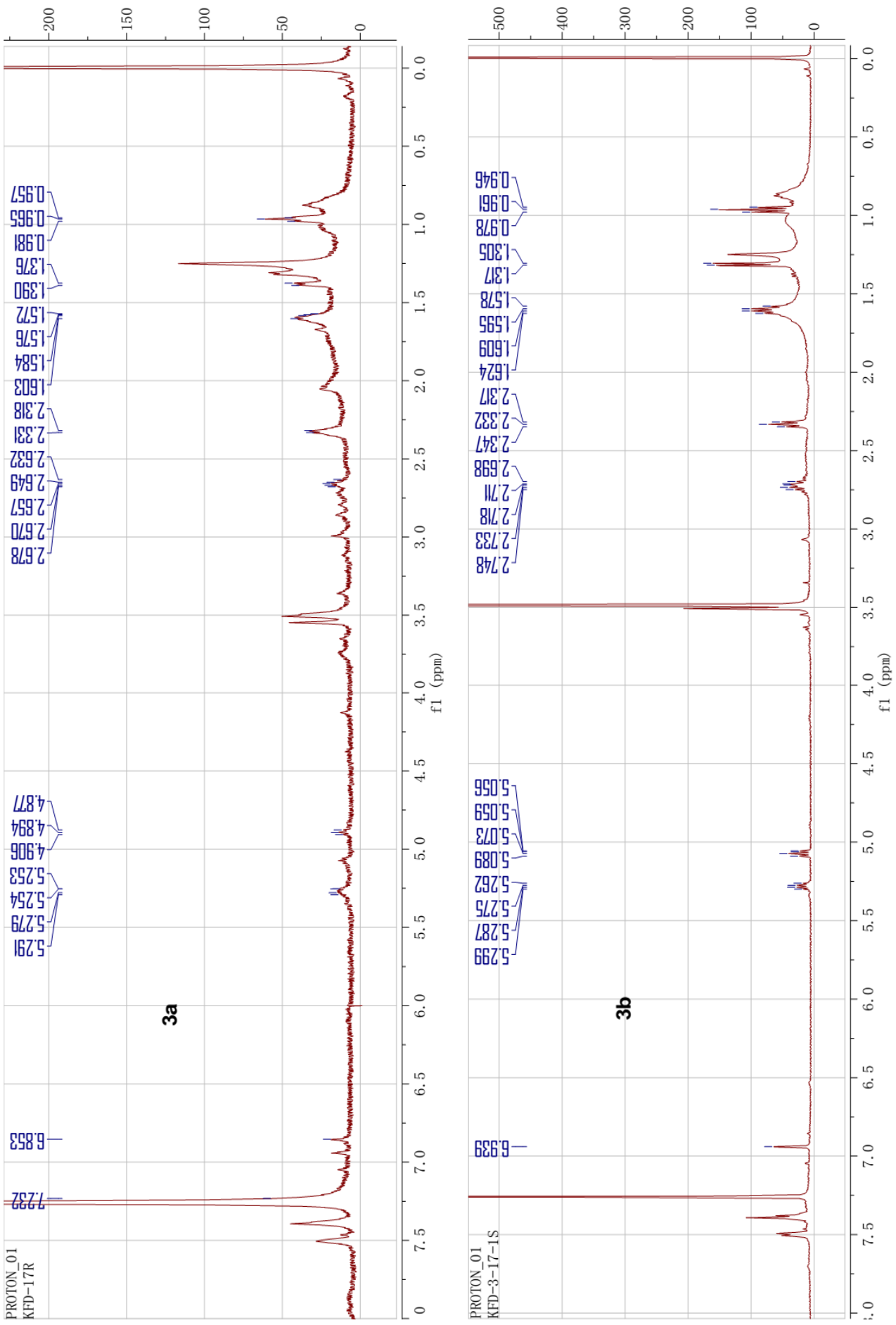

Figure S115. The ^{1}H-NMR spectrums of compounds **5a** and **5b** in $CDCl_3$

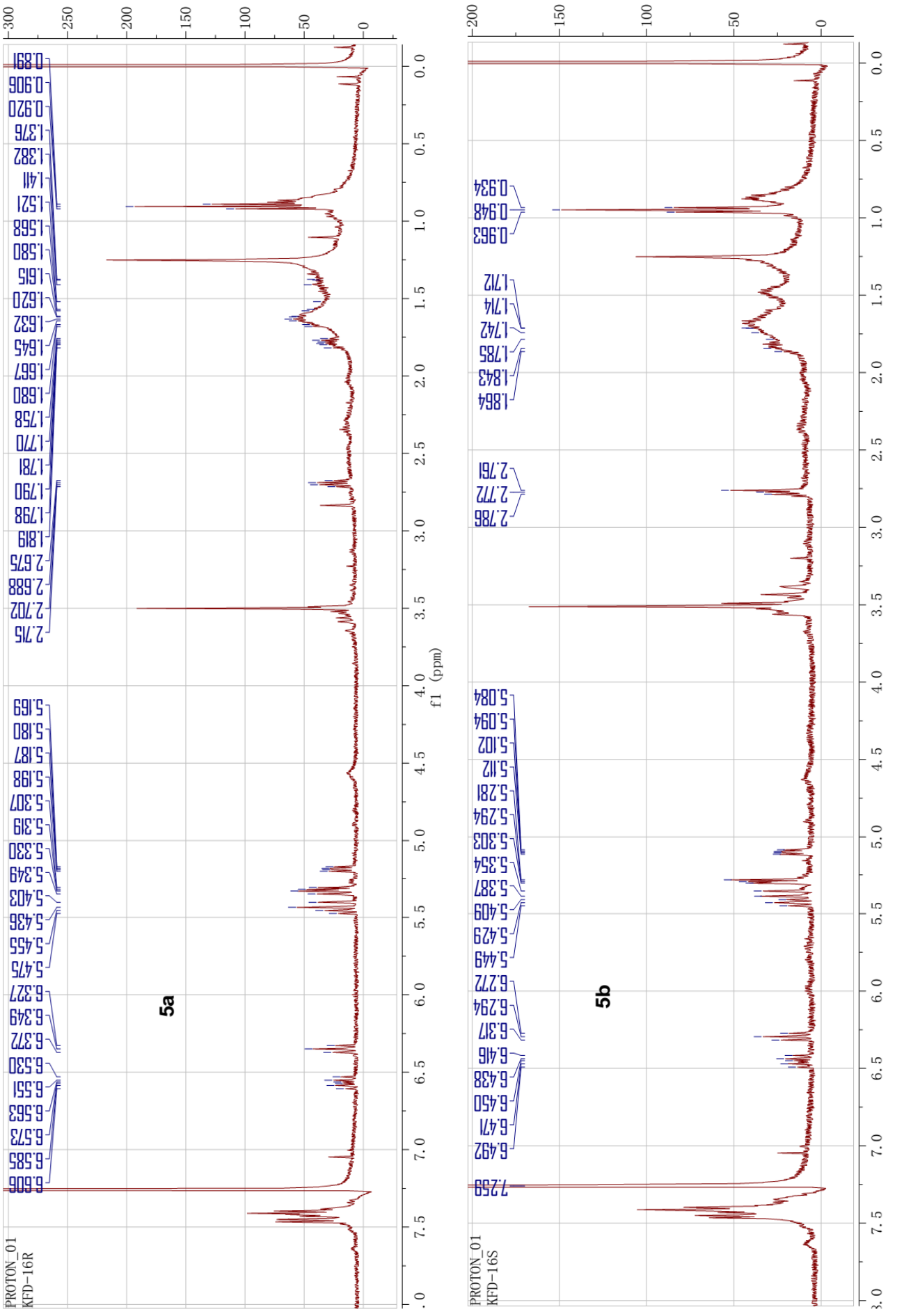

Figure S116. The ^{1}H-NMR spectrums of compounds **6a** and **6b** in $CDCl_3$

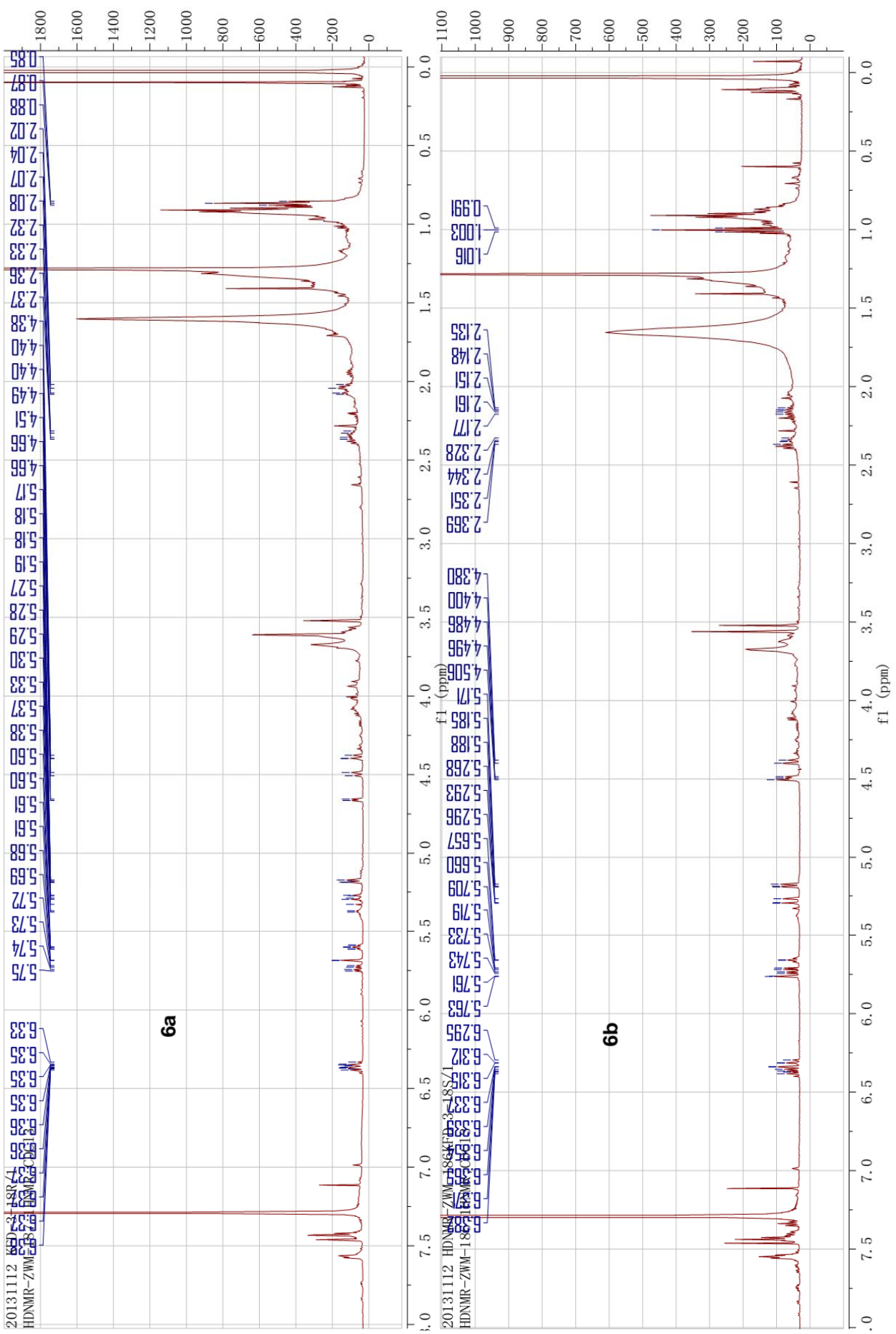

Figure S117. The ^{1}H-NMR spectrums of compounds **7a** and **7b** in $CDCl_3$

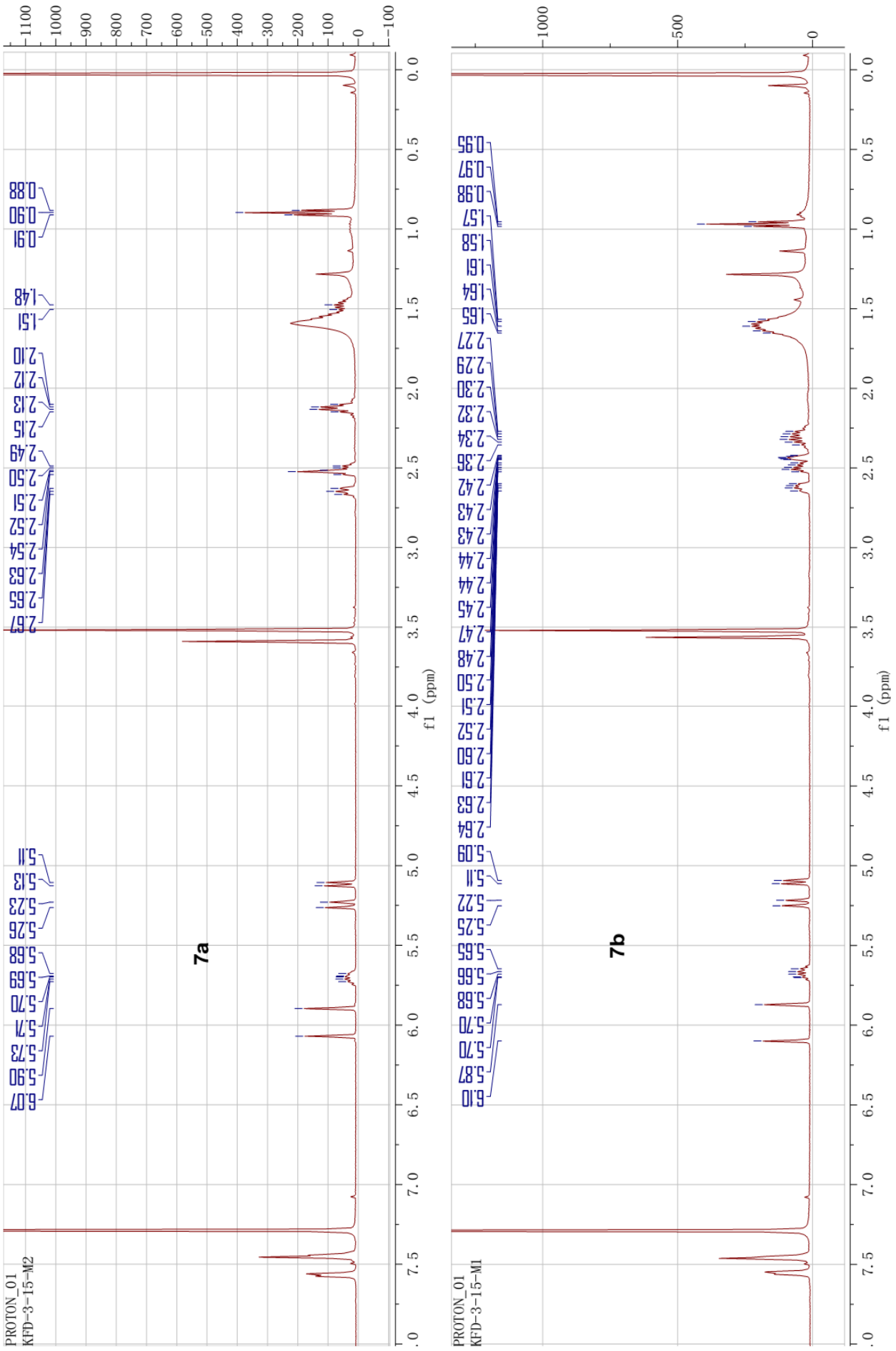

Figure S118. The ^{1}H-NMR spectrums of compounds **12aa** and **12ab** in $CDCl_3$

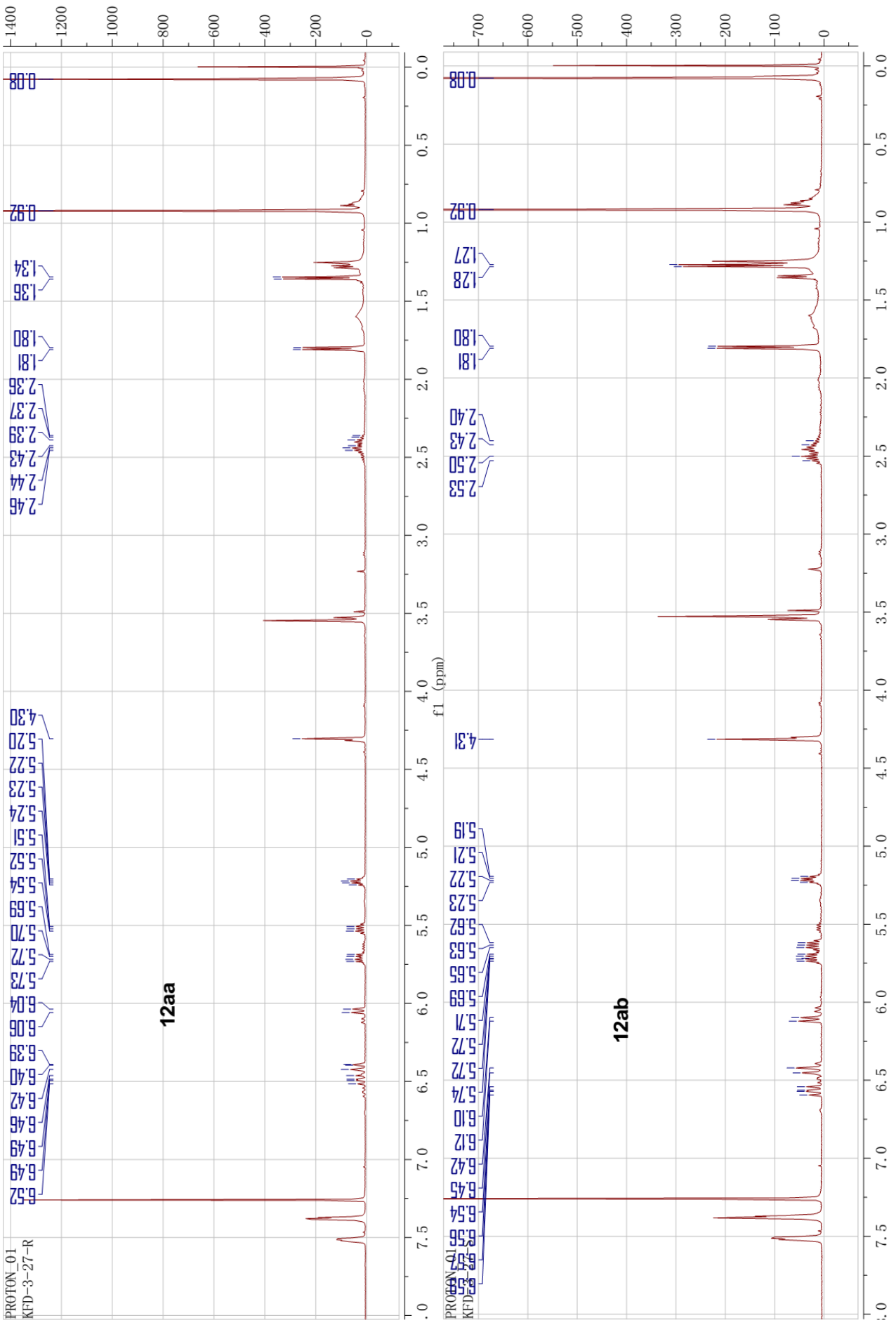

Figure S119.The HPLC analysis and the ESIMS of the reaction liquid of **12** to **12a**.

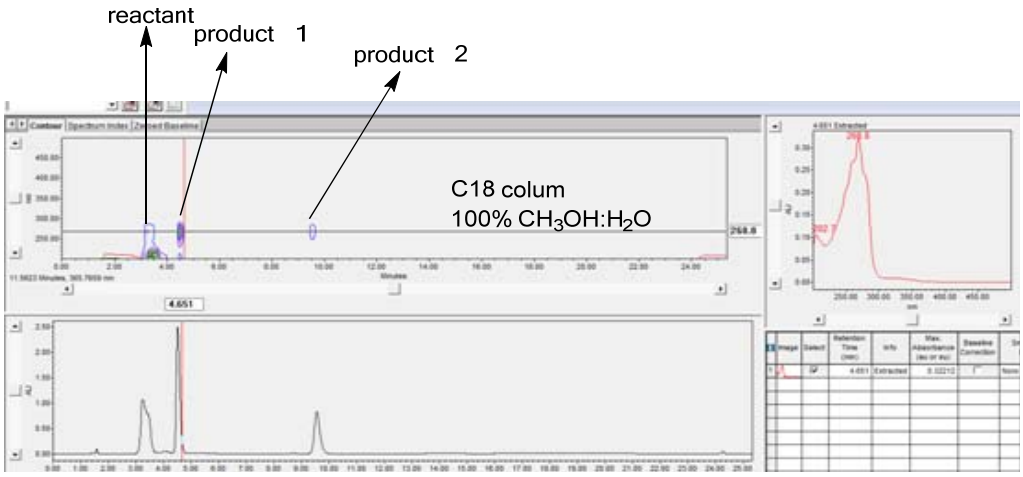

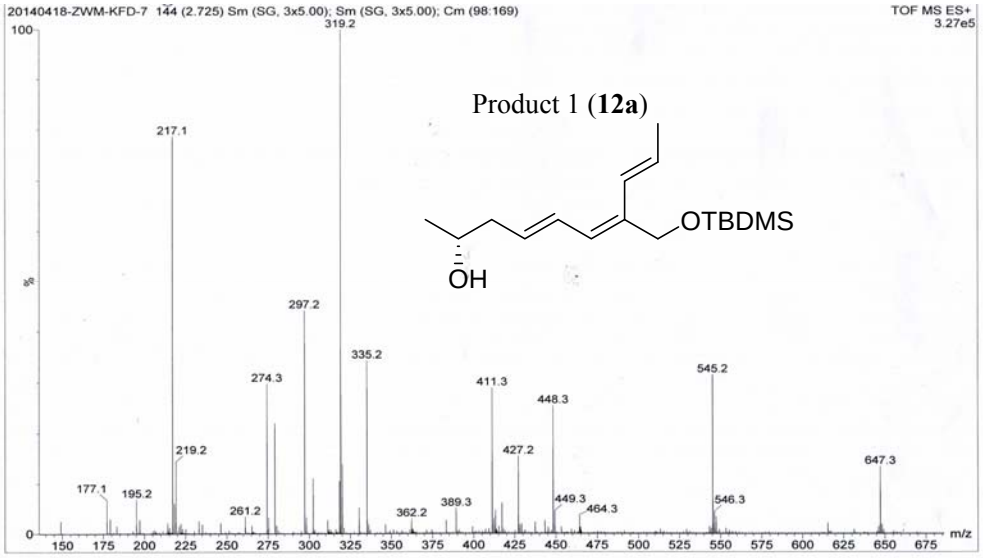

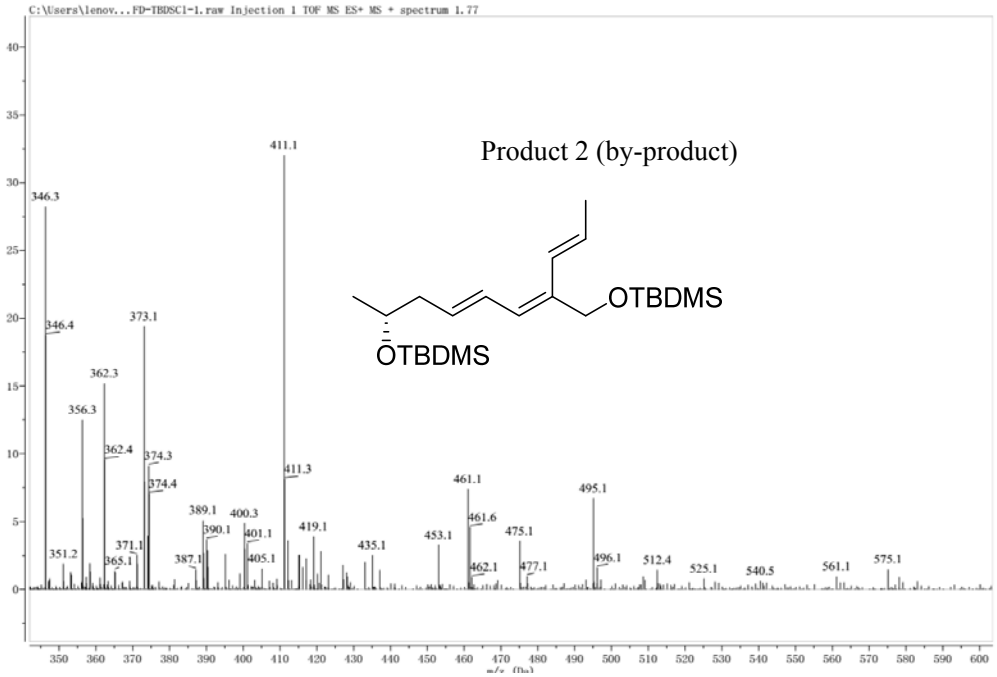

Figure S120. The HPLC analysis of compound **16** and synthetic **15** (ODS, 10% MeOH/H_2O, v/v).

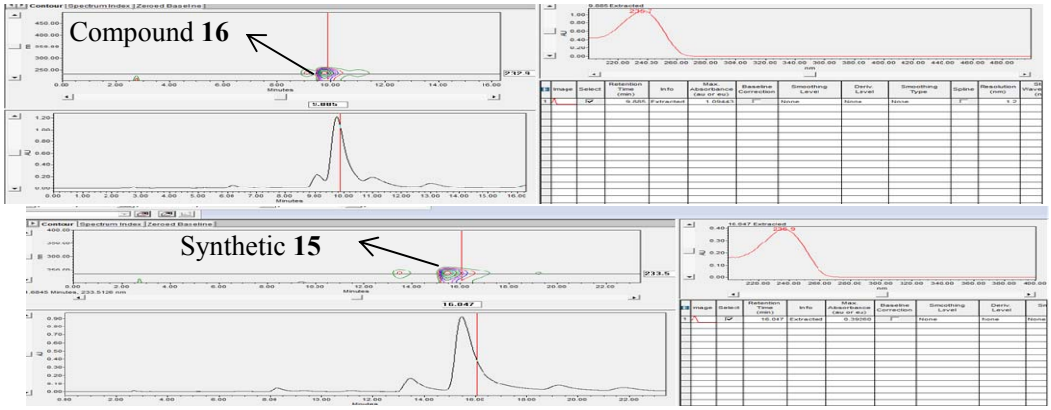

Figure S121. The HPLC analysis of **14** and the synthetic **14** (ODS, 20% MeOH/H_2O, v/v).

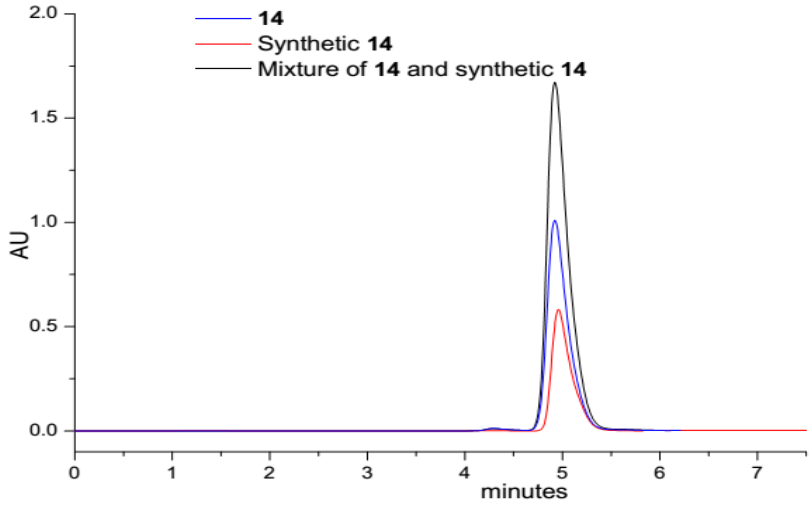

Figure S122. The HPLC analysis of **15** and the synthetic **15** (ODS, 15% MeOH/H_2O, v/v).